

TEXTE

120/2019

Environmentally friendly air conditioning for trains – Field data measurement and analysis on the ICE 3 air- cycle system

Testing, measurement and evaluation of systems with
natural refrigerants for sustainable cooling and heating
in means of public transport – Substitution of
fluorinated greenhouse gases
Final report

TEXTE 120/2019

Environmental Research of the
Federal Ministry for the
Environment, Nature Conservation
and Nuclear Safety

Project No. (FKZ) 3714 95 311 0
FB000132/ENG

Environmentally friendly air conditioning for trains – Field data measurement and analysis on the ICE 3 air-cycle system

Testing, measurement and evaluation of systems with natural refrigerants
for sustainable cooling and heating in means of public transport –
Substitution of fluorinated greenhouse gases

Final report

by

Reinhard Aigner, Andreas Krawanja, Dr. Christian Luger, Maik Wollweber
Liebherr-Transportation Systems GmbH & Co KG, Korneuburg


Dr. Peter Claus, Leonhard Hörth, Dr. Mario Streng
DB Systemtechnik GmbH, Munich

On behalf of the German Environment Agency

Imprint

Publisher:

Umweltbundesamt
Wörlitzer Platz 1
06844 Dessau-Roßlau
Tel: +49 340-2103-0
Fax: +49 340-2103-2285
buergerservice@uba.de
Internet: www.umweltbundesamt.de

 /umweltbundesamt.de

 /umweltbundesamt

Study performed by:

Liebherr-Transportation Systems GmbH & Co KG
Liebherrstrasse 1
2100 Korneuburg
Austria

Study completed in:

October 2018

Edited by:

Section III 1.4 Substance-related Product Issues
Gabriele Hoffmann

Publication as pdf:

<http://www.umweltbundesamt.de/publikationen>

ISSN 1862-4804

Dessau-Roßlau, October 2019

The responsibility for the content of this publication lies with the author(s).

Abstract

Current air-conditioning systems for railway vehicles predominantly use fluorinated refrigerants, which will be phased down in the coming years because of their damaging impact on the climate. Motivated by the need to implement environmentally friendly technologies that will be available for the long term for the air conditioning of passenger trains, Liebherr and Deutsche Bahn conducted a comparison of the annual energy consumption and the Total Cost of Ownership (TCO) of railway heating, ventilation, and air-conditioning systems (HVAC) using air and R-134a as refrigerants. Systems in operation and advanced systems were both assessed. Measurement data and model calculations obtained from systems in operation formed the basis for evaluation. For the average primary annual energy consumption for cooling, the air-cycle systems, which use air as refrigerant, had savings of 16% and 28%, respectively, compared to the R-134a systems that were considered. The higher investment costs of air-cycle systems are compensated by lower operating costs, particularly lower energy costs, and by lower maintenance costs, so that air-cycle systems have the advantage in terms of economic efficiency. As a result, air-cycle systems are an environmentally friendly, economical and reliable solution to the refrigerant issue.

Index

List of figures	7
List of tables.....	12
List of abbreviations	13
Summary.....	15
1 INTRODUCTION.....	26
1.1 Task	27
1.2 Requirements for the project	27
1.3 Project design and workflow	28
1.3.1 WP 1: Develop and prepare the measurement program	28
1.3.2 WP 2: Perform measurement	28
1.3.3 WP 3: Compare with other air-conditioning systems	29
1.3.4 WP 4: Evaluate the measurement program.....	29
1.3.5 WP 5: Technical discussion and publication	29
1.3.6 Schedule	29
1.4 Scientific and technical status before the start of the project	31
1.4.1 Compact air-conditioning unit on the ICE 3 (air).....	31
1.4.2 Air-conditioning system on the ICE-T (R134a)	35
1.4.3 Previous measurements to determine energy consumption	37
1.5 Collaboration with other project partners	39
2 DETAILED PRESENTATION OF THE PROJECT	40
2.1 Develop and prepare the measurement program (WP1).....	40
2.1.1 Measuring concept.....	40
2.1.2 Preparation of additional measurement equipment.....	41
2.1.2.1 Temperature and humidity of fresh air	42
2.1.2.2 Temperature and humidity of recirculated air	43
2.1.2.3 Position, speed and direction of the train	43
2.1.2.4 Solar radiation	44
2.1.2.5 Control cabinet	45
2.1.3 Installation of measurement equipment	48
2.1.3.1 Installation of control cabinet modules	49
2.1.3.2 Installation of temperature and humidity sensors	51
2.1.3.3 Installation of occupancy counter	52
2.1.3.4 Installation of solar sensors	53
2.1.4 Calibrating the measurement equipment.....	54

2.1.5	Concept for processing and evaluating field data.....	58
2.1.5.1	Data storage	60
2.1.5.2	Visualisation of data for manual assessment and processing	60
2.1.5.3	Program-supported processing of data	62
2.1.6	Creating the evaluation software.....	62
2.2	Perform measurement (WP2)	63
2.2.1	Data recording and processing.....	65
2.2.2	Repairs to the measurement equipment.....	65
2.2.2.1	Repairs to the solar sensors on 20 April 2016	66
2.2.2.2	Repair of occupancy counter on 23 June 2016	67
2.2.3	Modifications and additions to the measurement equipment.....	68
2.2.3.1	Replacement of the UMTS routers on 20 April 2016	68
2.2.3.2	Installation of a second GPS receiver on 20 April 2016	71
2.2.3.3	Improvement of data recording and backup in October 2016	72
2.2.4	Availability of data recording	72
2.2.5	Organisational matters.....	75
2.3	Evaluate the measurement program (WP 4).....	76
2.3.1	Creating the evaluation software.....	76
2.3.2	Analysis of power and energy consumption for the air-cycle system on the ICE 3	77
2.3.2.1	Methodology	77
2.3.2.2	Overview of existing measurement signals as the basis for investigations and measurement data processing	78
2.3.2.3	Processing measurement signals	79
2.3.2.4	Passenger occupancy signal in TW7	80
2.3.2.5	Solar radiation signal in W/m ² and mapping of DWD data	80
2.3.2.6	Determining the electric power consumption	81
2.3.2.7	Heating capacity supplied and cooling capacity withdrawn on the air side	82
2.3.2.8	Results from the analysis of example train trips from summer and winter service	83
2.3.3	Comparison of different HVAC systems with respect to electric power and energy consumption	89
2.3.3.1	Introduction and motivation	89
2.3.3.2	Factors influencing electric power and energy consumption	89
2.3.3.3	Primary, secondary and total power/energy consumption	90
2.3.3.4	HVAC systems to be compared	91
2.3.3.5	Source data	96
2.3.3.6	Methods of comparison	103

2.3.3.7	Summary of differences between the analyses in this project and the work by Meister (Meister, 2012)	123
2.3.4	Comparison of different HVAC systems in terms of maintenance effort	124
2.3.4.1	Extent of maintenance activities for the ICE 3 air-conditioning system	125
2.3.4.2	Extent of considered maintenance activities for the ICE-T	127
2.3.4.3	Collected maintenance data for the ICE 3 and ICE-T – cost comparison	128
2.4	Comparison with other air-conditioning systems (WP 3).....	129
2.4.1	Comparison of the electric power and energy consumption of different HVAC systems	129
2.4.1.1	Comparison of the primary power consumption according to the classification	129
2.4.1.2	Comparison of annual energy consumption	132
2.4.2	Complete analysis of Life Cycle Costs (LCC) and Total Costs of Ownership (TCO).....	151
2.4.2.1	Design of the Cost Assessment Tool (CAT)	151
2.4.2.2	Specific comparison of the HVAC systems	152
2.4.2.3	Input variables for the analysis of economic efficiency	153
2.4.2.4	Result of the analysis of economic efficiency	156
2.4.3	Discussion of results & conclusions	159
2.4.3.1	Results for power and energy consumption	159
2.4.3.2	Conclusion on economic efficiency	160
2.5	Technical discussion and publication (WP 5).....	162
2.6	Need for and relevance of the project	163
2.7	Applicability of the results	163
2.7.1	Economic prospects of success	163
2.7.2	Prospects for scientific success	163
2.7.3	Prospects for scientific and commercial follow-up projects.....	163
2.8	Advances by other bodies.....	163
2.9	Publications.....	164
3	Bibliography.....	165

List of figures

Figure 1:	Comparison of primary annual energy consumption in cooling operation for the air-cycle system ACS (ICE 3) (system 1) and the vapour cycle system VCS (ICE-T) (system 2)	20
Figure 2:	Comparison of the primary annual energy consumption in cooling operation for the air-cycle system (ACS) with direct loop (system 6) and the vapour cycle system (VCS) with variable-speed compressor and refrigerant bypass (system 3)	21
Figure 3:	Work packages in the project structure	28
Figure 4:	Scheduling.....	29
Figure 5:	Photo of press conference in Munich on 27 October 2016	30
Figure 6:	Photo of press conference in Munich on 27 October 2016	30
Figure 7:	Air-cycle compact air-conditioning unit for the ICE 3.....	31
Figure 8:	Schematic of air-conditioning and process air circuit	32
Figure 9:	Air ducting in the compact air-conditioning unit.....	32
Figure 10:	ICE 3 – class 403, trainset 301 of Deutsche Bahn AG	33
Figure 11:	Carriage overview of the first half train ICE 3 - class 403 Ts 301(carriages 1 to 4)	34
Figure 12:	Carriage overview of the second half train ICE 3 - class 403 Ts 301 (carriages 5 to 8)	34
Figure 13:	Air-conditioning unit ICE-T - Compression refrigeration system with the refrigerant R134a	35
Figure 14:	Schematic of the refrigeration circuit and components of the compression refrigeration system with the refrigerant R134a.....	36
Figure 15:	Carriage overview of the ICE-T train for comparison	36
Figure 16:	Annual energy consumption for cooling generation per seat according to previous study	38
Figure 17:	Positions of installed sensors and connections on the compact air-conditioning unit No. 4 in the roof of ICE 3 – carriage TW7	41
Figure 18:	Position of the temperature and humidity sensor in the compact air-conditioning unit.....	42
Figure 19:	Graphical representation of the position of the temperature and humidity sensor in the recirculated air	43
Figure 20:	GPS module including sheet metal bracket installed in the compact air-conditioning unit.....	44
Figure 21:	Solar sensors: Two prepared connection points for the solar sensors (left), the two solar sensors with cable ends (top right), one individual solar sensor (bottom right).....	45
Figure 22:	Installation studies for the additional measurement equipment in the control cabinet for the compact air-conditioning unit in carriage TW7	46
Figure 23:	Installation space studies for the additional measurement equipment in the control cabinet	46

Figure 24:	Test installation of the additional measurement equipment (modules) in the control cabinet (on side).....	47
Figure 25:	Ethernet switch (left), barometric air pressure sensor (right) and occupancy counter unit (centre) – test installation	47
Figure 26:	MVB (fieldbus) reader (top left), additional air-conditioning system computer (BK3, bottom centre), power supply of sensors (top right) and USB hub (bottom right) – test installation	48
Figure 27:	Compact air-conditioning unit No. 4 installed in the roof of carriage TW7 of ICE 3 – class 403.....	49
Figure 28:	Control cabinet module with measurement equipment for carriage TW7 of ICE 3 – class 403.....	49
Figure 29:	Installed and connected top control cabinet module in carriage TW7 of ICE 3 – class 403	50
Figure 30:	Installed and connected bottom control cabinet module in carriage TW7 of ICE 3 – class 403.....	50
Figure 31:	Control cabinet with the two additional modules on the door and cabling in carriage TW7 of ICE 3 – class 403	51
Figure 32:	Installed temperature and humidity sensor in ICE 3 – class 403, carriage TW2 (same as TW7)	52
Figure 33:	Installed sensors for occupancy counting in the passages of carriage TW7 (top left and right) and a single sensor (bottom left).....	53
Figure 34:	Installation drawing for the two roof sensors (solar radiation)	53
Figure 35:	Screen for calibrating the analogue inputs in carriages TW7 and TW2	54
Figure 36:	Screen for calibrating and checking the occupancy counter.....	55
Figure 37:	Screen for checking the read MVB (fieldbus) data.....	55
Figure 38:	Online access to the additional measurement data (excerpt from the display screen)	56
Figure 39:	Online access to the position and speed of the train.....	56
Figure 40:	Test setup for calibrating the solar sensors (excerpt)	57
Figure 41:	Comparison of PV cell and star pyranometer.....	57
Figure 42:	Concept of data flow and the processing of field data.....	59
Figure 43:	Screenshot of the Grafana program: Example of a graphical display (plot)	61
Figure 44:	Screenshot of the Grafana program: Dialogue screen for simple and convenient selection of the graphical data display (dashboard)	62
Figure 45:	2015 ICE railway network	64
Figure 46:	Defective solar cell (cable break) on the air conditioning unit of ICE 3 carriage TW7	66
Figure 47:	Installation of the new solar cell on ICE 3 carriage the TW7 with additional cable attachment	66
Figure 48:	Damage to the sensor cable of the DILAX sensor for occupation counting	67

Figure 49:	Damage to the DILAX sensors for occupation counting	67
Figure 50:	Two new sensors for occupation counting and a new connecting cable after installation	68
Figure 51:	3G/UTMS router PEPWAVE MAX BR1	69
Figure 52:	Router as installed	69
Figure 53:	Installation of the new router (black) and removal of the USB hub (blue)	70
Figure 54:	Installation of the new mobile communication antennas in the compact air-conditioning unit in carriage TW2	70
Figure 55:	Position of the new mobile radio antennas on the train (at the level of the fresh air grids)	71
Figure 56:	Complete overview of the modified control cabinet in carriage TW7 after the initial adjustments	71
Figure 57:	Installation study of SSD in the control cabinet	72
Figure 58:	Example analysis of data recording for October 2015	73
Figure 59:	Data for March 2016 with data gap due to faulty communication between electronic components	73
Figure 60:	Data gap in April 2016 due to scheduled work on the train.....	74
Figure 61:	Data gap in August 2016 due to faulty server communication.....	74
Figure 62:	Signs on the Ts 301 “Freiburg im Breisgau”	75
Figure 63:	Overview of implemented workflow for data processing based on train trips.....	78
Figure 64:	Diagram for the mapping of weather data from the German Meteorological Service to the location of the train	81
Figure 65:	Schematic of the air path in the HVAC system with integrated components and relevant measuring points.....	83
Figure 66:	Temperature curves of the outside ambient temperature for the winter trip (left) and the summer trip (right).....	84
Figure 67:	Number of passengers for the winter trip (left), relative humidity of fresh air during the summer trip (right).....	85
Figure 68:	An example visualisation of the route showing passenger occupancy	85
Figure 69:	Electrically introduced heating capacity during example winter trip.....	86
Figure 70:	Comparison of electrically supplied power at the main heater (black) with power determined on the air side (red) against the time of day in hours	87
Figure 71:	Cooling capacity & electric power consumption in kW	88
Figure 72:	Diagram of a passenger rail vehicle with HVAC system, as well as loads and influencing factors	90
Figure 73:	Diagram of this air-cycle system with the open process air circuit (system 1)	92
Figure 74:	Diagram of vapour cycle system (R134a) with variable-speed compressor and reheating for the low part-load range (system 2)	93

Figure 75:	Diagram of vapour cycle system (R134a) with variable-speed compressor and projected bypass for the low part-load range (system 3)	94
Figure 76:	Diagram of air-cycle system with direct loop	96
Figure 77:	Source data for ICE-T (vapour cycle system) and ICE 3 (air-cycle system)	97
Figure 78:	Investigated ICE 3 central carriage	98
Figure 79:	Scatter diagram of valid data points for the measurements on the ICE 3	99
Figure 80:	Number of operating points from valid train trips, shown per hours of a 24-hour day.....	99
Figure 81:	Investigated ICE-T central carriage	100
Figure 82:	Target temperature (left) and difference between target and actual temperature (right) (absolute value) for ICE-T.....	101
Figure 83:	Scatter diagram of valid data points from the ICE-T data	102
Figure 84:	Schematic for the system comparison of power and energy consumption for the air-cycle system (ACS) on the ICE 3 and the R134a vapour cycle system on the ICE-T ...	104
Figure 85:	Diagram showing classification of the point-by-point measurement data	105
Figure 86:	Classification of measured values for the ICE 3, cooling	107
Figure 87:	Classification of measured values for the ICE-T with reheating, cooling	108
Figure 88:	Classification of measured values for the ICE 3, heating.....	109
Figure 89:	Results of the classification of measured values on the ICE 3 and ICE-T for cooling	110
Figure 90:	Results of the classification of measured values on the ICE 3 for heating.....	110
Figure 91:	Weighting matrix for the share of cooling.....	112
Figure 92:	Reference cities for meteorological data [Google Maps].....	114
Figure 93:	Temperature distributions of three different climatic zones in Germany in comparison (data from DIN 4710, analysis of 24-hour days)	115
Figure 94:	Weighting matrix for the distribution of model input parameters based on a test reference year for Braunlage (cool)	117
Figure 95:	Weighting matrix for the distribution of model input parameters based on a test reference year for Kassel (moderate).....	117
Figure 96:	Weighting matrix for the distribution of model input parameters based on a test reference year for Mannheim (warm).....	117
Figure 97:	Weighting matrix for the distribution of model input parameters based on the field data acquired on the ICE 3.....	118
Figure 98:	Temperature distributions from test reference years of Deutscher Wetterdienst (DWD) for the cities Braunlage and Mannheim compared to DWD data of 2-year period of measurement on ICE 3 2106/2017	120
Figure 99:	Design of the ICE 3 air-conditioning system	125
Figure 100:	Schematic of the ICE 3 air-conditioning system	126
Figure 101:	Compact air-conditioning unit of the ICE 3, 2nd series	127

Figure 102:	Primary power consumption for cooling, comparison for systems with actual measurement data	130
Figure 103:	Primary power consumption for heating, comparison for systems with actual measurement data	130
Figure 104:	Primary power consumption for cooling, comparison for systems with data from models/calculation	131
Figure 105:	Primary power consumption for heating, comparison for systems with data from models/calculation	132
Figure 106:	Comparison of primary annual energy consumption in cooling operation for the air-cycle system ACS (ICE 3) and the vapour cycle system VCS (ICE-T).....	133
Figure 107:	Comparison of primary annual energy consumption in heating operation for the air-cycle system ACS (ICE 3) and the vapour cycle system VCS (ICE-T).....	135
Figure 108:	Comparison of total primary annual energy consumption for the air-cycle system ACS (ICE 3) and the vapour cycle system VCS (ICE-T).....	136
Figure 109:	Comparison of total secondary annual energy consumption for the air-cycle system ACS (ICE 3) and the vapour cycle system VCS (ICE-T).....	139
Figure 110:	Comparison of total primary and secondary annual energy consumption for the air-cycle system ACS (ICE 3) and the vapour cycle system VCS (ICE-T).....	141
Figure 111:	Comparison of the primary annual energy consumption in cooling operation for the air-cycle system (ACS) with direct loop and the vapour cycle system (VCS) with variable-speed compressor and refrigerant bypass	143
Figure 112:	Comparison of primary annual energy consumption in heating operation for the air-cycle system with direct loop and the vapour cycle system with variable-speed compressor and refrigerant bypass.....	144
Figure 113:	Comparison of the total primary annual energy consumption in heating and cooling for the air-cycle system with direct loop and the vapour cycle system with variable-speed compressor and refrigerant bypass	145
Figure 114:	Comparison of the total secondary annual energy consumption for the air-cycle system with direct loop and the vapour cycle system with variable-speed compressor and refrigerant bypass.....	148
Figure 115:	Comparison of the total secondary annual energy consumption for the air-cycle system with direct loop and the vapour cycle system with variable-speed compressor and refrigerant bypass.....	150
Figure 116:	Design of the Cost Assessment Tool (CAT)	151
Figure 117:	Overview for system comparison using the Cost Assessment Tool (CAT)	153
Figure 118:	Source data for the Life Cycle Costs (LCC) model	154
Figure 119:	Comparison A: Total Cost of Ownership – Index determined using the Cost Assessment Tool (CAT)	157
Figure 120:	Comparison B: Total Cost of Ownership – Index determined using the Cost Assessment Tool (CAT)	159
Figure 121:	Programme for the technical discussion of the air-conditioning project, held in Berlin on 25 January 2018	162

List of tables

Table 1:	Comparison A of heating, ventilation and air-conditioning systems (HVAC systems) based on field data	16
Table 2:	Comparison B of advanced heating, ventilation and air-conditioning systems (HVAC systems) based on data from models and simulation	17
Table 3:	Basic formulas for determining the electric power consumption.....	82
Table 4:	Overview of the train trips in winter and in summer, analysed as examples	84
Table 5:	Comparison of temperature distributions of the test reference year with the distribution of the 2-year period of measurement	121
Table 6:	Comparison of the annual maintenance costs of the ICE-T and the ICE 3	128
Table 7:	Comparison of primary annual energy consumption for the air-cycle system (ICE 3) with the vapour-compression refrigeration system (ICE-T)	137
Table 8:	Comparison of the secondary annual energy consumption for the air-cycle system (ICE 3) with the vapour-compression refrigeration system (ICE-T)	138
Table 9:	Comparison of total combined primary and secondary annual energy consumption for the air-cycle system (ICE 3) with the vapour-compression refrigeration system (ICE-T).....	140
Table 10:	Comparison of the primary annual energy consumption for the air-cycle system with direct loop and the vapour cycle system with variable-speed compressor and refrigerant bypass.....	146
Table 11:	Comparison of the secondary annual energy consumption for the air-cycle system with direct loop and the vapour cycle system with variable-speed compressor and refrigerant bypass.....	147
Table 12:	Comparison of the primary and secondary annual energy consumption combined for the air-cycle system with direct loop and the vapour cycle system with variable-speed compressor and refrigerant bypass	149
Table 13:	Annual energy consumption for the Cost Assessment Tool (CAT) related to the reference vehicle, based on the field data	154
Table 14:	Comparison A - Maintenance Cost for the ICE-T and ICE 3 2nd series air-conditioning systems on the reference vehicle according to calculation in the Cost Assessment Tool (CAT).....	155
Table 15:	Comparison B - Maintenance Cost for three optimised air-conditioning systems on the reference vehicle according to calculation in the Cost Assessment Tool (CAT).....	155
Table 16:	Comparison A: Total Cost of Ownership – Index determined using the Cost Assessment Tool (CAT)	157
Table 17:	Comparison B: Total Cost of Ownership – Index determined using the Cost Assessment Tool (CAT)	158

List of abbreviations

3G	Third generation wireless mobile standard
ACS	Air-cycle system
ANN	Artificial neural network
API	Application Programming Interface
Apmzf	Air-conditioned first-class open-plan carriage with lounge (8 seats)
Avmz	Air-conditioned first-class carriage with compartment/open-plan area
BK3	Name of the current air-conditioning system computer from LVF
Bpmbz	Air-conditioned second-class open-plan carriage, wheelchair accessible
Bpmz	Air-conditioned second-class open-plan carriage
Bpmzf	Air-conditioned second-class open-plan carriage with lounge (10 seats)
BRmz	Air-conditioned restaurant carriage
Bvmz	Air-conditioned second-class carriage with compartment and open-plan area
CACU	Compact air conditioning unit
COP	Coefficient of Performance
DB	Deutsche Bahn AG
DWD	German Meteorological Service
EMC	Electromagnetic Compatibility
ENVIRONM	Environmental Cost
EW	End carriage
GPS	Global Positioning System
GSM	Global System for Mobile Communications
GUI	Graphical User Interface
GWP	Global Warming Potential
HVAC	Heating, Ventilation, Air Conditioning
HX	Heat Exchanger
ICE	InterCity Express
LCC	Life-Cycle Costs
LVF	Liebherr-Transportation Systems GmbH & Co KG
MACM	Motorised air-cycle machine/turbomachine
MC	Maintenance Cost
MTBF	Mean Time Between Failures
MVB	Multifunction Vehicle Bus
MW	Central carriage

NRC	Non-Recurring Cost
OC	Operating Cost
PAX	Passengers
PV	Photovoltaics
R&D	Research and Development
RC	Recurring Cost
SSD	Solid State Drive
SW	Converter carriage
TCO	Total Cost of Ownership
TRY	Test Reference Year
TW	Transformer carriage
Ts	Trainset
UBA	German Federal Environment Agency
UMTS	Universal Mobile Telecommunications System
USB	Universal Serial Bus
UNFCCC	United Nations Framework Convention on Climate Change
VCS	Vapour Cycle System
WP	Work package

Summary¹

Energy efficiency and environmental friendliness are today's key topics for heating, ventilation and air-conditioning systems (HVAC systems) in passenger rail vehicles.

Typically, up to 30% of the total energy consumption of a train is for air conditioning (Schmitt & Berlitz, 2014). Consequently, reducing the energy consumption is a powerful lever for reducing the operating costs (energy costs) and the environmental impact of energy supply.

The hydrofluorocarbon (HFC) refrigerants R-134a and R-407C, which are the most common refrigerants used in today's railway air conditioning, have a high direct global warming potential and consequently contribute to global warming. To reduce HFC emissions, the quantity of HFC available on the market has gradually been phased down since 2016 on the basis of the European F-gas Regulation (EU, 2014) with the goal of reaching only 21% of the total quantity stipulated by the EU by 2030.

The reduced availability of HFC refrigerant has already led to drastic increases in refrigerant prices. How the price will develop in the future remains completely uncertain. In addition, the availability of refrigerants has fallen, so that railway operators are also having difficulty procuring the quantities required.

Currently available fluorinated refrigerants with lower GWP, such as those being considered as alternatives for the automotive industry, are not an option for the railway industry because of their flammability or toxicity.

To ensure air conditioning of railway vehicles without limitations in the future, there are only two environmentally friendly alternatives that are sustainable in the long term from today's perspective:

- ▶ Air conditioning systems with air as natural refrigerant (the proven air-cycle system)
- ▶ Air conditioning systems with R744 (CO₂) as refrigerant

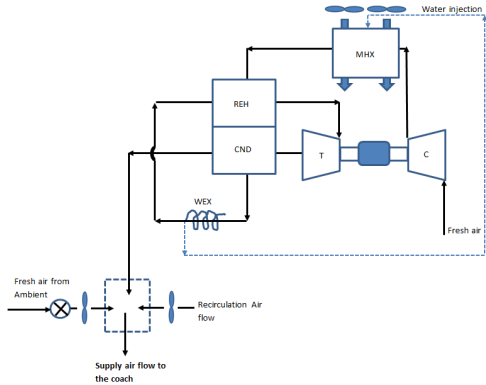
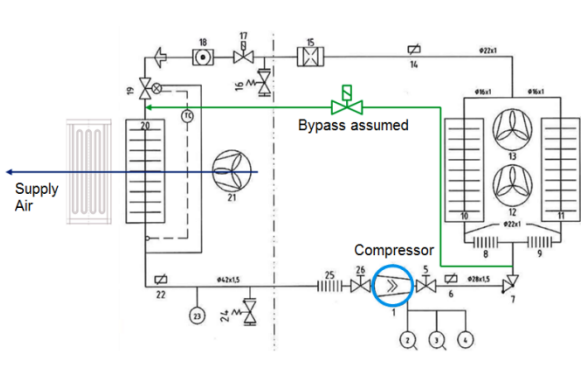
The air-cycle system was the focus of this research project conducted by Liebherr-Transportation Systems, in collaboration with Deutsche Bahn - DB Systemtechnik GmbH and DB Fernverkehr AG, on behalf of the German Federal Environment Agency and funded by the German Federal Ministry for the Environment, Nature Conservation and Nuclear Safety (Claus, 2016). The goal of the project was to determine the energy consumption and the Total Cost of Ownership (TCO) of the air-cycle system and conduct a comparison with systems that use conventional HFC refrigerants - specifically on the basis of measurement data obtained during real-world operation.

The first step consisted of installing additional measurement equipment and systems for collecting and transferring operating data transfer on an ICE 3 train owned by Deutsche Bahn, which had been fitted with new air-cycle systems. Over a period of 2 years while the train was in standard passenger service, operating data were recorded and transmitted to a stationary database. This was followed by extensive processing of the data.

The assessed data were then used to analyse the annual energy consumption of various HVAC systems. The primary annual energy consumption for cooling operation had average savings of 28% across the climate zones under consideration for an air-cycle system with reverse loop (ICE 3) compared to an R-134a vapour cycle system with variable-speed compressor and optional reheating (ICE-T). The advanced air-cycle system with direct loop (simulation) had savings of 16% compared to an improved vapour cycle system with variable-speed compressor and refrigerant bypass (calculation). This shows

¹ This summary has similarly been published in (Luger et al., 2018) and in (Krawanja et al., 2018).

Table 2: Comparison B of advanced heating, ventilation and air-conditioning systems (HVAC systems) based on data from models and simulation

System 6: Air-cycle system (ACS) with direct loop and variable-speed turbomachine	System 3: Vapour cycle system (VCS, R-134a) with variable-speed compressor and refrigerant bypass
<ul style="list-style-type: none"> ▶ Refrigerant: air (natural/environment-friendly) ▶ New optimised Liebherr technology ▶ Data from simulation using the Liebherr software EOLE 	<ul style="list-style-type: none"> ▶ Refrigerant: R134 (high global warming potential) ▶ Bypass assumed for low part-load range (model) ▶ Data derived from the ICE-T field data
	

The system diagrams are inserted here for orientation only, they can be found enlarged and clearly legible in Figures 76 and 75.

Field data were available for the comparison of systems 1 and 2; no field data were available for systems 6 and 3. Therefore, relevant variables for systems 6 and 3 were derived or calculated on the basis of assumptions and models. (Meister, 2012) compared system 1 with system 2. The current comparison follows that of (Meister, 2012) and extends it.

From a technical point of view, there is no difference in terms of heating operation for the four HVAC systems compared here. It was therefore possible to derive the unavailable data for heating operation for systems 2, 3 and 6 from the data for system 1.

When sufficient data are available, it will also be possible to compare a vapour cycle system with the natural refrigerant carbon dioxide (R744).

Analyses and comparisons of power and energy consumption

The electric energy consumption is an essential factor when assessing heating, ventilation and air-conditioning systems (HVAC systems) in terms of economic efficiency and environmental impact. The energy consumption gives rise to operating costs (energy costs) and environmental impact/emissions – to varying degrees depending on the energy mix – due to the energy supply. The different railway HVAC systems were therefore compared in terms of their energy consumption.

The power or energy consumption of a railway HVAC system is the sum of the primary consumption, particularly for heating, cooling and air flow, and the secondary consumption for the drive (traction), which is provided by the vehicle drive. For the primary power or energy consumption, the compressor or turbomachine (depending on system), heater, supply air fan, condenser fan, cooling fan, controller and magnetic bearing controller were taken into account.

The traction required as a result of the mass of the HVAC system was not taken into account because of the relatively small share of the total energy consumption and the low differences in mass between the systems under consideration. The impulse resistance, which is created by the stationary air being drawn into the moving train, has a significantly greater impact on the required traction. The intake air mass flow was taken into account for every system. An analytical approach was used for the investigation.

Data sources

Field data for systems 1 and 2 were prepared, filtered for valid values, and processed with software tools (in particular Python and Matlab). For system 2 (ICE-T), the passenger occupancy was derived from a stationary model for CO₂ concentration in the carriage and process parameters for fresh air supply. For system 1 (ICE 3), the passenger occupancy was counted with optical door sensors. The data stream from the counters was split into individual train journeys for further processing.

The comparison was based on the intersection of available variables and signals for the systems: The two independent input variables, outside temperature and passenger occupancy rate, were mapped onto the output variable, electric power consumption, for cooling in comfort mode. Other relevant factors influencing a railway HVAC system, such as solar radiation, could not be explicitly taken into account. The pre-conditioning and parking modes were not taken into account due to insufficient data.

Methods of comparison

The comparison methodology followed the work of (Meister, 2012) and included the following three steps:

- ▶ Step 1: Classification of the electric power consumption
→ Model of the electric power consumptions of different HVAC systems
- ▶ Step 2: Weighting and summing of the classes for specific operating conditions
→ Average electric power consumption of the HVAC systems
- ▶ Step 3: Scaling to typical number of operating hours/year (6,570 h/year)
→ Electric energy consumption per year of the HVAC systems

Step 1: The electric power consumption values determined for the different systems were classified according to the outside temperature and passenger occupancy. For the outside temperature in °C, 9 classes were used with the class boundaries at {below -5, -5, 0, 5, 10, 15, 20, 25, 30, above 30}. For the passenger occupancy in percent, 3 classes of different ranges were used with the class boundaries at {0, 30, 50, above 50}. The mean power value (arithmetic mean) was calculated for each class.

Step 2: The result of step 1 is a matrix with mean power consumptions in cooling operation and in heating operation, respectively, for different HVAC systems. These matrices were multiplied element-by-element by two types of weighting matrices, and the resulting weighted power values were added together. This results to the

- ▶ Matrix for share of cooling and heating and the
- ▶ Matrix for distribution of the model input parameters of temperature and passenger occupancy.

The matrix for the share of cooling and heating describes the likelihood that cooling or heating operation is within a given class. The matrix was derived from field data for system 1. The matrix for the distribution of model input parameters describes how often specific classes occur under different realistic operating conditions. The matrices for the distribution of model input parameters against temperature distributions were derived from test reference years for the German cities of Braunlage

(cool), Kassel (moderate), and Mannheim (warm), taking realistic operating times in comfort mode from 04:00 to 24:00 hrs into account, as well as data for passenger occupancy from DB. The matrix for class weighting was derived from the frequencies of the field data recorded in this project.

Results of the comparison of electric power consumption

It was clear that passenger occupancy has a much smaller influence on the primary electric power consumption than the outside temperature.

At very high outside ambient temperatures in the range of 35 °C, the primary electric power consumption of the air-cycle systems was significantly higher than the primary power consumptions of the vapour cycle systems. This matches expectations based on theoretical/physical considerations for the respective thermodynamic cycles. But for lower temperatures in the range of, for example, 10 °C or 15 °C, the air-cycle systems were significantly more efficient than the vapour cycle systems. The advantage of energy-efficient part-load control is evident in this range. The key question was then which temperature ranges occur in real-world operation with what frequency.

Results of the comparison of electric energy consumption

The technical difference between the systems comes down to cooling operation. Results of comparison for the primary annual energy consumption in cooling operation are shown in Figure 1 (system 1 compared to system 2) and Figure 2 (system 6 compared to system 3). The results are for comfort mode of the HVAC systems (6,570 operating hours per year), where comfort mode means passenger service. The underlying operating conditions (weighting matrices), in particular the distribution of the outside ambient temperature, affect the result. The temperature distribution during the measurement period shifted to higher temperature levels compared to the temperature distribution of representative years (test reference years), as demonstrated by an examination of the temperature measurement data from the German Meteorological Service. This is reflected in the higher primary annual energy consumption for cooling for the operating conditions "according to the field data", compared to the operating conditions for "cool (Braunlage)", "moderate (Kassel)" and "warm (Mannheim)". In the comparisons with the respective vapour cycle systems, the air-cycle systems show savings in all cases. Depending on the operating conditions, the savings for system 1 compared to 2 are between 21% and 36% and for system 6 compared to system 3 between 5% and 27%.

Assuming that a train is operated with equal frequency in the climate zones (cool (Braunlage), moderate (Kassel) and warm (Mannheim)), the air-cycle system with reverse loop (ICE 3) resulted in average savings of 28% for primary annual energy consumption in cooling operation, compared to a vapour cycle system with variable-speed compressor and reheating option for the low part-load range (ICE-T). The advanced air-cycle system with direct loop (simulation) produces savings of 16% compared to a vapour cycle system with variable-speed compressor and refrigerant bypass (bypass assumed by calculation).

(Meister, 2012) carried out a generally comparable study, but with some different general conditions (operating hours, distributions of model input parameters (weighting matrices), lower limit temperature for the classification, etc.). The absolute figures for the primary annual energy consumption for cooling differed accordingly, while the relative comparisons yielded very similar results.

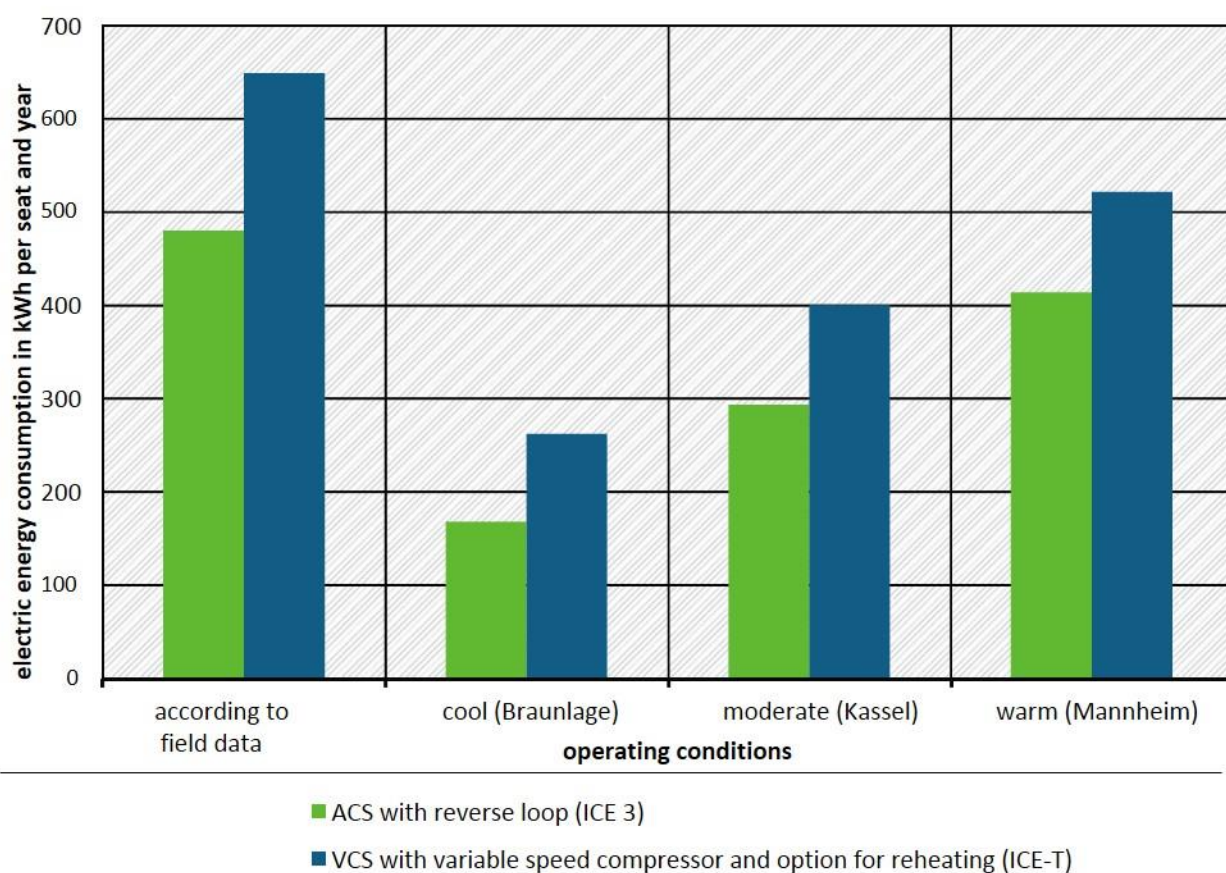
The main reasons for the advantage of air-cycle systems in terms of the primary annual energy consumption for cooling are the result of that fact that the cooling capacity of the air-cycle systems can be efficiently regulated over the entire output range, compared to the vapour cycle systems

considered, and the air-cycle systems have a high proportion of load requirements in the lower performance range in the course of the year for the operating conditions considered.

Significant savings for air-cycle systems in secondary energy consumption for cooling are the result of the lower consumption for intake air of 56% to 59% for system 1 compared to system 2 or of 41% to 46% for system 6 compared to system 3.

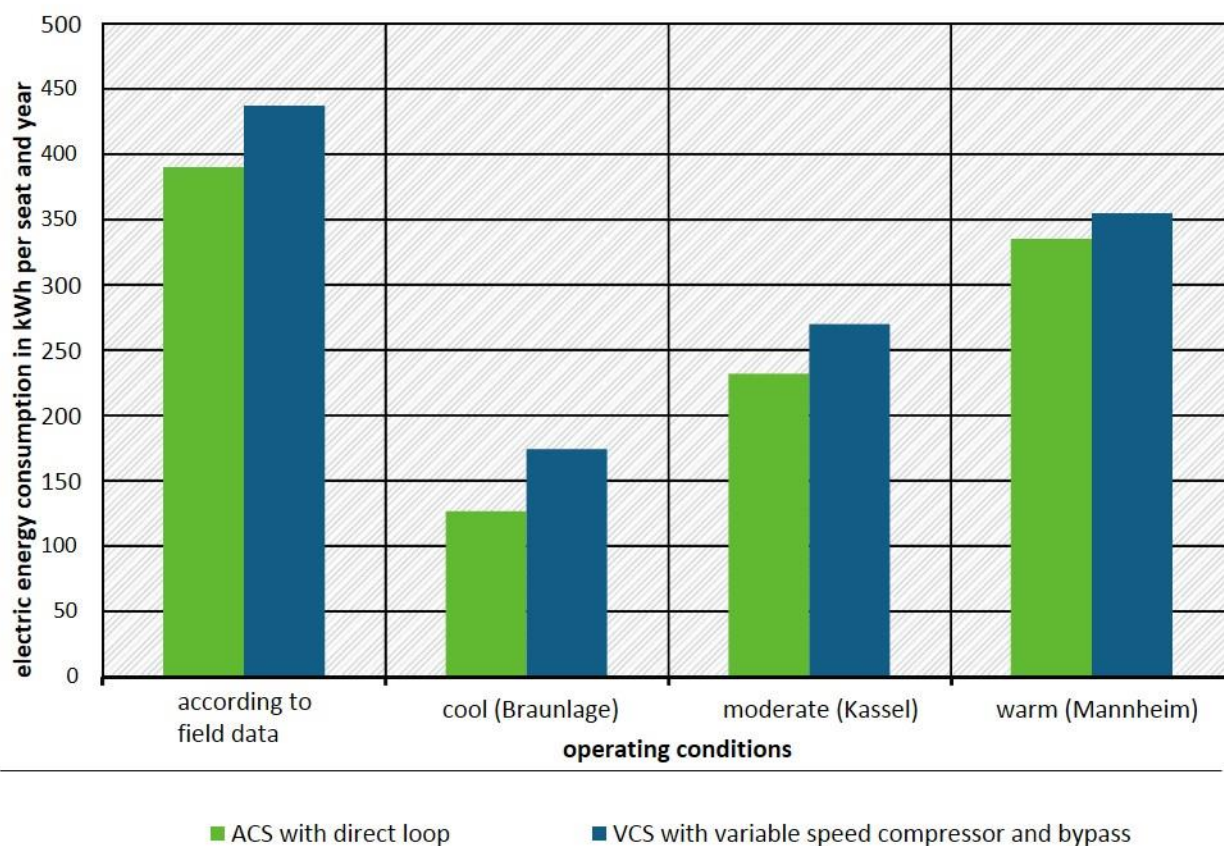
In heating operation, there are no relevant differences between the systems in terms of primary and secondary energy consumption. The savings in cooling operation reduce the total annual energy consumption; the percentage reduction of the total annual energy consumption depends on the ratio of heating and cooling operation in the given year.

Figure 1: Comparison of primary annual energy consumption in cooling operation for the air-cycle system ACS (ICE 3) (system 1) and the vapour cycle system VCS (ICE-T) (system 2)



Annual energy consumption in cooling operation for the air-cycle system (ACS) with reverse loop (based on implementation in ICE 3) and the vapour cycle system (VCS) with variable-speed compressor and option for reheating (based on implementation in ICE-T) (source data: field data); energy consumption is based on 6,570 operating hours in comfort mode per year. Energy consumption is at the device interface, i.e. excluding the efficiency of the on-board power supply up to the pantograph. Source: own illustration, Liebherr

Figure 2: Comparison of the primary annual energy consumption in cooling operation for the air-cycle system (ACS) with direct loop (system 6) and the vapour cycle system (VCS) with variable-speed compressor and refrigerant bypass (system 3)



Comparison of annual energy consumption in cooling operation for the air-cycle system (ACS) with direct loop from simulation with the vapour cycle system with variable-speed compressor (VCS) based on the ICE-T and with projected refrigerant bypass instead of reheating; Energy consumption based on 6,570 operating hours in comfort mode per year; Energy consumption is at the device interface, i.e. excluding the efficiency of the on-board power supply up to the pantograph. Quelle: own illustration, Liebherr

Analyses and comparisons of economic efficiency

Design of the Cost Assessment Tool (CAT)

An extensive cost analysis was performed to compare the economic efficiency of the different HVAC systems. The Cost Assessment Tool (CAT), developed for aviation, was used for this purpose. CAT can be used to compare the costs for different equipment variants on aircraft. The outcome of analysis is the cost over the life cycle of the aircraft ("Total Cost of Ownership") per flight hour that are incurred with the applicable equipment.

When using the CAT for railways, the costs are stated in Euros per year per HVAC system (carriage) against the life cycle of the railway vehicle.

It is possible to compare existing and future systems. Various tools are linked to generate the results.

The input data are taken from cost planning (item for item cost planning) or from the bill of materials, which are used to determine the production costs and the unit weights. Based on the bills of materials,

the Maintenance Cost is determined in the LCC Tool using reliability data for the components and information from the operator about the method of operation and maintenance.

The system simulation relies on the performance data of the components and calculates a forecast of the energy consumption using the operating profile of the vehicle and the climate data.

The result is a distribution of different cost types based on the annual costs per HVAC system for each version of a system considered.

- ▶ RC - Recurring Cost
- ▶ NRC- Non-Recurring Cost (development costs, engineering, prototype production, tests)
- ▶ MC - Maintenance Cost
- ▶ OC - Operating Cost
- ▶ ENVIRONM/Environmental Cost (CO₂ tax, retrofitting for environmentally friendly refrigerant)
- ▶ CAT Index/Sum of all costs per year

In principle, the LCC Tool can also be used to perform a dynamic analysis. Dynamic developments can be investigated by specifying indexes for imputed interest or inflation indexes, in general or separately for energy and environmental costs. In this project, this was treated as neutral, without taking into account imputed interest, development of the equity of the operating company, inflation, or energy price and environmental cost progression.

Comparison of the HVAC systems

It is essential for comparison that identical operating conditions are simulated for the HVAC systems. For this reason, all the systems were based on a reference vehicle, carriage TW7 of trainset 301 (ICE 3, 2nd series) from the field data analysis.

In the first step (comparison A), both of the systems, which have been in operation for many years, were compared or projected onto the reference vehicle:

- ▶ ICE-T (system 2)
- ▶ ICE 3, 2nd series (system 1)

The second step (comparison B) shows a future scenario. In this case, the R-134a vapour-compression refrigeration system and the air-cycle system with the described potential for improvement as well as the next generation air-cycle system technology were compared:

- ▶ ICE-T system concept, energy-optimized (system 3)
- ▶ ICE 3 system concept, maintenance-optimized (corresponds to system 1; however, potential improvements identified during analysis of the maintenance data were taken into account in the maintenance cost model)
- ▶ Next generation air-cycle system, open direct loop (system 6)

Input variables for the analysis of economic efficiency

NRC – Non-Recurring Cost

The development costs were compensated for to ensure a fair comparison of conventional and future technologies, as the development costs for a new technology are not transferred to just one production series or type of carriage. It was assumed that the NRC in the long term would approach €1,000,000 per HVAC system and vehicle type for all systems. The current CAT model is based on a series of 500 carriages, across which the stated NRC is distributed.

RC - Recurring Cost

The manufacturer's recommended prices for the reference vehicle, as expected for the current market, are as follows:

- ▶ RC for vapour cycle system: €40,000 (without refrigerant bypass)
- ▶ RC for vapour cycle system: €41,000 (with refrigerant bypass)
- ▶ RC for ACS reverse loop, analogous to ICE-3, 2nd series: €65,000
- ▶ RC for ACS direct loop, "Next generation ACS": €55,000

The manufacturing costs of air-cycle systems are a little higher than for vapour cycle systems, but the potential for economies of scale has not been taken into account. As demand for air-cycle technology increases and the quantities of corresponding components increases, one would expect a reduction in unit costs.

OC - Operating Cost:

The annual energy consumption according to Table 13 was used to determine the Operating Cost. The Operating Cost for primary energy consumption (operation of the HVAC system) and secondary energy consumption (travel resistance from exchanging air with the environment) was calculated based on an electricity tariff of 11.59 Euro cents/kWh.

MC – Maintenance Cost:

A model showing the corrective and preventive maintenance cost for the reference vehicle based on field data, information from the operating company and the source data from the Liebherr customer service is used to determine the Maintenance Cost.

The input variables are:

- ▶ Operating hours for cooling and heating for the reference vehicle according to the field data analysis
- ▶ Hourly rate of €90/h for work and infrastructure according to the operating company, DB AG
- ▶ Quantity and price of repairs, quantity and price of delivery of spare parts, based on documentation from Liebherr customer service
- ▶ Preventive maintenance according to the system manual

For the new "next generation ACS" with direct loop in comparison B, there are, of course, no data from customer service or the maintenance manual. For this reason, data were taken from the other systems or model values based on the manufacturer's data for analogous components were used. Table 14 shows the Maintenance Cost for the CAT reference vehicle (comparison A), and Table 15 shows the Maintenance Cost (comparison B).

ENVIRONM – Environmental Cost:

In comparison A (retrospective), the Environmental Cost for the vapour cycle system (systems 2 and 4) is calculated based on refrigerant leaks and is made up of the Emission Cost per CO₂ equivalent, refrigerant leaks and costs for filling refrigerant.

- ▶ Total filling quantity: 9 kg R-134a
- ▶ GWP of R-134a: 1430
- ▶ Leaks: 5% per annum
- ▶ Refrigerant price: €36/kg R-134a
- ▶ Emission Cost assessment of refrigerant leaks: €4.55/t CO₂ equivalent*)

Comparison B (future scenario) assumed the system will change to a refrigerant drop-in after 5 years of operation. The selected refrigerant drop-in R-513A (blend of R-1234yf and R-134a) has limited durability and it is assumed that the refrigerant must be replaced every 2 years due to the high number of operating hours in railway operations.

- ▶ Total filling quantity: 9 kg R-134a
- ▶ Changeover to R-513A after 5 years
- ▶ Drop-in, no retrofitting costs required for the HVAC system
- ▶ GWP of R-513A: 547
- ▶ Leaks: 5% per annum
- ▶ Complete replacement of refrigerant every 2 years
- ▶ Refrigerant price: €50/kg R-513A
- ▶ Emission Cost assessment of refrigerant leaks: €4.55/t CO₂ equivalent*)

*) European Union Emissions Trading System (European Energy Exchange AG, 2016).

Since the Emission Cost from electricity generation is already included in the electricity price, the value for the Environmental Cost of the air cycle systems is set at €0.

Result of the analysis of economic efficiency

Costs per annum and HVAC system for tested systems (comparison A):

It is clear that the NRC and Environmental Cost play a secondary role and are practically negligible. The largest share of the costs comes from energy consumption. Although the air cycle system has benefits, they are offset again by the higher Recurring Cost (RC). The Maintenance Cost is about the same for the two systems. The CAT Index, i.e. the sum of the cost components, is within the same order of magnitude for both systems, whereby the air cycle system has a small cost advantage of approx. €200/year.

Breakdown of annual costs for the future scenario (comparison B):

In contrast to comparison A with tested systems, the Environmental Cost for the future scenario is of greater importance. The new vapour cycle system is energy-optimised, i.e. it is at the same level as the air cycle system with reverse loop in terms of energy consumption. However, this improvement is partially offset by the Environmental Cost. The largest share of the costs is still from energy consumption.

For the next generation of air-cycle systems, one would expect improvements compared to today's air-cycle systems in terms of procurement costs and energy consumption, which would result in a cost benefit of approx. €1,000/year compared to state-of-the-art cold vapour systems.

Conclusion and outlook

Air-cycle railway air-conditioning systems are a successfully tested, environmentally friendly and economical alternative to conventional vapour cycle systems with fluorinated refrigerants. For the HVAC systems compared here, which have been in regular passenger service for many years, it is evident that the proven environment-friendly air-cycle technology is at least equivalent in terms of economic efficiency. If the potential for optimisation identified in the course of the study and new developments are exploited, then the air-cycle system is more economically efficient.

The higher investment costs for the air-cycle air-conditioning technology are offset by lower operating costs. In general, investment costs play a subordinate role compared to energy and maintenance costs. They amount to approx. 10% annually for conventional vapour cycle systems and approx. 14% for air-cycle systems.

The primary annual energy consumption in cooling operation has average savings of 28% across the climate zones for an air-cycle system with reverse loop (ICE 3) compared to an R-134a vapour cycle system with variable-speed compressor and optional reheating (ICE-T). By analogy, there are savings of 16% for the advanced air-cycle system with direct loop (simulation) compared to a vapour cycle system with variable-speed compressor and refrigerant bypass (calculation). For the annual energy consumption for cooling operation, the air-cycle technology therefore has a clear advantage.

In the course of the project, additional potential for improvement was identified for the maintenance of the existing system ICE 3, 2nd series. One would expect that the implementation will lead to a significant reduction in costs.

The potential of air-cycle technology is far from exhausted. There is a very positive outlook for the air-cycle air-conditioning of railway vehicles as the architecture is further developed.

1 INTRODUCTION

Emissions of greenhouse gases have to be reduced globally. This is a requirement of international agreements, such as the Montreal Protocol and the Framework Convention on Climate Change (UNFCCC).

Based on these framework agreements, nations around the world have made more and more far-reaching commitments that are intended to reduce greenhouse gas emissions and contribute to climate protection. Particular mention should be made of the Kyoto Protocol (2007), the Paris Agreement (2015) and the Kigali Agreement (2016), in particular for the phasedown of certain hydrofluorocarbons (HFCs). To meet the obligations under these agreements, the European Union has set itself ambitious climate protection targets.

Germany committed to a pioneering role in climate protection at an early stage. By 2050, the emissions of greenhouse gases in Germany are to be reduced by 80% to 95% compared to 1990.

In addition to gases such as carbon dioxide and methane, greenhouse gases also include perfluorocarbons and hydrofluorocarbons. The main field of application for the group of hydrofluorocarbons (HFCs) is refrigeration and air-conditioning systems. The greenhouse effect of HFCs can be as much as 14,800 times higher than that of the same quantity of carbon dioxide.

Air conditioning is now standard for new local public transport vehicles. Consequently, the share of air conditioning and resulting HFC refrigerant emissions from vehicle air-conditioning systems is increasing. The refrigerant emissions from buses and railway vehicles in Germany was 124 tonnes of R134a refrigerant in 2016, which is equal to 179,000 tonnes of CO₂ equivalents. In addition, CO₂ emissions arise from energy consumption for cooling and heating.

The use of hydrofluorocarbons (HFCs) must decrease drastically in the future. The applicable HFC bans and the reduction of the HFC quantities with an high impact on global warming are stipulated by the European Regulation (EU) No. 517/2014 on fluorinated greenhouse gases. In 2030, only 21% of the CO₂-equivalent quantities of HFCs for the year 2015 shall enter the European market. The Kigali Agreement requires a further reduction of HFCs by industrialised nations to 15% by 2036.

The European F-gas Regulation on fluorinated greenhouse gases (EU) No. 517/2014, which has been in effect since 1st January 2015, does not contain a specific ban on HFCs for air conditioning units in local public transport vehicles, such as railway vehicles or buses. However, HFCs have already become more expensive and scarce today due to the phase-down regulations of the F-gas Regulation. Thus, all users of HFCs now have to make an effort to find alternatives.

However, the development and testing of alternative air-conditioning concepts in local public transport vehicles has been very slow worldwide so far. Even Germany has very few documented examples and little experience in air conditioning for local public transport vehicles using natural refrigerants, which could convince operating companies to acquire such technologies on a large scale.

Air-cycle systems based on air compression as well as compression refrigeration circuits with the refrigerant carbon dioxide (CO₂; refrigerant designation R744) are promising alternative technologies for railway vehicles. Depending on the technology used, greenhouse gas emissions from refrigerants can be avoided or drastically reduced by using environmentally friendly, natural refrigerants. Similarly, energy consumption could be reduced by applying optimisation measures or new technical approaches to heating.

1.1 Task

The objection of the project was to provide scientifically valid evidence about the viability and practical suitability of alternative air-conditioning concepts in railway vehicles. For this purpose, innovative air-conditioning concepts for railway vehicles using environmentally friendly, natural refrigerants suitable for railway applications in real-world operation should be investigated in the project.

In railway vehicles with state-of-the-art air-conditioning systems cooling with natural refrigerants, a program for measurement during regular train operation should be designed and implemented. Measurements should be taken at least once over all seasons, including the heating period. The test vehicles and air-conditioning systems had to be provided by the contractor. It was to be ensured, that the test vehicles operated on rails for the time period required for the measurements.

The data obtained has to be analysed and used to make statements about the efficiency of the air-conditioning systems, including analysis over the life cycle. A comparison has to be made with commonly used existing air-conditioning systems with conventional hydrofluorocarbon refrigerants (HFCs).

Based on the results, requirements specifically for standard passenger service for the future development of air-conditioning systems should be identified.

1.2 Requirements for the project

Air (standard refrigerant designation R729) is currently a well-suited natural refrigerant for use in air-conditioning systems for railway vehicles, of which there is the longest practical experience.

However, air-cycle systems (ACS) are at a significant disadvantage compared to other systems in terms of investment costs because of high development costs and the still low number of units to date. Demonstrating the cost benefit for the operating company over the operating time of the system could provide important impetus for further introducing air-cycle systems.

The different systems cannot be compared in the lab, as real operating conditions cannot be replicated adequately. The operating and ambient conditions on the track, such as air temperature, solar radiation, air humidity, air pollution, shading, operating times, trips through tunnels, occupancy, travel speed, voltage interruptions, network performance, etc., together make up an operating and load profile that has a decisive influence on the performance and service life of the air-conditioning system. In-the-field operating profiles are therefore essential for extensive comparisons of air-cycle systems with vapour cycle systems (VCS). They can also provide indications for further development.

After a total of 13 trains in the ICE 3 second series had been fitted with air-cycle systems from 2004, Deutsche Bahn AG (DB) once again appointed Liebherr-Transportation System GmbH & Co KG (LVF) in October 2014 to equip an ICE 3 train with air-cycle systems in the course of the redesign of the ICE 3 first series. This provided the opportunity to fit the train and the new air-cycle systems with measurement equipment to create an extensive operating profile in real-world train service for the first time. Working with DB, the Total Cost of Ownership (TCO) was analysed by tracking the maintenance activities.

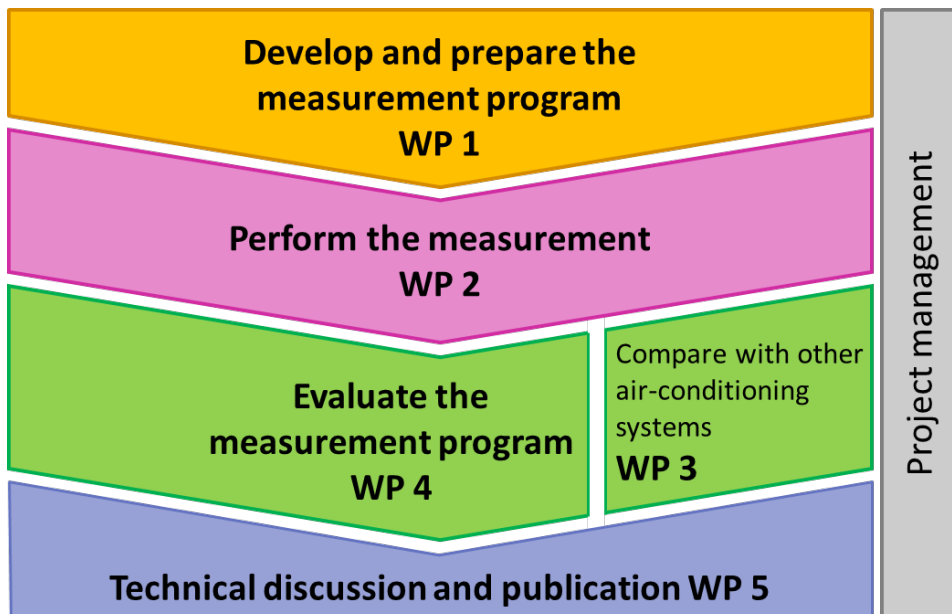
1.3 Project design and workflow

The project was divided into five work packages (WP):

- ▶ WP 1: Develop and prepare the measurement program
- ▶ WP 2: Perform measurement
- ▶ WP 3: Compare with other air-conditioning systems
- ▶ WP 4: Evaluate the measurement program
- ▶ WP 5: Technical discussion and publication

The work packages fell into three project phases: preparation of the measurement campaign, collection of measurements and evaluation with comparable analyses, and discussion of the results. The project structure is shown in Figure 3.

Figure 3: Work packages in the project structure



Work packages in the project structure. Source: own illustration, Liebherr

The content of the individual work packages is briefly described below. Completion of the work packages and the corresponding results are described in detail in section 2.

1.3.1 WP 1: Develop and prepare the measurement program

A measurement program was designed for standard passenger service that records all the parameters required for statements about the efficiency of the air-conditioning systems. The system for recording the necessary data in service was designed and developed. The sensors and data storage were installed in air-conditioning systems and train and checked to ensure they were functioning correctly.

1.3.2 WP 2: Perform measurement

The measurements on the train were performed as planned from the beginning of 2016 until the end of 2017.

1.3.3 WP 3: Compare with other air-conditioning systems

Since no parallel measurement could be performed on the same or a similar train for comparison with state-of-the-art air-conditioning systems, DB provided data from earlier measurements from an R134a air-conditioning system on an ICE-T train.

1.3.4 WP 4: Evaluate the measurement program

The data obtained in work packages 2 and 3 were analysed, compared and assessed. In the process, the results were obtained for energy consumption and the Total Cost of Ownership.

1.3.5 WP 5: Technical discussion and publication

In January 2018, a technical discussion was held in Berlin with the German Federal Environment Agency (UBA). This was where LVF and DB presented and discussed the results of the project. The presentations at the technical discussion can be found on the UBA website²

1.3.6 Schedule

The schedule is shown in Figure 4. All work packages (WPs 1 to 5) were processed as planned within the project timeframe. WP 1 was extended because the measurement equipment needed to be improved. For details, see section 2.

Figure 4: Scheduling

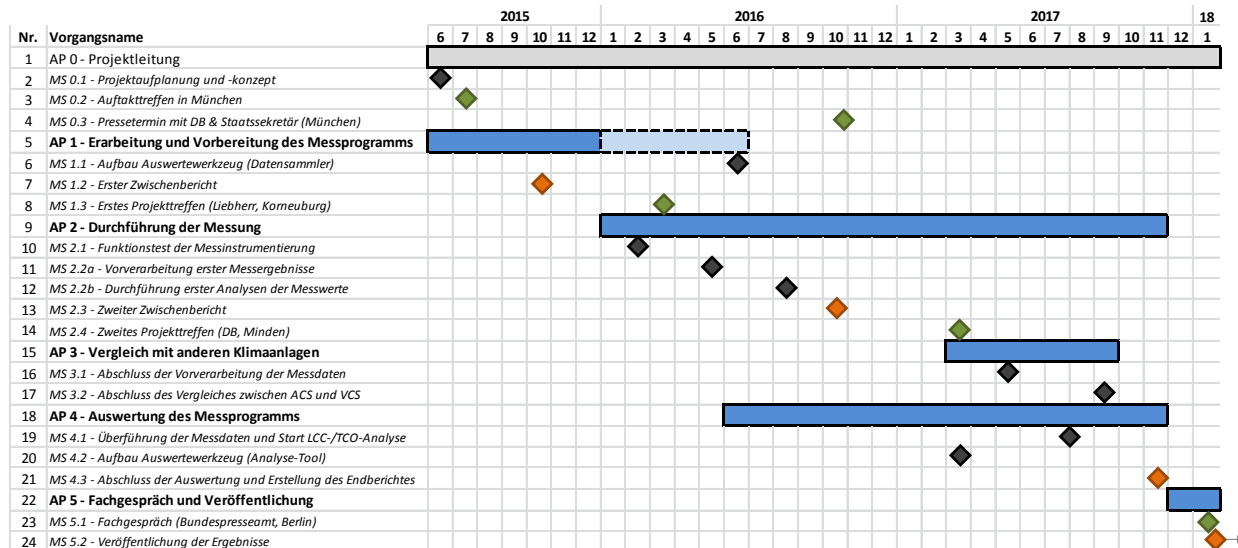


Illustration of the timeline. Source: own illustration, Liebherr

On 27 October 2016, a press conference was held at the ICE plant in Munich with Deutsche Bahn (DB), Liebherr-Transportation System GmbH & Co KG (LVF) and the German Federal Ministry for the Environment (BMU) to introduce the project to the public. Jochen Flasbarth (State Secretary at the BMU) and Ronald Pofalla (Board of DB) were updated on the status of the project on the ICE 3

² <https://www.umweltbundesamt.de/service/termine/fachgespraech-klimatisierung-von-zuegen>, 12/03/2018

“Freiburg im Breisgau” itself and discussed the need for new air-conditioning solutions. Press releases were also published by BMU³ and LVF⁴. A sign on the train provided details of the project. Below are two photos from the event.

Figure 5: Photo of press conference in Munich on 27 October 2016



Ronald Pofalla (Deutsche Bahn, left) and State Secretary Jochen Flasbarth (BMUB, right) next to the ICE 3 “Freiburg im Breisgau” in front of the sign on the train with information about the project. Source: Copyright Deutsche Bahn AG/ Uwe Miethe

Figure 6: Photo of press conference in Munich on 27 October 2016



Participants of BMUB, DB and LVF listen to the technical introduction on the roof of the ICE 3 at the opened air-conditioned air conditioning system at the press conference. Source: Copyright Deutsche Bahn AG / Uwe Miethe

³ <https://www.bmub.bund.de/pressemitteilung/klimaanlagen-ohne-fluorierte-treibhausgase/>, 13/03/2018

⁴ <https://www.liebherr.com/de/deu/aktuelles/news-pressemitteilungen/detail/umweltstaatssekret%C3%A4r-jochen-flasbarth-und-bahnvorstand-ronald-pofalla-informieren-sich-%C3%BCber-testprogramm-an-luftgest%C3%BCtzte-klimaanlagen-news.html>, 13/03/2018

1.4 Scientific and technical status before the start of the project

The two air-conditioning technologies for air refrigerant and the fluorinated refrigerant R134a, which were the subject of the investigation, have been in use at Deutsche Bahn for several years. Both types of system are installed in the vehicle roof of high-speed trains.

Air-conditioning systems with air refrigerant are used in first and second series ICE 3 trains.

Air-conditioning systems with R134a refrigerant are operated on DB's ICE-T, as well as on most other ICE trains. The two systems and how they operate are explained in more detail below.

1.4.1 Compact air-conditioning unit on the ICE 3 (air)

Figure 7 shows the pre-assembled air-cycle compact air-conditioning unit (CACU) developed by Liebherr-Transportation Systems (LVF). The manufacturer describes the system as the air-cycle System Heating, Ventilation, Air Conditioning (ACS HVAC), or simply ACS.

Figure 7: Air-cycle compact air-conditioning unit for the ICE 3

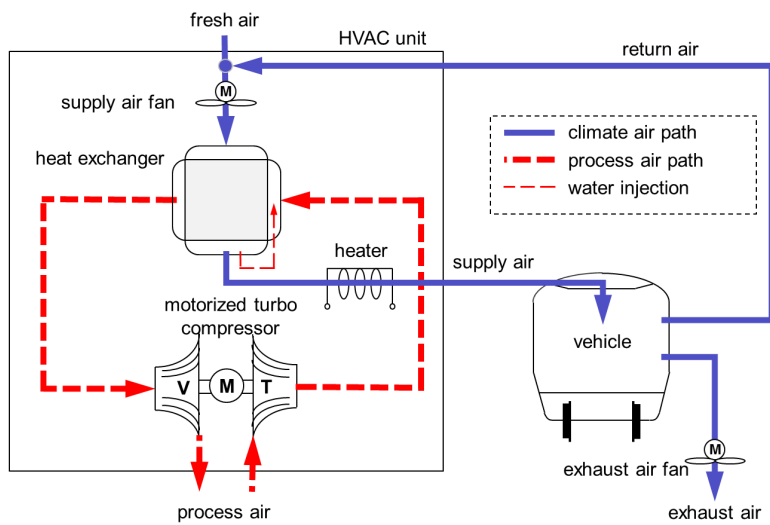


Air-cycle compact air-conditioning unit on transport frame and without cover. Source: own illustration, Liebherr

This system uses air as refrigerant. The fresh air is cooled in the system in an independent circuit. This process air uses a heat exchanger to indirectly cool the conditioned air, which air conditions the passenger compartment and comes into contact with the passengers. The circuits are shown in Figure 8.

Air-cycle systems have been in use at Deutsche Bahn since 2000.

Figure 8: Schematic of air-conditioning and process air circuit

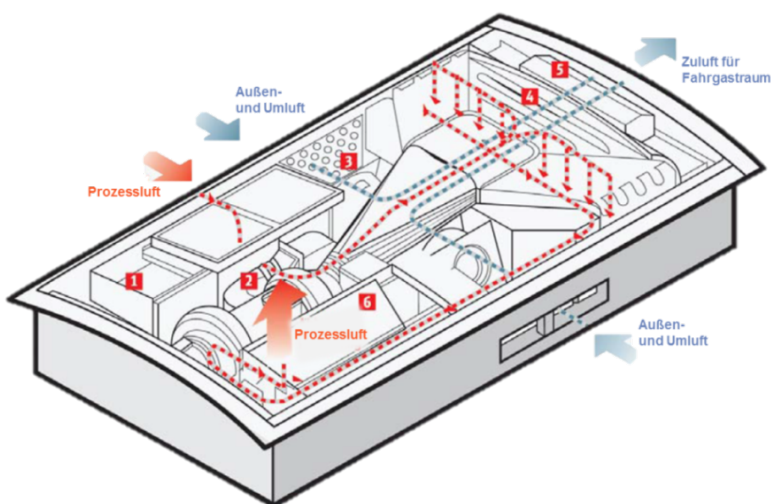


Schematic of air-conditioning circuit (blue) and process air circuit (red) (motorised air-cycle machine consists of compressor (V), motor (M) and turbine (T)). Source: own illustration, Liebherr

The air ducting within the air-cycle compact air-conditioning unit (CACU) is shown in Figure 9 with the main components:

1. Process air inlet box
2. Motorised air-cycle machine (MACM, turbomachine)
3. Supply air fan
4. Heat exchanger
5. Main heater
6. Process air outlet box

Figure 9: Air ducting in the compact air-conditioning unit



1 - Process air inlet box, 2 - Motorised air-cycle machine, 3 - Supply air fan, 4 - Heat exchanger, 5 - Main heater, 6 - Process air outlet box. Source: own illustration, Liebherr

The operating principle of the air-cycle compact air-conditioning unit (CACU) is also illustrated in Figure 9. The process air is drawn in from the outside via the process air inlet box (1) of the motorised air-cycle machine (MACM, 2).

In the MACM, the process air is cooled by lowering the pressure and directed to the heat exchanger (4) via the process air duct. From there, it flows from top to bottom and cools the supply air. The heated process air is fed to the connection socket via a piping system with sound absorber, drawn in by the MACM and released to the environment via the process air outlet (6). A cooling air fan guides a cooling airflow over the synchronous motor of the MACM, which is then released to the environment at the cooling air outlet.

The supply air fans (3) draw the air from the mixed air boxes and feed the air to the heat exchanger, which is installed underneath the process air duct. The supply air is then either cooled by the cold process air or heated by the main heater (5). The conditioned supply air is then blown further into the supply air duct system over the supply air sound absorber.

The air-cycle machine (MACM) is driven by a synchronous motor with variable speed control. This provides continuous control of the cooling capacity.

As part of a commercial trial for a redesign of ICE trains by DB in 2015, on an ICE 3, class 403, 1st series, trainset 301, in all carriages (total of eight), one of the air-cycle compact air-conditioning units shown in Figure 9 was installed.

Figure 10: ICE 3 – class 403, trainset 301 of Deutsche Bahn AG



Two ICE 3 class 403, Source: Copyright Deutsche Bahn AG / Claus Weber

Figure 11 and Figure 12 show the eight carriages of the trainset (Ts) 301. The individual carriage types are:

- ▶ EW – End carriage
- ▶ TW – Transformer carriage
- ▶ SW – Converter carriage
- ▶ MW – Central carriage

Figure 11: Carriage overview of the first half train ICE 3 - class 403 Ts 301(carriages 1 to 4)



Complete overview of the first half of the train (carriages 1 to 4). Source: (Deutsche Bahn AG, Fahrzeuglexikon für den Fernverkehr 2016, 2017)

Figure 12: Carriage overview of the second half train ICE 3 - class 403 Ts 301 (carriages 5 to 8)



Complete overview of the second half of the train (carriages 5 to 8). Source: (Deutsche Bahn AG, Fahrzeuglexikon für den Fernverkehr 2016, 2017)

1.4.2 Air-conditioning system on the ICE-T (R134a)

For comparison in this project the air conditioning unit developed by Liebherr-Transportation Systems GmbH & Co KG (LVF) for the ICE-T was used. An image of the uninstalled system is provided in Figure 13.

This system is a conventional vapour-compression refrigeration system – it is also referred to as a vapour cycle system (VCS). The refrigerant is a hydrofluorocarbon with the refrigerant designation R134a, the chemical name of which is 1,1,1,2-tetrafluoroethane.

This system type has been in use at Deutsche Bahn since 1999.

Figure 13: Air-conditioning unit ICE-T - Compression refrigeration system with the refrigerant R134a



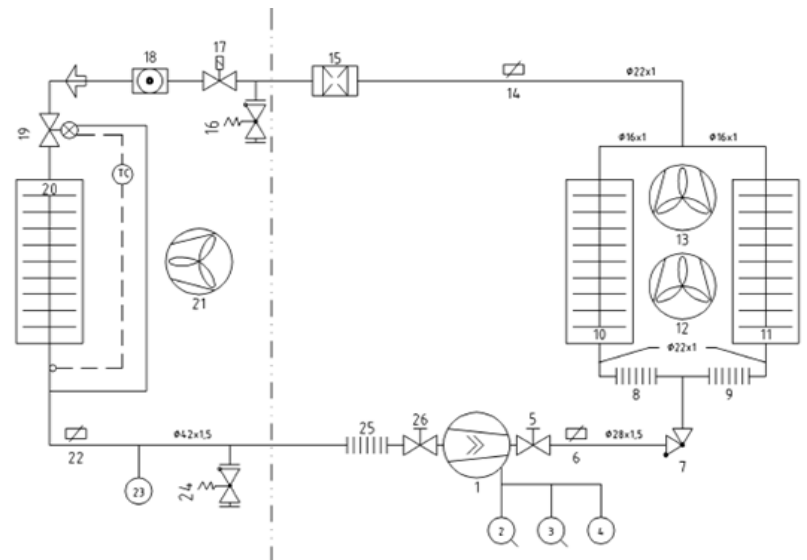
ICE-T air-conditioning unit in transport frame and without cover. Source: own illustration, Liebherr

The operating principle of the VCS air-conditioning unit is described below. The comments in parentheses refer to Figure 14.

The refrigerant compressor (1) draws in the gaseous refrigerant and compresses it. Compressing also increases the temperature of the refrigerant. The refrigerant flows into the heat exchangers (condensers, 10 and 11), where it transfers the heat to the condenser air and liquefies it at high pressure. The condenser fans (12 & 13) draw air through the condenser upwards into the open.

The liquid highly-pressurised refrigerant in the refrigerant circuit reaches the expansion valve (19) after additional components, where the refrigerant depressurises to the evaporation pressure and cools in the process. The expansion valve controls the refrigerant supply to the evaporator (20). In the second heat exchanger (evaporator, 20), the refrigerant evaporates and the heat required for evaporation is taken from the air flowing over the evaporator. The gaseous refrigerant then passes into the compressor again at low pressure.

Figure 14: Schematic of the refrigeration circuit and components of the compression refrigeration system with the refrigerant R134a



1 - Refrigerant compressor, 10 & 11 - Heat exchangers (condensers), 12 & 13 - Condenser fans, 19 - Expansion valve, 20 - Heat exchanger (evaporator), 21 - Supply air fan, the heater is not shown here, see figure 76. Source: own illustration, Liebherr

The capacity of the refrigeration system is controlled by frequency control of the compressor in the range from 25 to 80 Hz. When the minimum frequency of the compressor is reached, the system produces too much cooling capacity for low cooling demand, which requires reheating by the heater.

Figure 15 shows the seven carriages of the ICE-T, i.e. this train features one carriage fewer than the ICE 3 with eight carriages (see Figure 11 and Figure 13).

The resulting differences in terms of passenger occupancy and annual energy consumption were taken into account for comparison of the systems.

Figure 15: Carriage overview of the ICE-T train for comparison





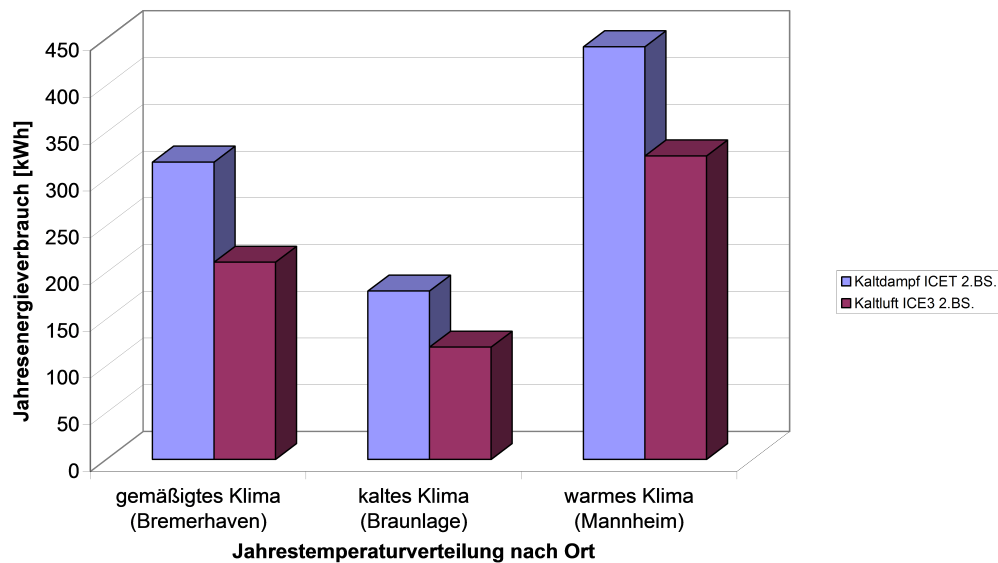
Overview of the seven carriages of the ICE-T train for comparison, source (Deutsche Bahn AG, Fahrzeuglexikon für den Fernverkehr 2016, 2017)

1.4.3 Previous measurements to determine energy consumption

Before this project, DB Systemtechnik GmbH had carried out an investigation of the energy consumption. (Meister, 2012) performed comparative operating measurements to determine the energy consumption of air-conditioning systems with the air and R134a refrigerants. The ACS and VCS air-conditioning systems described in the sections 1.4.1 and 1.4.2 were compared. In 2008 and 2009, the power consumption and relevant operating parameters were recorded in the field for these air-conditioning systems. A basis for comparison was established and the annual energy consumption in cooling operation was determined for the two HVAC systems.

Based on the comparison of the thermodynamic properties of both refrigerants, (Meister, 2012) originally expected a higher energy efficiency for the R134a system across the entire output range. However, overall the observation by (Meister, 2012) showed that the annual energy consumption of the air-cycle system is lower than the vapour cycle system with conventional refrigerant, as shown in Figure 16. For the ICE 3 system (ACS), (Meister, 2012) identified a saving in annual energy consumption for cooling operation of 26% (Mannheim) to 34% (Bremerhaven) compared to the ICE-T system (VCS). (Meister, 2012) lists the following reasons for this: “the cooling capacity that is adjustable over the entire output range of the ICE 3 system, the control concept of the ICE-T system in the low-end load range and the generally high share of low load requirements over the course of the year”.

Figure 16: Annual energy consumption for cooling generation per seat according to previous study



Source: (Meister, 2012)

The study by (Meister, 2012) is the basis and reference for the present study in many areas. In particular, the field data used by (Meister, 2012) for the VCS system on an ICE-T were also used in this study. Regarding the comparison methodology (classification, weighting of classes), the present study is modelled on the work by (Meister, 2012).

In this study, however, the analyses for comparison go significantly further and the approaches by Meister have been further developed. Specifically, the study by (Meister, 2012) did not investigate economic efficiency. An investigation of economic efficiency is an important contribution by the present study. Besides the analysis of the ACS and VCS system as by (Meister, 2012), this study also compared advanced/optimised ACS and VCS systems.

Regarding power and energy consumption, the key differences between the study by (Meister, 2012) and the present study are described in section 2.3.3.7. Particular mention should be made of the investigation of cooling and heating (instead of examining the cooling only), the use of other and more up-to-date source meteorological data (test reference years) and consideration of typical operating times in comfort mode, the new source data for ACS and the comparison based on the operating profile (train trips) according to the field data acquired in the course of this study.

1.5 Collaboration with other project partners

Liebherr-Transportation Systems GmbH & Co KG, as the contractor, was responsible for the overall execution of the project and brought in Deutsche Bahn (DB) as sub-contractor for this purpose.

The key points regarding the allocation of responsibilities among the three project partners are broken down below.

Liebherr-Transportation Systems GmbH & Co KG

- ▶ Build and provide the compact air-conditioning unit (CACU)
- ▶ Create the measurement program (concept)
- ▶ Install additional measurement equipment
- ▶ Record and analyse the data
- ▶ Analyse the Total Cost of Ownership in collaboration with DB
- ▶ Discuss and coordinate the methodology and results

DB Systemtechnik GmbH

- ▶ Analyse and provide the Operating Cost of DB
- ▶ Support analysis of measurement results
- ▶ Provide the data for comparison vehicles and maintenance data
- ▶ Discuss and coordinate the methodology and results

DB Fernverkehr AG

- ▶ Provide the train
- ▶ Install the compact air-conditioning unit (CACU)
- ▶ Provide support for installation of measurement equipment
- ▶ Discuss and coordinate the methodology and results

Several work meetings were held between these three project partners over course of the project. In addition, there were three project meetings of the project partners with the UBA, a press conference and discussion event with additional representatives of the parties involved in the project and a final technical discussion to present the results.

2 DETAILED PRESENTATION OF THE PROJECT

This section provides a detailed description of the measures and results for the individual work packages (WP). The objective is briefly explained at the beginning of each WP. For chronological reasons, the analysis of the measurement results on ICE3 – class 403, Ts 301 (WP4) is discussed first before the comparison with other systems (WP3).

For this reason, the arrangement of the WPs in this section is as follows:

- ▶ WP 1: Develop and prepare the measurement program
- ▶ WP 2: Perform measurement
- ▶ WP 4: Evaluate the measurement program
- ▶ WP 3: Compare with other air-conditioning systems
- ▶ WP 5: Technical discussion and publication

2.1 Develop and prepare the measurement program (WP1)

The first work package (WP 1) involved preparing all other WPs for this project to acquire field data for the air-cycle system. The measuring concept was created as part of this work package and coordinated with the operating company (Deutsche Bahn AG), the measurement equipment was installed, commissioned and tested, and an assessment concept was prepared.

The installation of the required measurement and data recording equipment was successfully completed by the end of 2015. From June to December 2015, all the measurement equipment and associated sensors were installed and tested on various dates in collaboration with Deutsche Bahn. During this period, measured values were already being recorded and, if usable, were used for the analysis in WP 4 (see section 2.3).

However, there were still some issues with the measurement equipment that required modifications and repairs, which are described in more detail in sections 2.1.5 and 2.2.2. The resulting availability of the data is shown graphically in section 2.2.2.

Given these necessary adjustments and repairs, WP 1 was completed in June 2016.

2.1.1 Measuring concept

In order to record the energy consumption of the air-cycle compact air-conditioning unit (CACU) in ICE3 – class 403, Ts 301 and show it against freely selectable parameters, a measuring concept was developed based on three areas for data collection.

The first set of data is the data that are generated by control of the CACU and stored in the air-conditioning system computer (BK3) for each unit (overall, there are eight CACUs). The second set of data is the data that can be read out from the train's fieldbus (MVB). The third set of data is from additional sensors and measuring devices installed in CACU No. 4 and in carriages TW7 and TW2.

This made it possible for the measurement equipment to read out and save all relevant air-conditioning data for the two half trains (transmitted via the MVB) at intervals of ten seconds. The values on the air-conditioning system computer were also recorded – also every ten seconds per half train.

The following values were additionally recorded once for the entire train:

- ▶ Relative humidity and temperature of outside air (fresh air)
- ▶ Position, direction and speed of the train (via GPS)
- ▶ Solar radiation (on the left and right on the roof of TW7)

As well as:

- ▶ Relative humidity and temperature of inside air (recirculated air in TW7 and TW2)
- ▶ Passenger occupancy of carriage TW7
- ▶ Barometric air pressure inside the train

All the data and information collected by the MVB Gateway, the BK3 and the additional sensors were collected on an additional measuring computer (also a BK3), assigned unique time stamps, and stored locally in log files. Each half train then carried out an hourly transfer via GSM USB modem and via mobile telecommunications network to stationary devices at the contractor LVF, where the data were then processed further (see section 2.1.5).

The additional installed sensors and measurement equipment are described in the following sections.

2.1.2 Preparation of additional measurement equipment

After completing the preliminary theoretical work and preparations and preparing the measuring concept, procurement or development and production of the hardware for measurement data acquisition then followed. Among other things, this included designing the connection points of the data acquisition system to the air-conditioning system and to the air-conditioning system of the vehicle.

Figure 17 shows the compact air-conditioning unit (CACU) No. 4 complete with the additional sensors and GPS, for carriage TW7. The individual elements are described in detail in the following sections.

Figure 17: Positions of installed sensors and connections on the compact air-conditioning unit No. 4 in the roof of ICE 3 – carriage TW7



Positions of GPS and installed sensors for solar radiation, air humidity/temperature and their connections on the compact air-conditioning unit No. 4 in the roof of ICE 3 – carriage TW7. Source: own illustration, Liebherr

Luftfeuchte=air humidity

It was possible to install some of the additional measurement equipment at the plant of the contractor LVF, other devices had to be installed on site in Ts 301 or connected with the systems already installed in CACU No. 4 and wired to the control cabinet.

2.1.2.1 Temperature and humidity of fresh air

Since the eight compact air-conditioning units (CACU) were manufactured as new by the contractor Liebherr-Transportation Systems GmbH & Co KG (LVF) for trial operation at Deutsche Bahn (DB), it was possible to adapt a CACU to the measuring requirements before integrating it into the carriage.

To determine the temperature and relative humidity of the air outside the train, a combined humidity/temperature sensor was installed in the process air inlet box (see Figure 18). As the system draws in process air from the environment, the sensor at this position is in a continuous stream of air, as long as the motorised air-cycle machine (MACM) is running.

Figure 18: Position of the temperature and humidity sensor in the compact air-conditioning unit



Position of the temperature and humidity sensor in the compact air-conditioning unit. Source: own illustration, Liebherr

Installing the sensor required revising the design drawing for the CACU and changes had to be made to the installation sequence. The sensor was then wired, the appropriate length of the cable was installed in the unit and prepared for connection to the control cabinet of carriage TW7.

2.1.2.2 Temperature and humidity of recirculated air

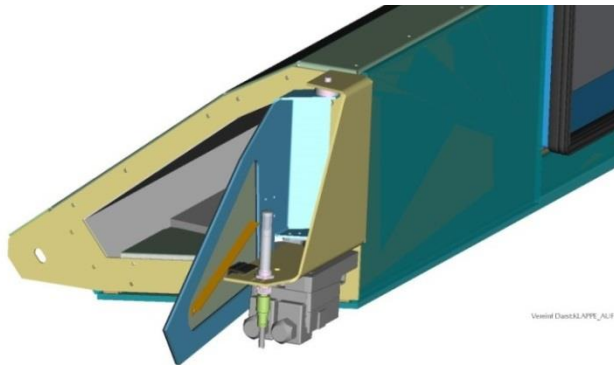
It was very important for the evaluation of the measurements to know the temperature and humidity of the recirculated air before it is returned to the compact air-conditioning unit (CACU). Although temperature sensors are located in the carriages, which were also assessed, the interior humidity was not recorded in any carriage so far.

For this reason, the same type of combined humidity/temperature sensor, as used to measure the temperature and relative humidity of the air outside of the train, was also used to measure the relative humidity and temperature inside the carriage. The sensors were installed in carriages TW7 and TW2. As a second-class carriage with 74 seats, the TW7 is nominally the most densely occupied; TW2 with 32+16 seats is nominally the least densely occupied.

It was decided to place the sensors at the inlet of the mixed air box to measure the relative humidity and temperature in the airflow of the returning recirculated air, before the recirculated air is mixed in the mixed air box with fresh air from the outside and becomes the new supply air for the passengers. This provided information about the current air situation in the carriage.

Figure 19 shows an installation study for the sensor in front of the recirculated air flap in the mixed air box. The sensor can be seen in the centre of the image, upright, with connection in green.

Figure 19: Graphical representation of the position of the temperature and humidity sensor in the recirculated air



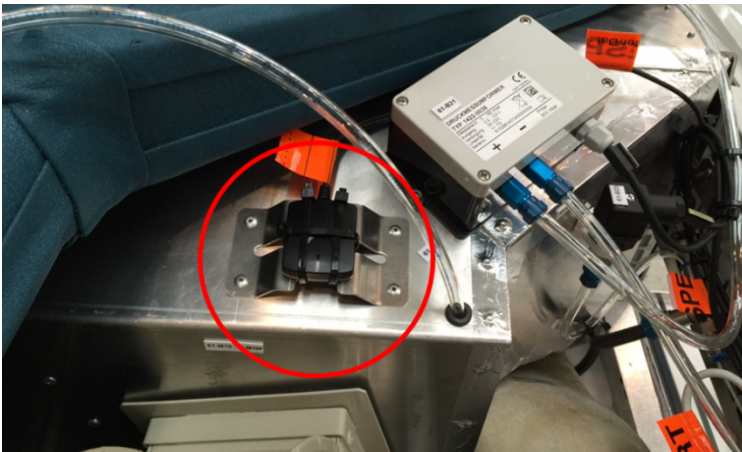
Graphical representation of the position of the temperature and humidity sensor in the recirculated air. Source: own illustration, Liebherr

2.1.2.3 Position, speed and direction of the train

As it was important for the planned assessment and, in particular, for comparison with local weather data, to know the position of the train and also the speed, a GPS module was procured and installed in the compact air conditioning unit (CACU) No. 4 (Figure 20). The GPS module can determine the coordinates, direction and speed of the train.

The CACU design drawing had to be revised to install the GPS and the assembly had to be modified. It was also necessary separately to design, draw, and manufacture a special sheet metal bracket and install it in the unit. The optimum cabling had to be determined as well, as the signals are transferred via USB, but the signal strength can travel only a short cable length. Ultimately, a cable length was found that met the requirements. The cable was prepared in advance for connection to the control cabinet of the TW7.

Figure 20: GPS module including sheet metal bracket installed in the compact air-conditioning unit



GPS module including sheet metal bracket installed in the compact air-conditioning unit. Source: own illustration, Liebherr

Where the GPS sensor is located has a significant impact on the reception of the satellite signals. After some deliberation, a position was finally found for the GPS in the unit, where the sensor is only covered by the cover of the CACU. As the cover is made of fibre glass, the signal does not deteriorate significantly.

2.1.2.4 Solar radiation

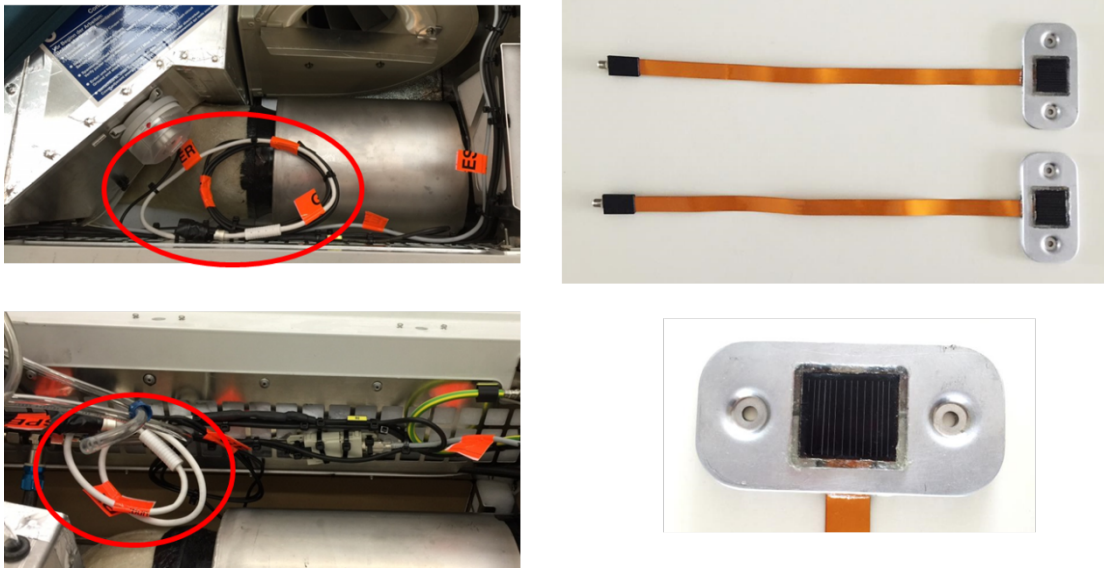
Another significant issue is the heat input from solar radiation. It is important to know the ratio of radiation and ambient heat in particular for control of the air-conditioning system. Hence, two solar sensors (photovoltaic cells or PV cells) were installed on the roof of the train on the frame of the compact air conditioning unit (CACU) No. 4.

Three PV cells were procured for this purpose. Two of these cells were converted to mountable units. A coaxial ribbon cable was soldered on for this purpose and each cell was provided with a load resistor. A special bracket was also designed and manufactured, which consists of three parts and is used to mount the PV cell and as the mounting base on the frame of the CACU.

The soldered cells were then secured on the bracket in a two-component adhesive bath. The cable ends of both sensors matched the prepared connection points in CACU No. 4, as shown in Figure 21.

Figure 21 shows the finished solar sensors and their connection points in CACU No. 4. The final installation of the solar sensors on the roof of the TW7 is described in detail in section 2.1.3.4.

Figure 21: Solar sensors: Two prepared connection points for the solar sensors (left), the two solar sensors with cable ends (top right), one individual solar sensor (bottom right)



Solar sensors: Two prepared connection points for the solar sensors (left), the two solar sensors with cable ends (top right), one individual solar sensor (bottom right). Source: own illustration, Liebherr

2.1.2.5 Control cabinet

For analysis of the measurement data of all sensors as well as the additional data from the fieldbus (MVB) and the air-conditioning system computer, it was necessary to install additional measurement equipment in the control cabinets of carriages TW2 and TW7, which is installed separately from the compact air-conditioning unit (CACU) in the applicable carriage of the train. Each CACU has its own control cabinet.

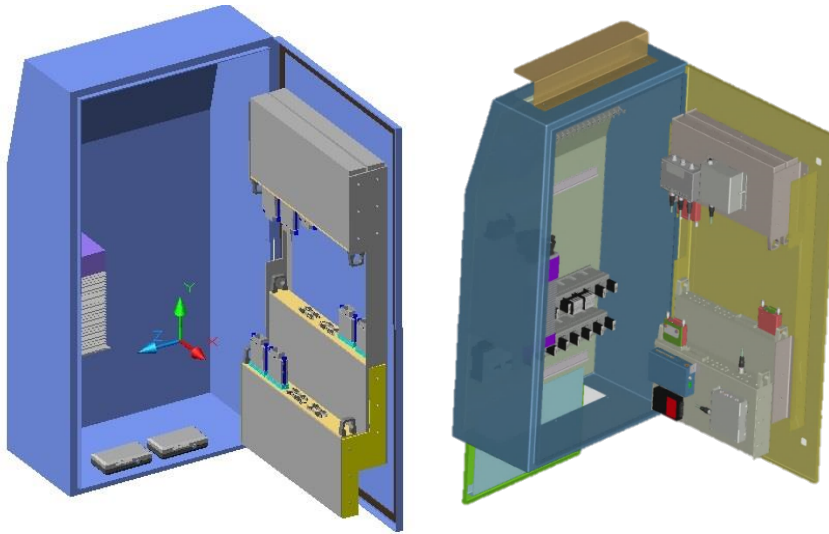
The integration of additional large components into each control cabinet proved to be a major challenge, as the available installation space is very limited and the additional measurement equipment creates additional heat input, which must not affect the proper functioning of the air-conditioning control system under any circumstances.

For these reasons, various installation studies were conducted with the necessary modules to identify a possible means of installation (see Figure 22).

The additional components to be integrated were:

- ▶ Air-conditioning system computer (BK3) for data acquisition and processing
- ▶ MVB Gateway for acquiring the data from the fieldbuses (MVB) of the half trains
- ▶ Counter to count occupancy in the TW7 carriage
- ▶ Barometric air pressure sensor to measure the air pressure inside the train (in carriage TW7 only)
- ▶ Additional temperature sensor to monitor the temperature in the control cabinet as a safety measure
- ▶ Ethernet switch for data acquisition connection
- ▶ USB hub to connect to the GPS sensor
- ▶ GSM USB modem for data transfer directly on the air-conditioning system computer BK3 with additional antenna
- ▶ Voltage supply for the additional sensors in the compact air-conditioning unit (CACU) and control cabinet

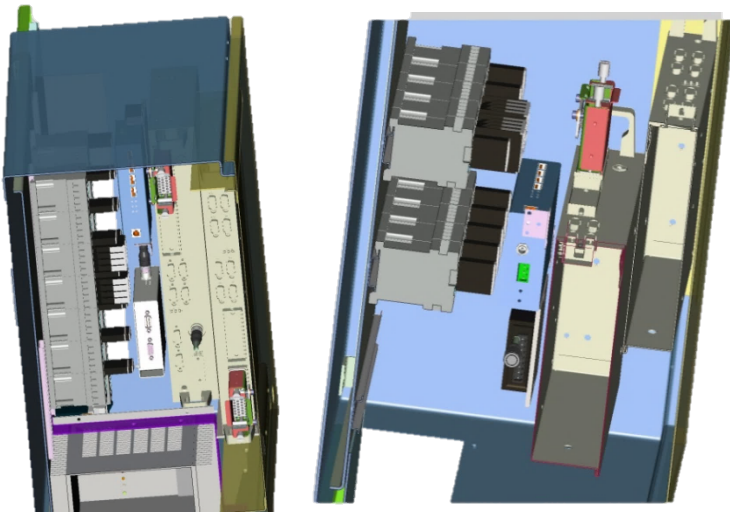
Figure 22: Installation studies for the additional measurement equipment in the control cabinet for the compact air-conditioning unit in carriage TW7



Installation studies for the additional measurement equipment in the control cabinet for the compact air-conditioning unit in carriage TW7. Source: own illustration, Liebherr

The following figure shows the high density of all units in the available installation space in the control cabinet with the planned modules.

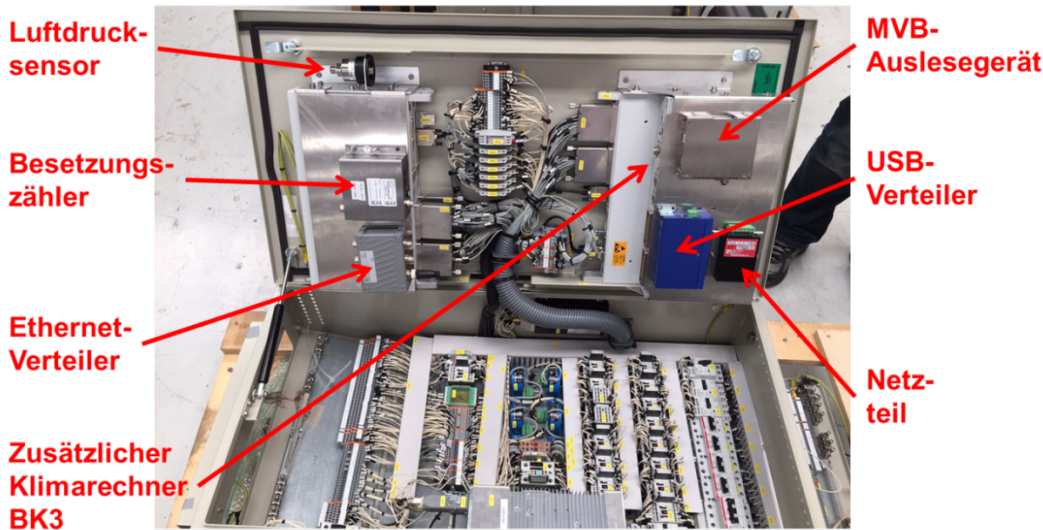
Figure 23: Installation space studies for the additional measurement equipment in the control cabinet



Installation space studies for the additional measurement equipment in the control cabinet. Source: own illustration, Liebherr

The solution found in the installation studies still had to be tested using a real control cabinet. For this purpose, two large-surface sheet metal brackets were designed and manufactured to support the listed additional components. The result was two control cabinet modules. One module with air pressure sensor, counter and Ethernet switch was installed in the upper part of the control cabinet. A second module was installed in the lower part of the control cabinet with the additional air-conditioning system controller BK3 under the bracket and the MVB Gateway, the USB hub and the voltage supply on the bracket (see Figure 24).

Figure 24: Test installation of the additional measurement equipment (modules) in the control cabinet (on side)



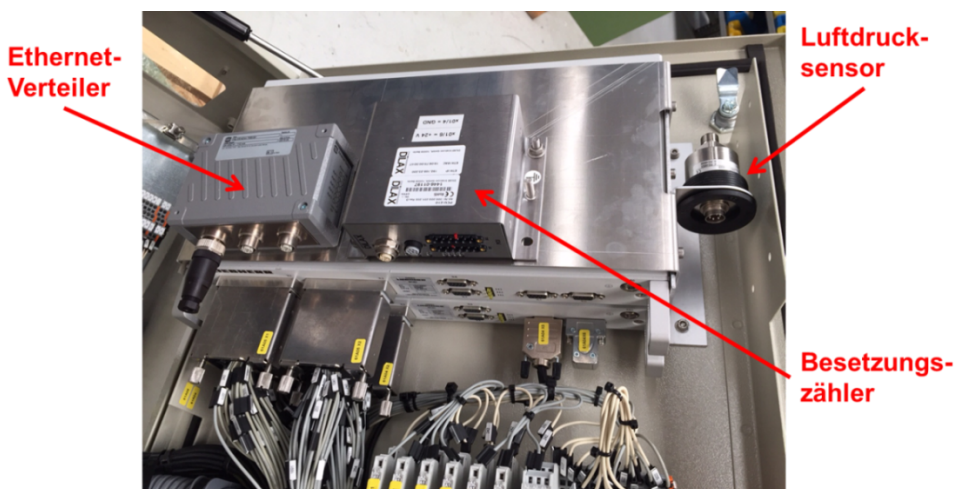
Test installation of the additional measurement equipment (modules) in the control cabinet (on side). Source: own illustration, Liebherr

Luftdrucksensor=air pressure sensor; Besetzungszähler=occupation counter; Ethernet Verteiler= Ethernet switch; Zusätzlicher Klimarechner BK3=additional air conditioning controller BK3; MVB Auslesegerät= MVB gateway; USB Verteiler=USB hub; Netzteil=voltage supply

The test installation of the two modules showed that installation in the control cabinets of carriages TW7 and TW2 is possible in principle. The cabling of the control cabinet could not be taken into account for the test installation, as the work could only be performed directly on the train (see Figure 31). The cabling is described in more detail in section 2.1.3.1.

Figure 25 shows the upper control cabinet module during test installation on the inside of the control cabinet door.

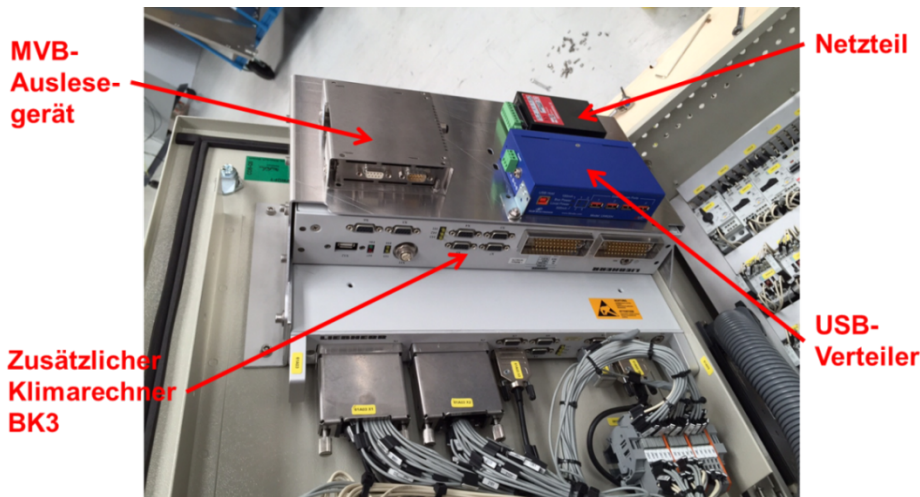
Figure 25: Ethernet switch (left), barometric air pressure sensor (right) and occupancy counter unit (centre) – test installation



Ethernet switch (left), barometric air pressure sensor (right) and occupancy counter unit (centre) – test installation. Ethernet Verteiler=Ethernet switch; Luftdruck sensor=air pressure sensor; Besetzungszähler=occupation counter, Source: own illustration, Liebherr

Figure 26 shows the lower control cabinet module during test installation on the inside of the control cabinet door.

Figure 26: MVB (fieldbus) reader (top left), additional air-conditioning system computer (BK3, bottom centre), power supply of sensors (top right) and USB hub (bottom right) – test installation



MVB (fieldbus) reader (top left), additional air-conditioning system computer (BK3, bottom centre), power supply of sensors (top right) and USB hub (bottom right) – test installation. Source: own illustration, Liebherr

MVB Auslesegerät=MVB gateway; Zusätzlicher Klimarechner BK3=additional air conditioning controller BK3; Netzteil=power supply; USB Verteiler=USB hub

After successful installation of the modules in the limited available installation space inside the carriage control cabinets, a solution had to be found for the increased heat input in the control cabinet from the waste heat of the additional components.

To prevent the measurement instrumentation from causing any interference of the normal process and to detect and, if possible, prevent possible risks for temperature-sensitive components them, an additional simple temperature sensor was installed inside the control cabinet and its temperature values were recorded. This sensor is shown in Figure 31 in section 2.1.3.1 (silver-coloured measuring head on brass-coloured screw bracket suspended in the control cabinet, marked in red).

2.1.3 Installation of measurement equipment

The installation phase for the eight compact air-conditioning units (CACUs) in trainset Ts 301 of ICE3 – class 403 was used to fit the additional measurement equipment.

After the eight CACUs were installed in the train (see Figure 27), the additional sensors were installed in the control cabinets, i.e. in carriages TW7 and TW2, on the roof of TW7 and in/on the compact air-conditioning unit No. 4. To carry out the extensive retrofitting, several additional visits to the DB plant in Nuremberg lasting several days were necessary.

The separate installation phases are explained and described separately below.

Figure 27: Compact air-conditioning unit No. 4 installed in the roof of carriage TW7 of ICE 3 – class 403



Compact air-conditioning unit No. 4 installed in the roof of carriage TW7 with additional sensors and cabling (marked in orange). Source: own illustration, Liebherr

The figure above shows the compact air conditioning unit (CACU) No. 4 installed in the roof of carriage TW7 and the roof platform necessary for this purpose. The orange markings indicate the additional measurement instrumentation. The frame of the CACU/the transition to the carriage roof is identified with yellow adhesive tape. The cables in the foreground on the right side were subsequently routed into the carriage and to the control cabinet.

2.1.3.1 Installation of control cabinet modules

The modules that were previously assembled in the test installation were finally assembled on site in the train. Figure 28 shows the lower module for installation in the control cabinet in carriage TW7.

Figure 28: Control cabinet module with measurement equipment for carriage TW7 of ICE 3 – class 403



Control cabinet module with measurement equipment for carriage TW7. Source: own illustration, Liebherr

The components installed on the sheet metal supports were then secured in the control cabinets using screw fasteners, fitted with the necessary cable connections and wired. The cable connections were soldered on site for permanent connection.

Figure 29 and Figure 30 show the two control cabinet modules as installed.

Figure 29: Installed and connected top control cabinet module in carriage TW7 of ICE 3 – class 403



Installed and connected top control cabinet module in carriage TW7. Source: own illustration, Liebherr

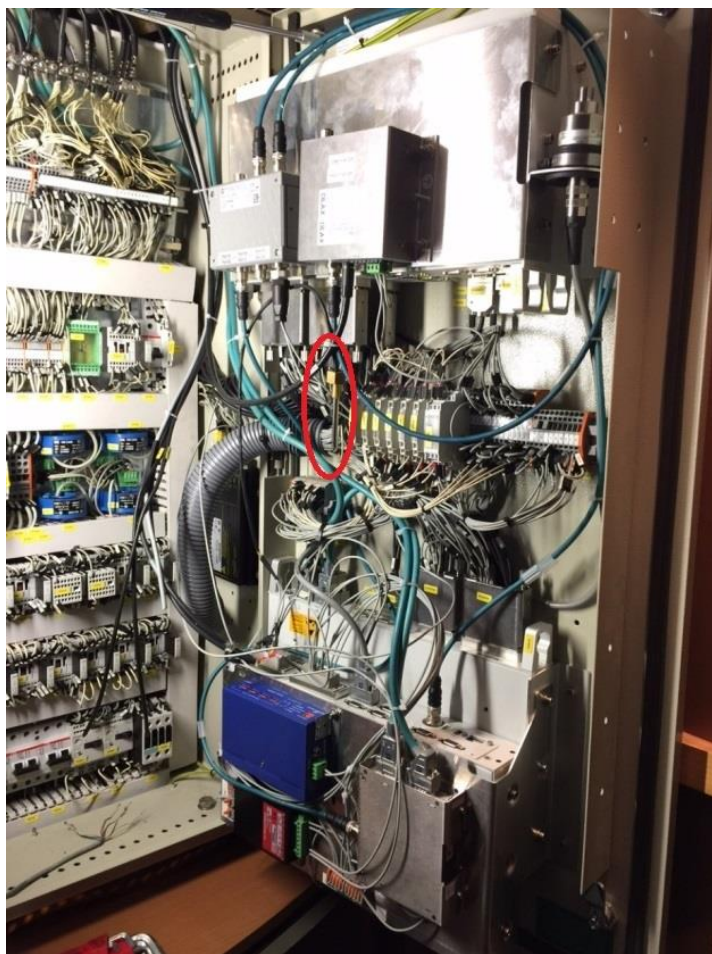
Figure 30: Installed and connected bottom control cabinet module in carriage TW7 of ICE 3 – class 403



Installed and connected bottom control cabinet module in carriage TW7. Source: own illustration, Liebherr

Figure 31 shows the TW7 control cabinet equipped with all the modules.

Figure 31: Control cabinet with the two additional modules on the door and cabling in carriage TW7 of ICE 3 – class 403

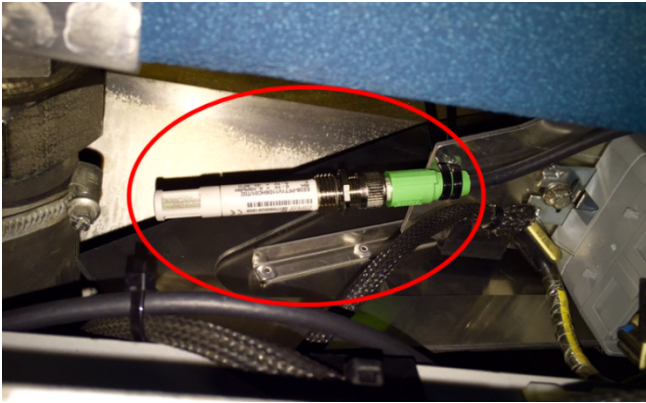


Control cabinet with the two additional modules on the door and cabling before the first function test (temperature sensor marked in red). Source: own illustration, Liebherr

2.1.3.2 Installation of temperature and humidity sensors

One combined humidity/temperature sensor each was installed in front of the inlet to the mixed-air box in carriages TW7 and TW2 (Figure 32). These sensors were checked at the DB plant in Nuremberg to ensure they were fully functional before installation of the measurement equipment.

Figure 32: Installed temperature and humidity sensor in ICE 3 – class 403, carriage TW2 (same as TW7)



Installed temperature and humidity sensor in TW2 (same as TW7). Source: own illustration, Liebherr

2.1.3.3 Installation of occupancy counter

Various options were available to determine the occupancy of the train. They ranged from weight on axles, analysis of the reservation system, to counting by a conductor up and CO₂ control (sensor). A technology that is already used in railway technology at some entrances and/or compartment doors was chosen, involving the recording passengers as they pass through both large entrances in carriage TW7. Boarding and alighting were recorded at both doors (see Figure 33).

The system then calculates the difference between boarding and alighting to determine the current occupancy of the carriage and saves this value in a log file. This was done in TW7 as a proxy for the whole train, as procuring and installing these sensors in all the carriages of the train would have been expensive. In general, it can be assumed that only minor changes will occur in the relative occupancy of the carriages on a long-distance train with just a few stops and longer runs.

The four sensors (two each per door/passage), the cable and the counting device were procured and installed in the roof by Deutsche Bahn (DB) in the Nuremberg plant. This is shown in Figure 33.

Then, using the software supplied, a brief function test of the sensors was carried out on-location and concluded successfully. The causes for initial minor inaccuracies in recording were identified and corrected during another meeting on site.

Figure 33: Installed sensors for occupancy counting in the passages of carriage TW7 (top left and right) and a single sensor (bottom left).

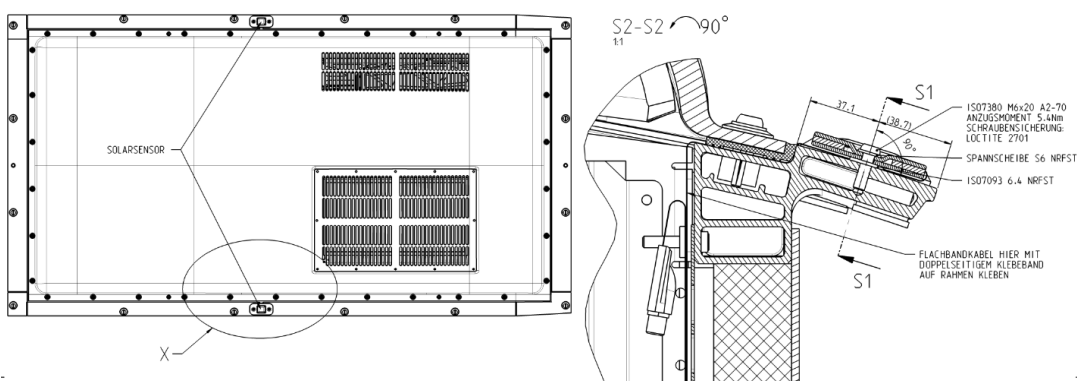


Installed sensors for occupancy counting in the passages of carriage TW7 (top left and right) and a single sensor (bottom left). Source: own illustration, Liebherr

2.1.3.4 Installation of solar sensors

To record the solar radiation, the two solar sensors described in section 2.1.2.4 were attached to the frame of the compact air-conditioning unit (CACU) No. 4, as per the following drawing (Figure 34). This positioning of the sensors had to be planned very precisely because of the frame design, as can be seen in Figure 34. The cables were then routed into the unit and connected to the previously prepared connectors.

Figure 34: Installation drawing for the two roof sensors (solar radiation)



Installation drawing for the two roof sensors (solar radiation). Source: own illustration, Liebherr

As the frame has a slightly falling angle on both sides, the sensors were able to detect the radiation in the entire space over the train and on the sides. The sensors delivered a voltage of up to 4 V, which was recorded by the system. To obtain not just qualitative information about the solar radiation, but also the best possible quantitative information, a correlation between the voltage and the radiation

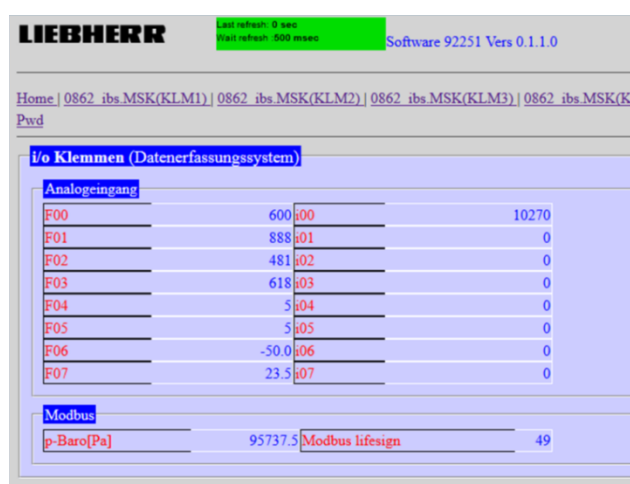
output in W/m^2 was established by using a third photovoltaic (PV) cell. This is described in more detail in the next section.

2.1.4 Calibrating the measurement equipment

After completing installation of the additional measurement equipment, an initial check and calibration were performed on site. To readjust the future procedure, the data transmission modems (GSM modems) were activated in carriages TW7 and TW2 and the data connection was established via the GSM network. Wireless communication proved to be very stable, where the mobile telecommunications network showed corresponding network coverage.

Figure 35 below shows the analogue inputs of the sensors to be calibrated on the air-conditioning system computer BK3.

Figure 35: Screen for calibrating the analogue inputs in carriages TW7 and TW2



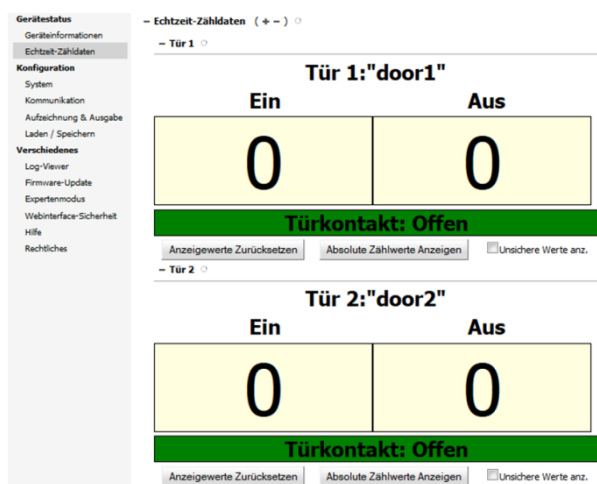
Screen for calibrating the analogue inputs in carriages TW7 and TW2. Source: own illustration, Liebherr

The signal inputs of the solar cells were activated and checked. The solar cells were then checked for humidity and temperature and, once signal reception was successful, an offset (compensation value) was set. The values obtained in this way were compared on site against a calibrated thermometer and confirmed. The pressure sensor was also activated and integrated into data acquisition. These sensors were of such high quality that further calibration was not necessary.

The last step for the additional measurement instrumentation involved incorporating the occupancy counter into the system. The supplied software (Figure 36) was used to activate the sensors. Recording of occupancy was then checked in several passages with real people. In the process, it was necessary to make several adjustments in order to obtain an initial, satisfactory result. These settings were initially kept.

However, real-world use showed that minor deviations in occupancy counting were still occurring. This was compared against a reference system from the manufacturer and confirmed. To obtain the required accuracy, additional modifications were made to the occupancy counter.

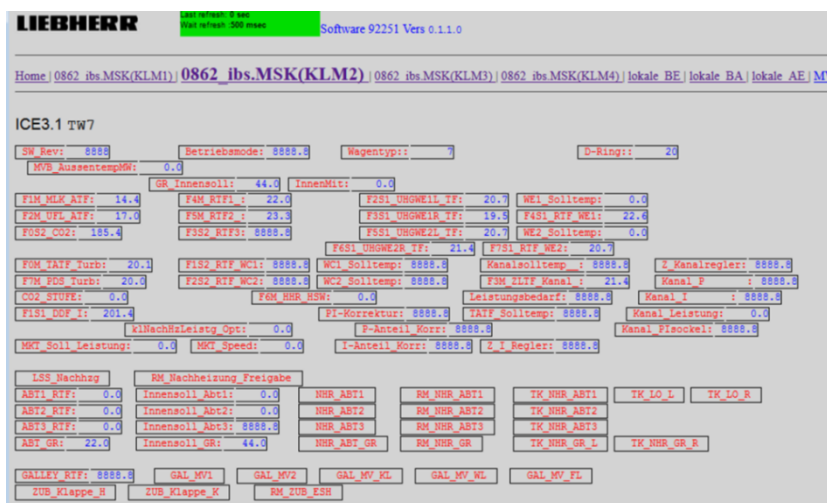
Figure 36: Screen for calibrating and checking the occupancy counter



Screen for calibrating and checking the occupancy counter. Source: own illustration, Liebherr

The next phase of calibration involved linking the data of the fieldbus (MVB) to the additional air-conditioning system computer BK3, which was used to record and process the measured values. For this purpose, the data of the MVBs in the four carriages of a half train were combined and supplied to the applicable air-conditioning system computer BK3 via cable. The BK3 could now monitor four carriages each on one screen (Figure 37). It is very important for the analysis that the time stamps of both recordings of the BK3s in each half train are synchronized. This was ensured by corresponding calibration.

Figure 37: Screen for checking the read MVB (fieldbus) data



Screen for checking the read MVB (fieldbus) data. Source: own illustration, Liebherr

After completing this measure, all connections were checked again and the completeness of incoming signals was also verified. The two access points of the modems on the two air-conditioning system computers (BK3) could now be used to access all four carriages of each half train and open the relevant air-conditioning data per carriage from each air-conditioning system computer, the fieldbus of the train (MVB) and the additionally installed sensors – and also remotely via GSM network.

Online access to current values was also set up, which were recorded at ten-second intervals. This mode of access to current values was not available continuously, as it depended on the reception of both GSM modems. Online access was used primarily for communication with the measurement equipment and to check that the sensors were working (failures, etc.), so continuous availability was not absolutely necessary. Excerpts from online monitoring are shown in Figure 38 and Figure 39.

Figure 38: Online access to the additional measurement data (excerpt from the display screen)

ICE3.1 TW7, lokale Sensorik				
T Frischluft [°C]	14.9	Phi Frischluft [%]	83	
T Umluft [°C]	21.5	Phi Umluft [%]	53	
Solar 1	5	Solar 2	314	
T Schaltschrank [°C]	34.5	ICE726		
p-Baro [mbar]	983			ZugNr
Personen	38			

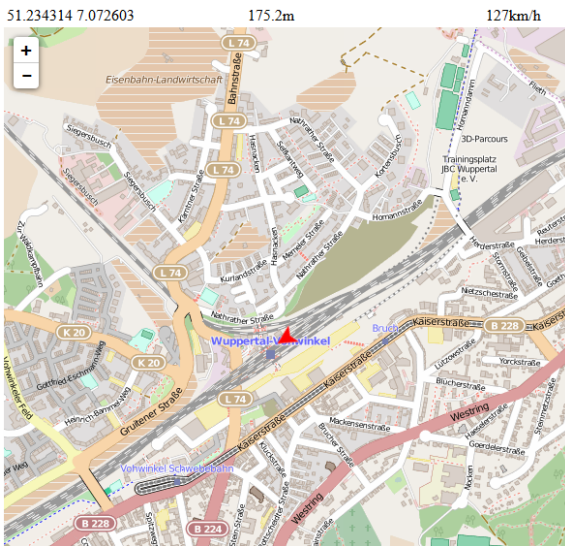
tech detail: doors

00 door(0).in:	43	01 door(0).out:	45
02 door(1).in:	47	03 door(1).out:	36
04 Pers:	38	06 uptime:	6151

ICE3.1 TW2, lokale Sensorik			
T Frischluft [°C]	-39.6	Phi Frischluft [%]	0
T Umluft [°C]	20.3	Phi Umluft [%]	52

Online access to the additional measurement data (excerpt from the display screen). Source: own illustration, Liebherr

Figure 39: Online access to the position and speed of the train



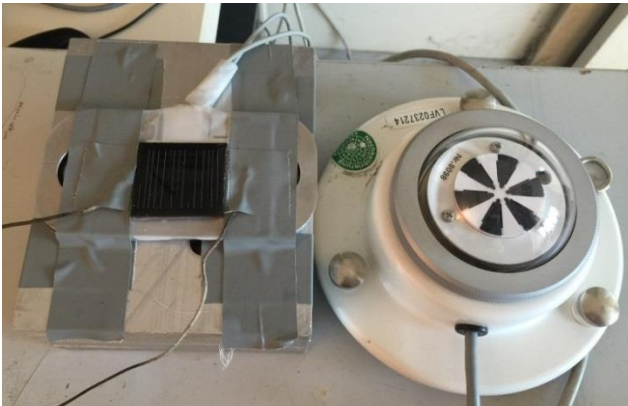
Online access to the position and speed of the train (map excerpt with train location indicated). Source: own illustration, Liebherr

Settings for the measurement equipment in the two half trains ensured that log files of all the measured values per carriage were saved on the two air-conditioning system computers (BK3) every hour. Depending on the GSM modem reception, they were also transmitted hourly to the contractor (LVF). If this was not possible, the system attempted the transfer in the next time window – until the

transfer was successful. The local copies were then deleted. The system automatically combined the hourly recordings into sessions. A session corresponded to a time slice between switching the train on and off. In the log files, the measured values were in ten-second intervals per time stamp and were available in this format for subsequent analysis.

A test to calibrate the solar sensors was performed in parallel by the contractor (LVF) (see Figure 40). A third photovoltaic (PV) cell was used for this purpose to obtain a correlation between the measured voltage and the radiation output at different angles, radiation intensities, ambient temperatures and degrees of pollution in comparison to a calibrated measuring device.

Figure 40: Test setup for calibrating the solar sensors (excerpt)

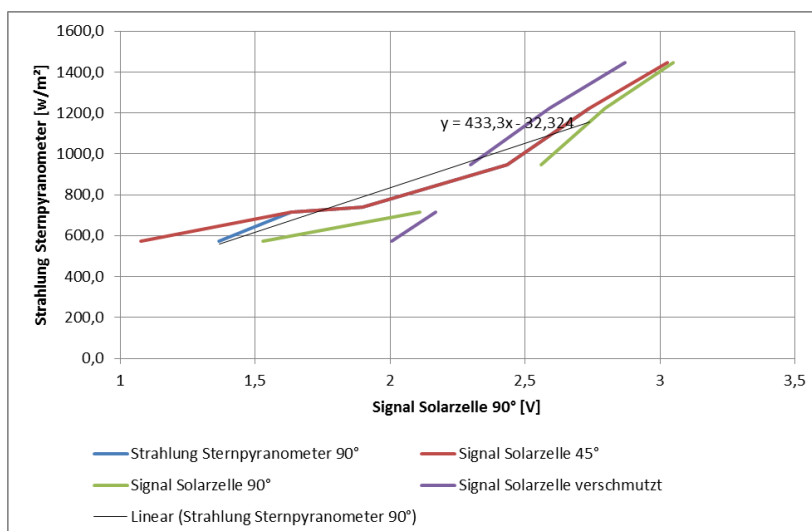


Test setup for calibrating the solar sensors – Comparison with a star pyranometer. Source: own illustration, Liebherr

This test showed that a nearly linear correlation exists between the emitted voltage of the PV cell and the radiation output, with sufficient accuracy. This result was included in the analysis in section 2.3.2. Details are provided in section 2.3.2.5.

Figure 41 shows some of the comparison measurements from the test of the photovoltaic cell.

Figure 41: Comparison of PV cell and star pyranometer



Comparison of PV cell and star pyranometer. Source: own illustration, Liebherr

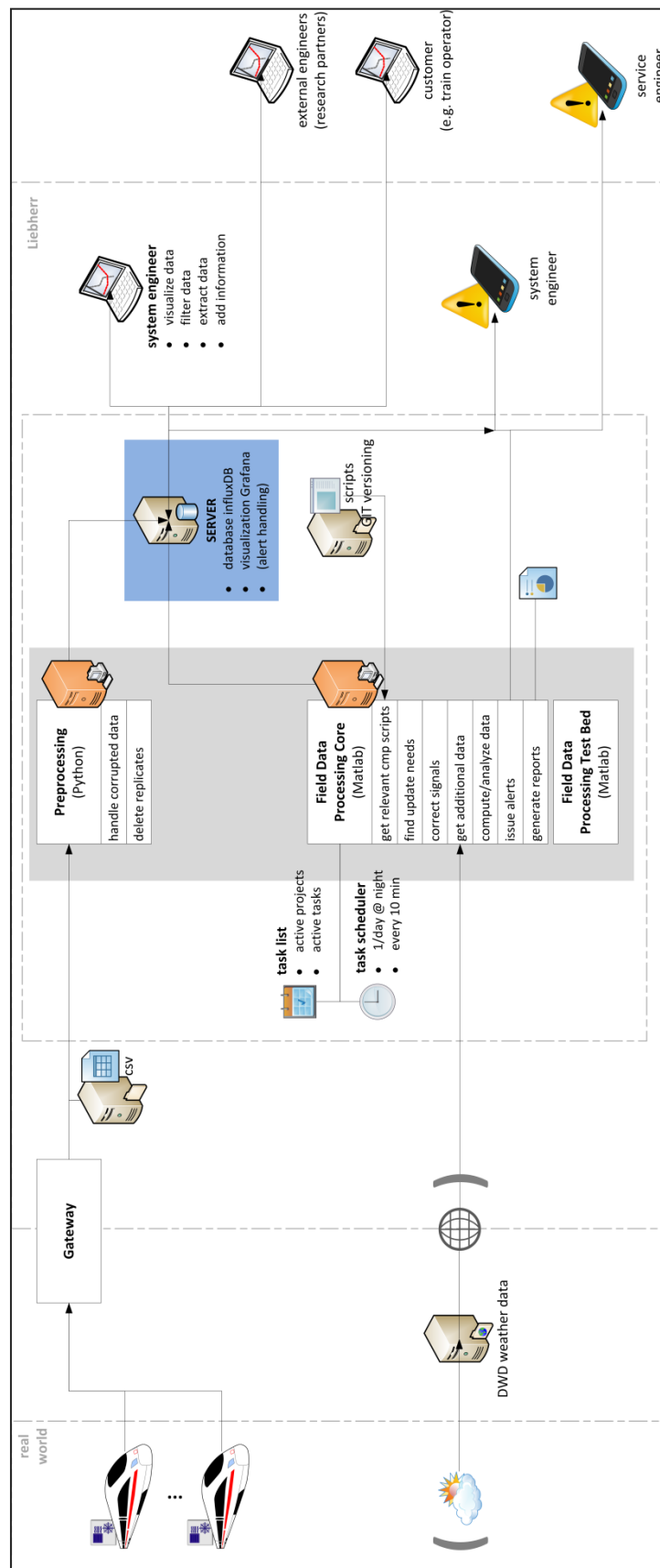
2.1.5 Concept for processing and evaluating field data

Figure 42 provides a diagram, representing the global concept for the data flow: Data from one or several trains running in the field are transmitted to Liebherr-Transportation Systems GmbH & Co KG (LVF) via a corresponding gateway, pre-processed and stored on a server in a suitable database for time series. Experts from LVF, external engineers or customers can access this database to visualise, filter and export data. The evaluation software created in the project also accesses the database. Additional interfaces, e.g. for using meteorological data, are planned.

While creating the concept, special attention was paid to ensure it can be extended flexibly. In the future, it will also be possible to acquire measurement data from other trains for similar comparisons. Alert handling, i.e. a process for generating and sending warning and error messages, will also be implemented in the future. In this project, the focus was on the functionality required immediately.

A detailed description of the analysis is provided in section 2.3 in particular.

Figure 42: Concept of data flow and the processing of field data



Flow chart for the concept of the data flow and the processing of field data. Source: own illustration, Liebherr

2.1.5.1 Data storage

The datasets (log files) created by the air-conditioning system computer BK3 on the train were transferred to a data server via the mobile telecommunications network. The data were then written to a database via a project-specific “importer” using the Python programming language. In the course of this import, the data were converted and preprocessed with the focus on filtering defective datasets. Defective or incomplete datasets, for example, were discarded.

To store the field data, a database was initially set up on an existing programming framework. A classic relational SQL database on a Windows server was used for this purpose. A suitable, flexibly adaptable database scheme was designed. However, the data import into this database revealed significant weaknesses in performance. Only a very slow write speed was possible and queries from the database required significant time. For this reason, suitable alternatives were sought.

An initial suggestion involved storing flat files in the file system with direct access from a client. Such an approach would allow for a variety of storage formats, such as json, csv, NetCDF, HDF, mat. The data would be stored in text or human-readable format or in binary and, as a result, would be very compact. Depending on the implementation, this approach would require significant effort for data and storage management with flat files in the file system.

After research, the preferred option was to provide special non-relational databases for the existing data (time series) that meet the special storage requirements and access patterns for time series. These types of database are referred to as Time Series Databases (TSDB). Typical functions of a TSDB are a time range query between two points, preprocessing and aggregation of the data (e.g. resampling), as well as compression of machine-generated raw data.

Examples of such time series databases are InfluxDB (www.influxdata.com), Open TSDB (<http://opentsdb.net>) and Graphite (<https://graphiteapp.org>). The final decision was for InfluxDB. This is a relatively new, widely used and open database that is also suitable for commercial applications. The database was centrally located on a server. Authorised users could write or query data over the network using a http-API. The database allowed several users or programs to access, view or process the data in parallel.

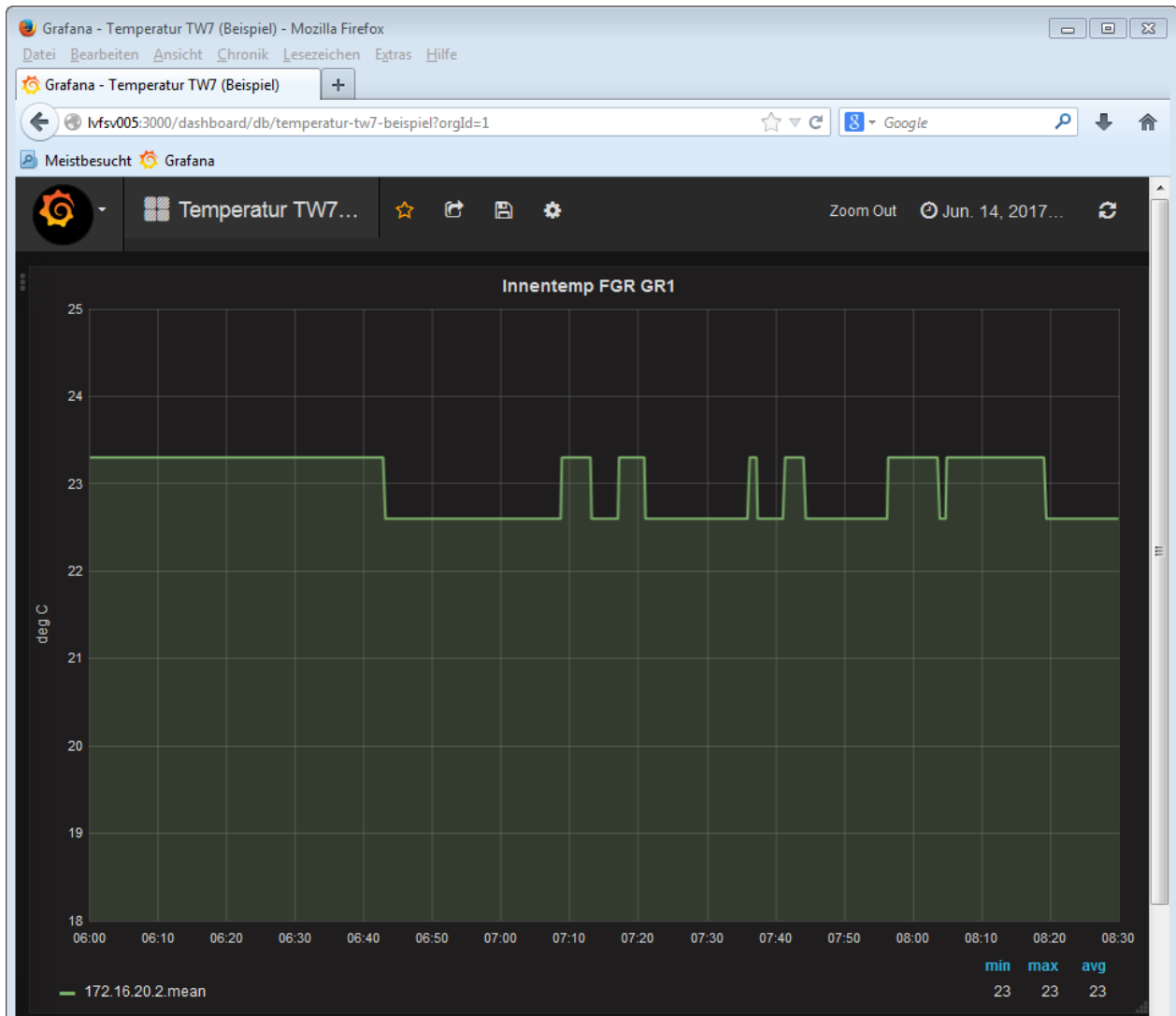
2.1.5.2 Visualisation of data for manual assessment and processing

To enable a convenient way to view signals, Grafana was introduced as a web-based tool for visualisation. Grafana (<https://grafana.com>) directly accesses the database and shows users the signals of interest as charts or tables in a graphical user interface (dashboard). A suitable tool was developed for automated creation of dashboards based on project-specific meta data in an Excel table.

In addition to the preconfigured project-specific dashboards, users can easily create their own database queries in Grafana and display the corresponding time signals. If needed, data can be exported from the database and processed further in Microsoft Excel. As Grafana is server-based, it can be used for effective collaboration in a team. Changes by one user are immediately available to all other users. Grafana also offers the option of defining alerts so that quick notification of a manager, e.g. via e-mail, is possible in case of defined statuses for a measurement signal.

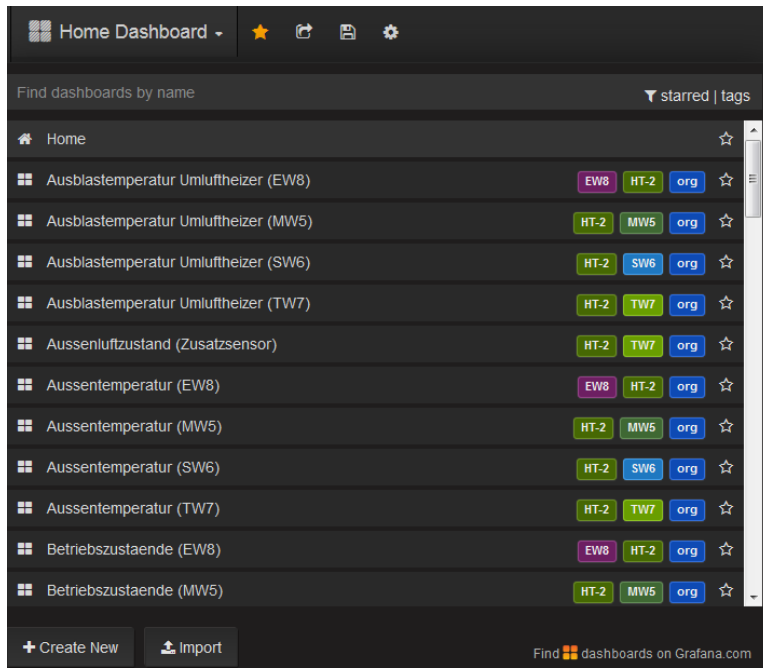
Figure 43 shows an example of a plot in Grafana. Figure 44 shows a screenshot of the selection window for various automatically created dashboards with important signals.

Figure 43: Screenshot of the Grafana program: Example of a graphical display (plot)



The example shown is a plot generated with the Grafana software of the inside temperature in carriage TW7 for a time period on 14 June 2017. Source: own illustration, Liebherr

Figure 44: Screenshot of the Grafana program: Dialogue screen for simple and convenient selection of the graphical data display (dashboard)



The following menu items are shown: Exhaust temperature, outside ambient temperature and operating conditions for various carriages of the ICE 3.

2.1.5.3 Program-supported processing of data

Modified data processing programs with database access were used to analyse the data. An exact description is provided in section 2.3. Source: own illustration, Liebherr

2.1.6 Creating the evaluation software

As part of WP 1, design considerations and smaller tests were conducted to clarify basic questions concerning the software design. All other activities were performed under WP 4. A detailed description is provided in section 2.3.

2.2 Perform measurement (WP2)

The purpose of work package WP 2 was to organise, conduct and monitor the planned measurement program. First, the equipment of the test train designed in the preceding WP 1 was verified. For this purpose, all the measuring instruments were successively checked again to ensure that they were operating correctly. After the recording of all data and parameters on ICE 3 trainset 301 (Ts 301) was working correctly, the system was switched over to continuous online data acquisition in cooling and heating operation. The measurements were run for the duration of the project over a period of two years in real passenger service for defined long-distance DB routes and parallel to the other activities in the project.

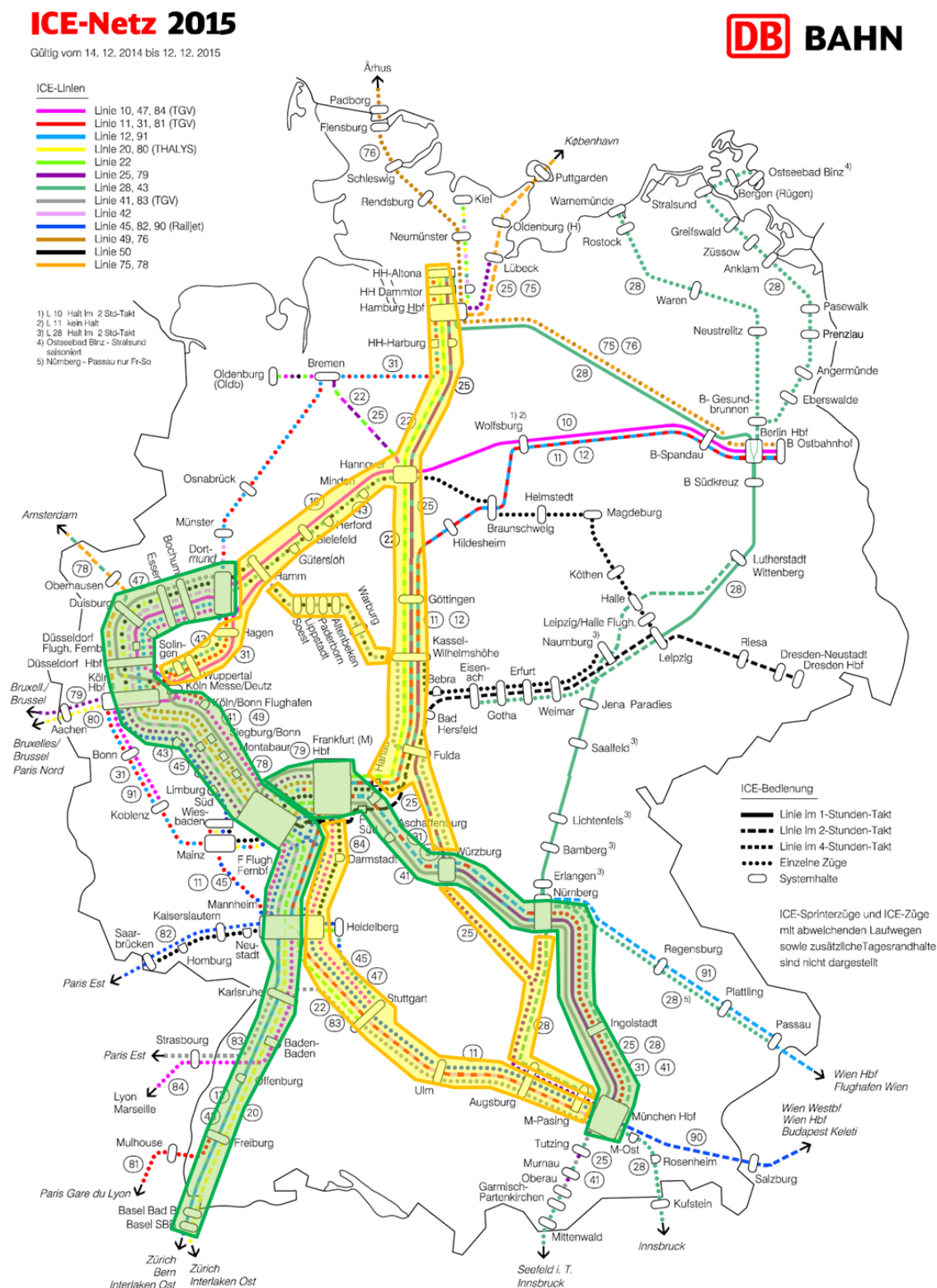
Figure 45 shows the railway network of the ICE fleet for 2015. The routes highlighted in yellow and green represent the main routes of the Ts 301. The routes Munich – Cologne/Dortmund and Dortmund – Basel (green) were travelled often and the routes marked in yellow, such as Munich – Dortmund via Stuttgart or Kassel and the routes to Hamburg were travelled less often. In addition, there were individual trips on other route segments that are not marked in colour here.

To provide an initial classification of the performance of the Ts 301: During the first period of measurement from 01/05/2015 to 30/05/2015, the train travelled for a total of 3,890.8 hours and covered 445,503 km. This resulted in an average of 9.8 hours of travel per calendar day.

The sensors, data transmission and data acquisition were checked regularly to ensure they were working and, in case of failures, were re-established immediately (see section 2.2.2). In addition, adjustments, additions and improvements were made to the measurement equipment (see section 2.2.3). The failures in data recording due to problems with the measurement equipment or other factors are discussed in section 2.2.2.

Section 2.2.1 describes the procedure for data recording and forwarding in more detail. The processing and analysis of data are discussed in detail in WP 4 in section 2.3.

Figure 45: 2015 ICE railway network



The most travelled routes (Munich – Cologne/Dortmund and Dortmund – Basel) are highlighted in green and the less travelled routes (e.g. Munich – Dortmund via Stuttgart or Kassel and routes to Hamburg) in yellow. Individual trips on other route segments are not marked in colour here. Source: own illustration, DB Systemtechnik

2.2.1 Data recording and processing

As outlined above, the total data volume to be recorded consisted of data from different sources. Specifically, the first set of data is the data generated by control of the CACU and stored in the air-conditioning system computer (BK3) of the unit. The second set of data is the data that can be read out from the train's fieldbus (MVB). The third and final set of data is from additional sensors and measuring devices installed in CACU No. 4 and in carriages TW7 and TW2.

This made it possible to read out all relevant air-conditioning data, which were transmitted via the MVB, read out by the measurement equipment and saved. This was done at intervals of ten seconds. The values on the air-conditioning system computer were also recorded – also every ten seconds per half train. Overall, approx. 4,500 measured values (raw data) were acquired for every ten-second interval. For a six-hour trip, this results in a total volume of approx. 9.7 million measured values as raw data. This volume of data was later assessed in WP 4.

All the data and information collected by the MVB Gateway, the BK3 and the additional sensors were collected on an additional measuring computer, assigned unique time stamps, and stored locally in log files. Each half train then carried out an hourly transfer via GSM USB modem and via mobile telecommunications network to stationary devices at the contractor LVF, where the data were then processed further (see section 2.1.5).

For this purpose, regular preliminary analysis of the raw data was carried and the measurements documented, as well as simultaneous acquisition of the maintenance data (preventive and corrective measures) in collaboration with the operating company.

Overall, approx. 60 gigabytes of raw data was produced for both half trains in the period from July 2015 to December 2017, which then had to be analysed in WP 4 (see section 2.3.1). However, the processing and preparation of these data also required adjustments to the servers at LVF to ensure a smooth operation of the database. This was started during this WP and successfully completed and implemented ultimately in WP 4.

Regular observation of the air-conditioning system made it possible to correct errors in the measurement setup at all times and ensure that the measurement devices were already ready for use.

Finally, all the measurement equipment has to be removed from the Deutsche Bahn train. Removal is scheduled as part of a longer stop for redesign at the Nuremberg plant, starting in November 2018.

WP 2 is completed at the end of the recording of all measured values over the scheduled time period, removal of the measurement devices and the preparation of a final report.

2.2.2 Repairs to the measurement equipment

In the course of work packages WP 1 and WP 2 in the period the end of 2015 to spring 2016, damage occurred to the measurement equipment. This damage subsequently led to a partial loss of the recorded data. Details are provided in detail in WP 2.

The relevant repairs were carried out as quickly as possible. The repairs and the possible causes of the damage are explained in the following sections.

2.2.2.1 Repairs to the solar sensors on 20 April 2016

The sensor cable on one of the two solar cells was damaged (Figure 46), possibly because the ribbon cable was wedged in due to repeated opening and closing of the cover of the CACU (TW7).

The fact that there was only one solar sensor to provide measured values for recording of the solar radiation was not a major problem, as lab measurements had already demonstrated (see section 2.1.4) that the directional dependency of the sensors only modified the measurement result negligibly.

However, the accuracy of the statements is greater if a sensor is available on both sides of the train and it was also necessary to ensure the redundancy of measurement. An additional solar cell was therefore produced and installed on the train as part of the scheduled tasks on the Ts 301 in April 2016.

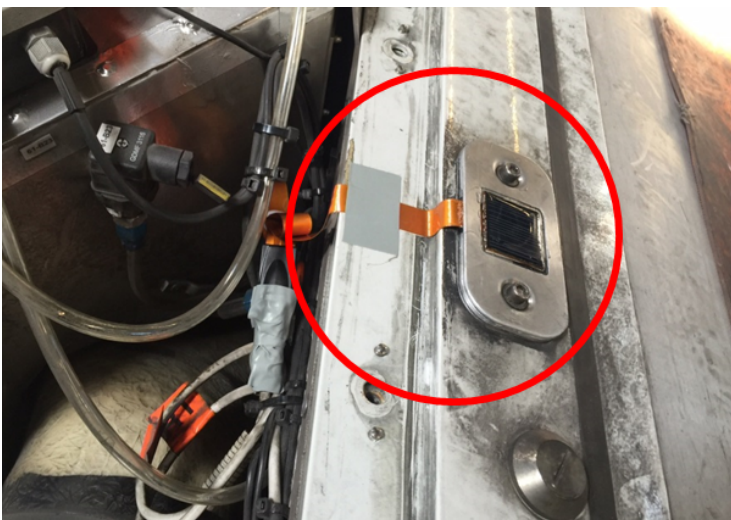
Figure 46: Defective solar cell (cable break) on the air conditioning unit of ICE 3 carriage TW7



Defective solar cell (cable break) on the air conditioning unit of ICE 3 carriage TW7. Source: own illustration, Liebherr

Figure 47 shows the installed solar cell with the cable attachment, which prevents further wedging of the cable when opening and closing the cover.

Figure 47: Installation of the new solar cell on ICE 3 carriage the TW7 with additional cable attachment



Installation of the new solar cell on the air conditioning unit of ICE 3 carriage TW7 with additional cable attachment. Source: own illustration, Liebherr

2.2.2.2 Repair of occupancy counter on 23 June 2016

During the scheduled tasks on the Ts 301 in April 2016, the occupancy counter (DILAX) sensors in TW7 were accidentally damaged, possibly at the ICE plant in Munich. The cause of the damage could not be established. Scheduled tasks may also have been performed on the doors inside the carriages, which may have required removal of the cover plate. The accidental damage may have occurred during the work.

Two of the four sensors (two per door or end of carriage) were rendered completely unusable, as their connecting plugs broke off (see Figure 48 and Figure 49). One connecting cable had also been removed and another one slightly damaged. There are therefore no measured values for occupancy for the period from the end of April to the middle of June 2016.

To prepare for repair, it was first necessary to find a date to determine what parts of the system had been damaged. This required removing the ceiling elements and checking the cables. This was done in early May 2016 during servicing on a CACU.

As a result, two new sensors and a new connecting cable between two sensors were ordered from DILAX. The delivery time was about four weeks.

Figure 48: Damage to the sensor cable of the DILAX sensor for occupation counting



Damage to the sensor cable of the DILAX sensor for occupation counting. Source: own illustration, Liebherr

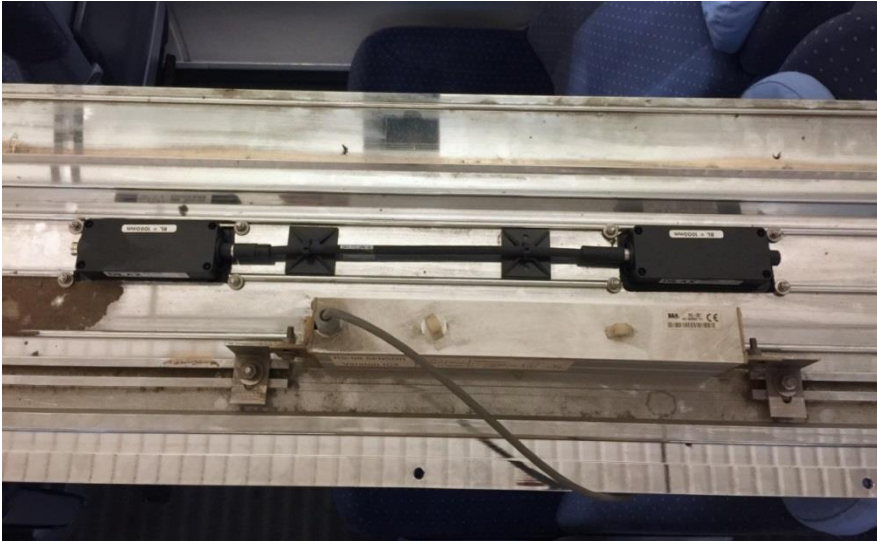
Figure 49: Damage to the DILAX sensors for occupation counting



Damage to the DILAX sensors for occupation counting. Source: own illustration, Liebherr

After the new sensors and cables arrived, a date was negotiated with DB for the repair. Liebherr replaced the two defective sensors and the missing cable on site at the ICE plant in Munich (see Figure 50). During repair, it was found that another cable was slightly damaged. The cable was installed across the entire length of the carriage and it was only possible to replace it with significant effort. However, as the contacts were not significantly damaged, it was still possible to record the sensor data without any problems.

Figure 50: Two new sensors for occupation counting and a new connecting cable after installation



Two new sensors for occupation counting and a new connecting cable after installation. Source: own illustration, Liebherr

To avoid this problem during future work on the doors, DB Systemtechnik gave further instructions to the DB maintenance team, noting the additional measurement equipment and the care to be taken when handling it.

2.2.3 Modifications and additions to the measurement equipment

In the course of the project, some modifications to the measurement equipment became necessary while in use on the ICE 3 Ts 301 to stabilise the acquisition and recording of data. The modifications are described below.

2.2.3.1 Replacement of the UMTS routers on 20 April 2016

During scheduled work by Deutsche Bahn on the Ts 301 in April 2016, DB expressed concern about the installed routers/transmitting antennas and their electromagnetic compatibility (EMC). It was therefore necessary to find new routers that meet particularly high EMC requirements. The positions of the transmitting antennas also had to be changed to be able to rule out any possible risk to these sensitive components.

3G/UMTS routers from PEPWAVE were eventually chosen. The model is the MAX BR1 (see Figure 51). It complies with all the required standards and has the advantage that communication with the air-conditioning system computer uses Ethernet, so the USB hub was then redundant, as the previously used USB modems could no longer be used.

The new router was also an improvement, as the new cabling rendered the USB hub redundant. For the time being, the USB hub was required in the TW2 and in the TW7 for communication of the USB interfaces with the air-conditioning system computer (BK3). However, for some unexplained reasons, constant communication problems occurred between the USB hub and the Linux card installed in the BK3. Among other things, this caused the GPS signal (position and speed of train) to be lost or mobile transmission to fail, as the modems were also connected via USB. The resulting interruptions are discussed in WP 2. Once the USB hub was removed, the communication problems due to interruptions also stopped.

Another advantage of this router is the option to use two SIM cards from different providers if necessary, so that it is possible to automatically switch from one network provider to another in case of poor coverage. Along the usual routes of the Ts 301, however, the coverage of one provider was adequate for communicating with the measurement equipment, so this option was not used.

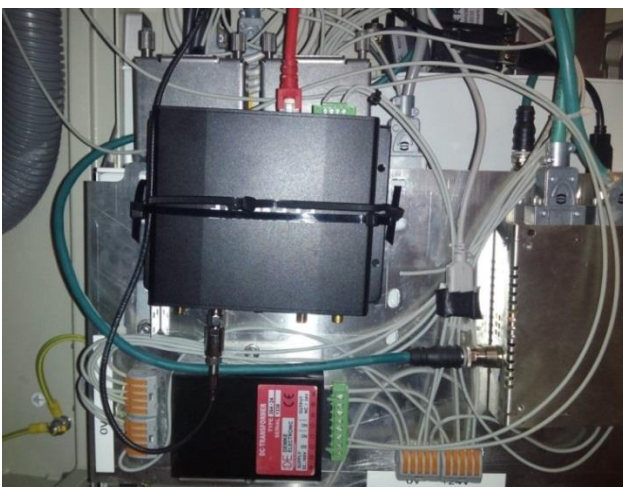
Figure 51: 3G/UTMS router PEPWAVE MAX BR1



3G/UTMS router PEPWAVE MAX BR1. Source: own illustration, Liebherr

During the period of these scheduled tasks, the new routers (modems) were installed and the corresponding antennas were better positioned.

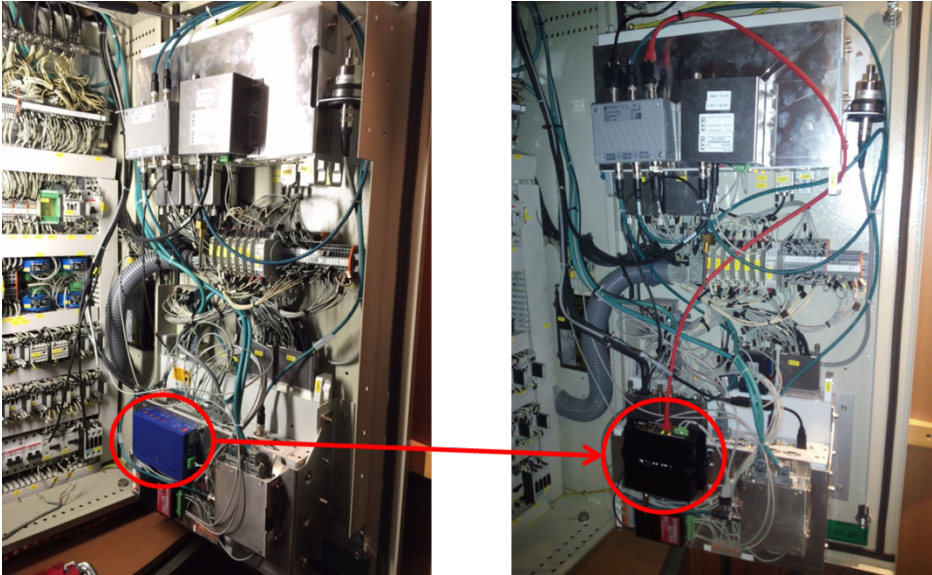
Figure 52: Router as installed



Router as installed in the control cabinet of the TW7. Source: own illustration, Liebherr

The free installation space in the control cabinet was extremely limited as explained above. Once the USB hub was no longer required, the router could be installed in the space that was then free in the control cabinet (Figure 53).

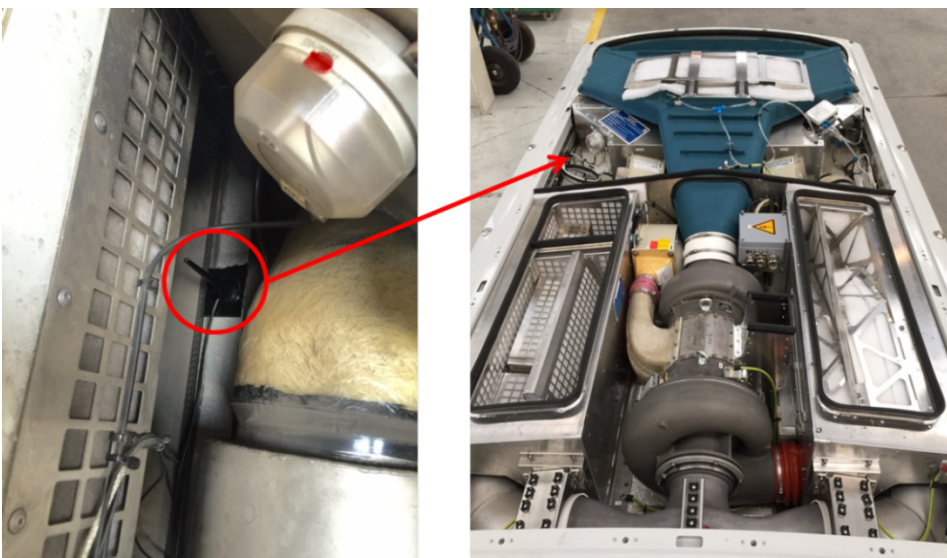
Figure 53: Installation of the new router (black) and removal of the USB hub (blue)



Installation of the new router (black) and removal of the USB hub (blue). Source: own illustration, Liebherr

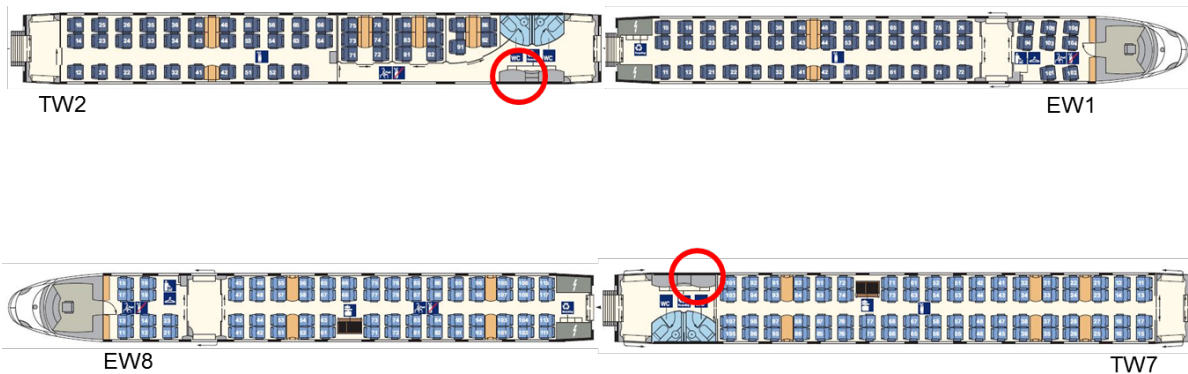
The following figures (Figure 54 and Figure 55) show the installation of the new antennas. The previous antennas were located near the control cabinet and, as such, next to the door control and the brake control of the train. The new antennas were installed directly in the compact air-conditioning unit (CACU), so that they are practically on the roof of the train. As the cover of the CACU and the side opening of the fresh air grid are made of plastic, signal transmission is interference-free.

Figure 54: Installation of the new mobile communication antennas in the compact air-conditioning unit in carriage TW2



Installation of the new mobile communication antennas in the compact air-conditioning unit in carriage TW2. Source: own illustration, Liebherr

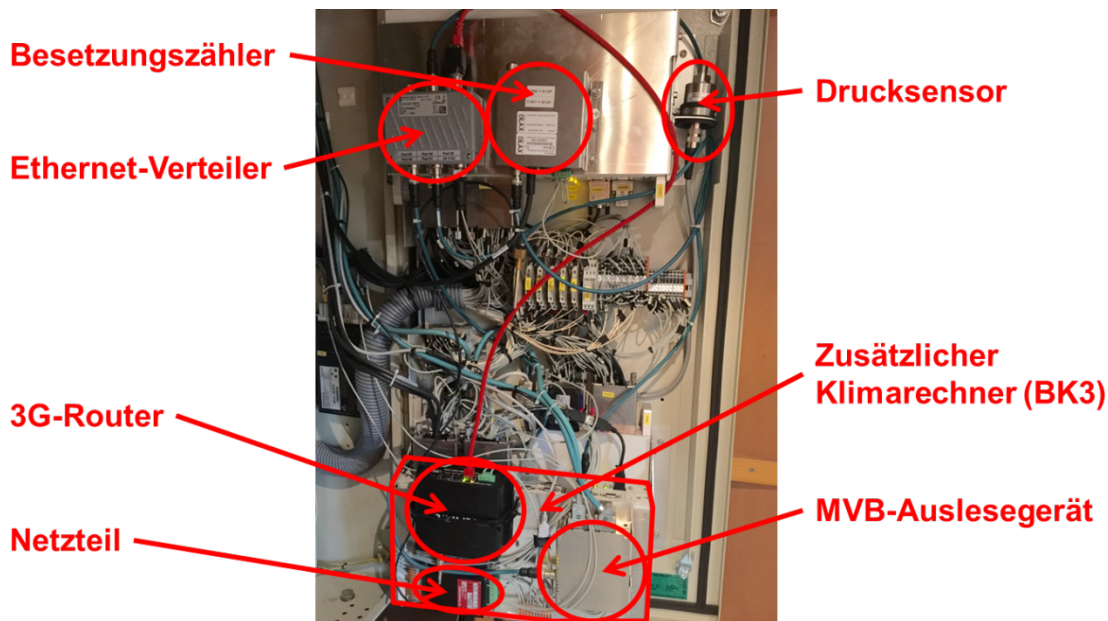
Figure 55: Position of the new mobile radio antennas on the train (at the level of the fresh air grids)



Position of the new mobile radio antennas on the train (at the level of the fresh air grids)

Figure 56 shows the control cabinet of ICE 3 carriage TW7 in the configuration that was reached after the initial adjustments. An additional change became necessary because of the modifications for data security, which is described in more detail in section 2.2.3.3.

Figure 56: Complete overview of the modified control cabinet in carriage TW7 after the initial adjustments



Complete overview of the modified control cabinet in ICE 3 carriage TW7 after the initial adjustments. Besetzungszähler=occupation counter; Ethernet Verteiler=Ethernet switch; 3G-Router=3G-Router; Netzteil=power supply; Drucksensor=pressure sensor; Zusätzlicher Klimarechner BK3=additional air conditioning controller BK3; MVB Auslesegerät=MVB gateway, Source: own illustration, Liebherr

2.2.3.2 Installation of a second GPS receiver on 20 April 2016

Access to the roof of the ICE 3, Ts 301 was possible during scheduled tasks in April 2016. This made it possible to install an additional GPS receiver in carriage TW2. This established redundancy for measurement of the position and speed of the train.

2.2.3.3 Improvement of data recording and backup in October 2016

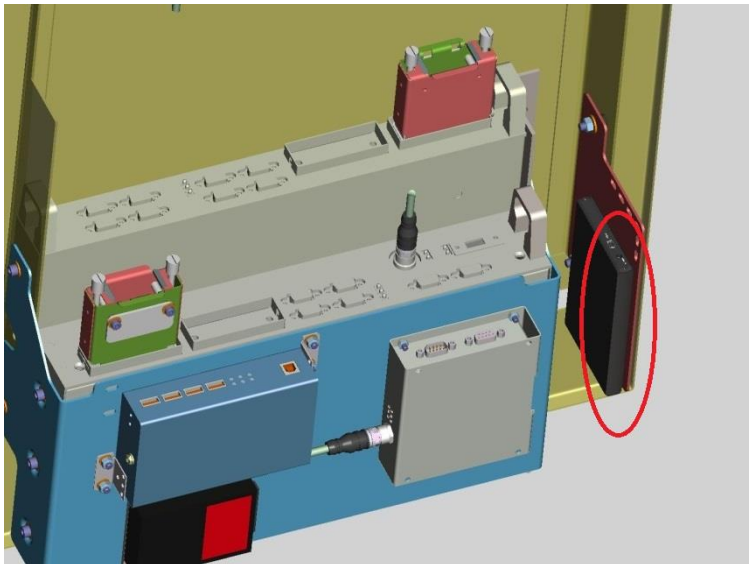
In August 2016, a communication error between the air-conditioning system computer (BK3) and the data acquisition server caused a two-week gap in the recording of the measured values. For details, see section 2.2.2.

The software was adapted to avoid data gaps in the future. To rule out additional problems with the transmission of data via mobile (3G), hardware was added/adapted at the end of October 2016.

This change included installing another computer, a Raspberry Pi, which had the task of copying all data records generated by the BK3 and backing them up on a local storage device in the control cabinet to be sent via mobile. The storage device was a 512 GB SSD (Solid State Drive). Figure 57 shows an example of the installation study for the positioning of the SSD in the control cabinet.

This changeover was intended to avoid total loss of data if the mobile link is interrupted. It would then be possible to copy the data directly on the train and add it for analysis in WP 4.

Figure 57: Installation study of SSD in the control cabinet



Installation study of SSD in the control cabinet. Source: own illustration, Liebherr

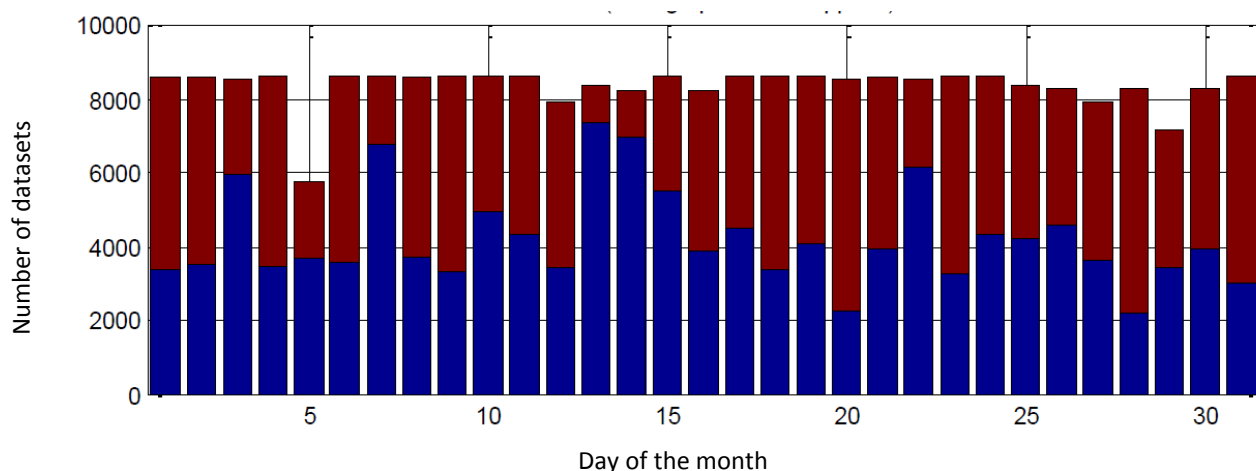
2.2.4 Availability of data recording

Breakdowns and other downtimes of the train occurred on the ICE 3 for operational reasons and led to missing period in the recording of the measured values.

To explain the missing times for data recording, the volume of recorded datasets was analysed against the travel speed. The data were recorded every 10 seconds. On the following graphs, the blue bars represent the number of datasets that were recorded at stop and the red bars represent the datasets that were recorded during travel (speed "v" greater than 0 km/h). The total of both is the number of datasets per day.

The first chart (Figure 58) shows an analysis of October 2015, as an example. The number of datasets per day while moving is shown as red bars and the number of datasets per day at stop is shown as blue bars. The abscissa axis (X-axis) represents the calendar days of the month of October 2015, the ordinate axis (Y-axis) represents the number of recorded datasets. In principle, one dataset was acquired every 10 seconds. The example month of October 2015 shows the typical distribution of travel and stop times of the train (Ts 301). This also matches the information from Deutsche Bahn.

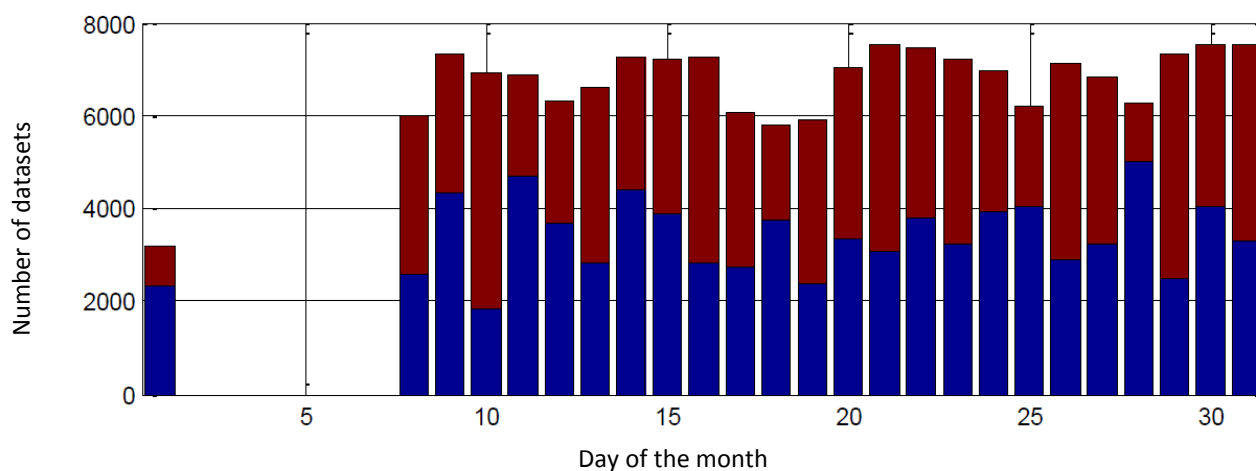
Figure 58: Example analysis of data recording for October 2015



Example analysis of data recording for all days in October 2015. Red bars: number of datasets per day during travel; blue bars: number of datasets per day at stop. Source: own illustration, Liebherr

The chart in Figure 59 clearly shows the loss of data in March 2016 due to faulty communication between electronic components, as there are missing bars. The failures caused by the USB hub were resolved by changing the UTMS routers (modems) in April 2016 (see section 2.1.5.1).

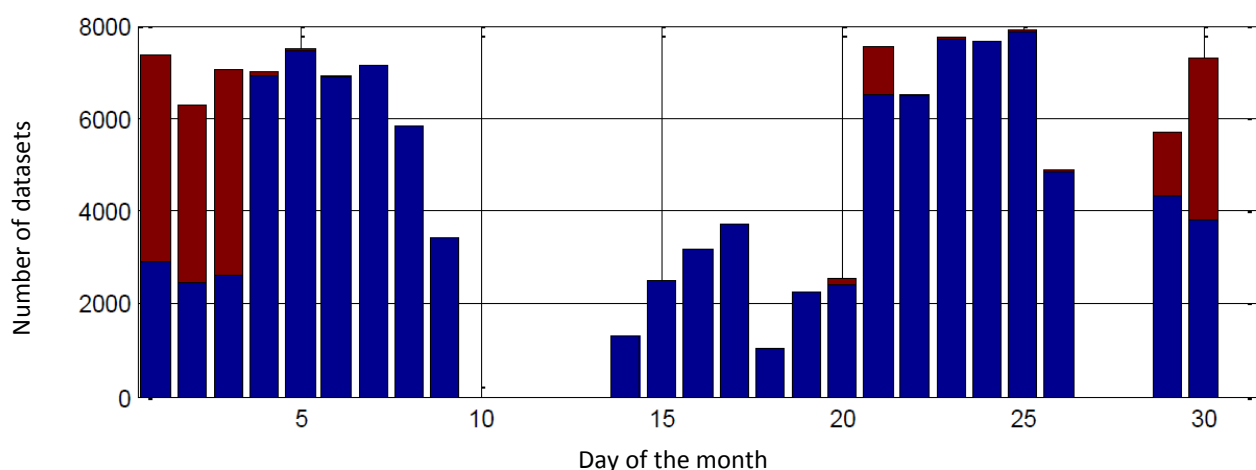
Figure 59: Data for March 2016 with data gap due to faulty communication between electronic components



Data record for all days in March 2016 with data gap of 6 days due to faulty communication of electronic components. Red bars: number of datasets per day during travel; blue bars: number of datasets per day at stop. Source: own illustration, Liebherr

The chart in Figure 60 shows a stop from 4 April to 28 April 2016. This was due to scheduled work, i.e. a regularly required inspection and maintenance of the ICE 3, Ts 301 by Deutsche Bahn. These scheduled tasks are required for proper operation of the train and are also carried out for all other ICE 3 vehicle of the Deutsche Bahn fleet, i.e. they are not due to breakdown or failure. During this time, no project-related measurement data for the air-conditioning systems could be collected. However, the downtime was used in a meaningful way by LVF for repairs and modifications to the measurement equipment (see also WP 1).

Figure 60: Data gap in April 2016 due to scheduled work on the train

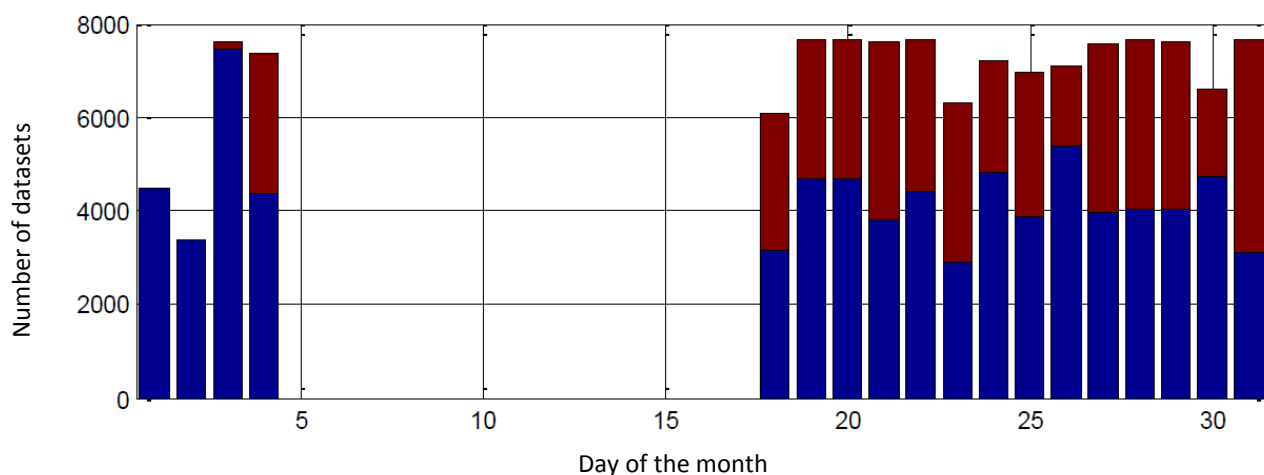


Data gap in April 2016 due to scheduled work on the train. Red bars: number of datasets per day during travel, blue bars: number of datasets per day at stop. Source: own illustration, Liebherr

The chart in Figure 61 shows missing data due to a communication error between the installed air-conditioning system computer (BK3) and the data acquisition server. As a result, the BK3 could no longer transmit the hourly data records to the server and only saved them. When the storage capacity of the BK3 was reached, the existing data were overwritten with new datasets. This was only noticed approx. two weeks later. The cause of the error could not be completely clarified. To avoid such errors in data recording, the software was modified.

To avoid further failures in the future, the measurement equipment was changed and an additional computer (Raspberry Pi) with connected storage (SSD) was integrated in order to have an additional local copy of all measured values in addition to the data transmitted via mobile (see section 2.1.5.1). This guaranteed long-term data security.

Figure 61: Data gap in August 2016 due to faulty server communication



Data gap in April 2016 due to faulty server communication. Red bars: number of datasets per day during travel, blue bars: number of datasets per day at stop. Source: own illustration, Liebherr

Figure 58 and Figure 59 show that approx. 50% of the acquired datasets per day are while the train is running (red bars), while the remaining approx. 50% are during stops (e.g. train parked or train in workshop) (blue bars).

The recording of the measured values, with the exception of the described issues and missing data, has been without errors since April 2016. The implemented modifications resulted in more reliable provision and storage of data.

2.2.5 Organisational matters

Since April 2016, external markings have indicated that the train is part of a UBA project. A total of four signs were attached (Figure 62) – two on each side of the train – to provide information about the project.

Figure 62: Signs on the Ts 301 “Freiburg im Breisgau”



Signs on the Ts 301 “Freiburg im Breisgau”. Source: own illustration, Liebherr

2.3 Evaluate the measurement program (WP 4)

The goal of work package WP 4 was detailed evaluation and analysis of the energy consumption of the air-conditioning units and a comparison between air-cycle system (air-cycle system, ACS) and a system based on the vapour compression process (vapour cycle system, VCS). This was based on the field data (WP 2) and the data obtained in WP 3 (see section 2.4).

As there is no standardised procedure for comparing the energy consumption, the initial step was to select a procedure. The result is a detailed presentation of the annual energy consumption of the vehicles and comparison on a quantitative basis.

Evaluation of the measurement data was followed by analysis of the Life Cycle Cost (LCC) and the Total Cost of Ownership (TCO). The goal of this evaluation is to make statements about the economic efficiency of a system over the entire observation period. Measurement and maintenance data created in collaboration with DB were taken into account. This complete analysis (LCC/TCO) provides a statement for all costs, from manufacturing up to disposal of the air-conditioning system, as well as an assessment of a system compared to other systems in terms of economic efficiency.

The analysis tool created in this project (Software, section 2.3.1) was used to evaluate and present the results. The results obtained were processed and compared using scientific methods.

2.3.1 Creating the evaluation software

Project-specific evaluation software was developed. Implementation was done primarily in Matlab. The evaluation software has a modular design. Program modules can be combined depending on application, modified as needed and, if necessary, added to a framework (programming framework) for automatic batch data processing. Among other things, modules were created for the following:

- ▶ Access to the database of measurement data
- ▶ Calculation of electric power consumption
- ▶ Calculation of air states and of heating and cooling capacity on the air side
- ▶ Import of data from other data sources (weather data from the DWD, measurement data from DB, etc.)
- ▶ Linking a Modelica/Dymola simulation for validation purposes
- ▶ Classification of data to derive a model for the electric power consumption
- ▶ Deriving class frequencies to weight for the annual energy consumption
- ▶ Calculation of annual energy consumption for different HVAC systems

Section 2.3.2 describes evaluation of the power and energy consumption based on an example train trip for the air-cycle system of the ICE 3, including determining the COP (Coefficient of Performance) of the system. Results from field data evaluation are also compared with calculation results from a corresponding simulation model. The analysis of different influencing factors and the calculation of air states at the interfaces of the HVAC device may form the basis of a system model for future investigations.

Section 2.3.3 focuses on comparison of different HVAC technologies. Important parts from of 2.3.2 are required for this comparison.

2.3.2 Analysis of power and energy consumption for the air-cycle system on the ICE 3

This section analyses selected data for the air-cycle system on the ICE 3 in terms of power consumption and energy consumption. This evaluation is initially independent of a comparison with any other air-conditioning unit.

The goal of analysis was to determine the following power/energy values:

- ▶ Electric power and energy consumption in heating and cooling operation (power: P_{el})
- ▶ Heating capacity/heating energy introduced on the air side and cooling capacity/cooling energy taken from the air (power: \dot{Q}_0)

This can be used to calculate the Coefficient of Performance (COP) according to equation (1):

$$COP = \frac{\dot{Q}_0}{P_{el}} \quad (1)$$

The specific analyses here were based on the data from individual train trips. This made it possible to interpret and verify the results intuitively (including checking plausibility in meetings of experts). In a future step, the analyses may be extended beyond train trips.

The focus for these analyses was on carriage TW7, as this carriage is equipped with the most extensive measurement equipment. The TW7 is one of the carriages with the highest required cooling load at the design point.

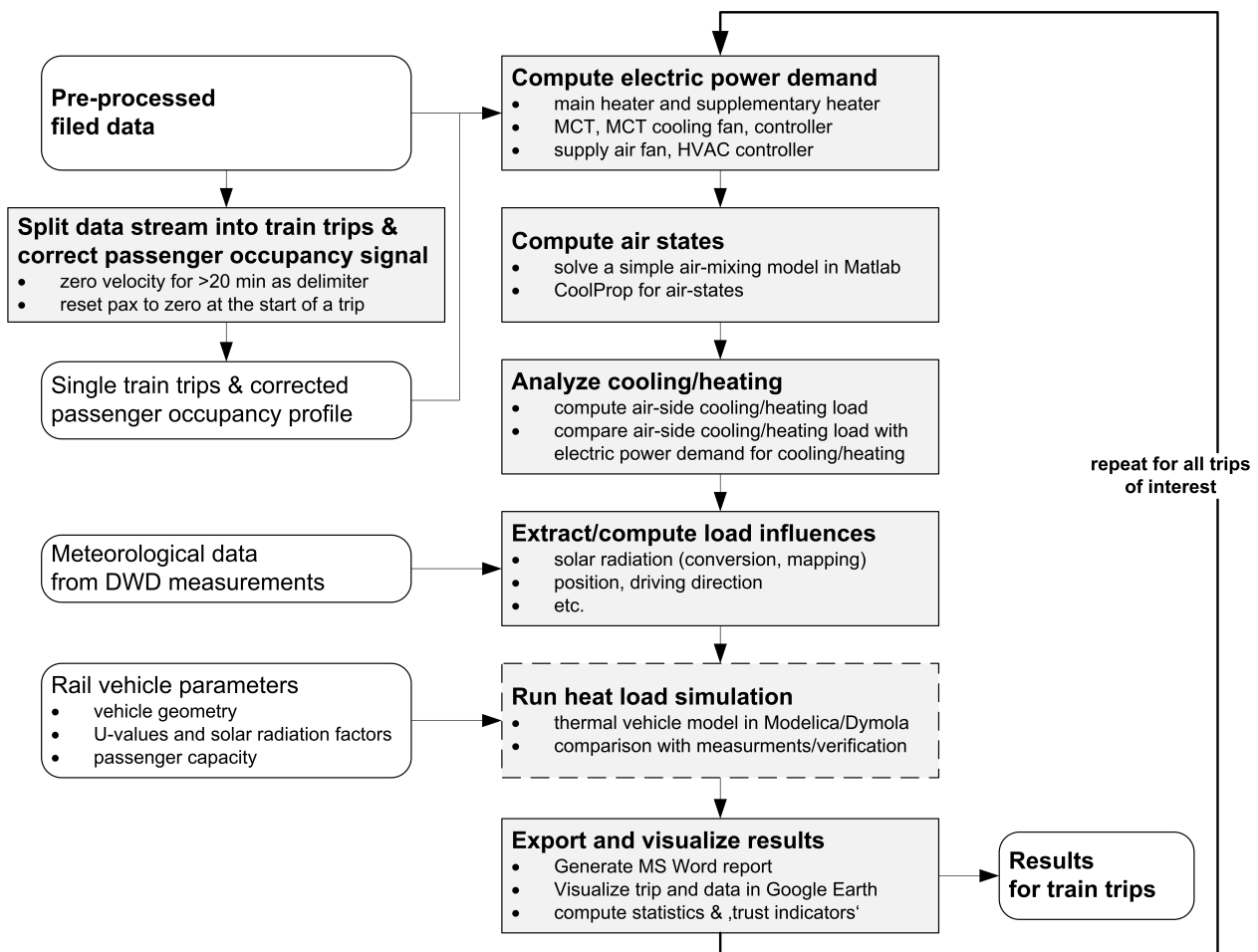
2.3.2.1 Methodology

Project-specific software tools were developed to automate the processing of the significant volumes of data. Implementation was in Python and Matlab. The Dymola simulation environment and Liebherr internal simulation models were also used for a sub-range focussing on checking plausibility and validation.

Figure 63 provides an overview of the workflow for processing data based on train trips. Details are provided in the sections below.

The evaluation software developed during the project was used to determine the electric power consumption of the HVAC unit as well as the air-side heating or cooling capacity, based on air states at different, relevant points in the air path. The influencing factors on the heating or cooling load were extracted from the raw data. As an additional step, represented in Figure 63 by the rectangle with a dashed border, calibration was performed with a thermal simulation model of the carriage. The results were exported as charts and visualised in Google Earth.

Figure 63: Overview of implemented workflow for data processing based on train trips



Rectangles with rounded corners represent input/output data, rectangles with grey shading represent processing steps.

Source: own illustration, Liebherr

U-values=Heat transmission factors; DWD=Deutscher Wetterdienst; MCT=Motorized cooling turbine (=motorized Aircycle Machine)

2.3.2.2 Overview of existing measurement signals as the basis for investigations and measurement data processing

Field data acquisition was used to acquire approx. 4,500 variables at a scan rate of approx. 0.1 Hz (i.e. every 10 seconds) at the train level (half train 1 and 2). The most extensive set of measurement data was collected for TW7 – a second-class open-plan carriage (see Figure 10). The signals recorded for the TW7 are summarised below by groups:

- ▶ Signals from sensors that are installed in the HVAC system as standard (temperature at various points on the air path, CO₂ concentration in the carriage, etc.)
- ▶ HVAC controller data (target temperature, fan speeds, position of flaps, etc.)
- ▶ GPS position as well as direction of travel and speed*
- ▶ Solar radiation from two photovoltaic sensors on the roof*
- ▶ Passenger occupancy via passenger counting system*
- ▶ Relative humidity of fresh air and recirculated air, as well as air pressure*
- ▶ Power consumption of various devices*
- ▶ Operating parameters of main control bus of the train

The signals marked with an asterisk (*) were acquired by additional measurement equipment installed in the TW7.

2.3.2.3 Processing measurement signals

In the course of evaluation, the available measurement data displayed various uncertainties, errors and gaps. This is to be expected from field data. Specific reasons for deviations from the ideal measurement signals were primarily due to the following in this project (see also sections 2.1.5 and 2.1.6):

- ▶ General measurement deviation and interference factors not immediately quantifiable affecting the parameter to be measured
- ▶ Problems with hardware and software for measurement data acquisition (e.g. overflow of value range)
- ▶ Temporary failure of individual sensors (e.g. failure of one of the two photovoltaic cells due to damage of the connecting line, failure of occupancy counting system after damage to the sensors on one carriage side in the course of train overhaul)
- ▶ Temporary failure of remote data transmission or temporary deactivation of remote data transmission due to concern of DB regarding EMC compatibility

Substantial effort was required for signal processing to be able to carry out the planned evaluation as well as possible based on the acquired signals.

When uncertainties or errors are identified in signals, one of the following approaches may be applied in principle:

- ▶ Ignore the uncertainty, if only minor impact on the final results is expected
- ▶ Suitable correction of the signal
- ▶ Replace the signal with data from another corresponding measurement
- ▶ Discard the entire time range if correction or replacement of the signal is not plausibly possible.

Note that not all uncertainties or errors can be detected or corrected with reasonable effort. Depending on the task and methodology of the evaluation, different signals are required at the same time. Hence, it is possible that the corresponding time range must be factored out if there is a temporary lack of a required signal.

For the observations described in this section for power and energy consumption, the following processing of the signals was carried out:

1. Discard signal values that fall outside a bandwidth that is meaningful for the relevant variable.
2. Identify and discard outliers
3. Interpolate missing or discarded data points
4. Flatten the signals over a floating mean (if required)
5. Scan rate conversion of signals for regular time stamp and, if necessary, reduced scan rate (if required)

2.3.2.4 Passenger occupancy signal in TW7

For passenger occupancy, counting pulses for boarding and alighting are added together to give the absolute number of people in the carriage. Incorrect counts (e.g. counting a suitcase as a person) can add up over the course of time. For as trustworthy a signal as possible for the absolute number of passengers on the train, automated resetting of the counter was therefore necessary. Specifically, the data stream on train trips was subdivided based on the signal for the travel speed and a minimum duration for stop. At the beginning of a train trip defined in this way, the occupancy counter was reset to zero for evaluation. In a subsequent step, the calculated occupancy signal was checked (number of passengers at the end of the trip, negative passenger occupancy in the carriage) and corrected accordingly or discarded. Further analysis could now be performed across the identified train trips or over the entire data stream.

2.3.2.5 Solar radiation signal in W/m^2 and mapping of DWD data

As described in section 2.1.3.4., two simple photovoltaic cells were implemented on the carrier roof, roughly in one horizontal plane. The photovoltaic cells can therefore be considered redundant. The original goal was to enable basic statements to be made about the solar radiation (e.g. at 3 levels). Lab measurements were conducted under different conditions with a photovoltaic cell and a star pyranometer. A correlation was derived on the basis of the measurement results, which enabled approximate mapping of the measured voltage in volts to the solar radiation in W/m^2 . Analysis of the solar radiation was therefore possible at higher quality than originally considered.

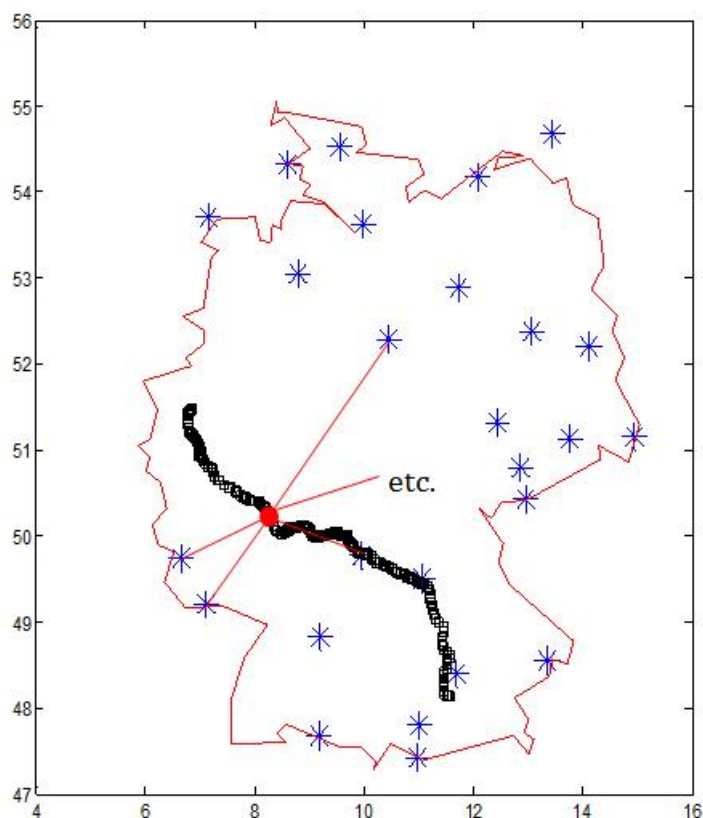
The solar radiation recorded via the photovoltaic cells represents the total radiation I_{total} , i.e. the total direct (direction-dependent) I_{dir} and diffuse (not direction-dependent) radiation I_{dif} .

For certain analyses, it is necessary to know the radiation value for the direct radiation separately. This direct direction-dependent radiation component is needed in particular, in conjunction with the radiation direction and the orientation of window surfaces of a train carriage, to be able to determine the heat introduced into carriages through windows due to direct solar radiation.

For the distribution of the types of radiation, additional stationary measurement data from the German Meteorological Service (DWD) from (Deutscher Wetterdienst, Climate Data Center, 2017) were used.

Specifically, the closest measuring station of the DWD for the current position of the train was used via the evaluation program as reference for the I_{dir}/I_{total} ratio for a given time. It was assumed that this I_{dir}/I_{total} ratio is also valid for the current position of the train. Effects, such as clouds, could not be mapped here directly. A diagram of the procedure is provided in Figure 64.

Figure 64: Diagram for the mapping of weather data from the German Meteorological Service to the location of the train



Weather data from the German Meteorological Service (DWD) were used to divide the measured total solar radiation into direct and diffuse radiation. The map shows DWD measuring stations in Germany as well as the position of the train on a specific train trip. Source: own illustration, Liebherr

2.3.2.6 Determining the electric power consumption

Table 3 shows the formulas for determining the electric power consumption of the individual consumers of the air-conditioning unit. 'MCRUN' is an operating variable of the MACM turbomachine. Variables preceded by a 'U' represent voltage values, variables with 'I' are current values. The indicated correlations were partially identified by lab investigations.

For the heating scenario, the electric output of the heaters is directly fed to the air.

Table 3: Basic formulas for determining the electric power consumption

Subsystem/function	Calculation formula
Heating	
Basic heater	$P_{el, \text{ Main heater}} = U \cdot I_M$
Secondary heater, entrance heater	$P_{el, \text{ Secondary heater}} = \frac{440}{\sqrt{3}} \cdot (I_{SH1} + I_{SH2} + I_{SH3})$
Cooling	
MACM	$P_{el, \text{ MACM}} = (-0.0007 \cdot MCRUN^2 + 0.5163 \cdot MCRUN + 1.0582) \cdot 1000 \quad \text{if } MCRUN > 0$ $P_{el, \text{ MACM}} = 0 \quad \text{if } MCRUN = 0$
MACM fan	$P_{el, \text{ MACM fan}} = 760 \quad \text{if } MCRUN > 0$ $P_{el, \text{ MACM fan}} = 0 \quad \text{if } MCRUN = 0$
General operation	
Supply air fans 1 & 2	$P_{el, \text{ Supply air fan}} = (I_{\text{Supply air fan}} \cdot U)$
Magnetic bearing controller for MACM	$P_{el, \text{ MagBear}} = \left(50 + \left(\frac{MCRUN}{100} \right) \cdot 300 \right)$
HVAC controller	$P_{el, \text{ Controller}} = 50$

SI units for current and voltage apply in each case; the unit for power is the Watt

2.3.2.7 Heating capacity supplied and cooling capacity withdrawn on the air side

Figure 65 shows a diagram of the air path of the HVAC system with the main components. The rectangle with the 'Loads' label represents the passenger compartment. Several measuring points are shown for temperature T , relative humidity φ and air volume flow rate \dot{V} , as well as for the passenger occupancy pax , the total solar radiation I_g and the measured electric power consumption P_{el} .

The heating capacity supplied to the air is from the heater in the HVAC unit. The cooling capacity withdrawn from the air is the capacity at the evaporator of the HVAC unit. For the air-cycle systems, the air is not cooled via an evaporator, as in a conventional air-conditioning unit, but via an air-to-air heat exchanger. Figure 65 shows the system boundary as a red dash-dotted line.

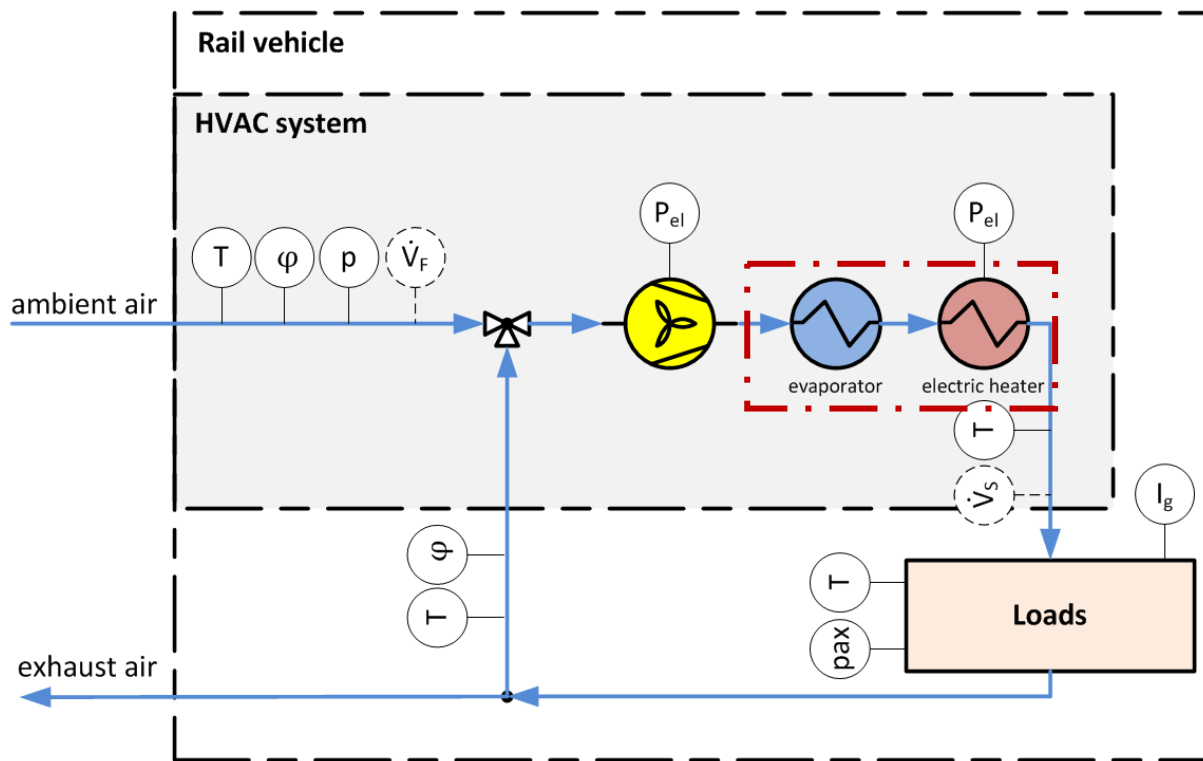
The capacity on the air side \dot{Q}_0 was determined by an equation (2). $h_{\text{supplyAir}}$ is the specific enthalpy of the supply air into the carriage; $\dot{m}_{\text{supplyAir}}$ is the corresponding mass flow. h_{mixedAir} is the specific enthalpy of the air after the supply air fan; $\dot{m}_{\text{mixedAir}}$ is the corresponding mass flow. A positive sign for \dot{Q}_0 indicates capacity at the heater (heating capacity), a negative sign indicates capacity at the evaporator (cooling capacity).

$$\dot{Q}_0 = h_{\text{supplyAir}} \cdot \dot{m}_{\text{supplyAir}} - h_{\text{mixedAir}} \cdot \dot{m}_{\text{mixedAir}} \quad (2)$$

To calculate the air states, the CoolProp (www.coolprop.org, version 5.1.2 (Bell, et al., 2014)) materials database was used. No measuring point is available for the relative humidity of the supply air downstream of the heat exchangers. For this reason, the relative humidity of the supply air had to be estimated for cooling. The mass flows were derived from the corresponding volume flows. As no direct measurement of the volume flows was performed in service, because installation of the relevant

measurement equipment was not possible, the data measured during the train's type test were used. Information about the flap positions was used and density differences were taken into account accordingly. Note that the volume flows during travel can differ slightly compared to the measurements at stop, which can fundamentally be attributed to other pressure ratios at the intake.

Figure 65: Schematic of the air path in the HVAC system with integrated components and relevant measuring points



Schematic of the air path in the HVAC system with integrated components and relevant measuring points. The sensors for volume flows have been circled with a dashed line to indicate that the volume flows were not measured in the field, but derived from available lab measurements and other process data. Source: own illustration, Liebherr

2.3.2.8 Results from the analysis of example train trips from summer and winter service

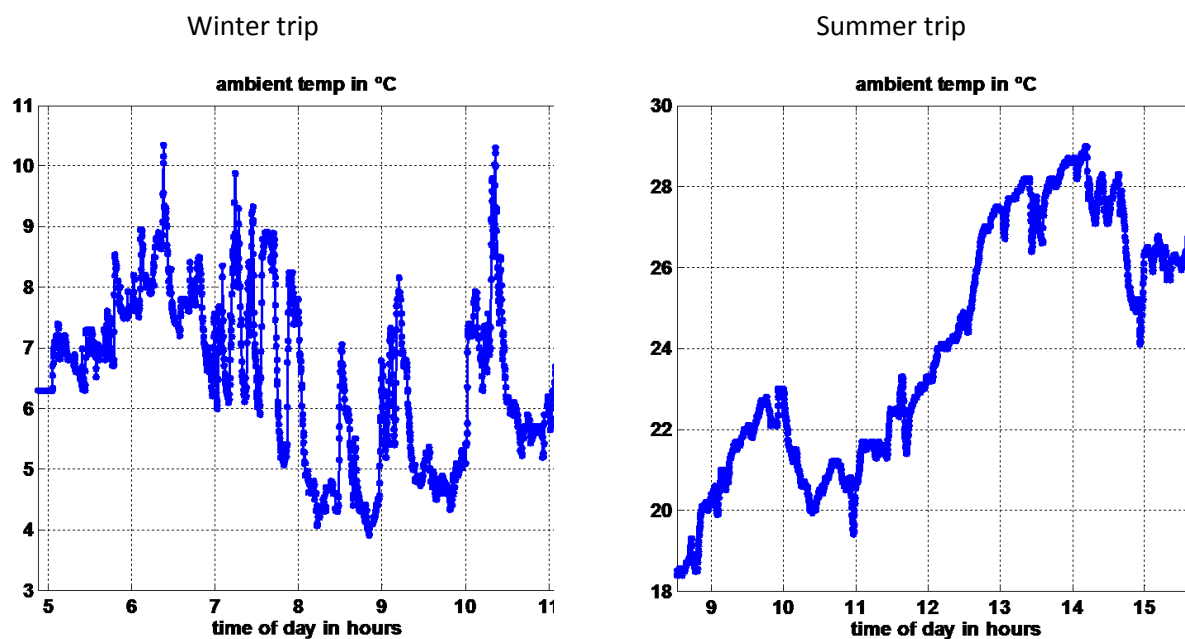
The developed methodology was applied to one train trip each in summer and winter service as an example.

Table 4 shows an overview of the two train trips that were considered. During selection, attention was paid to selecting train trips at relatively low and relatively high outside ambient temperatures. Figure 66 shows the temperature curves for each trip over the entire train trip. Relatively heavy temperature fluctuations can be seen. At an expert workshop, they were considered to be possible or plausible.

Table 4: Overview of the train trips in winter and in summer, analysed as examples

Season	Winter	Summer
Start of train trip - date	12/02/2016	06/06/2016
Start of train trip -time	05:03	08:31
Duration of train trip	6.4 h	7.5 h
Outside ambient temperature - Average	6.5 °C	24.1 °C
Outside ambient temperature	3.9 °C (Minimum)	29.0 °C (Maximum)

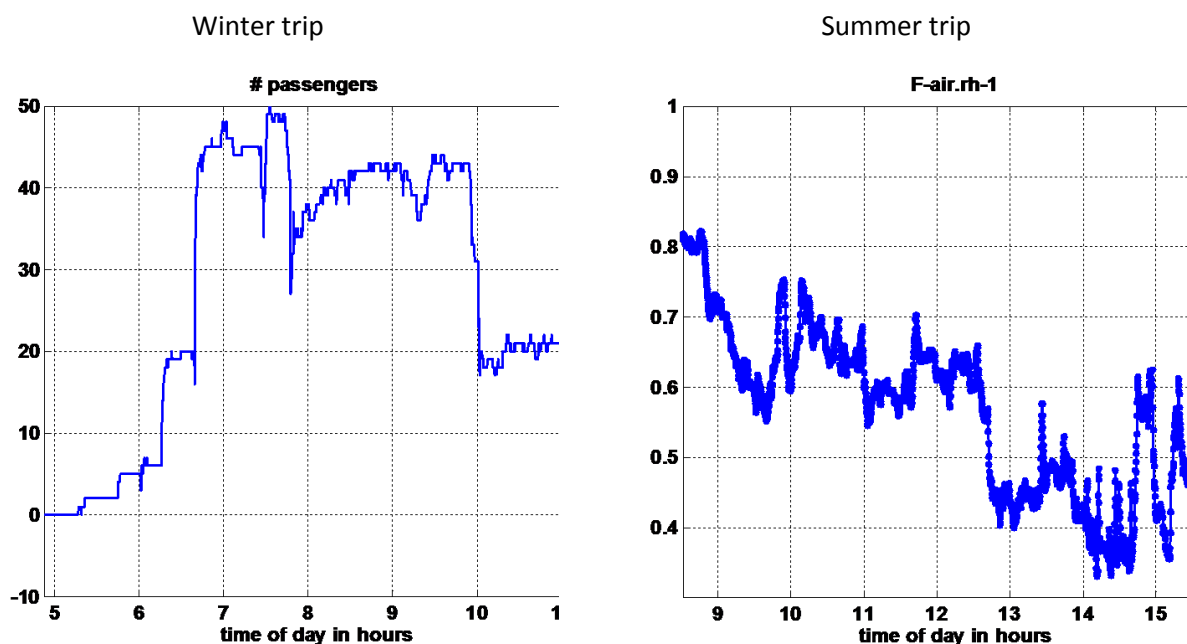
Figure 66: Temperature curves of the outside ambient temperature for the winter trip (left) and the summer trip (right)



The Y-axis shows the outside ambient temperature in °C in each case. Source: own illustration, Liebherr

Figure 67 shows the passenger occupancy signal for the winter trip on the left and the relative humidity signal for the fresh air for the summer trip on the right.

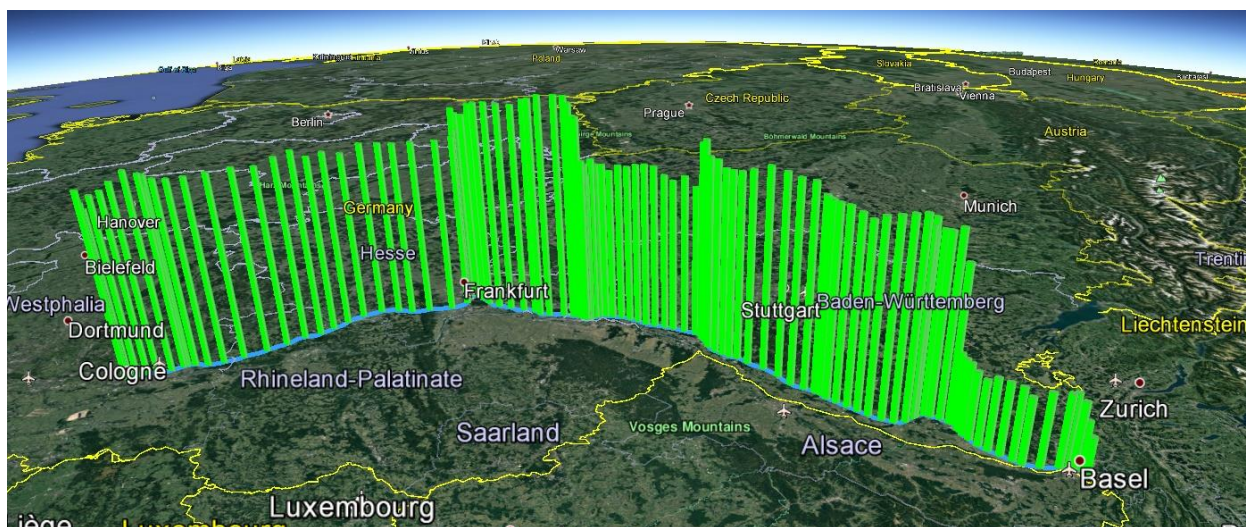
Figure 67: Number of passengers for the winter trip (left), relative humidity of fresh air during the summer trip (right)



The left chart plots the number of passengers on the Y-axis. The right chart plots the relative humidity of the fresh air on the Y-axis. Source: own illustration, Liebherr

Google Earth was used to visualise the data by location and time. In fact, any signals can be converted into a corresponding data format for analysis and verification and loaded in Google Earth. Figure 68 shows the passenger occupancy for the specific trip on 7 June 2016 over the route, as an example. Stations along the route are Cologne main railway station, Siegburg/Bonn, Frankfurt(M) airport mainline railway station, Mannheim main railway station, Karlsruhe main railway station, Offenburg, Freiburg (Breisgau) main railway station, Basel Bad railway station, Basel SBB.

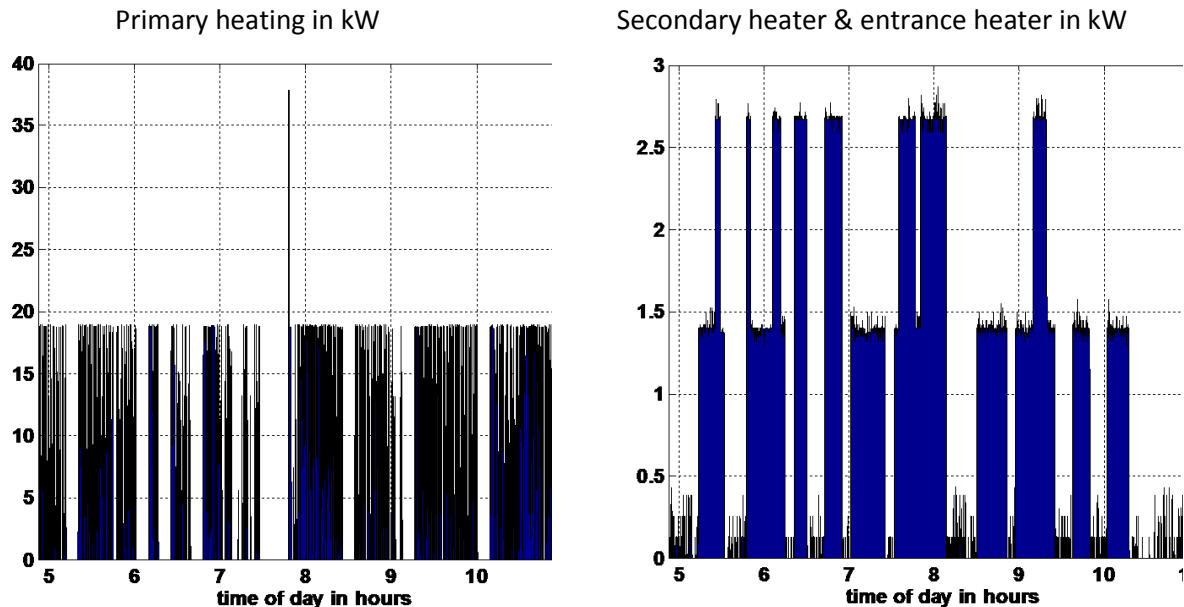
Figure 68: An example visualisation of the route showing passenger occupancy



An example visualisation of the route, showing of passenger occupancy. Trip with start time on 07/06/2016 at 12:55. Shown in Google Earth. Source: own illustration, Liebherr

The electric power consumptions against time for primary heating, secondary heating and the entrance heater during the winter trip are shown in Figure 69. The heaters are run in cycles at different levels. The cycling of the heaters is difficult to see on the charts because the time axis is compressed.

Figure 69: Electrically introduced heating capacity during example winter trip



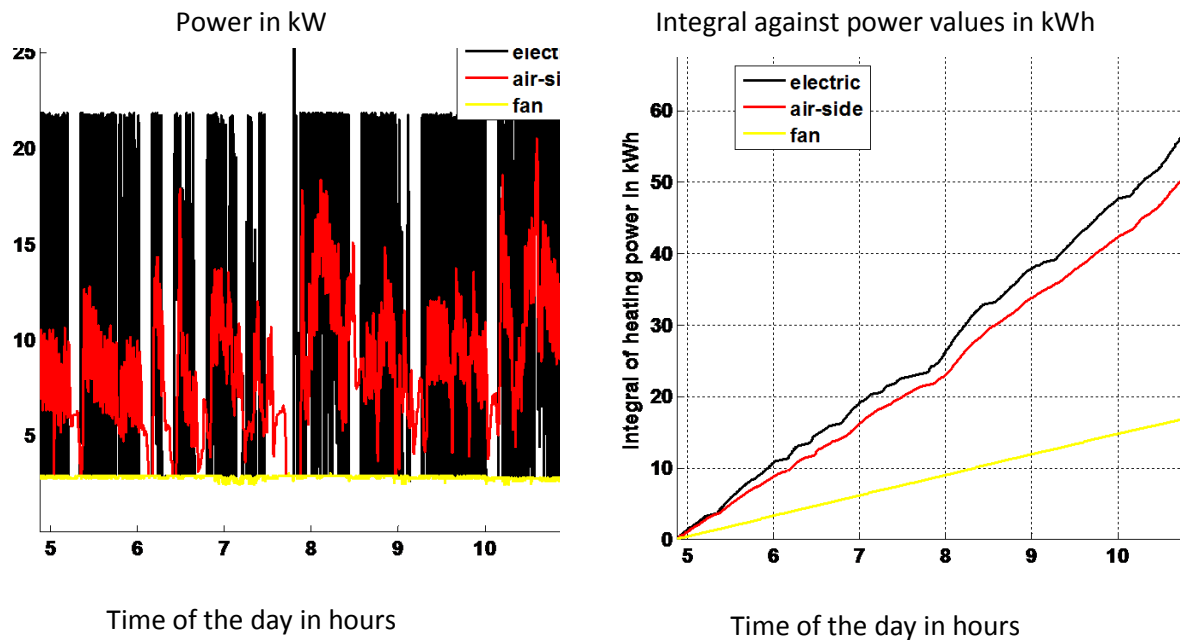
The dissipation of the fans is not included. The Y-axes show the electric heating capacity in kW. Source: own illustration, Liebherr

As electric heaters are used for heating, the COP_{Heater} is nearly 1 in the real-world scenario. This makes a direct comparison of the electrically introduced power with the power determined on the air side possible. Figure 70 provides a visualisation of the comparison.

On the right, Figure 70 shows the integral of the power values against time. A slight deviation between the curve for the electric and the air-side energy supply is apparent. At the end time, the deviation of the heating energy for the two variants is approx. 10% for the example train trip. When applied to the average deviation of the power, this deviation corresponds to less than 3% of the installed heating capacity. This relatively low deviation is a positive result in terms of verification and validation of the whole methodology.

The total electric power consumption (including fans, controllers, etc.) of the HVAC unit for the winter trip under consideration was determined using the formulas in section 2.3.2.6 and integrated for the energy consumption over the 6.4 h of the train trip. The mean electric power was approx. 10.2 kW and the total energy consumption was 69.3 kW.

Figure 70: Comparison of electrically supplied power at the main heater (black) with power determined on the air side (red) against the time of day in hours



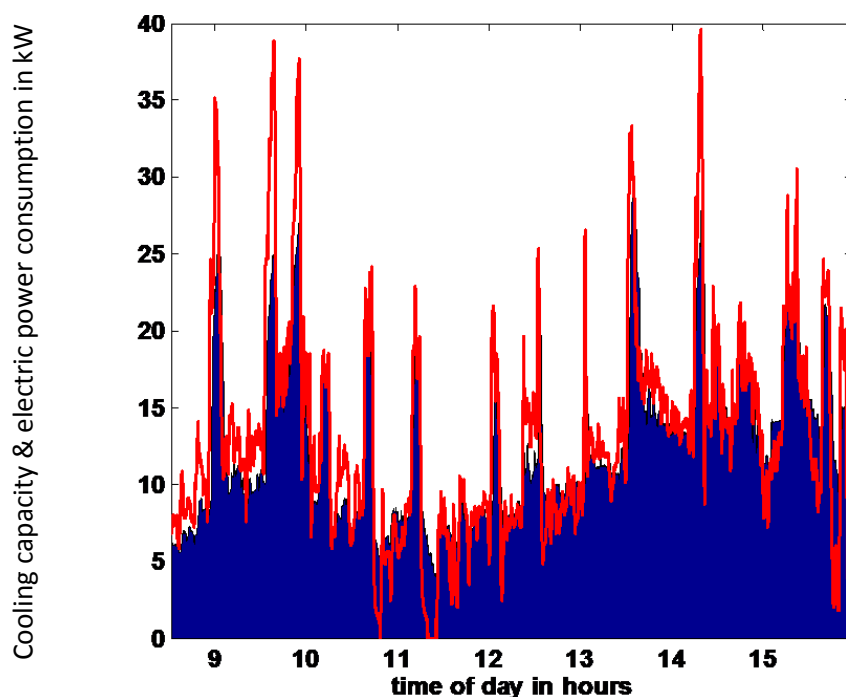
The Y-axis on the left chart shows the power in kW. The Y-axis on the right chart shows the energy in kWh. Source: own illustration, Liebherr

For the cooling capacity during the summer trip, Figure 71 shows the comparison of electric power consumption of the turbomachine (red) with the cooling capacity determined on the air side (blue).

In contrast to heating, the COP is not constant for cooling and not known in advance. The COP_{MACM} (cooling capacity at evaporator against electric power consumption of the MACM turbomachine) can be determined from the measurement data. The train trip under consideration had an average $COP_{MACM} = 0.96$. This value was considered realistic by the group of experts. In this context, reference must be made again to the relatively high outside ambient temperatures during the selected train trip. They represent a rather unfavourable operating point with relatively low COP of the ACS HVAC system. However, high outside ambient temperatures are relatively rare during the course of the year, so that the ACS HVAC system usually has significantly better COP values.

As in the procedure for the winter trip, the total electric power consumption and energy consumption (including fans, controllers, etc.) of the HVAC unit were determined using the formulas in section 2.3.2.6 for the selected summer trip. The 7.5 h summer trip had an average electric power consumption of approx. 16 kW and a total energy consumption of 119.7 kWh.

Figure 71: Cooling capacity & electric power consumption in kW



Comparison of electric power consumption of the turbomachine (red) with the cooling capacity determined on the air side (blue). Source: own illustration, Liebherr

Calibration of measurement results with a thermal simulation model in Modelica/Dymola was performed for validation and verification. As a detailed description of the corresponding simulation model for the carriage, the procedure and the results are not immediately relevant to this report, see (Luger, Virtual development and optimization of HVAC systems in rail vehicles, 2017) at this point. The selected train trips showed sufficiently good agreement between measurement data and simulation results. It was therefore possible to show that relevant measurement signals are consistent and valid.

2.3.3 Comparison of different HVAC systems with respect to electric power and energy consumption

2.3.3.1 Introduction and motivation

This section describes the general conditions and methodology for comparing different HVAC systems in terms of electric power and energy consumption. The results are presented and discussed in section 2.4.1.

The electric power consumption is relevant in terms of the required connection power or dimensioning of the on-board power supply inverter.

The electric energy consumption over a certain observation period (for example, over a year with representative operating conditions) is an essential factor for evaluating an HVAC system in terms of economic efficiency. The energy consumption is reflected in the operating costs (energy costs) and in environmental impact and emissions of different magnitudes for providing the energy depending on the energy mix being used.

In passenger rail transport, typical HVAC systems require up to 30% of the total energy consumption (Schmitt & Berlitz, 2014). A reduction of the energy consumption represents an important means of reducing operating costs and environmental impact.

2.3.3.2 Factors influencing electric power and energy consumption

Figure 72 provides a diagram of a passenger rail vehicle with heating, ventilation, air-conditioning system (HVAC system) and the most important factors influencing the thermal loads that have to be compensated by the HVAC system. All of these factors affect the electric power and energy consumption.

In cooling operation, the ambient temperature causes heat flows into the carriage and in heating operation it causes heat flows out of the carriage, i.e. heat losses. The heat load due to solar radiation is affected by the changing lighting of the vehicle side walls and windows, depending on the orientation of the railway track to the sun. Changes between the trip in the open and in a tunnel cause abrupt changes in radiation and must be taken into account, particularly for underground lines.

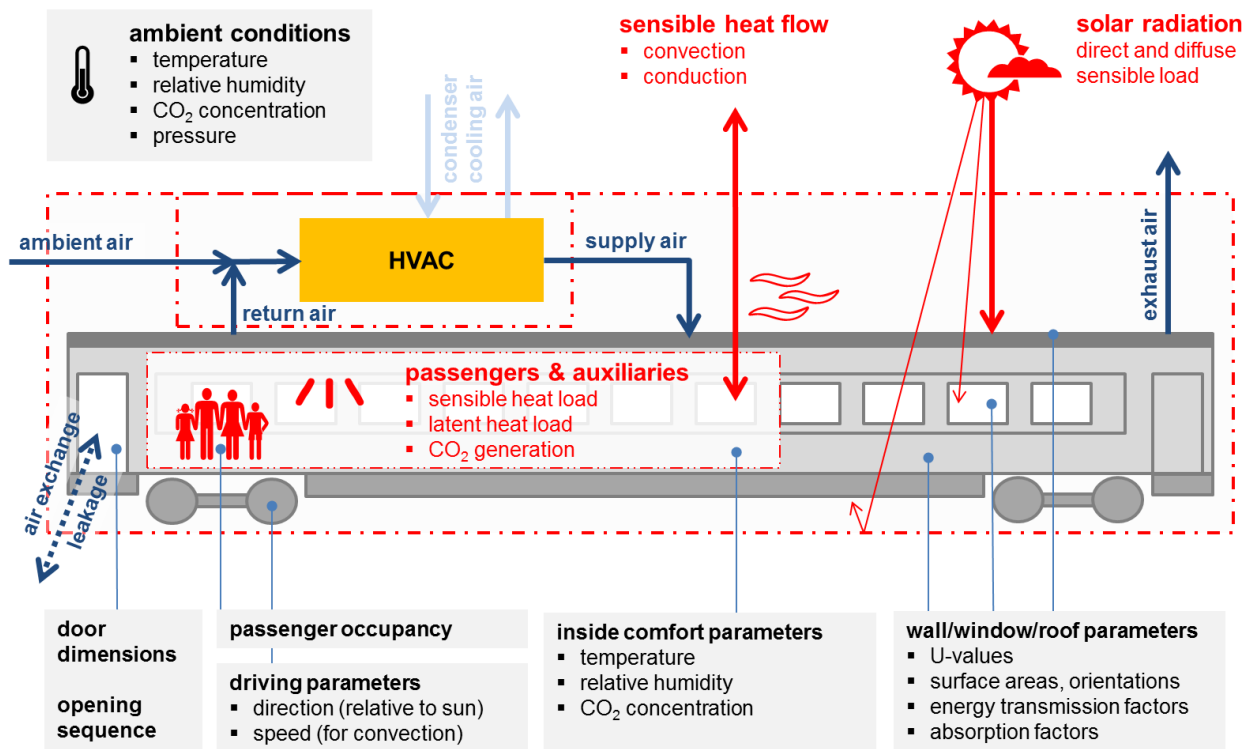
When opening doors at stations, the ambient air enters and the passenger occupancy may change quickly. Passengers cause sensitive and latent heat loads and require a certain volume flow rate of fresh air supply to compensate the CO₂ from human metabolism. The impact of heat transfer from convection on the external vehicle skin and the impact of solar radiation vary, as the external coefficient of heat transfer depends on the travel speed.

The selected comfort parameters or controlled variables, such as inside temperature, inside humidity, tolerances and regulating times, also have an impact on the power and energy consumption of an HVAC system.

The operating mode or operating profile affects the power and energy consumption of a railway HVAC system. Different operating modes have different requirements, controlled variables and different additional influencing factors, in particular the number of passengers (from comfort mode including passenger service, park mode for maintaining a specific temperature to preconditioning).

Besides the listed factors, technical aspects of the HVAC system, such as refrigerant, selection of components and dimensioning of electric power and energy consumption, are also influencing factors.

Figure 72: Diagram of a passenger rail vehicle with HVAC system, as well as loads and influencing factors



Typical air flows are indicated by blue arrows. (Luger, Kallinovskiy, & Rieberer, Identification of representative operating conditions of HVAC systems in passenger rail vehicles based on sampling virtual train trips, 2016). Source: own illustration, Liebherr

U-values=heat transmission factors

2.3.3.3 Primary, secondary and total power/energy consumption

The total power/energy consumption of an HVAC system is the sum of the primary and secondary energy consumption. The primary consumption is caused directly by the HVAC system for heating, cooling, dehumidifying, air movement, flap drives and actuators, etc. For the HVAC systems considered here, the primary consumption is supplied by electric current. The secondary power/energy consumption refers to the traction power consumption/traction energy from the mass of the HVAC system on the one hand and the impulse resistance of the intake air by the HVAC system on the other. The secondary energy consumption must be provided by the vehicle drive.

Based on model calculations for different system configurations for a high-speed train in Germany according to (Aigner, 2007), (Morgenstern & Ebinger, 2008) identified average values. They found that the total annual energy consumption therefore consists of 51% from own consumption for heating (primary consumption), 22% from own consumption for cooling (primary consumption), 22% from consumption for air intake (impulse resistance, secondary consumption) and 5% for traction due to system mass (secondary consumption). It is therefore clear that the secondary energy consumption has an impact on the total energy consumption that should not be underestimated.

"The impulse resistance is caused by the acceleration of the intake air into the ventilation units, and this air must be accelerated to the travel speed of the train", (Deutsche Bahn AG, Verringerung des Impulswiderstandes des ICE 3 Option durch den Einsatz des offenen Unterdrucksystems, 2001). Put

another way, the air is initially at rest and slows down the train when it is drawn in. To overcome the braking effect, a correspondingly higher traction force must be applied. The calculation is shown in section 2.3.3.6.

2.3.3.4 HVAC systems to be compared

Below is a description of the heating, ventilation and air-conditioning systems (HVAC systems) that were used for comparison. The details of systems 1 to 6 are described further below in this section.

(Meister, 2012) compared an air-cycle system with reverse loop (ICE 3) as in (system 1) with a vapour cycle system with variable-speed compressor and reheating (ICE-T) (system 2). The current comparison is based on the procedure followed by (Meister, 2012), but it expands this comparison, as described in detail further below.

The comparison in this project includes the following HVAC systems:

- ▶ System 1: Air-cycle system with reverse loop (ICE 3)
- ▶ System 2: Vapour cycle system (R134a) with variable-speed compressor and reheating (ICE-T)
- ▶ System 6: Air-cycle system with direct loop (new architecture, simulation)
- ▶ System 3: Vapour cycle system (R134a) with variable-speed compressor and projected bypass (based on ICE-T)

As there are no measurement data available from extensive field data records for an R134a system with bypass (system 3), there is only limited comparability here. This should be taken into account when interpreting the results.

System 1 and system 2 are installed in trains. System 6 and system 3 are advanced, optimised HVAC systems with air or R134a as refrigerant. This study compares one air-cycle system and one vapour cycle system, which are systems currently installed on trains, as well as advanced and improved systems for both technologies.

While field data was available for the comparison of systems 1 and 2, this was not the case for systems 6 and 3. Instead of field data, relevant variables for the comparison of systems 6 and 3 were derived or calculated on the basis of assumptions and models. A direct comparison of the calculated results for system 6 and 3 with the results from actual measurements for system 1 and 2 would not be appropriate and might even be misleading. Hence, the results are shown clearly separated from each other on the result charts.

From a technological point of view there is no difference in terms of heating operation for the HVAC systems compared here. Conventional electric resistance heaters are used in all of the systems. A heat pump circuit is not present in any of the HVAC systems under consideration, but would technically be possible in principle for systems 2, 3, and 6. Hence, the comparison shows the differences in cooling operation of the systems.

As described in the section on system 4, much consideration was given to the comparison with other conventional HVAC systems. However, the general conditions and the insufficient data available made such comparison impractical. In the context of an ongoing research project, the section on system 5 provides an advanced look at a comparison planned for the future with a vapour cycle system using the natural refrigerant R744.

System 1: Air-cycle system with reverse loop (ICE 3)

An air-cycle system with reverse loop (open process air circuit) is installed in the ICE 3 (see Figure 73). The process air is drawn in from the environment, expanded via the turbine at full load to approx. 0.5 bar and cooled in the process and also directed over an air-to-air heat exchanger. In the heat exchanger, heat from the supply air (which is later supplied to the carriage) is transferred to the cool process air, which cools down the supply air and heats up the process air. The process air is compressed to the ambient pressure and discharged to the environment.

Turbine and compressor are located on a mechanical shaft and are driven by an electric motor. The cooling capacity of the air-cycle system can be regulated steplessly via the exact speed control of the synchronous motor that is used. As a result, additional devices to regulate the cooling capacity (e.g. a bypass or heater for reheating) are not required in this system.

Figure 73: Diagram of this air-cycle system with the open process air circuit (system 1)

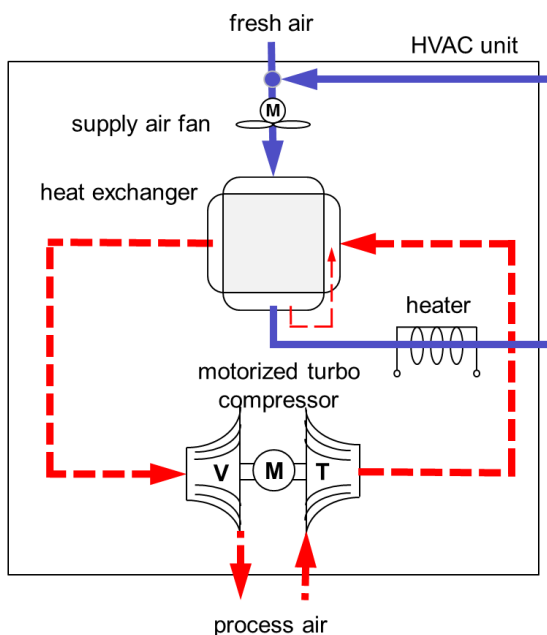


Diagram of this air-cycle system with the open process air circuit, as implemented in the ICE 3. Source: own illustration, Liebherr

System 2: Vapour cycle system (R134a) with variable-speed compressor and reheating for the low part-load range (ICE-T)

A diagram of the refrigeration circuit implemented in the ICE-T is provided in Figure 74. This is a vapour cycle system with the R134a refrigerant. This greenhouse refrigerant with a GWP (Global Warming Potential) of 1,430 is affected by the phasedown under the EU F-Gas Regulation 517/2014 and will be increasingly more difficult to obtain and significantly more expensive.

The ICE-T system features a variable-speed screw compressor for regulating the cooling capacity. However, speed control, which is itself energy-efficient, is only possible up to a certain minimum speed due to technical limitations (in particular, oil return). If the cooling capacity achieved at minimum speed is higher than the required cooling capacity, the overcooled air is heated again via an electric heater in this system. It is obvious that this capacity control concept does not meet today's requirements for high energy efficiency for the low part-load range. As reheating for capacity control is no longer state of the art, it is often explicitly excluded in current requirement specifications.

Figure 74: Diagram of vapour cycle system (R134a) with variable-speed compressor and reheating for the low part-load range (system 2)

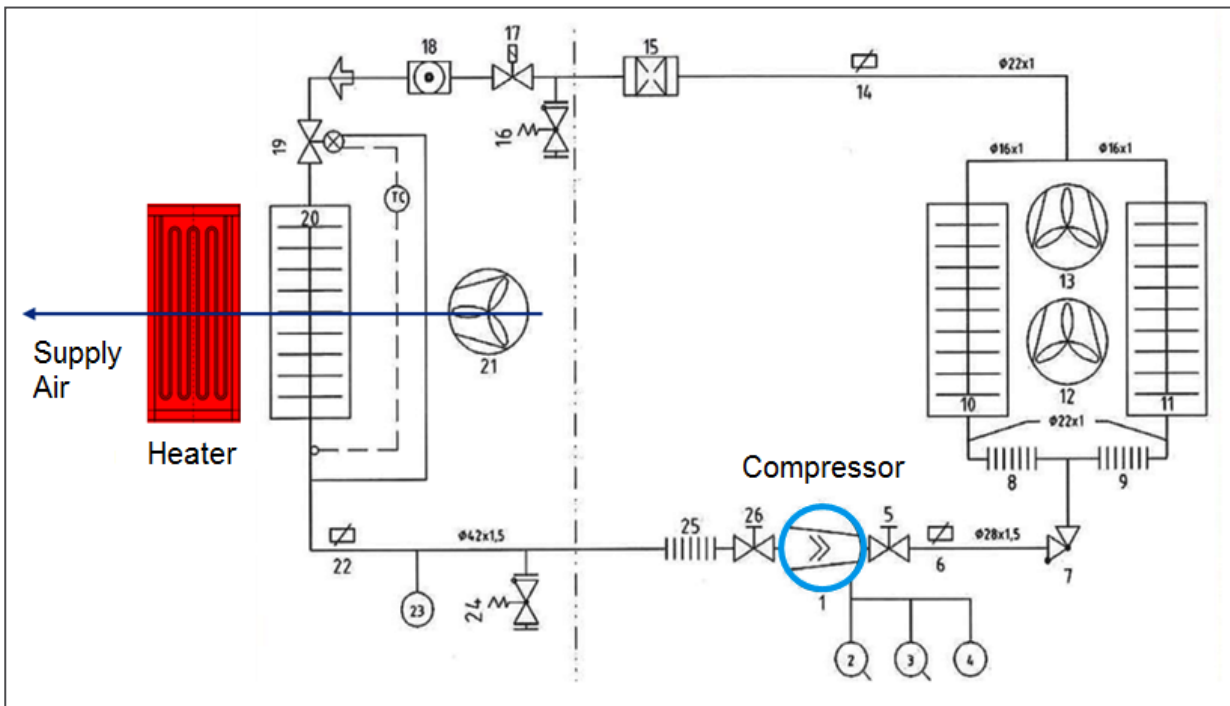


Diagram of vapour cycle system (R134a) with variable-speed compressor and reheating for the low part-load range, as used in the ICE-T. Source: own illustration, Liebherr

1 - Refrigerant compressor, 10 & 11 - Heat exchangers (condensers), 12 & 13 - Condenser fans, 19 - Expansion valve, 20 - Heat exchanger (evaporator), 21 - Supply air fan.

System 3: Vapour cycle system (R134a) with variable-speed compressor and projected bypass for the low part-load range

The HVAC system is basically the same as system 2. The refrigerant used is the greenhouse R134a. The refrigeration circuit of the system features a variable-speed screw compressor. The cooling capacity can be regulated continuously via the electronic speed control, between maximum speed and minimum speed. For a reduction of the cooling capacity below the minimum speed of the compressor, a conventional bypass circuit is used here, instead of reheating as in system 1. At approx. constant power consumption of the compressor (operation at minimum speed), the cooling capacity is lowered further by the bypass, so that the COP of the system becomes increasingly worse. In contrast to the original case, no additional heating capacity is supplied, which would lead to a significantly worse COP.

Figure 75: Diagram of vapour cycle system (R134a) with variable-speed compressor and projected bypass for the low part-load range (system 3)

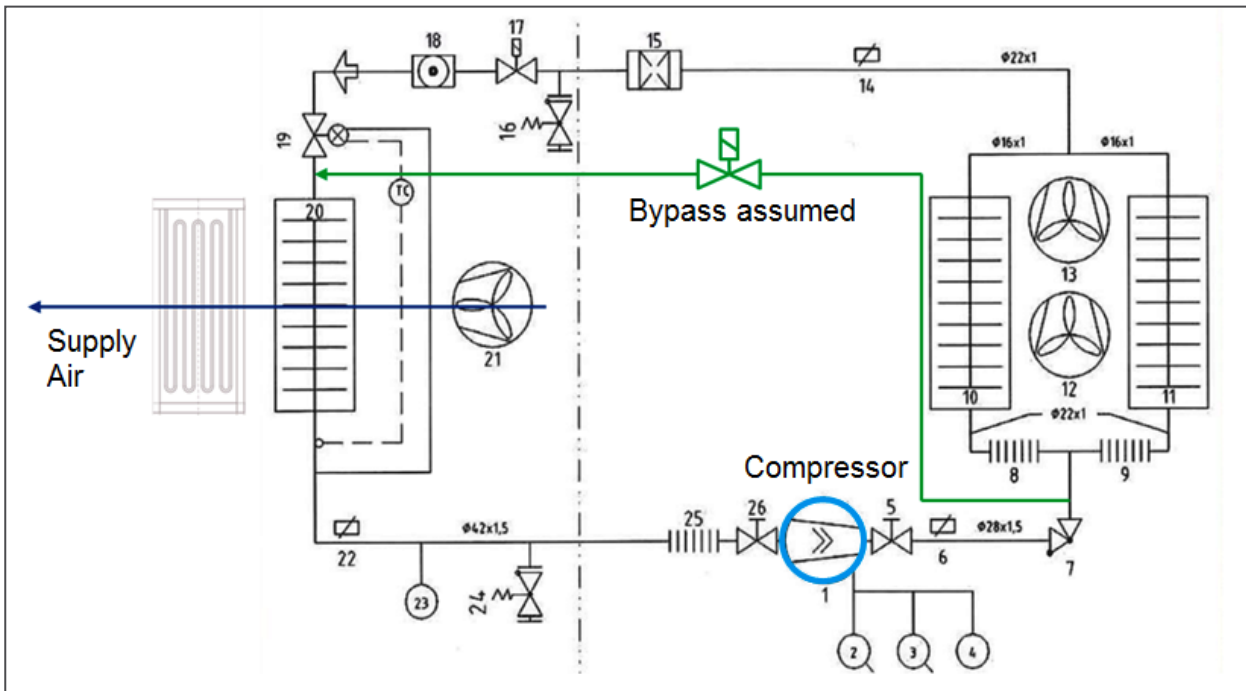


Diagram of vapour cycle system (R134a) with variable-speed compressor and projected bypass for the low part-load range (system 3). Source: own illustration, Liebherr

1 - Refrigerant compressor, 10 & 11 - Heat exchangers (condensers), 12 & 13 - Condenser fans, 19 - Expansion valve, 20 - Heat exchanger (evaporator), 21 - Supply air fan.

System 4: Advanced vapour cycle systems that were considered for potential comparison

To check the extent to which comparisons with other and advanced vapour cycle systems are possible, various DB and LVF projects were checked for suitability.

DB ICE-4

The ICE-4 features an advanced dual circuit system with the refrigerant R134a and a cooling capacity of 44 kW. No frequency-controlled compressor is used for capacity control.

For the ICE-4, there are measured values for some stationary points from the RTA climatic wind tunnel in Vienna. The measurement results were used to extrapolate annual consumption, based on assumption of certain weighting factors. Measurement data from actual field operation similar to ICE 3 and ICE-T, however, are not available at this time. The train was not commissioned until December 2017. Sufficiently extensive field data acquisition using the same approach as for the ICE 3, therefore, was not possible in the remaining time of the UBA project. Hence, a comparison of the ICE 3 (air-cycle system) with the ICE-4 (vapour cycle system) based on field data is not possible in the UBA project.

A possible solution that was considered was to compare data from the ICE-4 measured in the climatic wind tunnel under lab conditions with the field data of the ICE 3. But the very low number of measuring points in the climatic wind tunnel is not sufficient for this purpose. In addition, it should be noted that measurement in the climatic wind tunnel is done under stationary conditions, while

dynamic fluctuations of various influencing factors occur in field operation. These aspects prevent a fair and robust comparison.

Deutsche Bahn (DB) Velaro train

For the high-speed Velaro train owned by DB, which is based on the ICE 3, there is an ongoing field data programme, but its focus is on predictive maintenance and not on observations about energy consumption.

For the Velaro, climate data and process data (flap settings, etc.) are collected in the field. The power consumption is not measured, but it would be of central interest for the comparison of the different systems. Field data are also not collected continuously. The data available for the Velaro, therefore, are not suitable for a comparison with the ICE 3.

Railjet train owned by the Österreichische Bundesbahnen (ÖBB, Austrian Federal Railways)

The Railjet long-distance train owned by the ÖBB is equipped with a vapour cycle system (R134a refrigerant) with a dual-circuit design. Cooling capacity control is handled via cylinder lifting of the compressor and a bypass for the low part-load range. There are no field data available for this system at present. Field data for this train will be acquired from the first quarter of 2018 (see also the comments for system 5). The quality of the recorded measurement data will essentially match the quality of the measurement data in this project. Experience and findings from our current project could be used for the design of the field data programme for the Railjet.

System 5: Vapour cycle system with CO₂ (R744) refrigerant for a possible future comparison

LVF is working in a consortium on an HVAC system with the natural refrigerant CO₂ (R744) as part of the eco2jet project, funded by the Austrian Research Promotion Agency (Forschungsförderungsgesellschaft, FFG). As a first step, a demonstrator will be implemented on a passenger train (Railjet) owned by the ÖBB; a near-production unit will be implemented as a second step. Field data as for the UBA project will be acquired for both units, as well as for a state-of-the-art reference system with the conventional refrigerant R134a.

In the future, these data could allow for advanced comparison of different technologies or systems with different refrigerants. Data, methods and findings from the present project provide an important basis for this purpose.

System 6: Air-cycle system with direct loop

There is an advanced air-cycle system, in the same as an advanced vapour-compression refrigeration system (VCS system) was considered in system 3. A schematic of the state-of-the-art air-cycle system with direct loop is provided in Figure 76.

In the air-cycle system with direct loop, air drawn in from the environment is first compressed to overpressure and thereby heated. The heat is dissipated to the environment via an exterior heat exchanger. During subsequent expansion to ambient pressure, the air is cooled and, after mixing with recirculated air from the passenger compartment, is fed directly to the passenger compartment as supply air.

Figure 76: Diagram of air-cycle system with direct loop

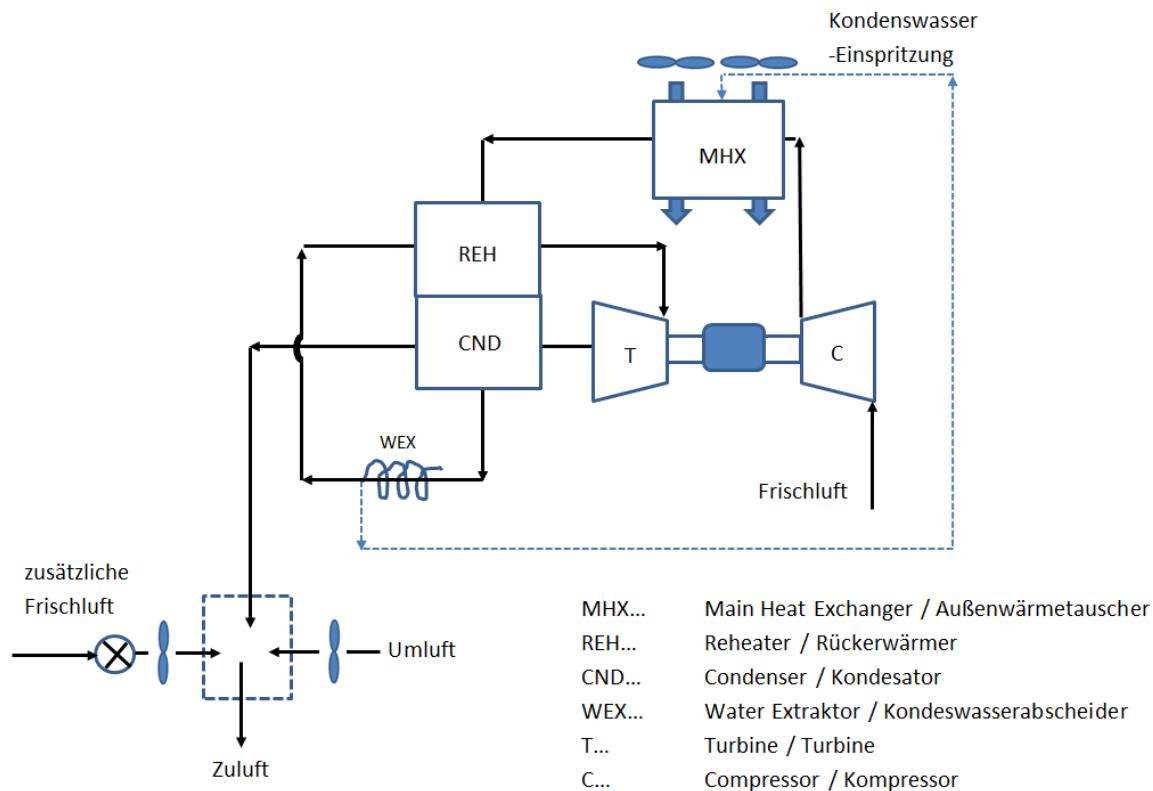


Diagram of air-cycle system with direct loop. Source: own illustration, Liebherr
 zusätzliche Frischluft=additional fresh air; Zuluft=supply air; Umluft=return air; Kondenswasser
 Einspritzung=condensate water injection

2.3.3.5 Source data

The available data determine what comparison is possible. The primary goal of this project is comparison based on data measured in standard service (field data). For proper comparison, it was decided not to compare field data from one system with simply calculated simulation data from another system. As far as possible and meaningful, the data were checked for plausibility. Data judged to be implausible were discarded.

The source data for system 1 (air-cycle system with reverse loop, ICE 3) is significantly more extensive than would be required for the comparison of a vapour cycle system with an air-cycle system described below. The extensive source data for ICE 3, however, does provide a valuable basis for advanced comparisons in future investigations. At the beginning of the project, it was not known how extensive the available data from the ICE-T measurement would be or whether comparisons with other conventional systems would be possible. For this reason, it was appropriate to design the time-consuming measurement data acquisition on the ICE 3 for the recorded signals as extensively as possible.

A review was carried out to identify to what extent missing data for the ICE-T could be derived from existing information or reconstructed by integrating additional data sources, such as the weather data from the DWD. For example, the missing information for solar radiation could have been estimated using the time stamp of the measurement data (time during the year, time during the day). However, all theoretically possible procedures would be associated with model assumptions and be subject to

significant uncertainties. This would not have significantly improved the effective quality of the comparison results. For this reason, it was decided not to reconstruct data for additional influencing factors.

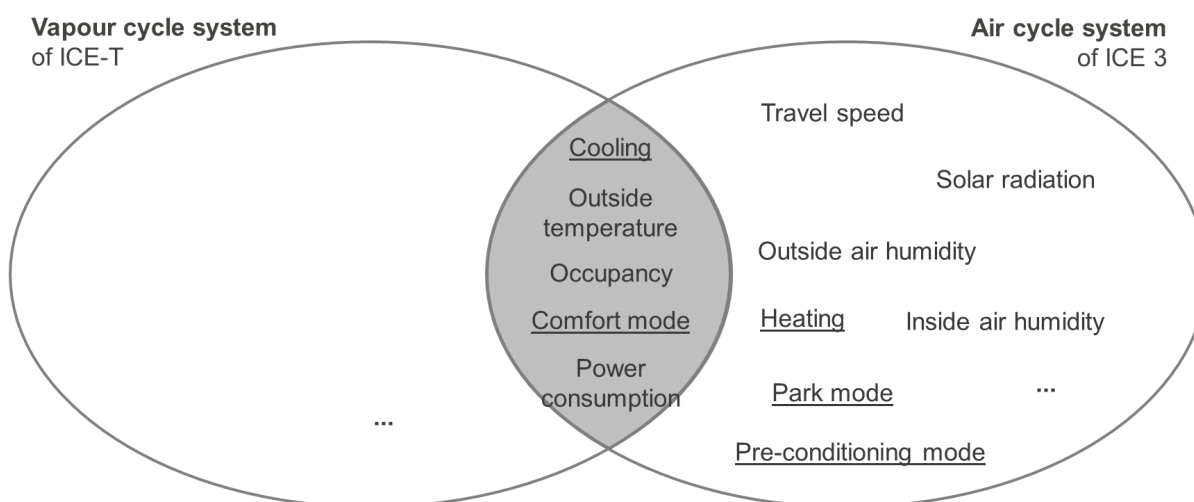
Furthermore, taking a larger number of observed influencing factors into account, i.e. greater dimensionality, would require a larger number of measuring points (samples). For the ICE-T, relatively few valid data points are available so that the dimensionality can hardly be increased beyond 2. This is obvious when it comes to the classification in section 2.3.3.5.

Intersection of the source data for comparison

Figure 77 shows the available data for system 2 (ICE-T) and system 1 (ICE 3) in the form of a Venn diagram. The data for ICE-T are from an older measurement programme by DB. The data for ICE 3 were acquired in this project. The diagram focuses on measurement signals and operating modes that are relevant to the comparison of HVAC systems in terms of power and energy consumption. It is immediately obvious that a proper comparison is only possible for the intersection of the two measurement programmes. Clearly, the limitations are essentially due to the limited availability of data for ICE-T.

The intersection includes the outside ambient temperature as well as the occupancy, as factors that influence the electric power consumption. Influencing factors such as the travel speed or the solar radiation cannot be taken into account. (For related comparisons, see 2.3.3.2 for the factors influencing electric power and energy consumption.) The comparison is for comfort operation, which includes passenger service. For park mode or pre-conditioning for the ICE-T, data are not available to the same extent. There is also not a sufficient quantity of data or there are no reliable measurement data for heating on the ICE-T.

Figure 77: Source data for ICE-T (vapour cycle system) and ICE 3 (air-cycle system)

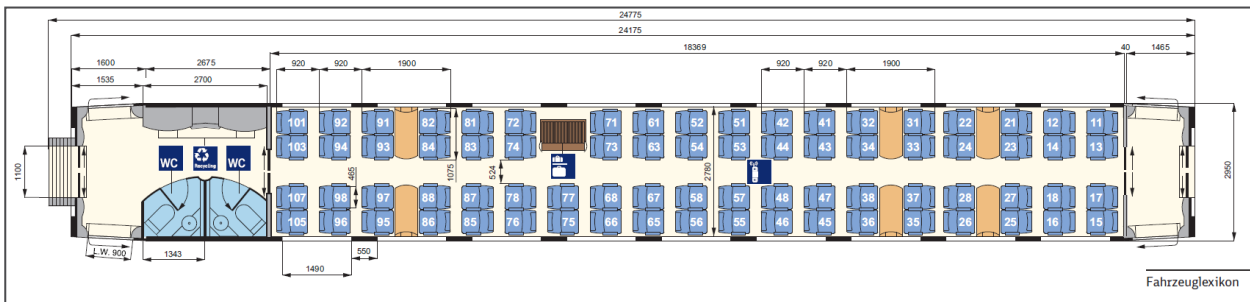


Source data for ICE-T (vapour cycle system) and ICE 3 (air-cycle system). Schematic of selected measurement signals and operating modes relevant to the comparison of HVAC systems. The elements in the intersection are used for the comparison. Source: own illustration, Liebherr

Data for system 1 – Air-cycle system with reverse loop on the ICE 3

For this project on the ICE 3, large-scale field data were acquired over a long period of time of approx. 2 years. Figure 78 shows once again the top view of the investigated carriage with 74 seats.

Figure 78: Investigated ICE 3 central carriage



Investigated ICE 3 central carriage; ICE 3, class 403, 2nd series (DB carriage type Bpmz 403.6). Source: (Deutsche Bahn AG, Fahrzeuglexikon für den Fernverkehr 2016, 2017)

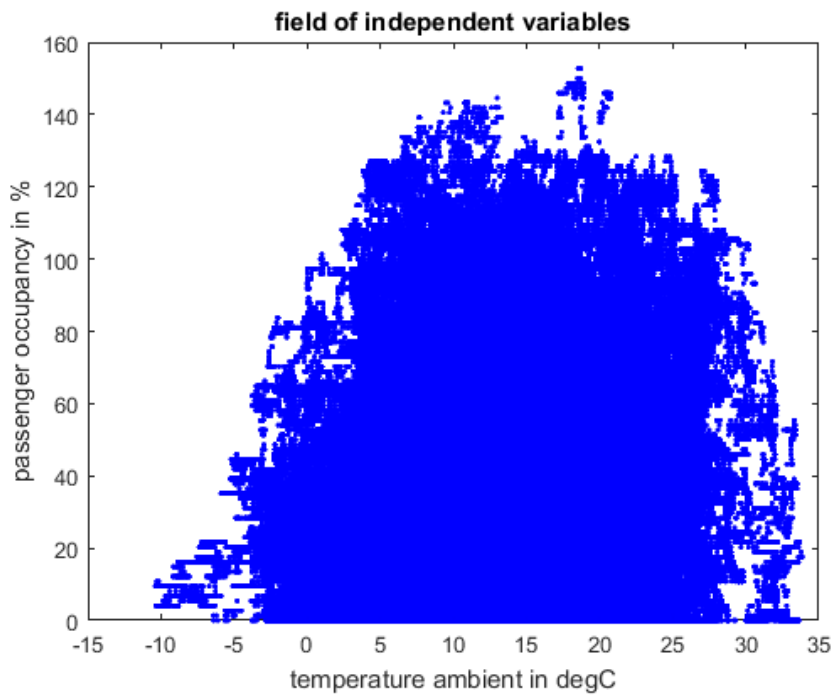
The comfort mode of the air-conditioning system (and therefore passenger service) was considered on the basis of the available ICE-T data.

The following basic approach was followed:

- ▶ Monthly pass of the speed signal and detection of stop times of at least 20 minutes. The basis for analysis was that a train trip typically starts with a stop phase of at least 20 minutes.
- ▶ Discard train trips that have a travel time of more than 24 h or travel times of less than 0.8 h. This made it possible to exclude short shunting movements or malfunctions/interruptions in data recording from the further analysis.
- ▶ Add up the counter readings of the four sensors for the occupancy count.
- ▶ Discard train trips with implausible passenger movements. See section 2.3.2.4.
- ▶ Calculate the electric power consumption according to section 2.3.2.6. For the plausible train trips, see also examples in section 2.3.2.8.

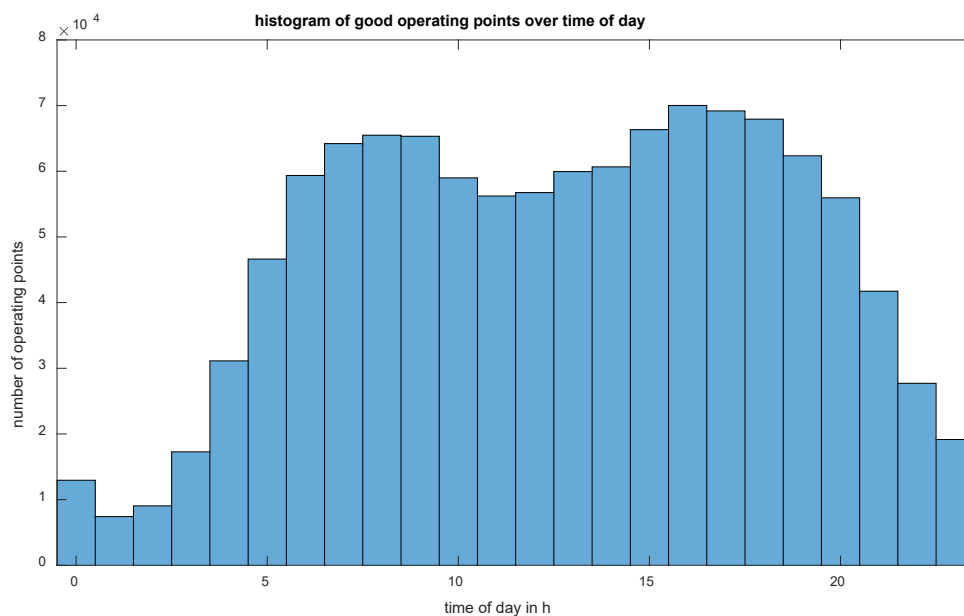
Figure 79 shows the scatter diagram of the measurement data that were finally used, plotted against the variables of outside ambient temperature and passenger occupancy, which were subsequently used as model input variables. The histogram in Figure 80 shows how many valid operating points are assigned to the respective hours of a day. It is immediately obvious and clear that there are significantly fewer valid train trips and consequently fewer operating points during the night compared to during the day.

Figure 79: Scatter diagram of valid data points for the measurements on the ICE 3



Scatter diagram of valid data points for the measurements on the ICE3. Source: own illustration, Liebherr

Figure 80: Number of operating points from valid train trips, shown per hours of a 24-hour day

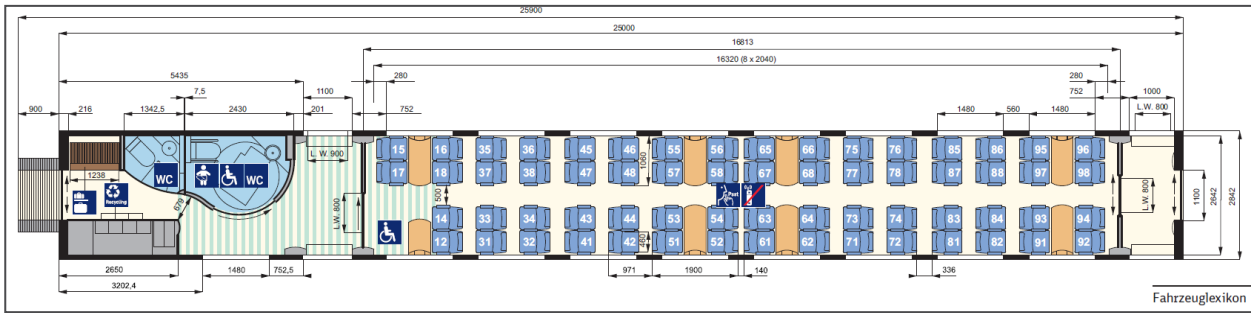


Data as of 01/10/2017. Source: own illustration, Liebherr

Data for system 2 – Vapour cycle system with variable-speed compressor and counter heater on the ICE-T

Data for the vapour cycle system on the ICE-T (system 2) were recorded by DB for two vehicles (TZ1168 and TZ1177) during an approx. one-year long period of field data acquisition (August 2008 to August 2009/September 2009). For information about field data acquisition, see (Meister, 2012). Figure 81 shows the top view of the ICE-T central carriage for investigation, which has 62 seats.

Figure 81: Investigated ICE-T central carriage



Investigated ICE-T central carriage; ICE-T, model 411, 1st series (DB carriage type Bpmbz 411.6). Source: (Deutsche Bahn AG, Vehicle lexicon for long-distance traffic [Fahrzeuglexikon für den Fernverkehr 2016, 2017])

The electric power consumption for the compressor was measured during field operation by a power meter, which was installed in the supply line between the inverter for cold and the compressor. The electric power consumption of the fans (supply air and condenser) and the heaters was determined using the switch-on signal and the related rated output.

On the ICE-T, no direct measurement as for the ICE 3 was performed for the occupancy of the carriage. It is possible to derive occupancy by using a model for the carbon footprint of a carriage occupied by passengers. The CO₂ content of the interior air recorded by the air-conditioning controller, as well as the fresh air volume flow set by the controller, are used as input for a model of this kind. (Meister, 2012) considers this to be an approximation method that is not particularly accurate. Owing to the limited accuracy of the occupancy data, no more than three occupancy classes are defined in the following classification. In this project, the model for the carbon footprint of a stationary carriage occupied by passengers was implemented and the occupancy was derived using this model.

Equation (3) shows the formula for determining the number of passengers: \dot{V}_{Zuluft} is the fresh air supply in m³/h, $C_{CO_2, Wagen}$ is the CO₂ content in the carriage in ppm based on sensor measurement, $C_{CO_2, außen}$ is the CO₂ content of the ambient air in ppm (400 ppm according to (DIN EN 13129:2016-12)) and $\dot{V}_{CO_2, per\ person}$ is the amount of CO₂ in l/h emitted per person (17.5 l/h according to (DIN EN 13129:2016-12)).

$$Number_of_passengers = \frac{\frac{\dot{V}_{Supply\ air}}{3600} \cdot \frac{(C_{CO_2, carriage} - C_{CO_2, outside})}{10^6}}{\frac{\dot{V}_{CO_2, per\ person}}{3600 \cdot 10^3}} \quad (3)$$

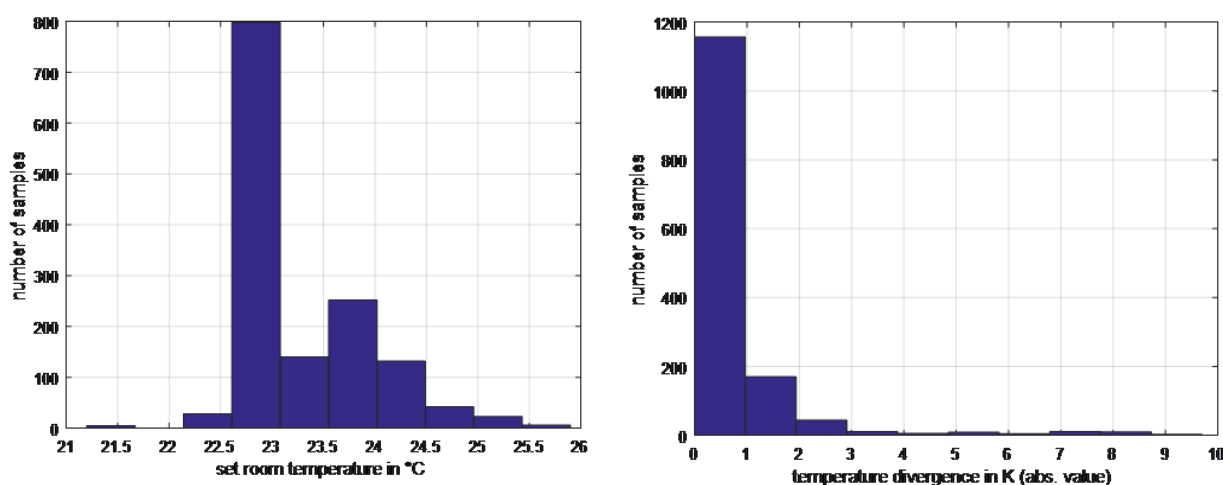
The data were sent to Liebherr by DB for comparison in the UBA project. Coordination between Liebherr and DB took place to ensure that both sides had the same understanding for interpretation of the data. The power consumption data were already prepared by DB. In particular, different data sources were already combined and the signal values were averaged in hourly increments. The raw data were only partially available. For this reason, the evaluations do not directly build on the raw data.

Ultimately, the source data included the following signals: electric power consumption of the compressor, electric power consumption of the heaters, electric power consumption of the condenser and supply air fans, room temperature target value, mean actual value of room temperature, difference between target and actual value of room temperature, outside ambient temperature, speed preset for the compressor, and the derived passenger occupancy.

After filtering for valid values, more than 1,400 datasets (time stamps) were available for comparison for the two carriages of the partial trains TZ1168 and TZ1177.

It was then a question of what operating mode (park mode, pre-heating/pre-cooling, comfort mode) the remaining data describe. If passengers are in the carriage, the system operates in comfort mode. The analysis of the target temperature as well as of the deviations between target and actual temperature (absolute value) in Figure 82 suggests that the majority of the datasets (samples) describe the comfort mode. Only a few samples show a temperature deviation >2.5 K. These samples were discarded.

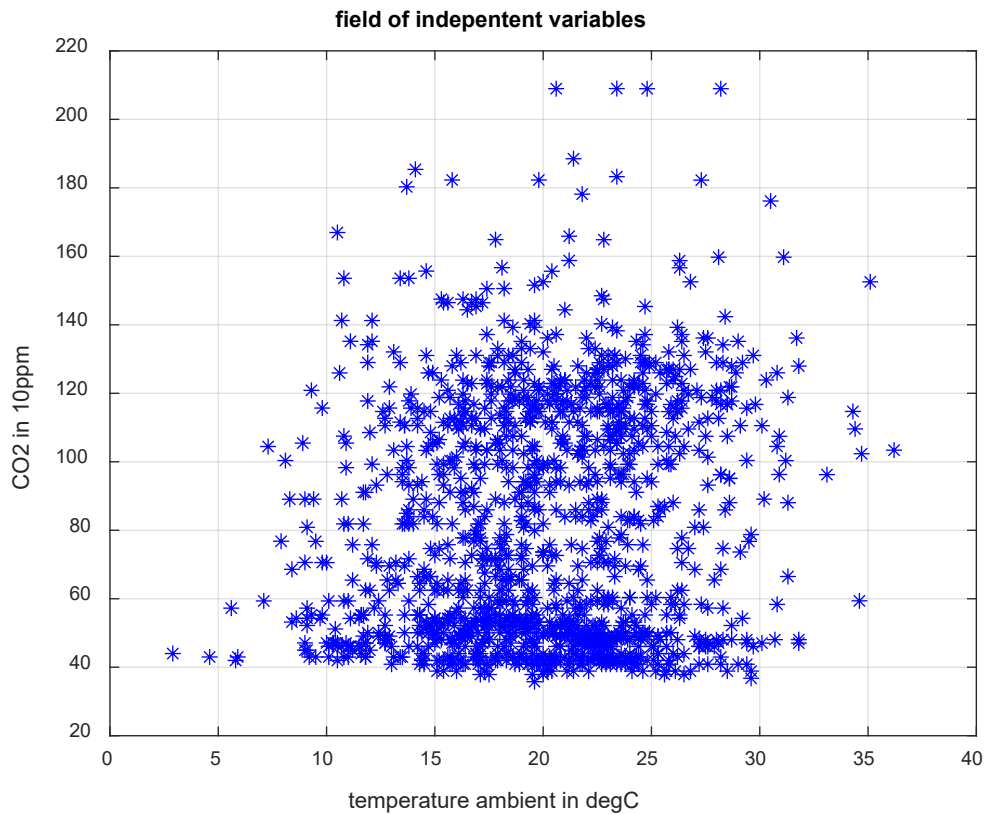
Figure 82: Target temperature (left) and difference between target and actual temperature (right) (absolute value) for ICE-T



The left chart plots the target temperature on the X-axis. The right chart plots the value for the difference between target and actual temperature. The Y-axis shows the number of datasets in each case. Source: own illustration, Liebherr

Figure 83 shows the data points valid for the comparison as a scatter diagram.

Figure 83: Scatter diagram of valid data points from the ICE-T data



Scatter diagram of valid data points from the ICE-T data. Source: own illustration, Liebherr

As hardly any or no data were available for low ambient temperatures, no direct statement could be made about the power consumption in heating operation. To be able nonetheless to make a comparison in terms of the annual energy consumption (cooling and heating), the data for heating operation on the ICE-T were derived in a suitable way from the field data for heating operation acquired on the ICE 3. This approach is justified because – as described in section 2.3.3.4 – there are no technical differences in heating operation between the systems compared here or between the ICE 3 and ICE-T.

The constant power consumption for the magnetic bearing controller for the air-cycle system on the ICE 3 was also taken into account for heating operation on the ICE 3, but factored out for the ICE-T since it does not have a turbomachine on active magnet bearings. Consequently, there is a minor advantage in terms of power and energy consumption for the vapour cycle system (ICE-T) compared to the air-cycle system (ICE 3).

Data for system 3 – Vapour cycle system (R134a) with variable-speed compressor and assumed bypass for the low part-load range

Measurement data for an R134a system with bypass were not directly available. The analysis was therefore done purely mathematically based on measurement data from the ICE-T. This means in practice that the heating capacity for reheating was not added to the power consumption of the compressor.

Note that a refrigerant-based bypass in a real system modifies the operating point of the compressor, which results in a slightly different electric power consumption for the compressor than assumed in a simplified way in the present analysis. The effort to integrate the change of operating point into available data would have been disproportionate. However, it can be assumed that the simplification leads to a workable approximation in terms of overall accuracy.

Data for system 6 – New air-cycle system with direct loop

There are currently no measurement data available for the new air-cycle system with reverse loop. Results from the numeric simulation were therefore used for the comparison. The architecture was mapped in Liebherr's internal EOLE simulation software for this purpose. The simulation software has proven its value in many years of use at Liebherr in various research and customer projects. The model for the turbomachine is based on characteristic maps. Characteristic maps were also used for various heat exchangers. Model inputs were temperature, humidity and mass flow rate of fresh air, the temperature and humidity of the recirculated air and the temperature and mass flow rate of the supply air. The model output was the electric power consumption of the turbomachine. The electric power consumption of additional components (e.g. HVAC controller) was added accordingly.

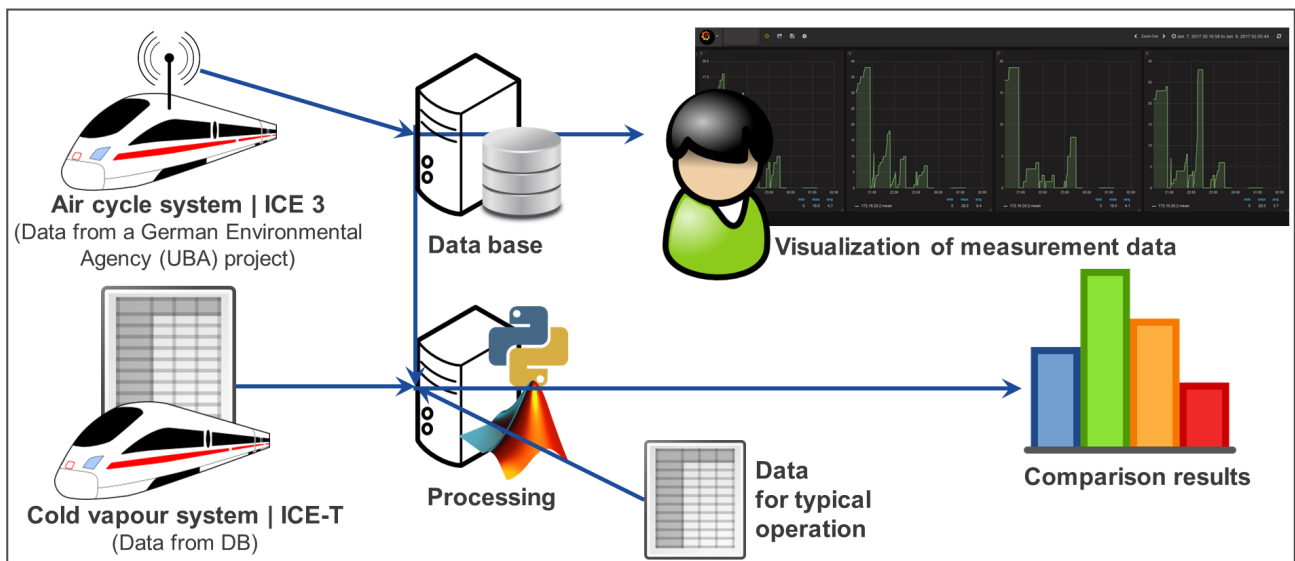
Comparing the new air-cycle system with the other HVAC systems required determining a value for the electric power consumption for every class according to the classification described in the following section 2.3.3.6. As a first step, the electric power consumption was calculated for one operating point per class, using the simulation software. This operating point per class was identified as follows: For the ICE 3, the above input variables into the model and the air-side heating capacity or cooling capacity \dot{Q}_0 according to section 2.3.2.7 were determined, based on measurement data for every time stamp of the corresponding measurement data. The second step was classification – substantially described in section 2.3.3.6. The mean of the air-side heating capacities and cooling capacities of the operating points assigned to the class was then calculated for each class. The operating point the heating capacity or cooling capacity of which showed the least deviation from the mean of the heating capacity or cooling capacity was used for further calculation. The operating point also provided all the input variables for the EOLE model.

2.3.3.6 Methods of comparison

Basic procedure and system limits

Figure 84 schematically describes the data flow for the system comparison based on field data (system 1 and 2). The project uses specially developed evaluation and calculation programs, which were integrated in particular into the Matlab software environment from TheMathWorks. These evaluation and calculation programs access ICE 3 field data via the integrated influxDB database and access files from DB with field data from the ICE-T. The results of comparison are finally generated on the basis of additional information and data for typical operation. The determined power consumptions for systems 3 and 6 were processed in a very similar way.

Figure 84: Schematic for the system comparison of power and energy consumption for the air-cycle system (ACS) on the ICE 3 and the R134a vapour cycle system on the ICE-T



Schematic for the system comparison of power and energy consumption for the air-cycle system (ACS) on the ICE 3 and the R134a vapour cycle system on the ICE-T. Source: own illustration, Liebherr

About the system limits: The analysis provided here of the power and energy consumption applies to the HVAC system including compressor or turbomachine, heaters, supply air fans, solenoid valves, servomotors for flap control drives and controllers. The power and energy consumption of the exhaust air fans was not included, as these fans are not installed in the HVAC systems and are used independently of the technology, i.e. for the ICE-T as well as the ICE 3. However, as the technology has an impact on the secondary energy consumption due to impulse resistance (depending on intake air volume), the secondary energy consumption was included in the analysis.

The comparison applies to one carriage. Carriage TW7 was used for the ICE 3, since this carriage was equipped with the most extensive measurement equipment, in particular the sensors for passenger counting were installed in the TW7. Furthermore, the TW7 is key to the dimensioning of the HVAC system for the entire train. As the selected carriages of the ICE 3 and ICE-T are not identical in terms of the number of seats, the power and energy consumption for a single seat was standardised – as proposed and done by (Meister, 2012) – for the purpose of comparison. (Meister, 2012) notes that other standardisations would also be possible, e.g. for the design cooling capacity. According to (Meister, 2012), the relationship of these variables corresponds “almost exactly to the ratio of number of seats so that no different tendencies would have been the result when comparing the air-conditioning systems of both series”.

The data for comparison was processed in the following steps, which are described below in more detail. The basic approach in this form was in essence proposed by (Meister, 2012).

- ▶ Step 1: Classification of the electric power consumption
 - Model of the electric power consumptions of different HVAC systems
- ▶ Step 2: Weighting and summing of the classes
 - Average electric power consumption of the HVAC systems
- ▶ Step 3: Scaling to typical number of operating hours/year (6,570 h/year)
 - Electric energy consumption per year of the HVAC systems

Due to the limited availability of data from the ICE-T, influencing factors such as solar radiation and travel speed could not be explicitly considered as model input variables in the system model (classification). For this reason, but also because of general measurement uncertainties, certain uncertainties must be assumed in the results. As the relevant influencing factors are not directly quantifiable, a quantitative statement of the (measurement) uncertainty is not possible. (Meister, 2012) also points out this issue.

Modelling via classification of the electric power consumption (Step 1)

As suggested in (Meister, 2012) and by DB in this project, a two-dimensional classification of the electric power consumption was carried out, i.e. the power consumption was expressed using two independent variables – outside ambient temperature and passenger occupancy.

Figure 85 shows the classification scheme for the point-by-point measurement data. From the point of view of Liebherr and DB, important influencing factors affecting operation of a railway HVAC system and consequently its electric power consumption are not explicitly taken into account here. This includes solar radiation (direct and diffuse radiation, as well as position of the sun in relation to the carriage alignment) and the speed of the train (effect on the thermal convection on the carriage shell) (see section 2.3.3.2). As explained in section 2.3.3.5, data for additional influencing factors are however not available for the comparison. The methodology for classification here is therefore the best possible.

Figure 85: Diagram showing classification of the point-by-point measurement data

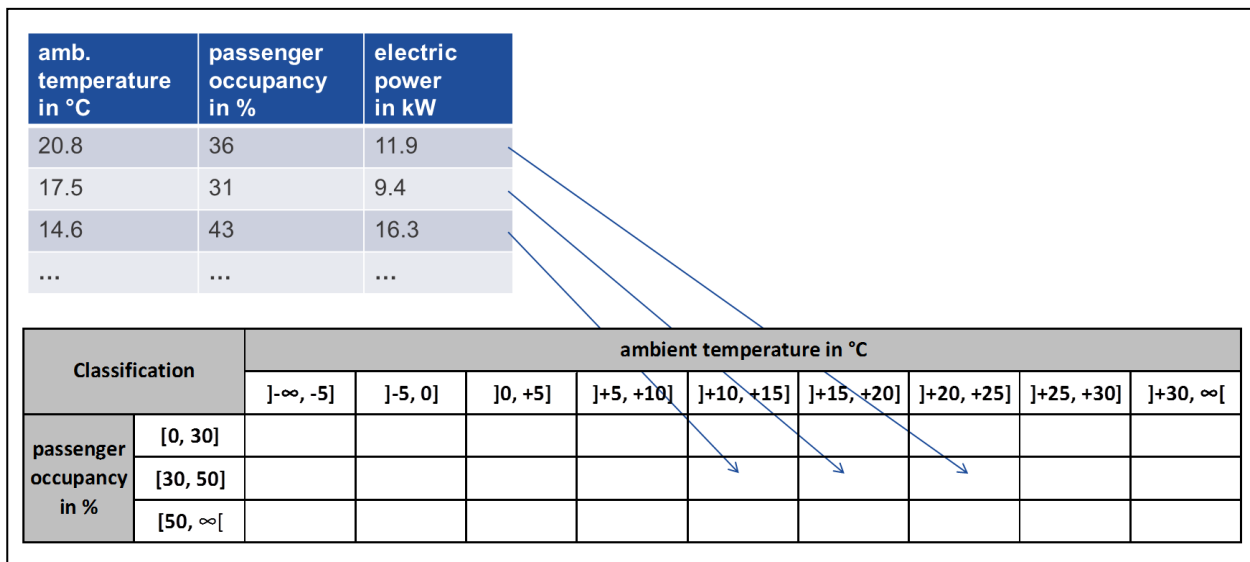


Figure 86, Figure 87 and Figure 88 show results of classification for cooling and heating on the ICE 3 and ICE-T in the form of histograms for the individual classes. For heating on the ICE-T, the histograms are not shown, since they essentially correspond to those of the ICE 3. The X-axis of the histograms is the electric power in kW, the Y-axis is the number of data points. It is immediately clear that the values for the electric power consumption within a class cover a very wide range.

Similar evaluation for this project by DB also showed large standard deviations within individual classes. An important reason is that only two and not all factors influencing the electric power

consumption can be taken into account in the classification. (For comparisons, see section 2.3.3.5.) As a result, a data point with a temperature of 24 °C, 40% passenger occupancy and no solar radiation (night trip) and a data point with a temperature of 24 °C, 40% passenger occupancy and very high solar radiation through the windows (day trip with corresponding orientation of the carriage in relation to the sun), for example, are mapped in the same class. But the two data points have significantly different cooling capacities and, therefore, electric power consumptions, which results in a large bandwidth within the class.

The three figures also show the number of points for each class. The number of cooling points decreases with decreasing outside ambient temperatures, while the number of heating points increases inversely. It can also be seen that the number of data points for ICE-T is significantly lower than for ICE 3. The number of data points within a class is related to the width of a class.

After classifying the measured values into the classes, the values within the individual classes are aggregated. This means that a suitable average is created for each class against the electric power consumption assigned to the respective class, so that each class is ultimately associated with one value. The mean (arithmetic mean) or the median (the 0.5 quantile) can be used for this average value. A mixed form of mean and median is also possible. The median provides a high degree of robustness in case of outliers in the underlying data; the commonly used mean is distorted more by outliers. How the average is formed affects the final result of the comparison. Calculations were made for both variants.

Ultimately, it was found that the arithmetic mean is a suitable mean value in the present case. One argument in favour of using the mean is that the data within a cell do not (should not) contain any true outliers. The broad spread of the data is caused by influencing factors, such as the solar radiation, that are not directly taken into account. True outliers or obviously wrong values were discarded with great care prior to creating the mean value. The mean was also used by (Meister, 2012).

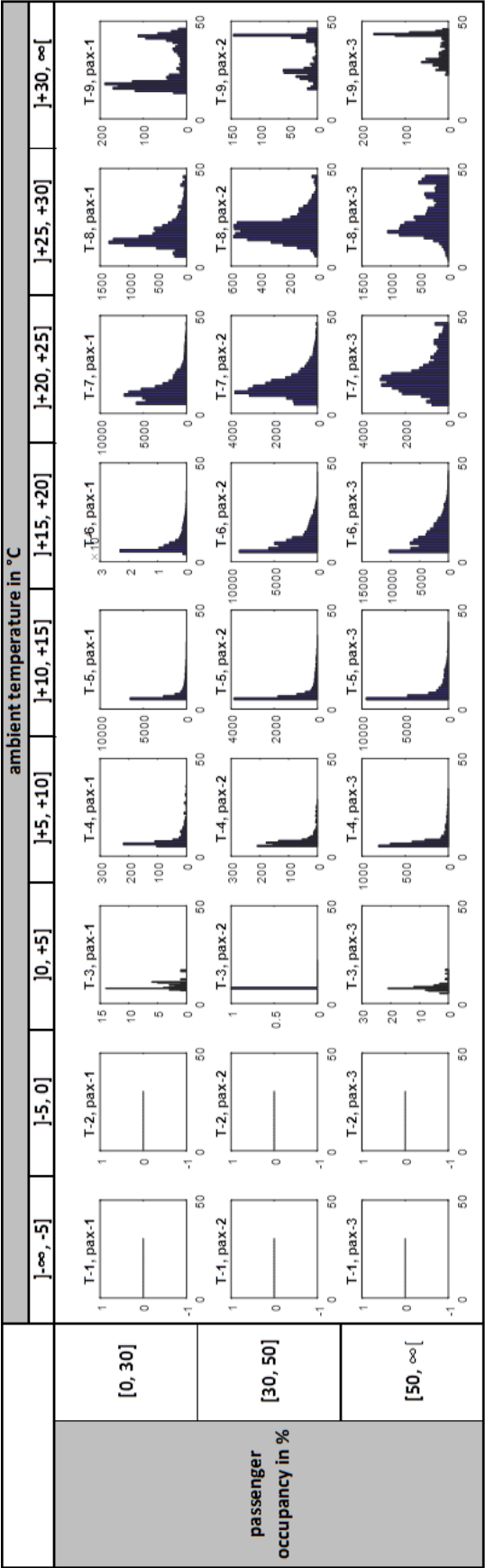
Other parameters for classification relate to the class definitions of the individual variables, as such: Limits of the classes, number of classes, width of classes (equidistant or varying). The selected width of the individual classes affects the resolution and the number of data points per class. Different classifications were considered in the project.

A classification with the class boundaries $\{-5, -5, 0, 5, 10, 15, 20, 25, 30, >30\}$ is used below for the outside ambient temperature in °C. This creates 9 classes. For the passenger occupancy in %, 3 classes of different widths were used with the class boundaries at $\{0, 30, 50, >50\}$ (see Figure 85).

The passenger occupancy was classified in consultation with DB, as in (Meister, 2012). The class boundaries for the outside ambient temperature in °C were defined by (Meister, 2012) as $\{15, 20, 25, >25\}$, so that there were only 3 classes. An essential difference with respect to the classification for the outside ambient temperature between the study by Meister and the present study is that the lowest temperature observed by Meister was 15 °C. For this reason, Meister did not consider the strong part-load range and the heating under it.

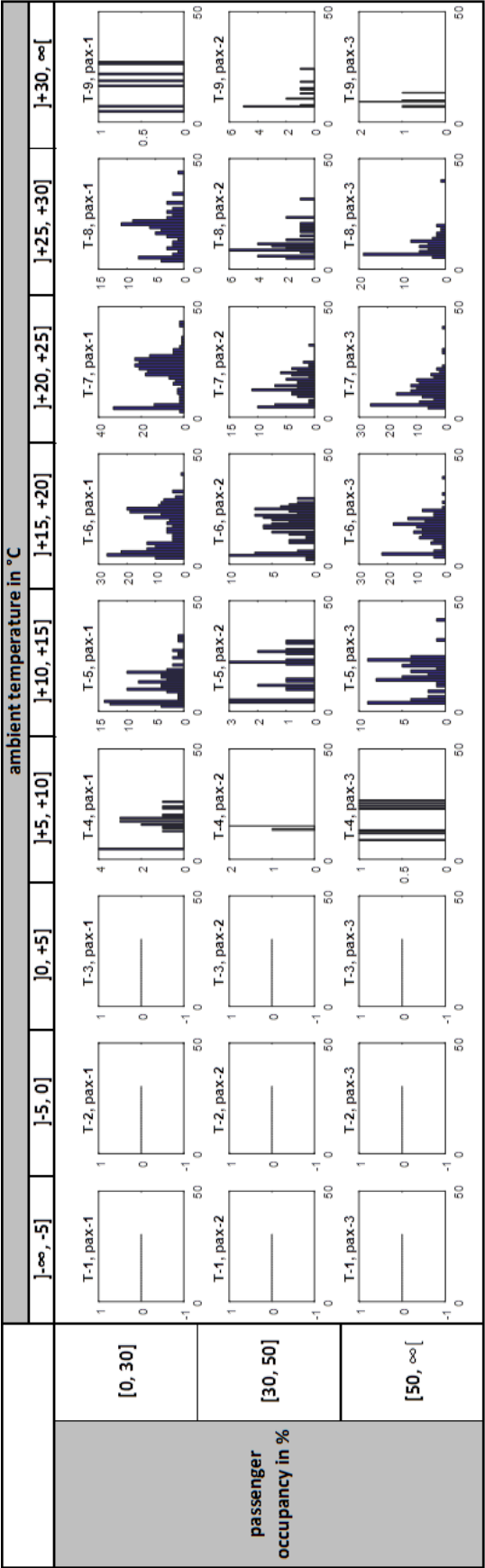
Figure 89 summarises the number of data points, the mean value and the standard deviation for each class for cooling on the ICE 3 and ICE-T. Figure 90 similarly summarises the number of data points, the mean value and the standard deviation for each class for heating on the ICE 3. The mean values are then used for the evaluation.

Figure 86: Classification of measured values for the ICE 3, cooling



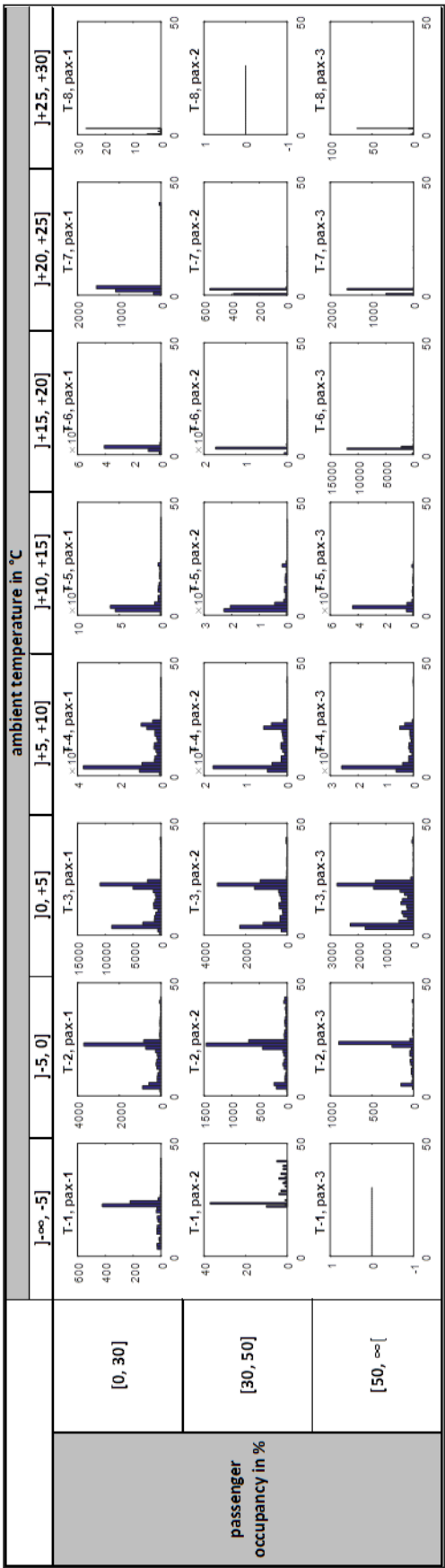
Classification for the ICE 3, cooling: The histograms show electric powers in kW for different measuring points assigned to a class. Source: own illustration, Liebherr

Figure 87: Classification of measured values for the ICE-T with reheating, cooling



Classification for ICE-T with reheating, cooling: The histograms show electric powers in kW for different measuring points assigned to a class. Source: own illustration, Liebherr

Figure 88: Classification of measured values for the ICE 3, heating



Classification for the ICE 3, heating: The histograms show electric powers in kW for different measuring points assigned to a class. Source: own illustration, Liebherr

Figure 89: Results of the classification of measured values on the ICE 3 and ICE-T for cooling

ICE 3

Samples		ambient temperature in °C								
]-∞, -5]]-5, 0]]0, +5]] +5, +10]] +10, +15]] +15, +20]] +20, +25]] +25, +30]] +30, ∞[
passenger occupancy in %	[0, 30]	0	0	49	645	13732	65808	51951	9543	1586
	[30, 50]	0	0	1	889	9277	41227	28586	5904	618
	[50, ∞[0	0	84	2690	24162	65206	37787	11216	948

Mean in kW		ambient temperature in °C								
]-∞, -5]]-5, 0]]0, +5]] +5, +10]] +10, +15]] +15, +20]] +20, +25]] +25, +30]] +30, ∞[
passenger occupancy in %	[0, 30]	0.00	0.00	9.30	8.87	7.64	9.19	12.40	16.59	26.04
	[30, 50]	0.00	0.00	7.83	7.91	8.28	10.76	14.81	19.41	32.35
	[50, ∞[0.00	0.00	8.30	7.95	8.93	12.76	19.43	26.08	36.80

Standarddeviation in kW		ambient temperature in °C								
]-∞, -5]]-5, 0]]0, +5]] +5, +10]] +10, +15]] +15, +20]] +20, +25]] +25, +30]] +30, ∞[
passenger occupancy in %	[0, 30]	0.00	0.00	2.18	5.13	4.43	5.15	6.53	7.66	11.02
	[30, 50]	0.00	0.00	0.00	3.83	5.28	6.00	6.78	6.57	10.06
	[50, ∞[0.00	0.00	2.04	4.21	5.59	6.96	9.24	10.11	7.05

ICE-T

Samples		ambient temperature in °C								
]-∞, -5]]-5, 0]]0, +5]] +5, +10]] +10, +15]] +15, +20]] +20, +25]] +25, +30]] +30, ∞[
passenger occupancy in %	[0, 30]	0	0	0	20	98	227	236	77	7
	[30, 50]	0	0	0	4	23	98	85	33	13
	[50, ∞[0	0	0	7	63	145	141	62	7

Mean in kW		ambient temperature in °C								
]-∞, -5]]-5, 0]]0, +5]] +5, +10]] +10, +15]] +15, +20]] +20, +25]] +25, +30]] +30, ∞[
passenger occupancy in %	[0, 30]	0.00	0.00	0.00	15.63	11.90	15.54	19.22	17.60	17.32
	[30, 50]	0.00	0.00	0.00	14.40	16.62	16.60	13.75	12.33	11.53
	[50, ∞[0.00	0.00	0.00	19.05	15.87	14.79	11.82	10.60	9.36

Standarddeviation in kW		ambient temperature in °C								
]-∞, -5]]-5, 0]]0, +5]] +5, +10]] +10, +15]] +15, +20]] +20, +25]] +25, +30]] +30, ∞[
passenger occupancy in %	[0, 30]	0.00	0.00	0.00	6.52	7.57	9.29	9.10	8.36	8.83
	[30, 50]	0.00	0.00	0.00	1.02	9.65	7.81	6.19	6.24	5.48
	[50, ∞[0.00	0.00	0.00	7.66	8.02	6.88	5.74	5.39	2.14

Figure 90: Results of the classification of measured values on the ICE 3 for heating

Samples		ambient temperature in °C								
]-∞, -5]]-5, 0]]0, +5]] +5, +10]] +10, +15]] +15, +20]] +20, +25]] +25, +30]] +30, ∞[
passenger occupancy in %	[0, 30]	984	9130	42947	104559	152058	53834	2863	38	0
	[30, 50]	77	4037	13559	48785	57556	18496	966	0	0
	[50, ∞[0	1768	13758	58085	61148	14721	2273	84	0

Mean in kW		ambient temperature in °C								
]-∞, -5]]-5, 0]]0, +5]] +5, +10]] +10, +15]] +15, +20]] +20, +25]] +25, +30]] +30, ∞[
passenger occupancy in %	[0, 30]	20.58	18.61	15.02	9.91	5.19	3.32	3.22	2.14	0.00
	[30, 50]	27.34	21.12	15.61	10.18	5.06	2.97	1.90	0.00	0.00
	[50, ∞[(27.34)	20.34	14.67	8.70	4.33	2.99	2.06	2.54	0.00

Standarddeviation in kW		ambient temperature in °C								
]-∞, -5]]-5, 0]]0, +5]] +5, +10]] +10, +15]] +15, +20]] +20, +25]] +25, +30]] +30, ∞[
passenger occupancy in %	[0, 30]	6.22	8.34	8.73	8.03	4.99	3.01	4.42	1.08	0.00
	[30, 50]	6.48	8.13	8.69	8.11	5.00	1.46	2.12	0.00	0.00
	[50, ∞[0.00	6.98	8.71	7.57	3.94	1.29	1.55	0.74	0.00

Modelling via artificial neural networks

As an alternative to a classification as described in step 1, the data on basis from the ICE-T were used to experiment with a model in the form of an artificial neural network (ANN).

ANNs have a unique ability to “learn” from complex, non-linear and multi-variant correlations via training based on input-output datasets. ANNs can be used as blackbox models without analytical knowledge of a system.

ANNs with different number of neurons were trained with temperature values and passenger occupancy values for the ICE-T as input and the electric power consumption as output. The subsequent validation based on a validation dataset from the ICE-T data that was not used for the training identified serious deviations between the model output and the corresponding measured values. As the validation results were not satisfactory, this approach was not pursued any further.

It is highly likely that the unsatisfactory validation results for the ANN model (at least to a significant extent) are attributable to the fact that important influencing factors for the electric power consumption cannot be expressed via the two input variables of temperature and passenger occupancy. The training data contain a variance that is not sufficiently described via the two input variables. However, this problem also occurs with the “modelling strategy” using the classification. In this context, reference is made to other influencing factors in section 2.3.3.2.

Evaluation of the models based on the classification with weighting matrices (step 2)

After models for electric power consumption (matrix **Power consumption**) depending on important factors influencing operation (outside ambient temperature and passenger occupancy) had been developed for the different HVAC systems in step 1, step 2 involve evaluating the models. The weighting shows how often a class and its assigned value for the electric power consumption occur.

Two matrices are derived and used for the weighting:

- a) Matrix for share of cooling/heating (**Operating ratio**_{Cooling} resp. **Operating ratio**_{Heating})
- b) Matrix **Class frequency** for distribution of the model input parameters of temperature and passenger occupancy

The matrix **Class frequency** for the distribution of the model input parameters of temperature and passenger occupancy was determined using statistical data for three reference cities on the one hand and by using the available field data on the other hand. The following sections describe the matrices and how they were determined in detail.

The power value assigned to a class from the classification is weighted using both weighting matrices. I.e., the power value is multiplied element by element by the assigned weighting factors from the weighting matrix for the share of cooling/heating and by the weighting matrix for the distribution of the model input parameters. These weighted power values for the individual classes are then added together to produce a scalar. The result is the mean electric power consumption of the HVAC system for heating over one year when using the weighting matrix **Operating ratio**_{Heating} or for cooling when using the weighting matrix **Operating ratio**_{Cooling}. The sum of the mean electric power consumption for heating/cooling gives the weighted total mean power consumption for analysis. Ventilation is not analysed separately, but added to heating instead. The turbomachine does not run in ventilation mode.

The equation (4) below states the calculation of the average electric power consumption $\widetilde{Pel}_{Cooling,system\ s}$ of a specific HVAC-system s in cooling operation. The calculation is analogous for heating operation. In the equation 'TC' stands for temperature class and 'OC' stands for occupancy class. Indices i and j allow to iterate through the classes.

$$\widetilde{Pel}_{Cooling,system\ s} = \sum_{all\ TC} \sum_{all\ OC} \left(\text{Power consumption}_{Cooling, System\ s_{TC\ i, OC\ j}} \cdot \text{Operating ratio}_{Cooling_{TC\ i, OC\ j}} \cdot \text{Class frequency}_{TC\ i, OC\ j} \right) \quad (4)$$

Matrix for the cooling and heating operating modes

One model (classification) was derived from the measurement data for each operating mode (cooling and heating), as shown in section 2.3.3.6. The question is then where does each model apply – depending on the model input variables of outside ambient temperature and passenger occupancy. Figure 91 shows an example of the weighting matrix for the share of cooling. It is immediately clear that only cooling consumption occurs at very high outside ambient temperatures and, therefore, no heating consumption, while the situation is reversed at very low outside ambient temperatures. For classes of moderate temperatures, cooling consumption or heating consumption occurs depending on additional influencing factors, which are not taken into account in the classification (such as solar radiation). In the example in the figure, the cooling consumption in the temperature class $[+15, +20]$ with average occupancy is within comfort mode approx. 70% of the time. The difference to 100% corresponds to the percentage of time for the share of heating.

Figure 91: Weighting matrix for the share of cooling

Cooling share		ambient temperature in °C								
		$]-\infty, -5]$	$]-5, 0]$	$]0, +5]$	$] +5, +10]$	$] +10, +15]$	$] +15, +20]$	$] +20, +25]$	$] +25, +30]$	$] +30, \infty[$
passenger occupancy in %	$[0, 30]$	0.0%	0.0%	0.1%	0.6%	8.4%	55.5%	94.3%	99.9%	100.0%
	$[30, 50]$	0.0%	0.0%	0.0%	2.0%	14.0%	69.8%	95.9%	99.9%	100.0%
	$[50, \infty[$	0.0%	0.0%	0.7%	4.4%	28.8%	82.9%	93.9%	99.3%	100.0%

The weighting matrices for the share of heating and cooling were derived as follows: For the ICE 3, heating and cooling was acquired as field data. Points for the two operating modes were classified separately. This resulted in a number of measuring points for cooling and heating for each class. The sum of the measuring points of a class (heating plus cooling) is 100%. The shares for heating/cooling were then easily calculated and added together in weighting matrices for the two operating modes.

The procedure described is based on the assumption that errors in measurement equipment are not dependent on the time of year, on average, so that no distortions occurred between heating and cooling over the duration of the measurement program. To support this assumption, a methodology for populating defective measuring points monthly was developed and applied. The result over these populated measuring points deviated from the directly determined results only insignificantly, thereby confirming the assumption.

For ICE-T, there is no sufficient information for heating. Hence, the information from the ICE 3 field data was applied to the ICE-T. The weighting matrices for the share of cooling/heating were therefore

also applied. After there are no technical differences between the two HVAC systems in this regard, this approach can be used to make statements comparing moderate and low temperatures.

(Meister, 2012) does not use such matrices for a share of cooling/heating. The lower temperature limit in (Meister, 2012) was 15 °C. In fact, Meister's investigation only focuses on cooling. As long as the share of cooling is close to 100%, so that there is no overlap of cooling and heating, an explicit analysis of the share of cooling is unnecessary. However, if the evaluation also includes lower temperatures (e.g. from 10 °C to 15 °C), where heating does occur with a non-negligible probability in addition to cooling, explicit analysis of the share of cooling and heating is necessary.

Especially at lower temperatures of e.g. 10 °C up to 15 °C (i.e. in heavy part-load operation), the advantage of the ACS system is its good part-load characteristic. Hence, lower temperatures should be included for a fair analysis. In addition, analysis of lower temperatures is required for heating.

Matrix for the distribution of the model input parameters of temperature and passenger occupancy from statistical data

Weighting the classes requires knowledge of the distribution of the temperature and the passenger occupancy.

Figure 92: Reference cities for meteorological data [Google Maps]



Reference cities for meteorological data. Source: Google Maps

Frequency distribution of outside ambient temperature:

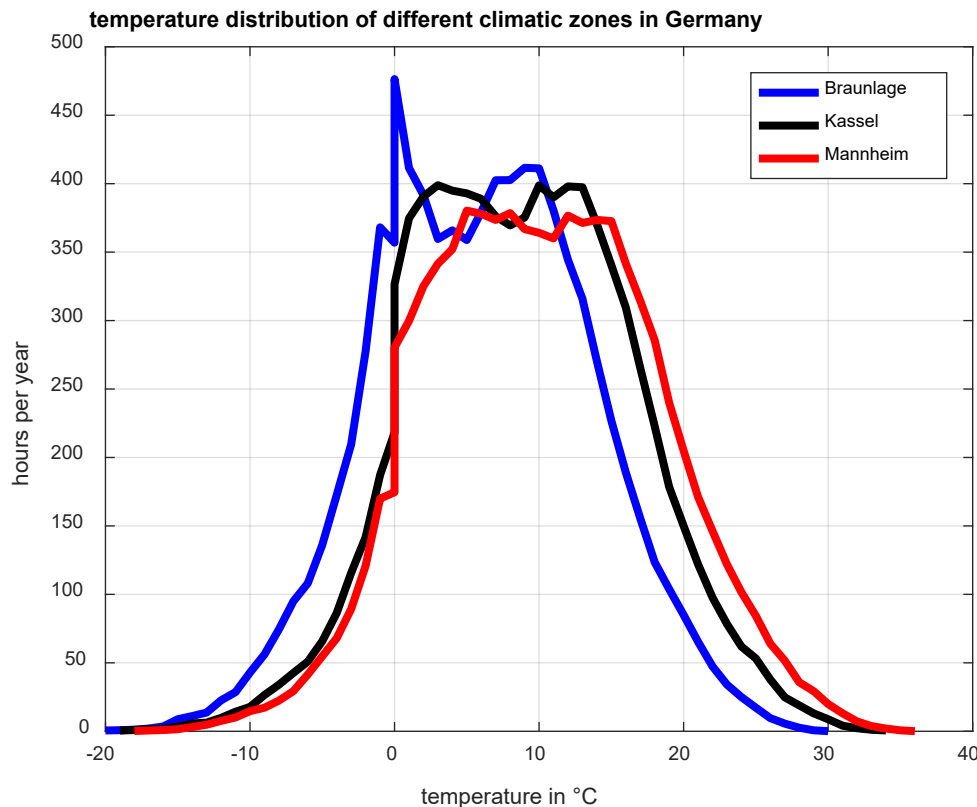
The frequency distribution of outside ambient temperatures was derived for three reference cities - DB suggested Braunlage (cool), Kassel (moderate) and Mannheim (warm) for the present study.

Figure 92 shows the reference cities on a map using Google Maps.

Frequency distribution of outside ambient temperature – Data from DIN 4710:2003-01

To derive the matrix for the distribution of model input parameters, (Meister, 2012) used meteorological data from (DIN 4710:2003-01). Figure 93 shows the temperature distribution from DIN 4710 for the three selected reference cities of Braunlage (cool), Kassel (moderate) and Mannheim (warm).

Figure 93: Temperature distributions of three different climatic zones in Germany in comparison (data from DIN 4710, analysis of 24-hour days)



Source: own illustration, Liebherr

The data used from DIN 4710 provides the number of hours for which the corresponding temperature occurs in an average year in 1 K increments (e.g. for Kassel, from -19 °C to 34 °C). The total number of hours therefore corresponds to a full year (365*24 h). This makes it possible to show temperatures for different times of the day and night evenly weighted. The data from the standard cannot be used to assign temperatures to times of day.

For comparison in this project, different HVAC systems are analysed in comfort mode (and therefore primarily in passenger service). The reason is the limited availability of data, as described in section 2.3.3.5.

In practice, a larger number of train trips takes place during the day instead of at night for a fleet, so that comfort mode occurs to a very limited extent during night hours, e.g. 00:00 to 04:00. Hence, a similar weighting of day and night for the temperature distribution is replicated only approximately by the actual train operating times. The use of data from DIN 4710 leads to a certain distortion towards lower temperatures. Generally speaking, cooler night temperatures decrease the cooling

capacity requirement and increase the heating capacity requirement. In the comparison between ICE-T and ICE 3, a low cooling capacity requirement, i.e. heavier part-load operation, is generally speaking more of a disadvantage for the ICE-T than for the ICE 3 in terms of energy. As such, the analysis generally favours ICE 3 in this regard. As there is no technical difference between ICE-T and ICE 3 in terms of heating, distortions in the demand for heating affect both trains equally.

The current DIN 4710:2003-01 uses temperature measurements from the time period from 1961 to 1990 as the basis for the three reference cities. As such, the data are on average (1975) more than 40 years old. The increase in average temperatures in recent years is therefore not included in the data. As a result, the data generally represent slightly lower temperatures than would be expected for more up-to-date meteorological data. Hence, the use of data from DIN 4710 favours the ACS system compared to the VCS to a certain extent.

Frequency distribution of outside ambient temperature – Data from test reference years (TRY)

To consider the different distribution of comfort mode over the day accordingly, this study used test reference years (TRY) from the DWD (Deutscher Wetterdienst, Testreferenzjahre von Deutschland für mittlere, extreme und zukünftige Witterungsverhältnisse, 2014) for meteorological data instead of (DIN 4710:2003-01).

Test reference years are hourly meteorological data in the form of a representative year for a specific geographical region. A representative meteorological year of this kind is typically derived from actual measurements over approximately 20 to 30 years. The form of the data makes it possible, as required for present purposes, deliberately to omit temperature measurements from night hours (e.g. between 00:00 and 04:00).

This study used TRY 2011 from the German Meteorological Service (DWD). The source data for the analysed reference cities comes from a reference period from 1988-2007, which makes the source data significantly younger/more recent than the source data of DIN 4710:2003-01, as the average age of the data is 20 years. The effect of increase in average temperatures in recent years is better expressed in the test reference years.

Distribution of occupancy:

For occupancy, data from the “Passenger Acquisition System” [ReisendenErfassungsSystem] GRIPS module 1 long-distance traffic (Deutsche Bahn AG, Daten zur Passagierbesetzung aus dem Reisenden-Erfassungs-System, 2008) was provided by DB. The data describe the average utilisation per train by day for the ICE-T line product. Specifically, this provides a matrix with hourly utilisation in percent over a full week (24*7 data points). The analysis period was from 01/01/2008 to 31/12/2008. Using the data, it was possible to derive the frequency for the passenger classes. The operating time of the system in comfort mode was taken into account for the occupancy distribution, consistent with the temperature distribution – as described above. As such, occupancy data from the time period, e.g. from 00:00 to 04:00, were excluded to avoid unrealistic distortion for low occupancies.

Examples of derived weighting matrices:

Combining the temperature distribution and occupancy distribution on the assumption of statistical independence between these two variables produces weighting matrices as the basis for analysis of the models (classification). Figure 94, Figure 95, Figure 96 show the weighting matrix for the typical operating times of a railway HVAC system in comfort mode, using test reference years for Braunlage (cool), Kassel (moderate) and Mannheim (warm). Comparing the weighting matrices shows a clear shift to higher temperatures from Braunlage to Mannheim.

Figure 94: Weighting matrix for the distribution of model input parameters based on a test reference year for Braunlage (cool)

Class weighting for Braunlage 04:00 to 24:00		ambient temperature in °C								
]-∞, -5]]-5, 0]]0, +5]] +5, +10]] +10, +15]] +15, +20]] +20, +25]] +25, +30]] +30, ∞[
passenger occupancy in %	[0, 30]	1,0%	4,2%	5,4%	5,9%	5,1%	3,0%	0,9%	0,1%	0,0%
	[30, 50]	1,5%	6,4%	8,1%	8,9%	7,6%	4,5%	1,4%	0,2%	0,0%
	[50, ∞[1,4%	5,9%	7,5%	8,3%	7,1%	4,2%	1,3%	0,2%	0,0%

Values based on typical times of use (04:00 to midnight) in comfort mode. Source: own illustration, Liebherr

Figure 95: Weighting matrix for the distribution of model input parameters based on a test reference year for Kassel (moderate)

Class weighting for Kassel 04:00 to 24:00		ambient temperature in °C								
]-∞, -5]]-5, 0]]0, +5]] +5, +10]] +10, +15]] +15, +20]] +20, +25]] +25, +30]] +30, ∞[
passenger occupancy in %	[0, 30]	0,3%	2,4%	5,1%	5,6%	5,8%	4,0%	2,0%	0,5%	0,1%
	[30, 50]	0,4%	3,6%	7,7%	8,3%	8,6%	6,0%	2,9%	0,8%	0,1%
	[50, ∞[0,4%	3,4%	7,1%	7,7%	8,0%	5,5%	2,7%	0,8%	0,1%

Values based on typical times of use (04:00 to midnight) in comfort mode. Source: own illustration, Liebherr

Figure 96: Weighting matrix for the distribution of model input parameters based on a test reference year for Mannheim (warm)

Class weighting for Mannheim 04:00 to 24:00		ambient temperature in °C								
]-∞, -5]]-5, 0]]0, +5]] +5, +10]] +10, +15]] +15, +20]] +20, +25]] +25, +30]] +30, ∞[
passenger occupancy in %	[0, 30]	0.2%	1.8%	3.7%	5.4%	5.6%	4.8%	2.8%	1.1%	0.2%
	[30, 50]	0.4%	2.7%	5.5%	8.2%	8.4%	7.2%	4.2%	1.7%	0.3%
	[50, ∞[0.3%	2.5%	5.1%	7.5%	7.8%	6.7%	3.9%	1.5%	0.3%

Values based on typical times of use (04:00 to midnight) in comfort mode. Source: own illustration, Liebherr

Matrix for the distribution of the model input parameters of temperature and passenger occupancy from field data from the ICE 3

Weighting the classes requires knowledge of the distribution of the temperature and the passenger occupancy. In contrast to the procedure above, it is not necessary to access statistical data for the outside ambient temperature in this case (e.g. from applicable standards or test reference years) or for the passenger occupancy. Instead, the weighting matrix in this section is derived from field data from the ICE 3 acquired as part of this project. By using this weighting matrix, calculated conditions are used for the HVAC systems as far as possible in this analysis, as if the HVAC systems to be compared had been used on the same train during the period of the field data acquisition. However, the field data operating points most probably not representative for use of trains on different routes over many years. During field data acquisition, it is possible that particularly hot summers could have occurred in combination with particularly mild winters or the relevant train may preferably have been operated on a route with particularly high or particularly low passenger utilisation.

To map the frequencies of the measured temperatures and passenger occupancies as correctly as possible, partial gaps in the data, e.g. due to maintenance, were populated. This was done month by month with a random replication process for all the months of a year. In detail, the procedure was as follows: The number of the month with the highest number of measurement data samples was defined as the target number for the measurement data samples (time stamp). The gap between the actually recorded number of measurement data samples and the target number was then populated for every calendar month by randomly taking the number of samples to be populated from the set of actually recorded measurement data samples for the month and assigning them to the month.

The weighting matrix derived from the field data is shown in Figure 106.

Figure 97: Weighting matrix for the distribution of model input parameters based on the field data acquired on the ICE 3

Distribution from field data of current project		ambient temperature in °C								
]-∞, -5]]-5, 0]]0, +5]] +5, +10]] +10, +15]] +15, +20]] +20, +25]] +25, +30]] +30, ∞[
passenger occupancy in %	[0, 30]	0,1%	0,7%	3,7%	9,7%	14,8%	12,2%	7,0%	1,4%	0,3%
	[30, 50]	0,0%	0,3%	1,2%	4,7%	5,8%	5,3%	3,8%	0,8%	0,2%
	[50, ∞[0,0%	0,1%	1,2%	5,5%	7,5%	7,3%	4,3%	1,7%	0,3%

The acquired field data were used in comfort mode. Source: own illustration, Liebherr

Comparison of the temperature distribution in the measurement period with a representative year

The question regarding the weighting matrices for the distribution of the model input parameters is whether the temperature distribution of the outside ambient temperature corresponds to the long-term average in the period of field data acquisition or whether those were particularly warm or cold years.

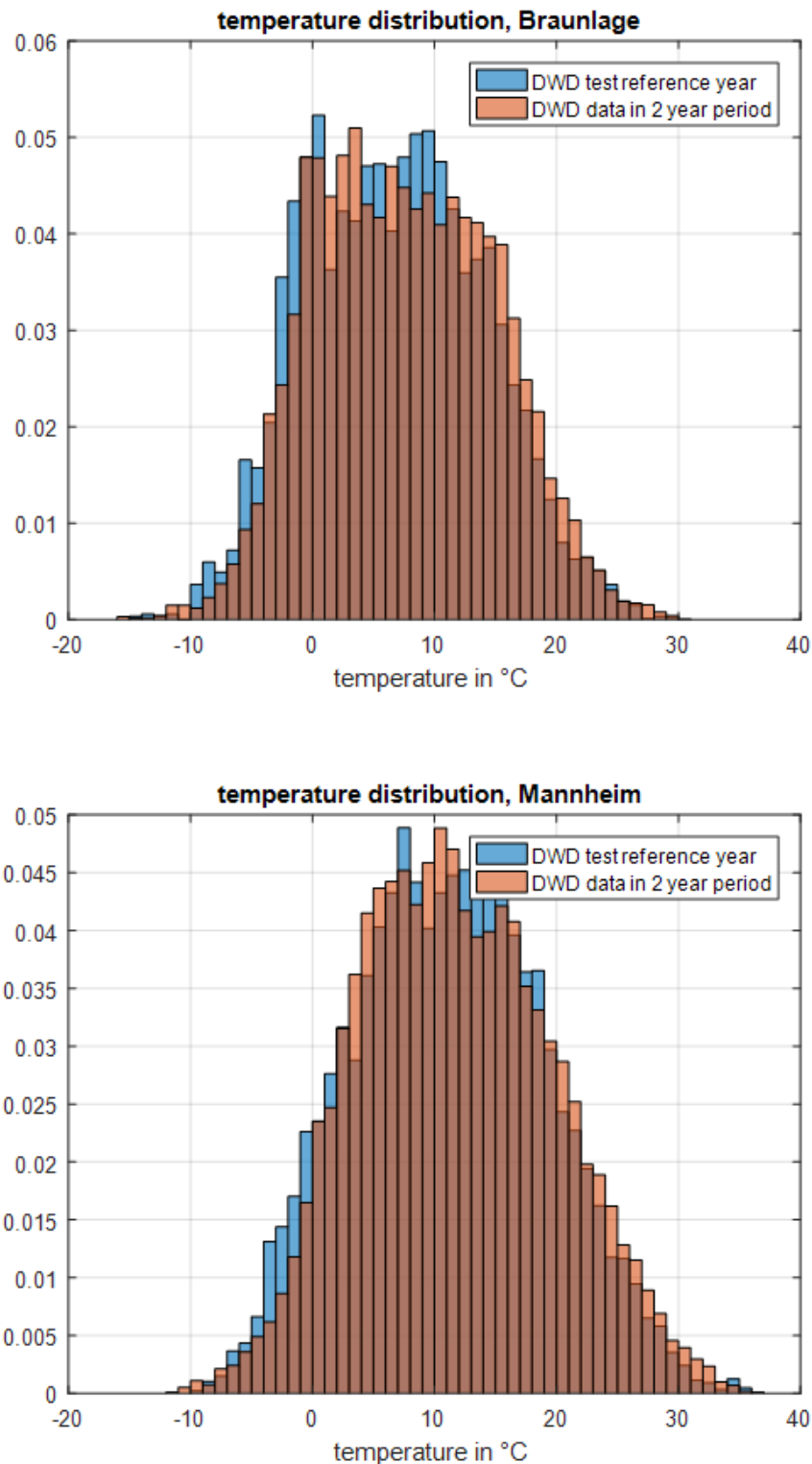
To answer this question, data from the German Meteorological Service were examined more closely for the reference cities of Braunlage and Mannheim. No current data were available for Kassel.

- ▶ Temperature frequencies from original measurement data from the DWD (unfiltered, i.e. complete 24 hours per day) for the reference cities of Braunlage and Mannheim and for a time period of 2 years from 01/11/2015 until 31/10/2017, which fell within the period of field data acquisition in this project; data source: (Deutscher Wetterdienst, Climate Data Center, 2017)
- ▶ Temperature frequencies from the test reference years for the reference cities of Braunlage and Mannheim; data source: (Deutscher Wetterdienst, Testreferenzjahre von Deutschland für mittlere, extreme und zukünftige Witterungsverhältnisse, 2014)

The temperature frequencies are shown in the histograms in Figure 98. The superimposed histograms clearly show that the orange range for the two years under observation falls further to the right and, therefore, at higher temperatures. The superimposition of the blue and orange histogram is shown in brown. The statistical data are summarised in Table 5.

Hence, the period of field data acquisition differs from the test reference years (representative years) with respect to the temperature distribution. It was warmer during the period under consideration.

Figure 98: Temperature distributions from test reference years of Deutscher Wetterdienst (DWD) for the cities Braunlage and Mannheim compared to DWD data of 2-year period of measurement on ICE 3 2106/2017



Source: own illustration, Liebherr

Table 5: Comparison of temperature distributions of the test reference year with the distribution of the 2-year period of measurement

Data source	Arithm. mean [°C]	Quantile [°C]				
		0%	25%	50%	75%	100%
Braunlage (cool)						
Test Reference Year	6.7	-14.8	0.8	6.7	12.0	29.2
2 year measurement	7.5	-15.3	1.8	7.2	13.1	30.3
Mannheim (warm)						
Test Reference Year	11.1	-9.3	5.4	11.1	16.7	36.3
2 year measurement	11.7	-11.2	5.8	11.2	17.3	35.3

Comparison of temperature distributions of the test reference year with the distribution of the 2-year period of measurement, temperature values in degrees Celsius.

Deriving the energy consumption for the operating hours in comfort mode (step 3)

After deriving the average electric power consumption over a year, the electric energy consumption is then calculated. For this purpose, the average electric power consumption is multiplied by the number of operating hours in comfort mode – the described classification model applies to comfort mode.

It is important to apply a realistic or representative number of operating hours in order to derive meaningful absolute figures for the annual energy consumption. In principle, different data sources can be used for the number of operating hours. In this case, information from the requirements specification for HVAC systems of a comparable train operated by DB was used, where 18 hours was the average number of operating hours per day. For the calculation in this project, 6,570 hours are applied as the basis for the annual energy consumption over 365 days.

Calculation of impulse resistance for the secondary energy consumption

In this project, the following equation (5) was used as an analytical approach for determining the impulse resistance.

$$W_{\text{Impulse resistance}} = \dot{m} \cdot v^2 \cdot t$$

$$\begin{aligned} \dot{m} & - \text{Intake air mass flow per class and system} \\ v & - \text{Travelling speed of the train} \\ t & - \text{Operating hours} \end{aligned} \quad (5)$$

The travelling speed of the train was derived as the root mean square based on the field data acquired in this project. This resulted in an average speed of $v = 133$ km/h for further calculation. This speed includes stop times (e.g. station stops) during train trips. The operating hours are the 6,570 hours from the calculation of the primary energy consumption.

The intake air mass flow was determined for each system and each class of the classification. Depending on the system, the air mass flow is comprised of the following components:

- ▶ The fresh air mass flow (fresh air supply for passengers) was determined for each temperature class and occupancy class according to the implemented control strategy. The fresh air supply is controlled on the basis of the CO₂ concentration in the carriage, depending on the occupancy. There are no differences between the systems observed with respect to fresh air mass flow. The fresh air mass flow depends on the outside ambient temperature and the passenger occupancy, according to the underlying standard.
- ▶ For the air-cycle system with reverse loop (system 1), measurement data in the trial were used to map the turbine speed onto the process air mass flow. By assigning turbine speeds to classes of the classification, it was possible to assign each class a process air mass flow. The mass flow rate for the cooling of the turbomachine was also included.
- ▶ For the air-cycle system with direct loop (system 6), the fresh air mass flow was increased depending on the required cooling capacity (high temperature class, high occupancy class) to avoid dropping below minimum temperatures at the supply air interface. The air mass flow also had to be considered for cooling (corresponds to a condenser air mass flow) for this system.
- ▶ For the vapour cycle systems (systems 2 and 3), the condenser air mass flow was controlled in two stages according to the controller implemented on ICE-T, depending on the heat to be dissipated via the condenser and the ambient temperature.
- ▶ In contrast to the vapour cycle system with reheating, it was assumed for the optimised vapour cycle system with bypass that the condenser fan did not have to run at the lowest setting for system optimisation for low ambient temperatures, but could be switched off completely when the train was operating.

The class-based air mass flows were finally weighted based on the weighting matrices, as for the determination of the power/energy consumption, then added together. Consequently, the secondary energy consumption depends on the operating conditions (temperature distribution, passenger distribution) and the system.

Consideration of efficiencies for on-board power supply and traction

To compare primary and secondary energy consumption directly or to add them together for the total energy consumption, it is first necessary to reference all consumptions to the same point. For analysis of the operating costs from energy costs, it is meaningful to reference all consumptions to the pantograph, i.e. the point of power supply into the train.

The primary energy consumptions analysed above from field data or the simulation are at the unit interface. An efficiency of 0.925 was set for the on-board power supply (inverter, etc.) between unit interface and pantograph. The secondary energy consumption must be provided by the vehicle drive. An efficiency of 0.870 was set for the entire efficiency chain from pantograph up to traction. The efficiencies match those in the investigation by (Aigner, 2007).

2.3.3.7 Summary of differences between the analyses in this project and the work by Meister (Meister, 2012)

The most important differences between the analysis in (Meister, 2012) and the analysis of the power and energy consumption in this project are summarised below.

- **Analysis of cooling and heating operation**

While (Meister, 2012) focused on cooling operation in which the analysed systems had technical differences, this project examined the cooling and heating operation. The analysis of the cooling operation in (Meister, 2012) was also limited to a minimum temperature of 15 °C. This project had no minimum temperature limitation, which made it possible to look at cooling at lower temperatures.

- **Comparison of systems/technologies**

In (Meister, 2012), the air-cycle system was compared with a vapour cycle system with a part-load control provided by reheating. Reheating for capacity control is no longer state-of-the-art. Further developments have also taken place for air-cycle systems. For this reason, this project makes an additional comparison between an advanced and improved air-cycle system and an improved vapour cycle system.

- **Operating mode – Comfort mode**

(Meister, 2012) makes not clear reference the examined operating mode of the system (comfort mode, pre-conditioning, parking operation). The scaling to 24*365 operating hours per year suggests that it was assumed that the data map to different operating modes. The analysis of the underlying data for the ICE-T in this project showed that the data primarily map to comfort mode. Consequently, the comparison in this study was performed explicitly for comfort mode. Comfort mode primarily means passenger service. This was taken into account in the definition of the class weighting matrix and in the number of operating hours per year.

- **Source for meteorological data**

While (Meister, 2012) used meteorological data from DIN 4710, this study uses test reference years in order to take into account the fact that comfort operation is less frequent during the night hours. The data from (DIN 4710:2003-01) and the test reference years (Deutscher Wetterdienst, Testreferenzjahre von Deutschland für mittlere, extreme und zukünftige Witterungsverhältnisse, 2014) differ in their form, the underlying method of generation and the underlying measurement source data. The test reference years are clearly more up-to-date and, as such, generally better represent the increase in average temperatures over recent years.

- **Source data for the air-cycle system**

The source field data for the air-cycle system differ between (Meister, 2012) and this project, particularly with respect to the period of measurement, the number of variables and the processing adapted to both.

- **Comparison based on operating conditions from current field data**

The different HVAC systems were compared not only by means of statistical data for temperature and passenger occupancy as in (Meister, 2012), but also on the basis of the specific distribution of temperature and passenger occupancy in the field data. As such, the comparison is also based on a very specific train.

► **Analysis of the secondary energy consumption due to the impulse resistance of intake air**

(Meister, 2012) did not perform an analysis of the secondary energy consumption. However, as the impulse resistance has an average share of 22% of the total annual energy consumption of the air conditioning for a high-speed train in Germany according to (Morgenstern & Ebinger, 2008), this secondary energy consumption was also analysed in this study. The analysis is based on an analytical approach.

The results in (Meister, 2012) and the results from this project differ, in particular due to the listed differences. In contrast to the study by (Meister, 2012), this project also extensively analyses the economic efficiency of the different systems.

2.3.4 Comparison of different HVAC systems in terms of maintenance effort

Data from the 2012-2014 time period were used for the complete analysis of the Life Cycle Cost (LCC). The data in DB's SAP maintenance system are used as the basis for analysis. The system contains the maintenance and servicing performed on the vehicles. In principle, the following series, which are equipped with vapour cycle systems, are suitable for a comparison with the air-cycle system on the ICE 3, 2nd series: Velaro D (BR 407), ICE 4 (BR 412) and ICE-T (BR 411).

The Velaro D was not commissioned until 2014, so that it has only been operating for a limited time. In addition, warranty repairs are not recorded in the SAP maintenance system.

The ICE 4 was not commissioned until 2017. The trial operation in 2016 is not suitable for analysis. In addition, there are no measurements for energy consumption or the Duty Cycle (Schmitt et al., 2015) of either vehicle. For these reasons, it was decided not to use these vehicles to compare the LCC/TCO.

The operating time of the ICE-T is comparable with that of the ICE 3, and measurements of the energy consumption were performed. As a result, the vapour cycle system on the ICE-T is compared with the air-cycle system on the ICE 3.

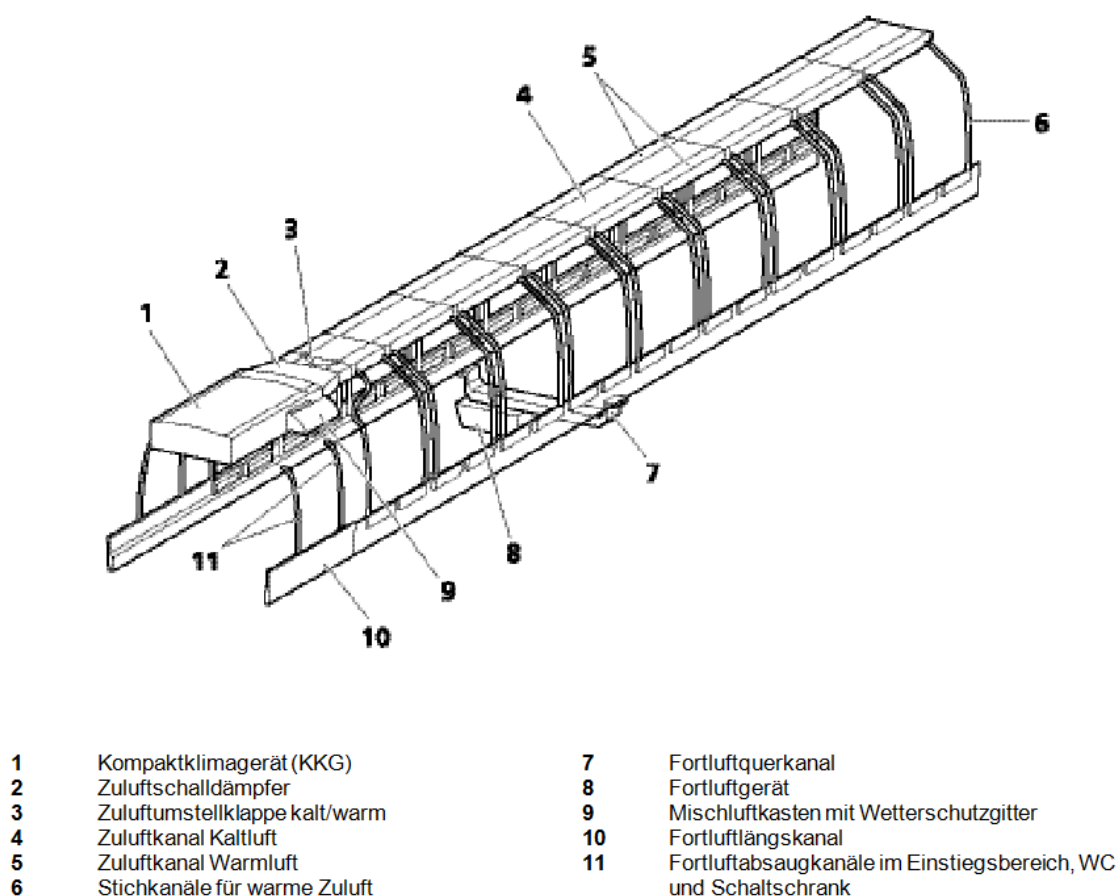
The maintenance and servicing for the ICE 3 and ICE-T under consideration, which was exported from SAP, was filtered in consultation with DB Systemtechnik and Liebherr for entries relevant to air-conditioning. They form the basis for the LCC in section 2.4.2 Complete analysis of Life Cycle Costs (LCC) and Total Costs of Ownership (TCO).

2.3.4.1 Extent of maintenance activities for the ICE 3 air-conditioning system

The air-conditioning system consists of several units that are distributed over the entire vehicle. The centrepiece is the compact air-conditioning unit (CACU).

The cooling or the main part of the heating energy is supplied via the duct system. The duct system features motorised flaps that ensure optimum distribution of cold or warm air. A sound absorber is integrated into the duct system to increase passenger comfort. Additional electric duct heaters are integrated into the duct system to regulate individual sections. Convection heaters are installed in the entrance area and the WC.

Figure 99: Design of the ICE 3 air-conditioning system



Design of the ICE 3 air-conditioning system. Source: own illustration, Liebherr

An exhaust air device, which is installed under the carriage body, is used to remove the exhaust air.

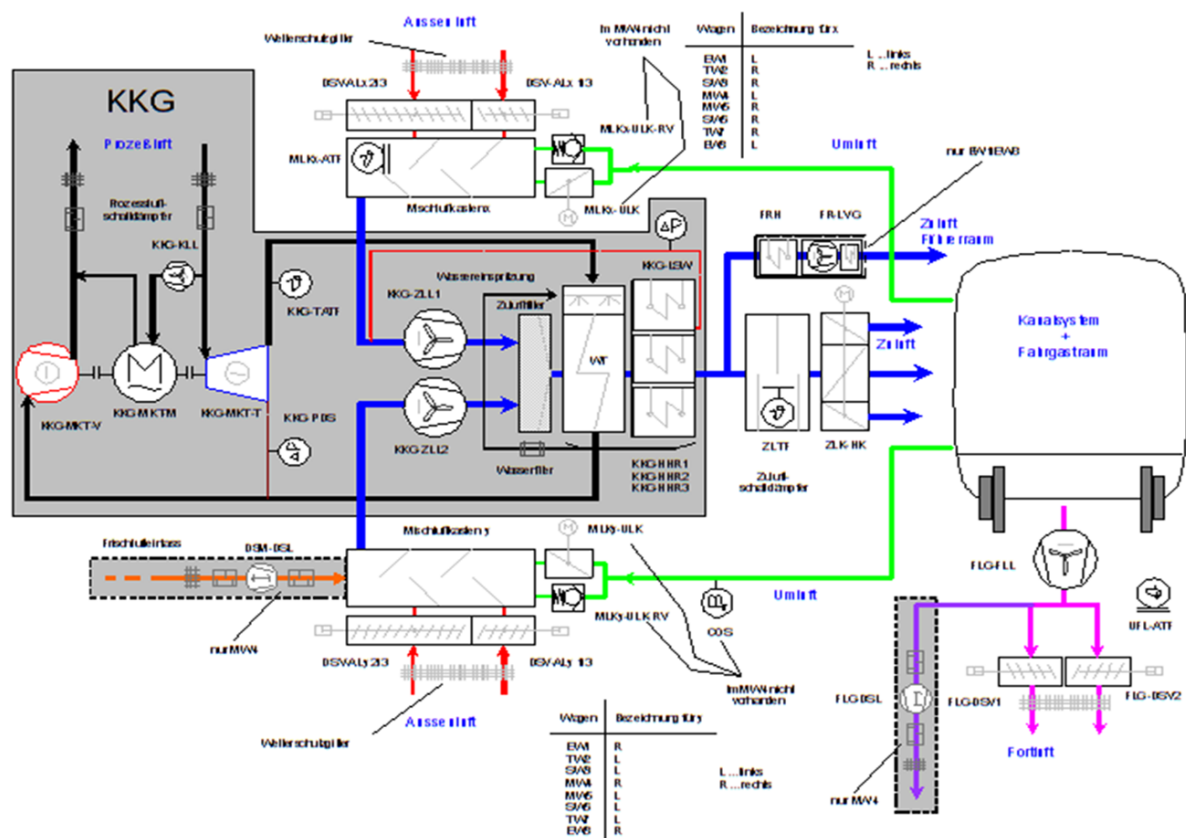
As the train is equipped with a passive pressure protection system, pressure protection flaps must be included at the exhaust air and fresh air opening.

For fresh air, these pressure protection flaps are located in the mixed-air boxes, which are installed on both sides of the compact air-conditioning unit.

As shown in Figure 99, there are a lot of components involved in the air conditioning. Aside from the CACU, these components are linked to the vehicle and not to an air-conditioning technology. Hence,

pressure protection is used only on high-speed trains, the duct system differs depending on the vehicle type, and not all railway vehicles have their own exhaust air device.

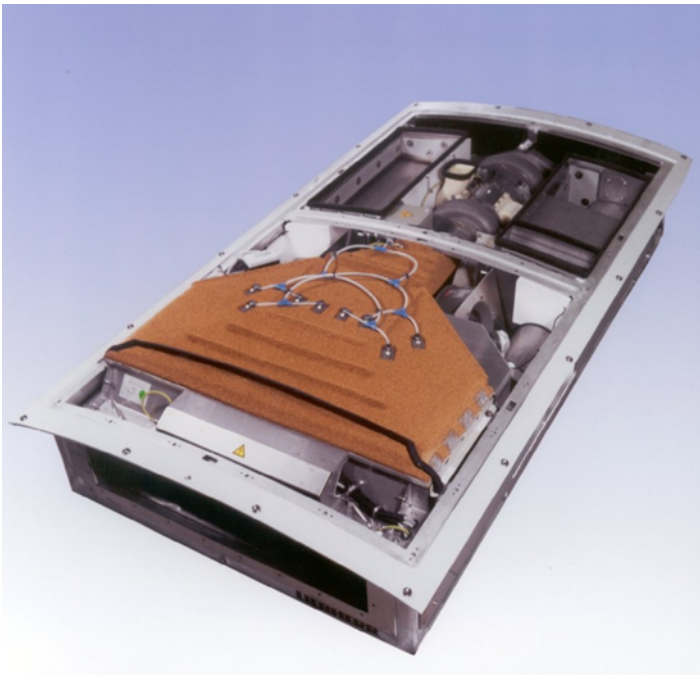
Figure 100: Schematic of the ICE 3 air-conditioning system



Schematic of the ICE 3 air-conditioning system, shaded in gray are the components of the compact air-conditioning unit (CACU). Source: own illustration, Liebherr

As an essential part of the maintenance work on the air-conditioning system only depends on the design and type of vehicle, the maintenance tasks that are not directly associated with the air-conditioning system itself were not taken into account. Hence, only those maintenance costs that are functionally associated with either the CACU (highlighted in grey in Figure 100) or the controller of the air-conditioning system were taken into account. The controller and CACU together represent one functional unit, which can be used in different vehicle scenarios.

Figure 101: Compact air-conditioning unit of the ICE 3, 2nd series



Compact air-conditioning unit of the ICE 3, 2nd series. Source: own illustration, Liebherr

Figure 101 shows the CACU on the 2nd series of the ICE 3, to which the charged maintenance costs apply. Overall, 104 units are installed in 13 partial trains.

The applicable main assemblies are:

- ▶ Process circuit: Motorised air-cycle machine (MACM), heat exchanger, condensate injection, seals
- ▶ Fans: Supply air and MACM cooling air
- ▶ Electric heating: Main heater, thermostats
- ▶ Electrical system and electronics: HVAC controller, open and closed-loop control components, magnetic bearing controller

Differences resulting from vehicle type, operating speed, installation type, specific conditions or requirements from the vehicle design are not shown in the comparison. This applies to CACU covers and screws, support frames and seals.

2.3.4.2 Extent of considered maintenance activities for the ICE-T

For the ICE-T, data from the central carriage unit (Figure 13) of 59 model 411 trains were analysed. In total, there were 295 carriages. The end carriages are not suitable for direct comparison, as they are designed with split units where the refrigeration circuit supplies the driver's cab as well as the passenger compartment.

The applicable main assemblies are:

- ▶ Refrigeration section: Variable-speed screw compressor, condensers, condenser fans, small components of the refrigeration circuit
- ▶ Air treatment section: Supply air fan, evaporator with expansion valve
- ▶ Electric heating: Main heater, thermostats
- ▶ Electrical system and electronics: HVAC controller, open and closed-loop control components

CACU covers and screws, support frame and seals are not included, as for the ICE 3.

2.3.4.3 Collected maintenance data for the ICE 3 and ICE-T – cost comparison

The period under investigation included extraordinary maintenance, which must be added to the life cycle of the system. For the ICE-T system, this was scheduled rolling overhaul of the screw compressors, which takes place once in the life cycle of 30 years. For the ICE 3, there was unscheduled refurbishment of the heat exchanger header, which was necessary because of insufficiently durable insulating material. As long-life insulating materials are now available, replacement of the insulating material is no longer relevant for a state-of-the-art air-cycle system, so that the item was excluded from the calculations.

The ICE 3 has an annual mileage that exceeds that of the ICE-T by a factor of 1.37. It was assumed that this does not affect the maintenance cost. It was also assumed that the ICE 3 and ICE-T have approximately the same annual operating time, so that no relevant impact is to be expected on the difference in terms of the maintenance costs.

A cooling capacity of 33 kW (rated cooling capacity of the ICE 3) was selected. As the ICE-T has a cooling capacity of only 30 kW, the maintenance costs for the cooling/ventilating function on the ICE-T were increased by 10%. The result is shown in Table 6:

Table 6: Comparison of the annual maintenance costs of the ICE-T and the ICE 3

Analysis of DB maintenance data	ICE-T model 411 (central carriage)	ICE 3, 2nd series
Cooling/ventilation	€3,402	€3,852
Heating system	€443	€556
Comparison of costs for cooling/heating/ventilation	€3,845	€4,408

Annual maintenance costs of the ICE 3 and the ICE-T

2.4 Comparison with other air-conditioning systems (WP 3)

In this work package, the Air-Cycle System (ACS) is compared with conventional Vapor Cycle Systems (VCS) in terms of power and energy requirements based on the measurements and for additional information on life-cycle costs (LCC respectively TCO). The results are presented and discussed below.

This work package focused on standardising and applying the obtained operating data to a reference system (comparison vehicle). A vehicle has to be selected for this purpose.

In WP 3, these operating and environmental data are examined, standardised, divided into classes selected in WP 1 and pre-processed to be well prepared for the next step – comparison with the air-cycle system. The work package also includes acquisition and processing of the maintenance costs (preventive and corrective measures) for the ICE-T, in the same way as in WP 2.

WP 3 is complete when all the data required for comparison of the systems is acquired and processed. The second project meeting is also part of WP 3.

2.4.1 Comparison of the electric power and energy consumption of different HVAC systems

2.4.1.1 Comparison of the primary power consumption according to the classification

Comparison of power consumption for the air-cycle system (ACS) on the ICE 3 (system 1) with the vapour cycle system (VCS) on the ICE-T (system 2)

Figure 102 and Figure 103 show the primary electric power consumption for cooling and heating for systems 1 and 2, i.e. for the systems for which field data were available. This uses the classification of the electric power consumption using the variables of outside ambient temperature and passenger occupancy as a model according to section 2.3.3.6. As explained above, the arithmetic mean was used as the aggregation function for the power values in the individual classes. To enable comparison between carriages with different passenger capacity, the power values were standardised for a seat. The power consumption values are at the unit interface, hence they do not include any efficiencies of the on-board power supply up to the pantograph.

The plots show that the passenger occupancy has a lower impact by far on the electric power consumption than the outside ambient temperature.

There are clear differences between the analysed systems in cooling operation. At very high outside temperatures in the range of 35 °C, the electric power consumption of the air-cycle system is significantly higher than the power consumption of the vapour cycle systems. This corresponds to expectations based on theoretical, physical considerations for the applicable circuit processes.

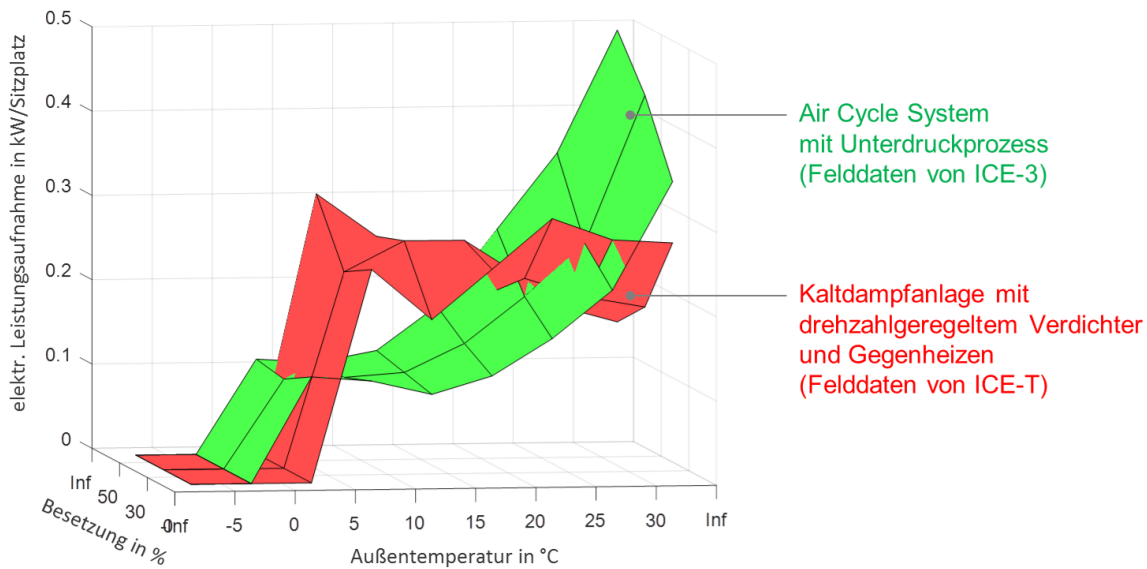
However, for lower temperatures in the range of e.g. 10 °C or 15 °C, the air-cycle system is significantly more efficient than the analysed vapour cycle systems. The advantage of energy-efficient part-load control is evident in this range. The figure clearly shows that part-load control with electric reheating in the part-load range, where the compressor speed can no longer be reduced, is a very inefficient strategy because of its power consumption.

The core question at this point is what temperature ranges or, in more general terms, what classes of temperature and passenger occupancy occur in actual operation, at what frequency and then what the annual energy consumption of the air-cycle system is. This question is discussed in section 2.4.1.2.

In heating operation, the electric power consumption of the air-cycle system lies only slightly above the power consumption of the investigated vapour cycle system. The difference cannot be seen in the figure. The difference between the air-cycle system and the vapour cycle system lies in the fact that the turbine is constantly being held in an elevated position, independent of cooling or heating operation,

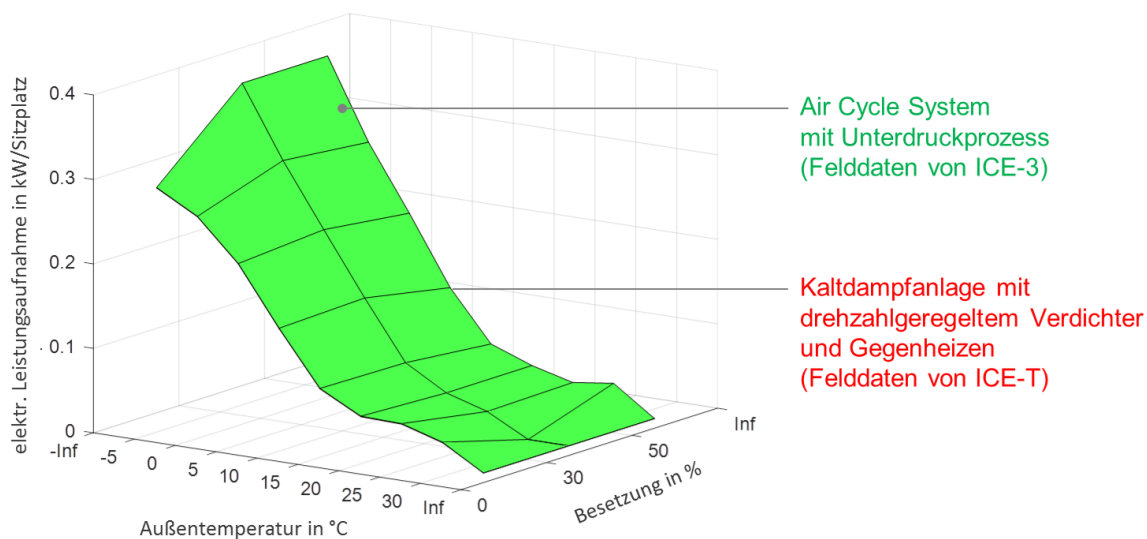
by active magnetic bearings for the air-cycle system in the investigated generation, in order to protect the turbine against potentially life cycle-reducing vibrations and shocks.

Figure 102: Primary power consumption for cooling, comparison for systems with actual measurement data



Power consumption at unit interface, i.e. without efficiencies of the on-board power supply. Source: own illustration, Liebherr

Figure 103: Primary power consumption for heating, comparison for systems with actual measurement data



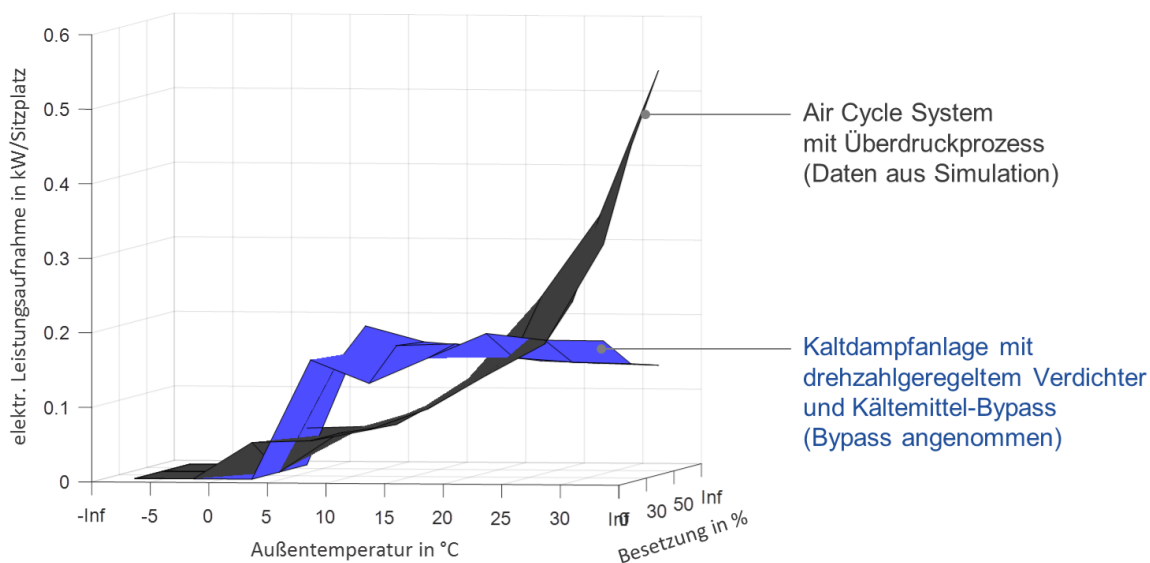
The area for the vapour cycle system is slightly below the green area for the air-cycle system and is covered by the green area. Power consumption at unit interface, i.e. without efficiencies of the on-board power supply. Source: own illustration, Liebherr

Comparison of power consumption for air-cycle system (ACS) with direct loop from simulation (system 6) with vapour cycle system (VCS) according to ICE-T, but with assumed bypass instead of reheating (system 3)

This is an advanced VCS or ACS system, so that no direct field data were available as the basis for comparison. As the sources of data were different, the results for systems 1 and 2 are also discussed separately from systems 3 and 6.

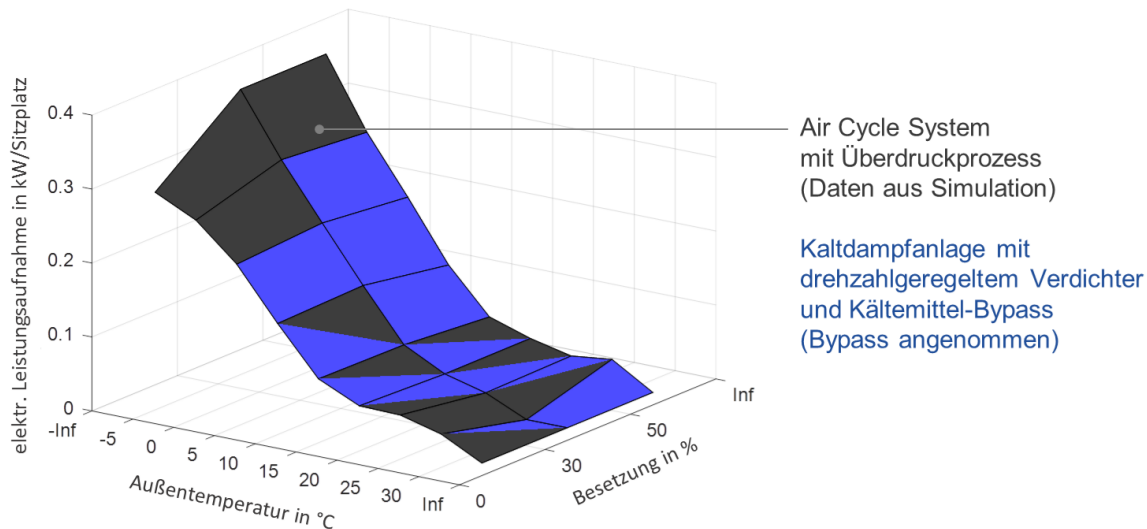
Figure 104 and Figure 105 show the primary electric power consumption for cooling and heating for systems 3 and 6, i.e. as in the previous section for systems 1 and 2. The power consumption values shown here are at the unit interface, hence they do not include any efficiencies of the on-board power supply up to the pantograph. In terms of quality, the comparison of the advanced ACS and VCS systems is similar to the comparison of systems 1 and 2 installed in the trains, which were discussed in the preceding section. Differences between the advanced ACS and VCS system can be seen in cooling operation, while the power consumptions of both systems are the same for heating operation. For the advanced ACS system, there is no power consumption for the magnetic bearing controller. On the other hand, Figure 104 clearly shows the efficiency benefit of the ACS system in the part-load range and the advantage of the VCS system in the high-load range.

Figure 104: Primary power consumption for cooling, comparison for systems with data from models/calculation



Power consumption at unit interface, i.e. without efficiencies of the on-board power supply. Source: own illustration, Liebherr

Figure 105: Primary power consumption for heating, comparison for systems with data from models/calculation



The two areas coincide. Power consumption at unit interface, i.e. without efficiencies of the on-board power supply.
Source: own illustration, Liebherr

2.4.1.2 Comparison of annual energy consumption

The absolute numbers for electric energy consumption are the basis for statements about Energy Cost as an essential part of the Life Cycle Cost (economic efficiency analysis) as well as for statements about environmental impact (particularly CO₂ emissions, depending on the electricity mix used).

The energy consumption reported in each case is based on 6,570 operating hours in comfort mode per year according to section 2.3.3.6. This number of operating hours corresponds to 18 hours per day for 365 days of the year.

The procedure described in section 2.3.3.6 (step 2) was used for class weighting. For temperature distribution, the test reference years for Braunlage, Kassel and Mannheim and an operating time in comfort mode from 04:00 to midnight were applied. The class weighting was derived from the frequencies in the field data. The results are presented in the following sections.

Comparison of energy consumption for the air-cycle system (ACS) on the ICE 3 (system 1) with the vapour cycle system (VCS) on the ICE-T (system 2)

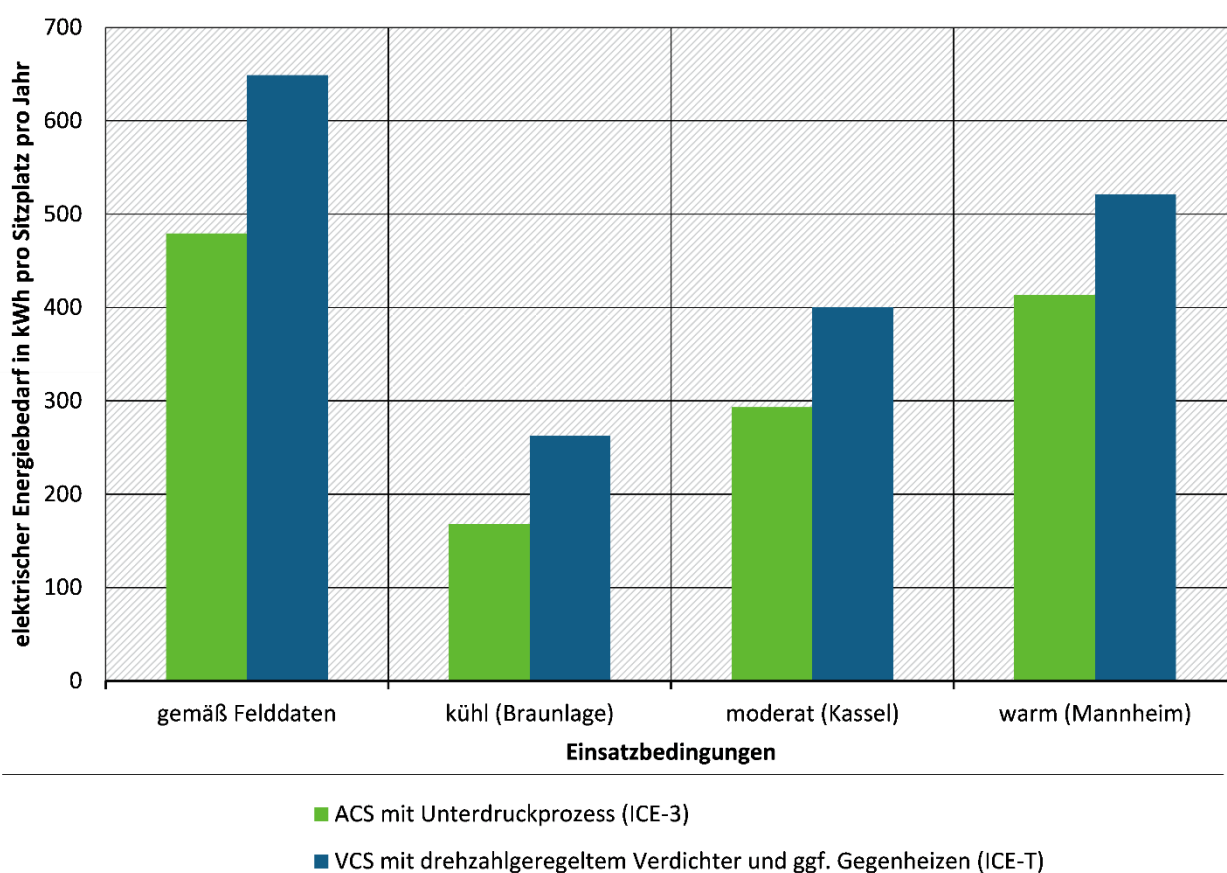
Figure 106, Figure 107, Figure 108 and Table 7 show the total primary energy consumption for cooling, for heating, as well as for cooling and heating for the HVAC systems (systems 1 and 2) that were analysed with measurement equipment. Note the adjusted scaling in each case on the ordinate axes (y-axes) of the charts. The stated energy consumptions are at the unit interface of the HVAC unit in each case. As such, efficiencies for the on-board power supply up to the pantograph are not included here. Table 7 provides a summary of the comparison results.

The technical difference between the systems is in cooling operation and can be clearly seen in Figure 106. The energy-saving potential with ACS, as measured on the ICE 3 in field operation, compared to the VCS with a variable-speed compressor and reheating for the lower part-load range, as measured on the ICE-T in field operation, depends on the operating conditions (temperature distribution and passenger distribution) and, therefore, on the climate zone. For cooling operation, the

evaluation shows a savings potential of 21% for the investigated warm climate zone (Mannheim) and up to 36% for the examined cool climate zone (Braunlage).

As shown in section 2.3.3.6, the temperature distribution during the measurement period was shifted to higher temperatures compared to the temperature distribution from the representative years (test reference years). The generally higher ambient temperatures are reflected in Figure 106 by the higher annual energy consumption for cooling for the operating conditions "according to field data" compared to the operating conditions for "cool (Braunlage)", "moderate (Kassel)" and "warm (Mannheim)". Both systems, ACS and VCS, are affected. For operating conditions "according to field data", the ACS has a lower energy consumption of about 26% compared to VCS. In heating operation, the higher ambient temperatures for the operating conditions "according to field data" lead to lower energy consumption compared to the other operating conditions.

Figure 106: Comparison of primary annual energy consumption in cooling operation for the air-cycle system ACS (ICE 3) and the vapour cycle system VCS (ICE-T)



Annual energy consumption in cooling operation for the air-cycle system (ACS) with reverse loop (based on implementation in ICE 3) and the vapour cycle system (VCS) with variable-speed compressor and option for reheating (based on implementation in ICE-T) (source data: field data); energy consumption is based on 6,570 operating hours in comfort mode per year. Energy consumption is at the device interface, i.e. excluding the efficiency of the on-board power supply up to the pantograph. Source: own illustration, Liebherr

elektrischer Energiebedarf in kWh pro Sitzplatz pro Jahr = electrical energy consumption in kWh per seat per year; gemäß Felddaten = according to the field data; kühl (Braunlage) = cool (Braunlage); moderat Kassel = moderate (Kassel); warm (Mannheim) = warm (Mannheim); Einsatzbedingungen = operating conditions; ACS mit Unterdruckprozess (ICE 3) = ACS with reverse loop (ICE 3); VCS mit drehzahlgeregeltem Verdichter und ggf. Gegenheizen (ICE-T) = VCS with variable-speed compressor and option for reheating (ICE-T)

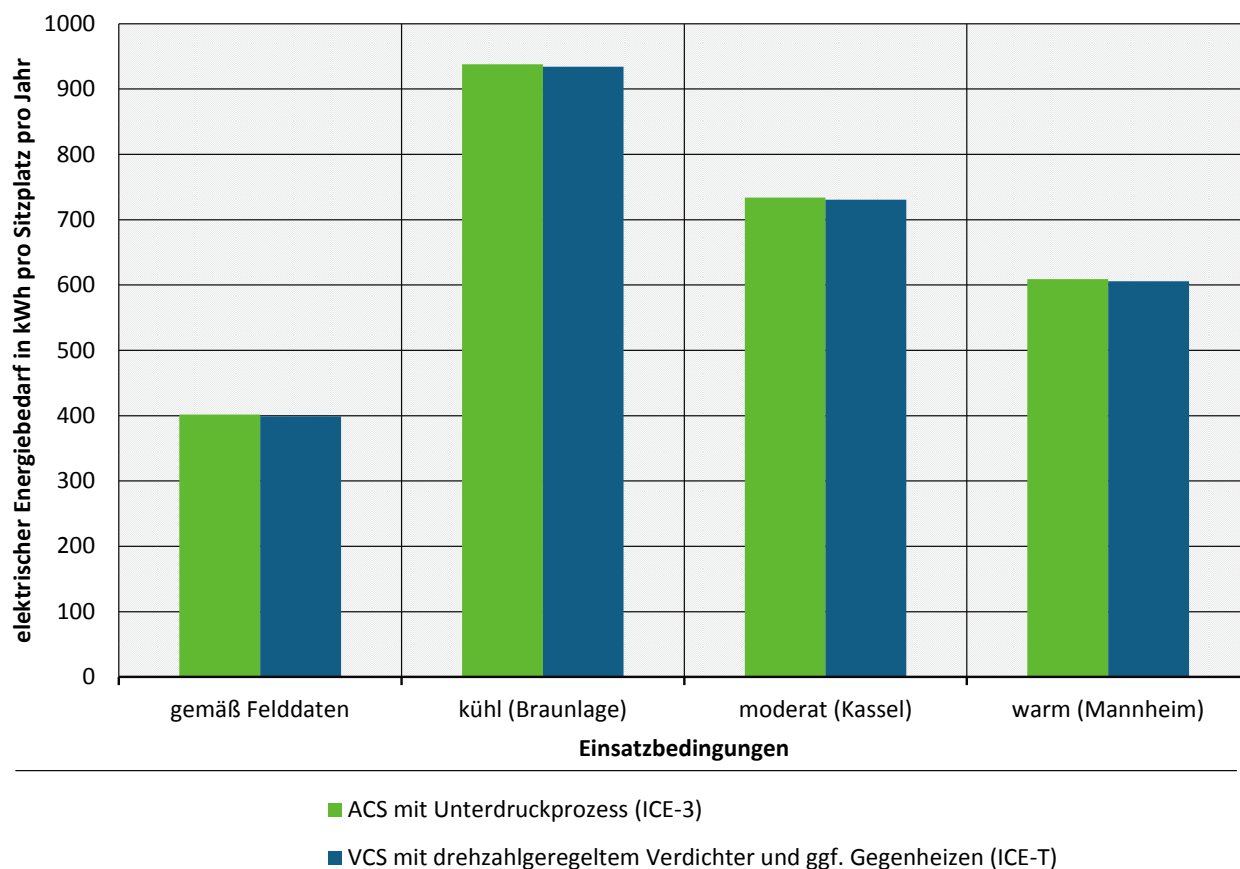
As can be seen in Figure 107, heating operation barely shows any differences, as the same heating technology is used in the investigated systems. The ICE 3 air-cycle system has a slightly increased consumption (1% or less) due to permanent activation of the magnetic bearings.

If the annual energy consumption in cooling operation and heating operation are examined together, the ACS has savings of 9% (Kassel and Mannheim, test reference years) to 16% (operating conditions according to field data) compared to VCS. The reason for the higher savings potential for the operating conditions according to field data is that the share of heating turns out to be lower for the identified temperature distribution compared to the share of cooling than it does for the other operating conditions. The advantages of ACS in cooling operation therefore have a stronger impact on the overall result.

As summarised in section 1.4.3, a very similar investigation was conducted by (Meister, 2012). However, the general conditions for the study by Meister and the present study are different (see section 2.3.3.7 on this point). Consequently, the results of the two investigations are different. The absolute numbers for the annual energy consumption differ in particular due to different underlying operating hours, different distributions of the model input parameters (weighting matrices) and a different lower limit temperature for the analysis of the cooling operation in the classification.

The relative comparison of the annual energy consumption for cooling operation of the examined systems provided very similar results for the two investigations with a difference of only a few percentage points. The comparison of the results shows that the results for the annual energy consumption in this study fall within a plausible order of magnitude.

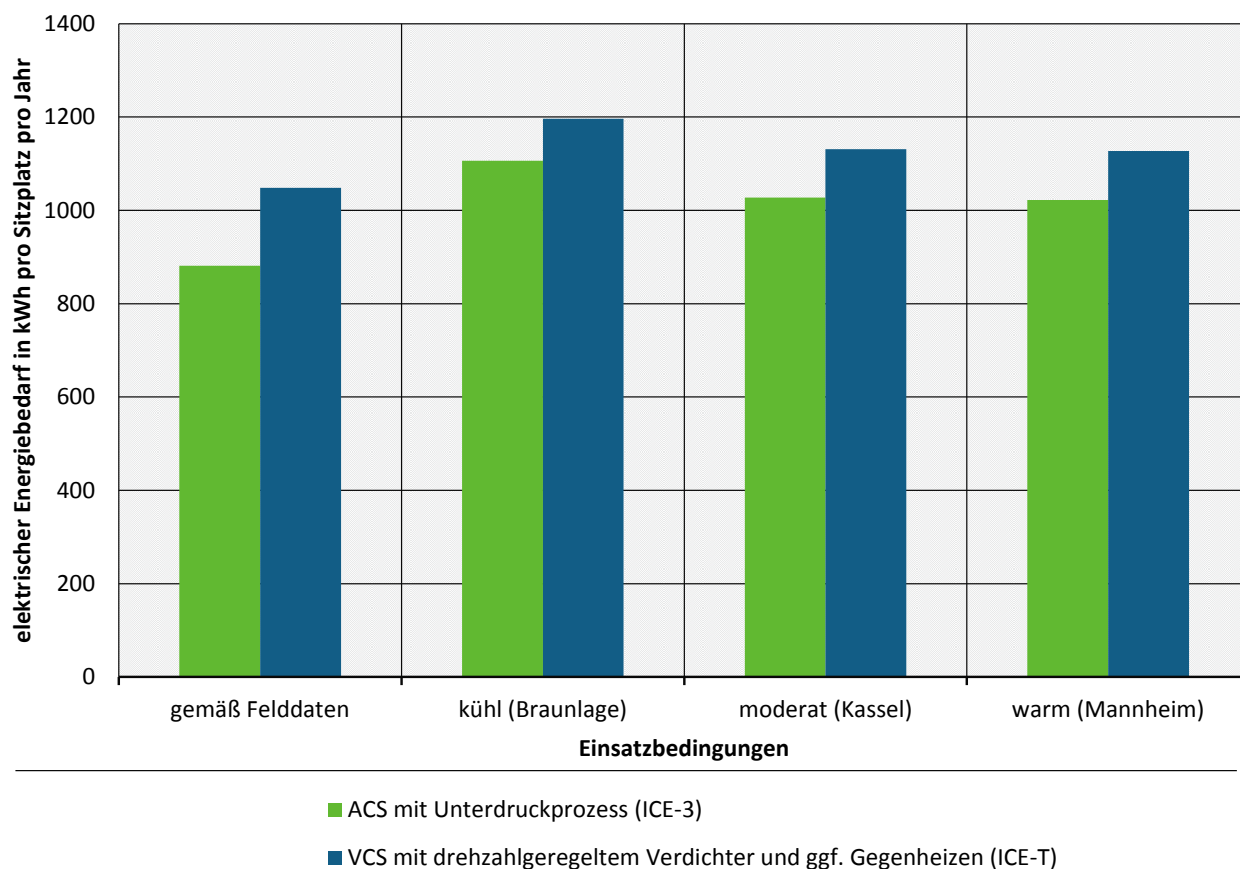
Figure 107: Comparison of primary annual energy consumption in heating operation for the air-cycle system ACS (ICE 3) and the vapour cycle system VCS (ICE-T)



Annual energy consumption in heating operation for the air-cycle system (ACS) with reverse loop (based on implementation in ICE 3) and the vapour cycle system (VCS) with variable-speed compressor and option for reheating (based on implementation in ICE-T) (source data: field data); energy consumption is based on 6,570 operating hours in comfort mode per year. Energy consumption is at the device interface, i.e. excluding the efficiency of the on-board power supply up to the pantograph. Source: own illustration, Liebherr

elektrischer Energiebedarf in kWh pro Sitzplatz pro Jahr = electrical energy consumption in kWh per seat per year; gemäß Felddaten = according to the field data; kühl (Braunlage) = cool (Braunlage); moderat Kassel = moderate (Kassel); warm (Mannheim) = warm (Mannheim); Einsatzbedingungen = operating conditions; ACS mit Unterdruckprozess (ICE 3) = ACS with reverse loop (ICE 3); VCS mit drehzahlgeregeltem Verdichter und ggf. Gegenheizen (ICE-T) = VCS with variable-speed compressor and option for reheating (ICE-T)

Figure 108: Comparison of total primary annual energy consumption for the air-cycle system ACS (ICE 3) and the vapour cycle system VCS (ICE-T)



Total annual energy consumption for the air-cycle system (ACS) with reverse loop (based on implementation in ICE 3) and the vapour cycle system (VCS) with variable-speed compressor and option for reheating (based on implementation in ICE-T) (source data: field data); energy consumption is based on 6,570 operating hours in comfort mode per year. Energy consumption is at the device interface, i.e. excluding the efficiency of the on-board power supply up to the pantograph. Source: own illustration, Liebherr

elektrischer Energiebedarf in kWh pro Sitzplatz pro Jahr = electrical energy consumption in kWh per seat per year; gemäß Felddaten = according to the field data; kühl (Braunlage) = cool (Braunlage); moderat Kassel = moderate (Kassel); warm (Mannheim) = warm (Mannheim); Einsatzbedingungen = operating conditions; ACS mit Unterdruckprozess (ICE 3) = ACS with reverse loop (ICE 3); VCS mit drehzahlgeregeltem Verdichter und ggf. Gegenheizen (ICE-T) = VCS with variable-speed compressor and option for reheating (ICE-T)

Table 7: Comparison of primary annual energy consumption for the air-cycle system (ICE 3) with the vapour-compression refrigeration system (ICE-T)

Operating conditions	Energy consumption in comfort mode		Comparison	
	ACS_UntDP ICE 3 Measurement kWh/(seat x year)	VCS_f/U_GH ICE-T Measurement kWh/(seat x year)	absolute ACS_UntDP - VCS_f/U_GH kWh/(seat x year)	relative ACS_UntDP/ VCS_f/U_GH
Cooling				
according to field data	479.5	649.0	-169.5	74%
cool (Braunlage)	168.4	262.5	-94.1	64%
moderate (Kassel)	293.4	400.5	-107.2	73%
warm (Mannheim)	413.2	521.5	-108.3	79%
Heating				
according to field data	401.8	399.1	2.7	101%
cool (Braunlage)	937.8	934.1	3.7	100%
moderate (Kassel)	733.9	730.6	3.3	100%
warm (Mannheim)	608.8	605.9	3.0	100%
Total				
according to field data	881.3	1048.1	-166.9	84%
cool (Braunlage)	1106.2	1196.6	-90.3	92%
moderate (Kassel)	1027.3	1131.1	-103.8	91%
warm (Mannheim)	1022.0	1127.4	-105.3	91%

ACS_UntDP: ACS with reverse loop

VCS_f/U_GH: VCS with variable-speed compressor and option for reheating

Comparison of annual energy consumption for the air-cycle system (ACS) on the ICE 3 with the vapour cycle system (VCS) on the ICE-T; Energy consumption based on 6,570 operating hours in comfort mode per year;

Energy consumption is at the device interface, i.e. excluding the efficiency of the on-board power supply up to the pantograph.

Table 8 summarises the comparison results for the secondary energy consumptions due to the impulse resistance of the intake air for systems 1 and 2. Figure 109 shows the secondary annual energy consumption for heating and cooling combined. In contrast to the primary energy consumptions presented above, these energy consumptions are not at the unit interface, but at the pantograph. Hence, the efficiencies for traction and on-board power supply are included.

Table 8: Comparison of the secondary annual energy consumption for the air-cycle system (ICE 3) with the vapour-compression refrigeration system (ICE-T)

Operating conditions	Energy consumption in comfort mode		Comparison	
	ACS_UntDP ICE 3 Measurement kWh/(seat x year)	VCS_f/U_GH ICE-T Measurement kWh/(seat x year)	absolute ACS_UntDP - VCS_f/U_GH kWh/(seat x year)	relative ACS_UntDP/VCS _f/U_GH %
Cooling				
according to field data	54.7	131.6	-76.9	42%
cool (Braunlage)	22.1	50.8	-28.7	44%
moderate (Kassel)	34.6	82.4	-47.7	42%
warm (Mannheim)	45.8	112.0	-66.2	41%
Heating				
according to field data	24.3	24.2	0.1	100%
cool (Braunlage)	36.5	36.4	0.1	100%
moderate (Kassel)	32.4	32.4	0.1	100%
warm (Mannheim)	28.8	28.8	0.1	100%
Total				
according to field data	79.0	155.8	-76.8	51%
cool (Braunlage)	58.6	87.2	-28.6	67%
moderate (Kassel)	67.1	114.7	-47.7	58%
warm (Mannheim)	74.6	140.8	-66.1	53%

ACS_UntDP: ACS with reverse loop

VCS_f/U_GH: VCS with variable-speed compressor and option for reheating

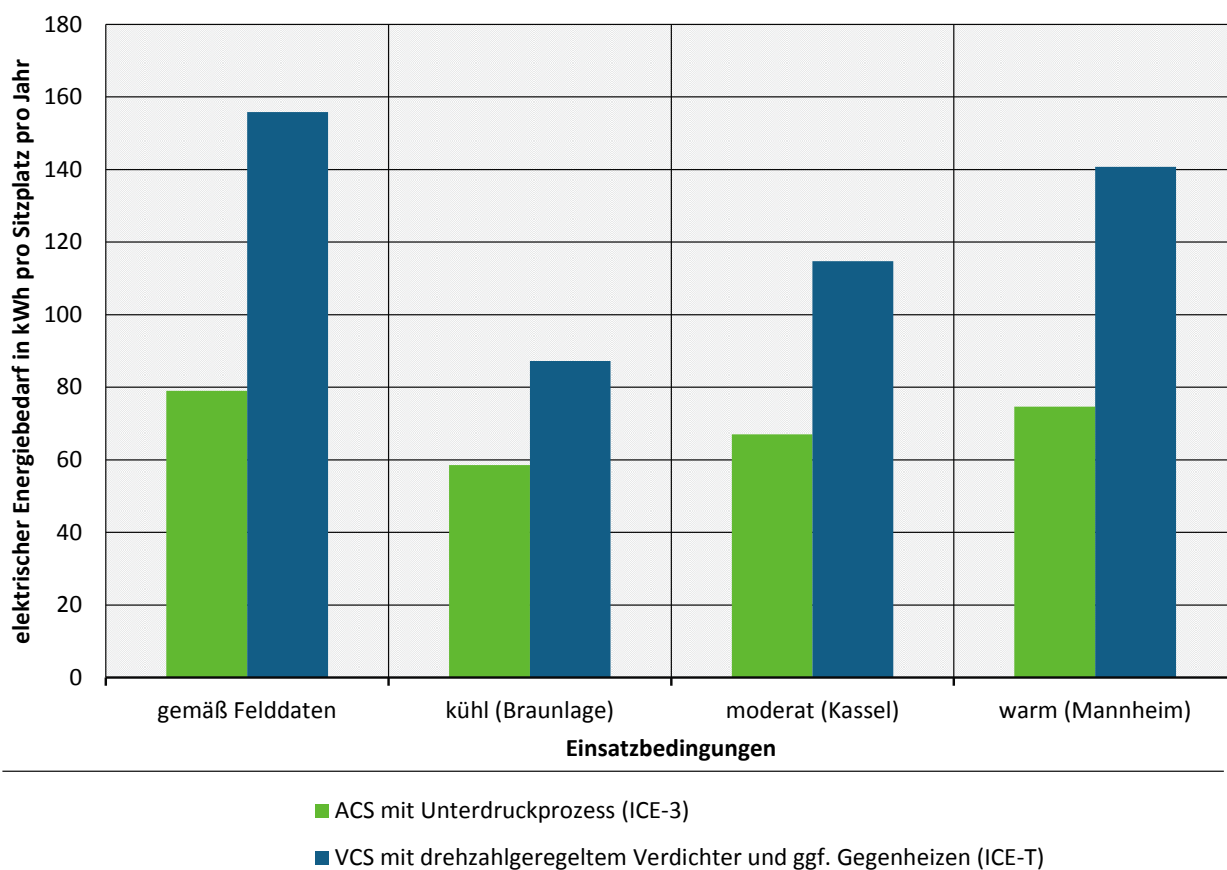
Energy consumption based on 6,570 operating hours in comfort mode per year;

Energy consumption at the pantograph, i.e. including efficiency for traction and on-board power supply

While there is no difference between the examined systems with respect to the required fresh air volume for the passenger compartment – the fresh air control in both systems is occupancy-dependent (control of CO₂ content in the passenger compartment), the required air mass flow to be drawn in to the air-cycle system for cooling (system 1; process air mass flow) is significantly lower than for the vapour cycle system (system 2; condenser air mass flow). It is immediately evident from Table 8 (column for relative comparison) that the air-cycle technology (system 1) allows for a considerable reduction in the secondary energy consumption for cooling operation of more than 50% compared to the vapour cycle system (system 2).

In heating operation, there is no difference between the technologies with respect to the air mass flow to be drawn in, because in heating operation the same amount of fresh air required for the passengers needs to be provided for all systems. In heating operation, the high air mass flow for condenser air or process air is completely omitted, since there is no heat pump operation for the investigated systems.

Figure 109: Comparison of total secondary annual energy consumption for the air-cycle system ACS (ICE 3) and the vapour cycle system VCS (ICE-T)



ACS according to implementation in ICE 3 versus VCS according to implementation in ICE-T (source of data: field data); Energy consumption based on 6,570 operating hours in comfort mode per year; Energy consumption at the pantograph, i.e. including efficiency for traction and on-board power supply. Source: own illustration, Liebherr
 elektrischer Energiebedarf in kWh pro Sitzplatz pro Jahr = electrical energy consumption in kWh per seat per year;
 gemäß Felddaten = according to the field data; kühl (Braunlage) = cool (Braunlage); moderat Kassel = moderate (Kassel); warm (Mannheim) = warm (Mannheim); Einsatzbedingungen = operating conditions; ACS mit Unterdruckprozess (ICE 3) = ACS with reverse loop (ICE 3); VCS mit drehzahlgeregeltem Verdichter und ggf. Gegenheizen (ICE-T) = VCS with variable-speed compressor and option for reheating (ICE-T)

Table 9 summarises the results for the total primary and secondary energy consumption for systems 1 and 2. Figure 110 shows the total primary and secondary energy consumption for heating and cooling combined. The stated energy consumptions are not at the unit interface, but at the pantograph. Hence, they include the efficiencies for traction and on-board power supply for primary and secondary energy consumption.

It should be noted at this point that the primary energy consumption for systems 1 and 2 was derived from field data, while an analytical approach was selected to calculate the secondary energy consumption due to the impulse resistance.

For the following analysis of economic efficiency, the sum of the primary and secondary annual energy demand was used.

Table 9: Comparison of total combined primary and secondary annual energy consumption for the air-cycle system (ICE 3) with the vapour-compression refrigeration system (ICE-T)

Operating conditions	Energy consumption in comfort mode		Comparison	
	ACS_UntDP ICE 3 Measurement kWh/(seat x year)	VCS_f/U_GH ICE-T Measurement kWh/(seat x year)	absolute ACS_UntDP - VCS_f/U_GH kWh/(seat x year)	relative ACS_UntDP/VCS_ f/U_GH %
Cooling				
according to field data	573.1	833.3	-260.1	69%
cool (Braunlage)	204.2	334.6	-130.4	61%
moderate (Kassel)	351.8	515.4	-163.6	68%
warm (Mannheim)	492.5	675.8	-183.3	73%
Heating				
according to field data	458.6	455.7	2.9	101%
cool (Braunlage)	1050.3	1046.2	4.1	100%
moderate (Kassel)	825.8	822.2	3.7	100%
warm (Mannheim)	687.0	683.8	3.3	100%
Total				
according to field data	1031.8	1289.0	-257.2	80%
cool (Braunlage)	1254.5	1380.8	-126.3	91%
moderate (Kassel)	1177.6	1337.6	-159.9	88%
warm (Mannheim)	1179.5	1359.5	-180.0	87%

ACS_UntDP: ACS with reverse loop

VCS_f/U_GH: VCS with variable-speed compressor and option for reheating

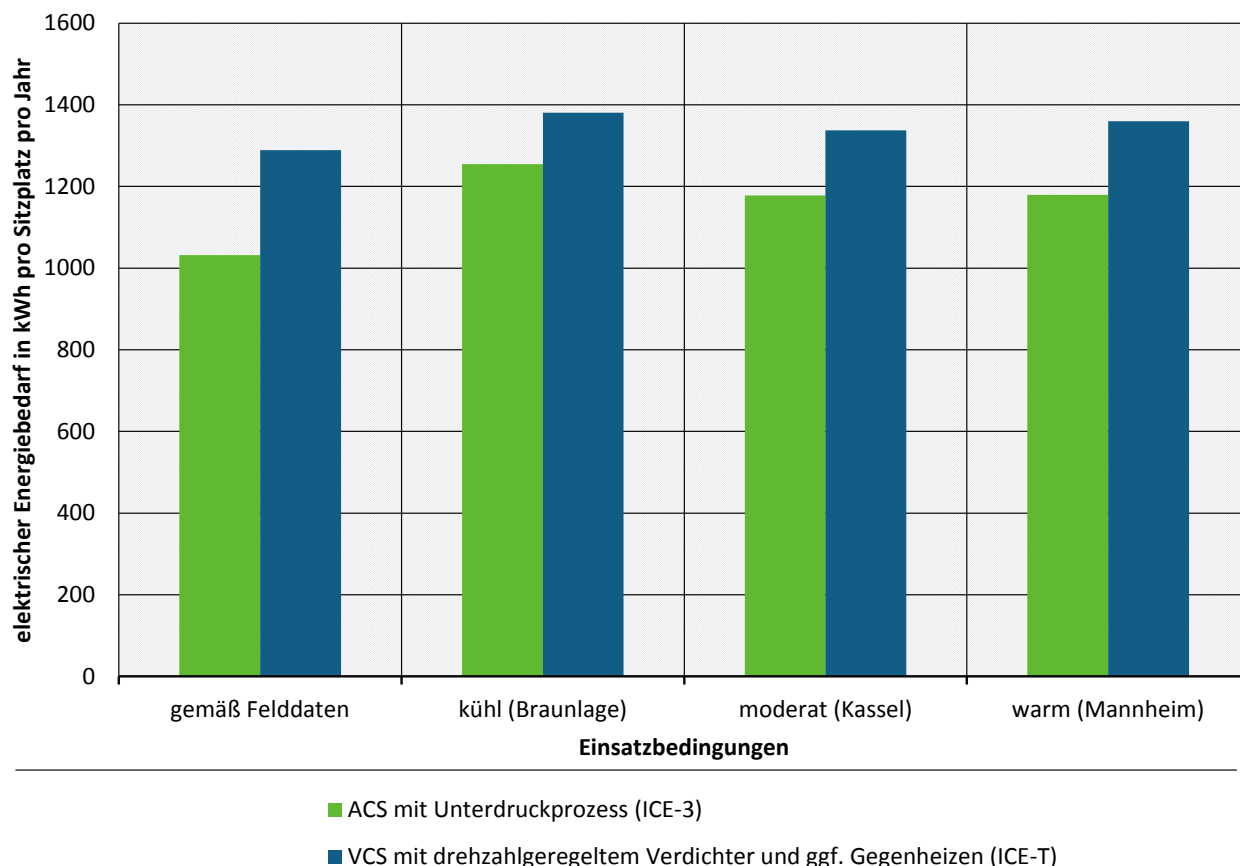
Energy consumption based on 6,570 operating hours in comfort mode per year;

Energy consumption at the pantograph, i.e. including efficiency for traction and on-board power supply

Comparing Table 7 (primary energy demand) and Table 9 (sum of primary and secondary energy demand), it becomes clear that a further energy efficiency advantage for the comparison system 1 (air-cycle system) over the comparison system 2 (vapour compression refrigerant system) by the lower secondary energy demand results: Depending on the operating conditions, for the air-cycle system (comparison system 1) a total saving of 9% to 20% compared to the considered vapour compression refrigerant system (comparison system 2) can be achieved in the overall consideration with secondary

energy consumption for cooling and heating operation (see Table 9, last line). For the cooling operation alone, the savings for the air cycle system are in the range of 27% to 39% compared to the vapour compression refrigerant system (see Table 9, 1st line).

Figure 110: Comparison of total primary and secondary annual energy consumption for the air-cycle system ACS (ICE 3) and the vapour cycle system VCS (ICE-T)



ACS according to implementation in ICE 3 versus VCS according to implementation in ICE-T (source of data: field data); Energy consumption based on 6,570 operating hours in comfort mode per year; Energy consumption at the pantograph, i.e. including efficiency for traction and on-board power supply. Source: own illustration, Liebherr
 elektrischer Energiebedarf in kWh pro Sitzplatz pro Jahr = electrical energy consumption in kWh per seat per year;
 gemäß Felddaten = according to the field data; kühl (Braunlage) = cool (Braunlage); moderat Kassel = moderate (Kassel); warm (Mannheim) = warm (Mannheim); Einsatzbedingungen = operating conditions; ACS mit Unterdruckprozess (ICE 3) = ACS with reverse loop (ICE 3); VCS mit drehzahlgeregeltem Verdichter und ggf. Gegenheizen (ICE-T) = VCS with variable-speed compressor and option for reheating (ICE-T)

Comparison of the air-cycle system (ACS) with direct loop from simulation (system 6) with the vapour cycle system (VCS) on the ICE-T, but with assumed bypass instead of reheating (system 3)

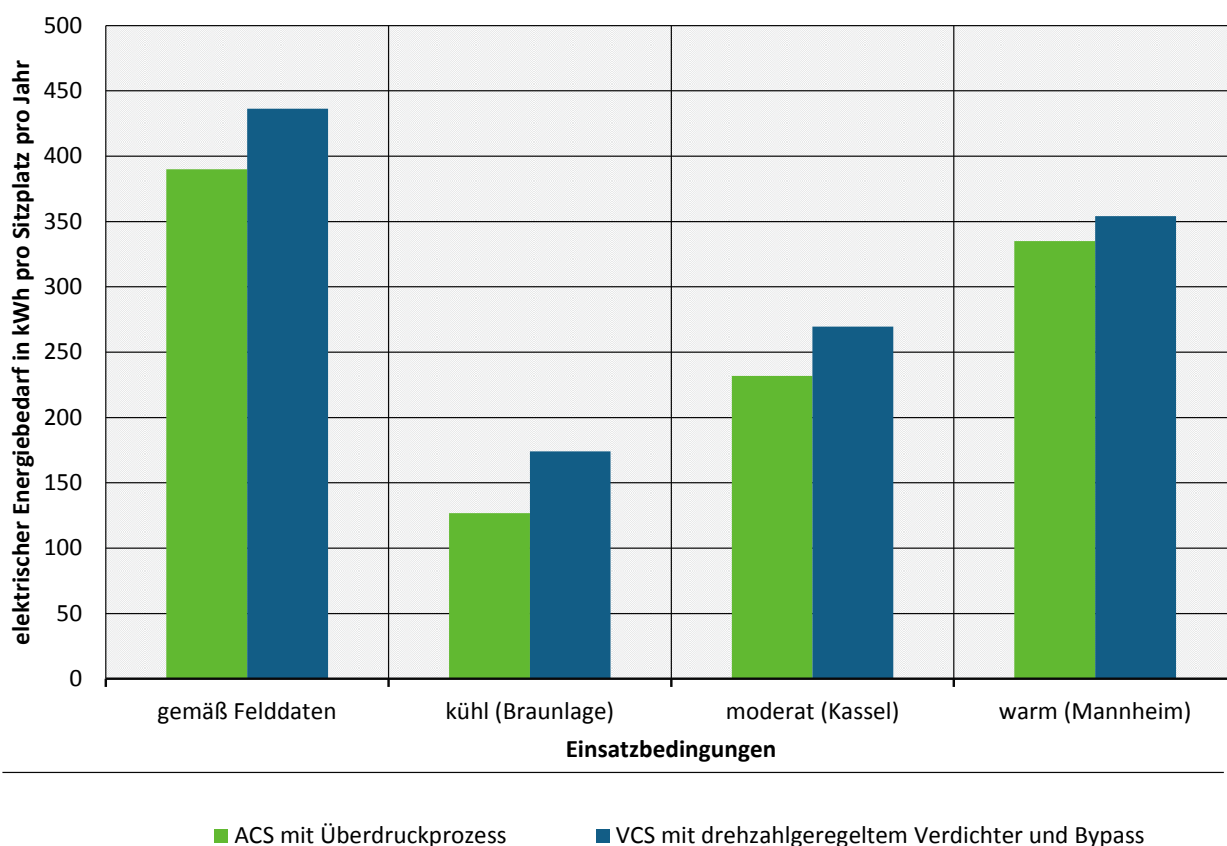
Figure 111, Figure 112, Figure 113 and Table 10 show the primary energy consumption for cooling, for heating, as well as for cooling and heating added together for the HVAC systems (systems 6 and 3) that were analysed on the basis of simulation/calculation. Note the adjusted and therefore the different scaling in each case on the ordinate axes (Y-axis) of the charts. The stated energy consumptions are at the unit interface of the HVAC unit in each case. As such, efficiencies for the on-board power supply up to the pantograph are not included here. Table 10 provides a summary of the comparison results.

The technical difference between the systems comes again down to cooling operation. In a comparison of the ACS system with the VCS system, the analysis shows savings potential of 5% for the investigated warm climate zone (Mannheim) to 27% for the investigated cool climate zone (Braunlage). The operating conditions according to field data show savings potential of 11% for the ACS. Note that the temperature distribution during the measurement period was shifted to higher temperatures compared to the temperature distribution from the representative years (test reference years).

As Figure 112 shows for the energy consumption in heating operation, there are no differences in heating operation since the advanced/optimised ACS system no longer has any permanently activated magnetic bearings.

If the annual energy consumption in cooling operation and heating operation are examined together, the air-cycle system has savings of 2% (Mannheim, test reference years) to 6% (operating conditions according to field data) compared to the improved vapour cycle system.

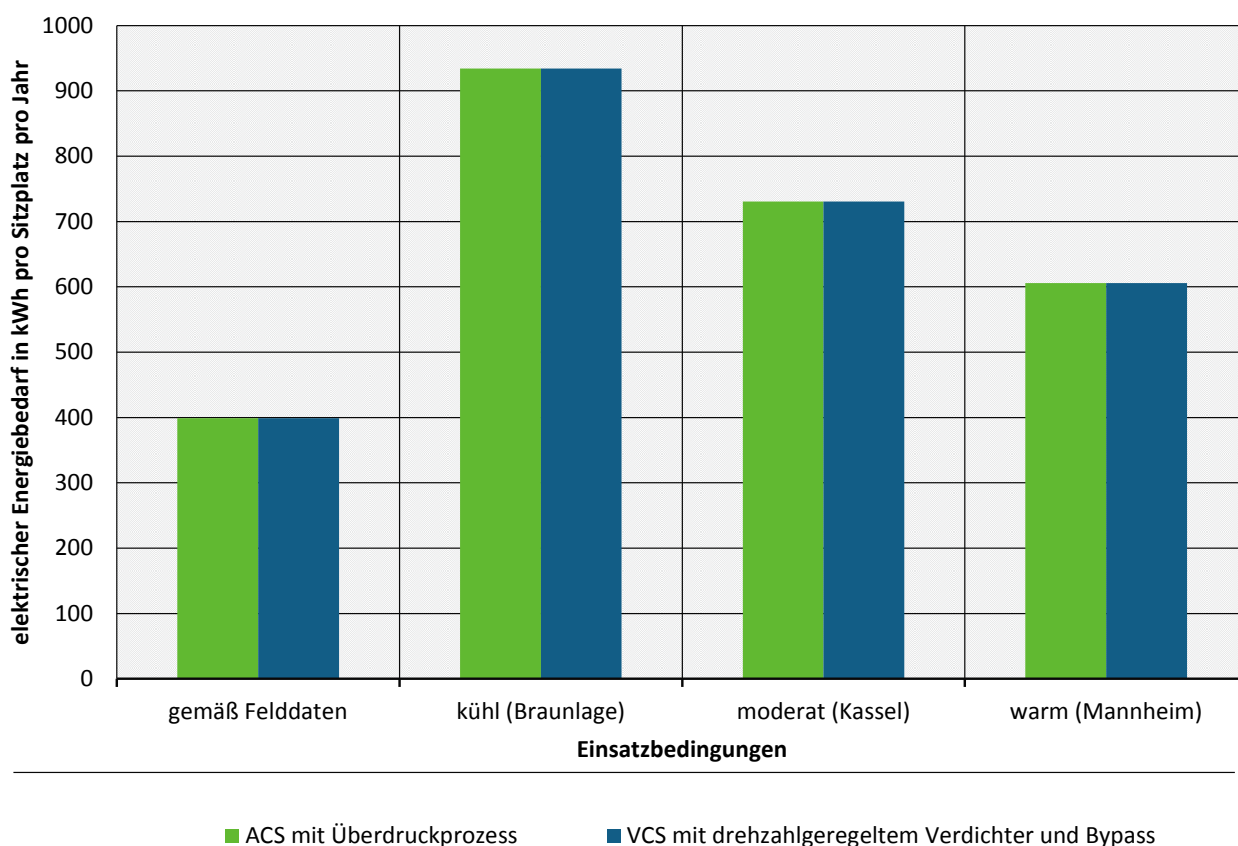
Figure 111: Comparison of the primary annual energy consumption in cooling operation for the air-cycle system (ACS) with direct loop and the vapour cycle system (VCS) with variable-speed compressor and refrigerant bypass



Comparison of annual energy consumption in cooling operation for the air-cycle system (ACS) with direct loop from simulation with the vapour cycle system with variable-speed compressor (VCS) based on the ICE-T and with projected refrigerant bypass instead of reheating; Energy consumption based on 6,570 operating hours in comfort mode per year; Energy consumption is at the device interface, i.e. excluding the efficiency of the on-board power supply up to the pantograph. Source: own illustration, Liebherr

elektrischer Energiebedarf in kWh pro Sitzplatz pro Jahr = electrical energy consumption in kWh per seat per year; gemäß Felddaten = according to the field data; kühl (Braunlage) = cool (Braunlage); moderat Kassel = moderate (Kassel); warm (Mannheim) = warm (Mannheim); Einsatzbedingungen = operating conditions; ACS mit Überdruckprozess = ACS with direct loop; VCS mit drehzahlgeregeltem Verdichter und Bypass = VCS with variable speed compressor and bypass

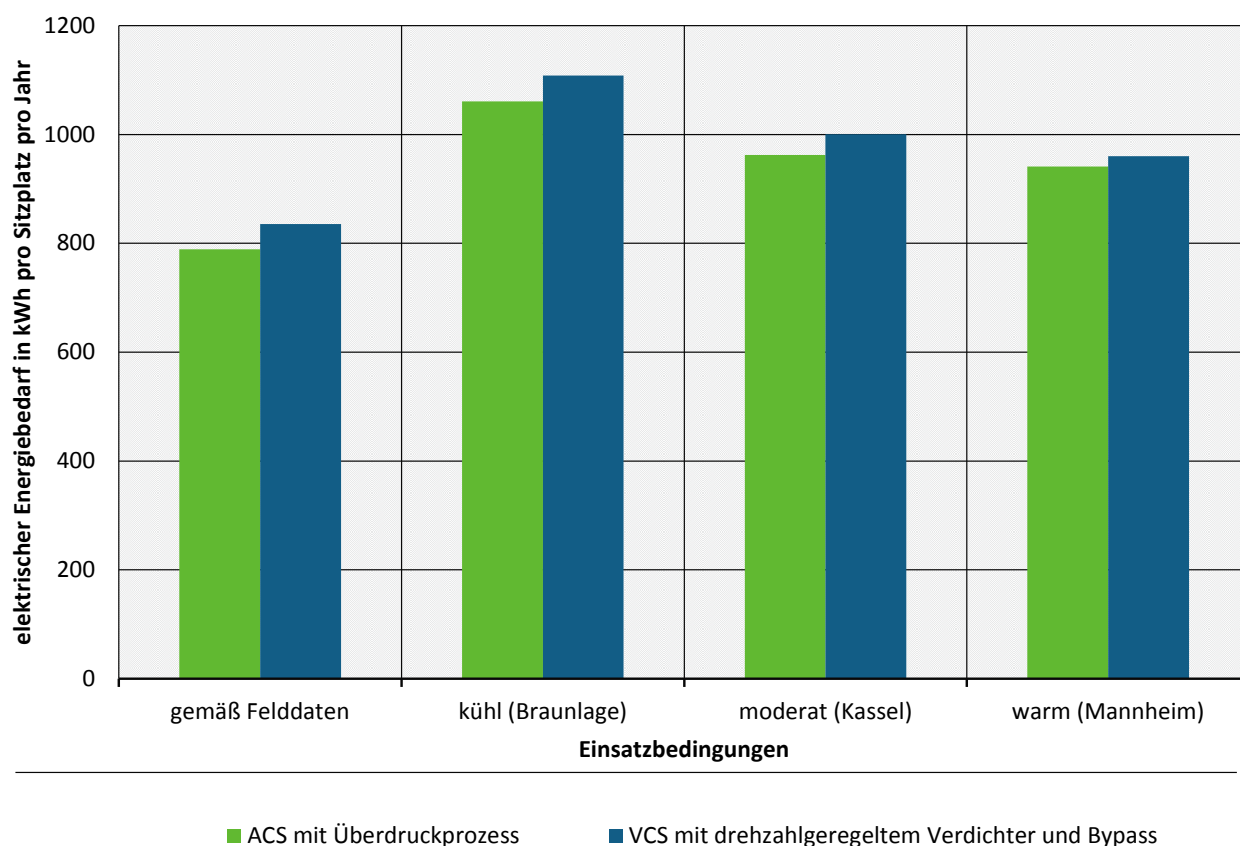
Figure 112: Comparison of primary annual energy consumption in heating operation for the air-cycle system with direct loop and the vapour cycle system with variable-speed compressor and refrigerant bypass



Comparison of annual energy consumption in heating operation for the air-cycle system (ACS) with direct loop from simulation with the vapour cycle system with variable-speed compressor (VCS) based on the ICE-T and with projected refrigerant bypass instead of reheating; Energy consumption based on 6,570 operating hours in comfort mode per year; Energy consumption is at the device interface, i.e. excluding the efficiency of the on-board power supply up to the pantograph. Source: own illustration, Liebherr

elektrischer Energiebedarf in kWh pro Sitzplatz pro Jahr = electrical energy consumption in kWh per seat per year; gemäß Felddaten = according to the field data; kühl (Braunlage) = cool (Braunlage); moderat Kassel = moderate (Kassel); warm (Mannheim) = warm (Mannheim); Einsatzbedingungen = operating conditions; ACS mit Überdruckprozess = ACS with direct loop; VCS mit drehzahlgeregeltem Verdichter und Bypass = VCS with variable speed compressor and bypass

Figure 113: Comparison of the total primary annual energy consumption in heating and cooling for the air-cycle system with direct loop and the vapour cycle system with variable-speed compressor and refrigerant bypass



Comparison of total annual energy consumption for the air-cycle system (ACS) with direct loop from simulation with the vapour cycle system with variable-speed compressor (VCS) based on the ICE-T and with projected refrigerant bypass instead of reheating; Energy consumption based on 6,570 operating hours in comfort mode per year; Energy consumption is at the device interface, i.e. excluding the efficiency of the on-board power supply up to the pantograph. Source: own illustration, Liebherr

elektrischer Energiebedarf in kWh pro Sitzplatz pro Jahr = electrical energy consumption in kWh per seat per year; gemäß Felddaten = according to the field data; kühl (Braunlage) = cool (Braunlage); moderat Kassel = moderate (Kassel); warm (Mannheim) = warm (Mannheim); Einsatzbedingungen = operating conditions; ACS mit Überdruckprozess = ACS with direct loop; VCS mit drehzahlgeregeltem Verdichter und Bypass = VCS with variable speed compressor and bypass

Table 10: Comparison of the primary annual energy consumption for the air-cycle system with direct loop and the vapour cycle system with variable-speed compressor and refrigerant bypass

Operating conditions	Energy consumption in comfort mode		Comparison	
	ACS_ÜbDP Simulation	VCS_f/U_BP Bypass: Assumption	absolute ACS_ÜbDP - VCS_f/U_BP	relative ACS_ÜbDP / VCS_f/U_BP
	kWh/(seat x year)	kWh/(seat x year)	kWh/(seat x year)	
Cooling				
according to field data	389.9	436.3	-46.4	89%
cool (Braunlage)	126.8	174.1	-47.4	73%
moderate (Kassel)	231.9	269.5	-37.7	86%
warm (Mannheim)	335.0	354.1	-19.1	95%
Heating				
according to field data	399.1	399.1	0.0	100%
cool (Braunlage)	934.1	934.1	0.0	100%
moderate (Kassel)	730.6	730.6	0.0	100%
warm (Mannheim)	605.9	605.9	0.0	100%
Total				
according to field data	789.0	835.5	-46.4	94%
cool (Braunlage)	1060.8	1108.2	-47.4	96%
moderate (Kassel)	962.5	1000.1	-37.7	96%
warm (Mannheim)	940.9	959.9	-19.1	98%

ACS_ÜbDP: Air-cycle system with direct loop

VCS_f/U_BP: Vapour cycle system with speed-controlled compressor and refrigerant bypass

Comparison of the annual energy consumption for the air-cycle system with direct loop and the vapour cycle system with variable-speed compressor and refrigerant bypass; Energy consumption based on 6,570 operating hours in comfort mode per year; Energy consumption is at the device interface, i.e. excluding the efficiency of the on-board power supply up to the pantograph.

Table 11 summarises the comparison results for the secondary energy consumptions due to the impulse resistance of the intake air for systems 6 and 3. Figure 114 shows the secondary annual energy consumption for heating and cooling combined. In contrast to the primary energy consumptions presented above, these primary energy consumptions are not at the unit interface, but at the pantograph. Hence, the efficiencies for traction and on-board power supply are included.

Table 11: Comparison of the secondary annual energy consumption for the air-cycle system with direct loop and the vapour cycle system with variable-speed compressor and refrigerant bypass

Operating conditions	Energy consumption in comfort mode		Comparison	
	ACS_ÜbDP Simulation kWh/(seat x year)	VCS_f/U_BP Bypass: Assumption kWh/(seat x year)	absolute ACS_ÜbDP - VCS_f/U_BP kWh/(seat x year)	relative ACS_ÜbDP/ VCS_f/U_BP %
Cooling				
according to field data	71.4	130.5	-59.1	55%
cool (Braunlage)	29.1	49.2	-20.1	59%
moderate (Kassel)	45.1	80.8	-35.7	56%
warm (Mannheim)	59.3	110.5	-51.2	54%
Heating				
according to field data	24.3	24.2	0.1	100%
cool (Braunlage)	36.5	36.4	0.1	100%
moderate (Kassel)	32.4	32.4	0.1	100%
warm (Mannheim)	28.8	28.8	0.1	100%
Total				
according to field data	95.7	154.8	-59.1	62%
cool (Braunlage)	65.6	85.6	-20.0	77%
moderate (Kassel)	77.5	113.2	-35.6	69%
warm (Mannheim)	88.1	139.3	-51.1	63%

ACS_ÜbDP: ACS with direct loop

VCS_f/U_BP: VSC with speed-controlled compressor and refrigerant bypass

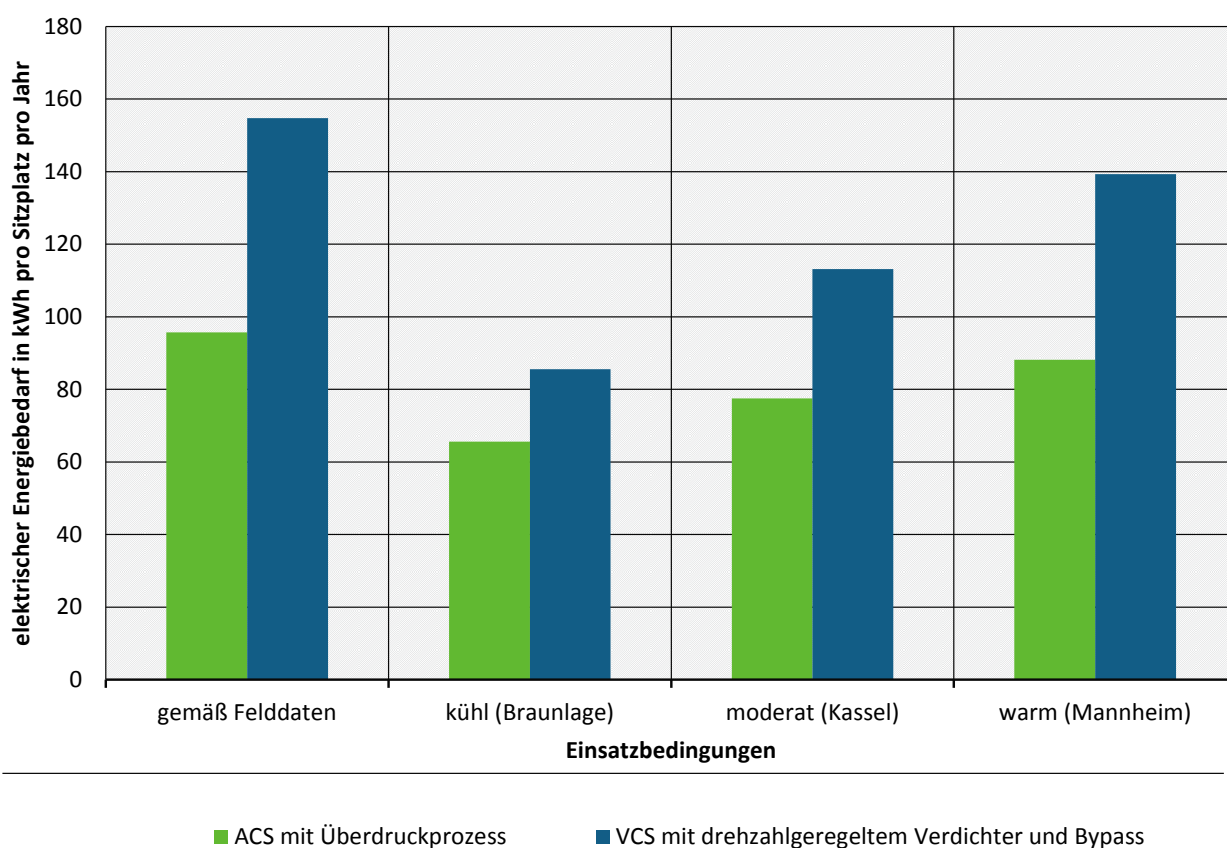
Energy consumption based on 6,570 operating hours in comfort mode per year;

Energy consumption at the pantograph, i.e. including efficiency for traction and on-board power supply

While there is no difference between the examined systems with respect to the required fresh air volume for the passenger compartment – the fresh air control in both systems is occupancy-dependent (control of CO₂ content in the passenger compartment), the required air mass flow to be drawn in to the air-cycle system for cooling (system 6) is significantly lower than for the vapour cycle system (system 3). It is immediately evident from Table 8 (column for relative comparison) that the air-cycle technology (system 6) allows for a considerable reduction in the secondary energy consumption for cooling operation of more than 40% compared to the vapour cycle system (system 3).

In heating operation, there is no difference between the technologies with respect to the air mass flow to be drawn in, because in heating operation the same amount of fresh air required for the passengers needs to be provided for all systems.

Figure 114: Comparison of the total secondary annual energy consumption for the air-cycle system with direct loop and the vapour cycle system with variable-speed compressor and refrigerant bypass



ACS with direct loop from simulations compared to VCS according to ICE-T, but with assumed bypass instead of reheating; Energy consumption based on 6,570 operating hours in comfort mode per year; Energy consumption at the pantograph, i.e. including efficiency for traction and on-board power supply. Source: own illustration, Liebherr
 elektrischer Energiebedarf in kWh pro Sitzplatz pro Jahr = electrical energy consumption in kWh per seat per year;
 gemäß Felddaten = according to the field data; kühl (Braunlage) = cool (Braunlage); moderat (Kassel) = moderate (Kassel); warm (Mannheim) = warm (Mannheim); Einsatzbedingungen = operating conditions; ACS mit Überdruckprozess = ACS with direct loop; VCS mit drehzahlgezieltem Verdichter und Bypass = VCS with variable speed compressor and bypass

Table 12 summarises the comparison results for the total primary and secondary energy consumption for systems 6 and 3. Figure 115 shows the total primary and secondary energy consumption for heating and cooling combined. The stated energy consumptions are not at the unit interface, but at the pantograph. Hence, they include the efficiencies for traction and on-board power supply for primary and secondary energy consumption.

The results for primary and secondary annual energy consumption added together were used for the subsequent analysis of economic efficiency.

Table 12: Comparison of the primary and secondary annual energy consumption combined for the air-cycle system with direct loop and the vapour cycle system with variable-speed compressor and refrigerant bypass

Operating conditions	Energy consumption in comfort mode		Comparison	
	ACS_ÜbDP Simulation kWh/(seat x year)	VCS_f/U_BP Bypass: Assumption kWh/(seat x year)	absolute ACS_ÜbDP - VCS_f/U_BP kWh/(seat x year)	relative ACS_ÜbDP/VCS_f /U_BP %
Cooling				
according to field data	492.9	602.3	-109.3	82%
cool (Braunlage)	166.2	237.5	-71.3	70%
moderate (Kassel)	295.8	372.2	-76.4	79%
warm (Mannheim)	421.5	493.3	-71.8	85%
Heating				
according to field data	455.8	455.7	0.1	100%
cool (Braunlage)	1046.3	1046.2	0.1	100%
moderate (Kassel)	822.2	822.2	0.1	100%
warm (Mannheim)	683.8	683.8	0.1	100%
Total				
according to field data	948.7	1058.0	-109.3	90%
cool (Braunlage)	1212.4	1283.7	-71.2	94%
moderate (Kassel)	1118.0	1194.4	-76.3	94%
warm (Mannheim)	1105.3	1177.1	-71.8	94%

ACS_ÜbDP: ACS with direct loop

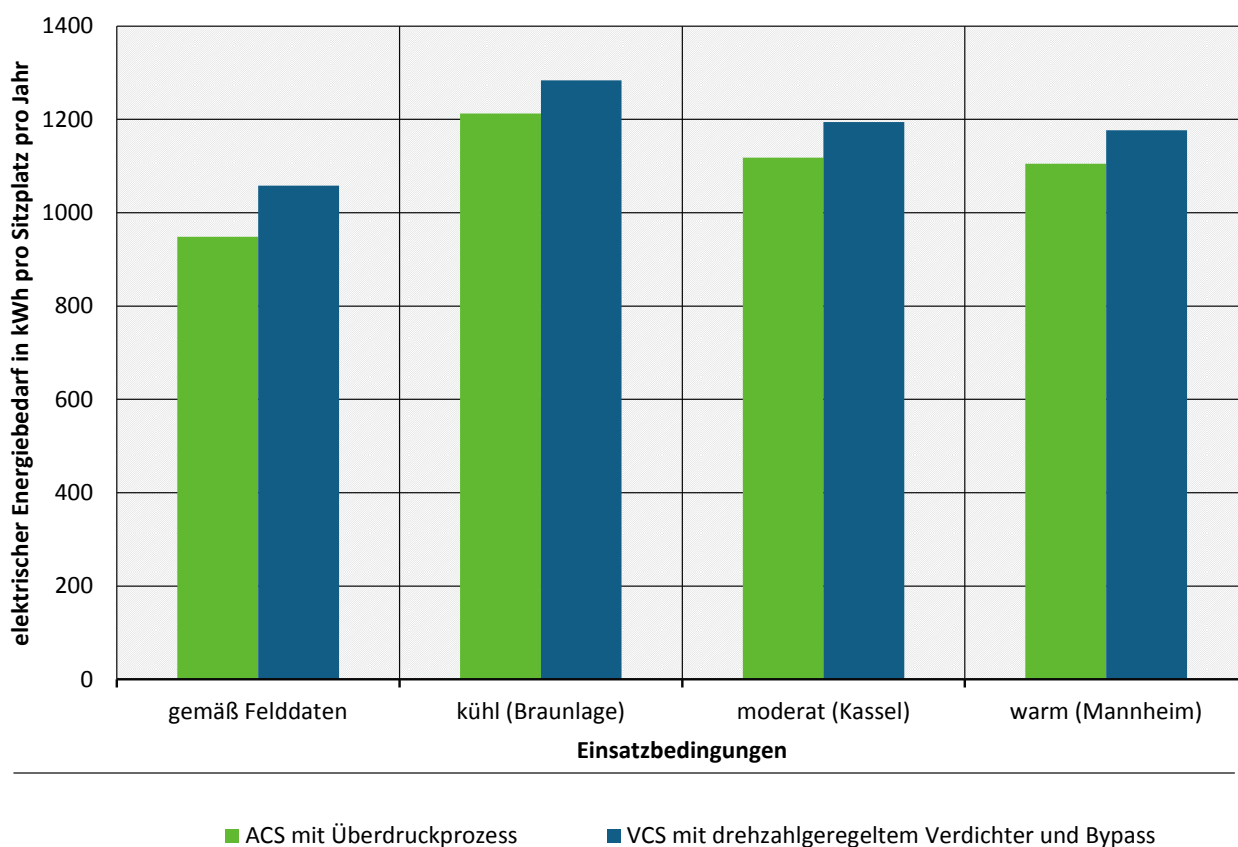
VCS_f/U_BP: VSC with speed-controlled compressor and refrigerant bypass

Energy consumption based on 6,570 operating hours in comfort mode per year;

Energy consumption at the pantograph, i.e. including efficiency for traction and on-board power supply

Comparing Table 10 (primary energy demand) and Table 12 (sum of primary and secondary energy demand), it becomes clear that a further energy efficiency advantage for the comparison system 6 (air-cycle system) over the comparison system 3 (vapour compression refrigerant system) by the lower secondary energy demand results: Depending on the operating conditions, for the air-cycle system (comparison system 6) a total saving of 6% to 10% compared to the considered vapour compression refrigerant system (comparison system 3) can be achieved in the overall consideration with secondary energy consumption for cooling and heating operation (see Table 12, last line). For the cooling operation alone, the savings for the optimized air cycle system are in the range of 15% to 30% compared to the optimized vapour compression refrigerant system (see Table 12, 1st line).

Figure 115: Comparison of the total secondary annual energy consumption for the air-cycle system with direct loop and the vapour cycle system with variable-speed compressor and refrigerant bypass



ACS with direct loop from simulations compared to VCS according to ICE-T, but with assumed bypass instead of reheating; Energy consumption based on 6,570 operating hours in comfort mode per year; Energy consumption at the pantograph, i.e. including efficiency for traction and on-board power supply. Source: own illustration, Liebherr

elektrischer Energiebedarf in kWh pro Sitzplatz pro Jahr = electrical energy consumption in kWh per seat per year; gemäß Felddaten = according to the field data; kühl (Braunlage) = cool (Braunlage); moderat Kassel = moderate (Kassel); warm (Mannheim) = warm (Mannheim); Einsatzbedingungen = operating conditions; ACS mit Überdruckprozess = ACS with direct loop; VCS mit drehzahlgeregeltem Verdichter und Bypass = VCS with variable speed compressor and bypass

2.4.2 Complete analysis of Life Cycle Costs (LCC) and Total Costs of Ownership (TCO)

2.4.2.1 Design of the Cost Assessment Tool (CAT)

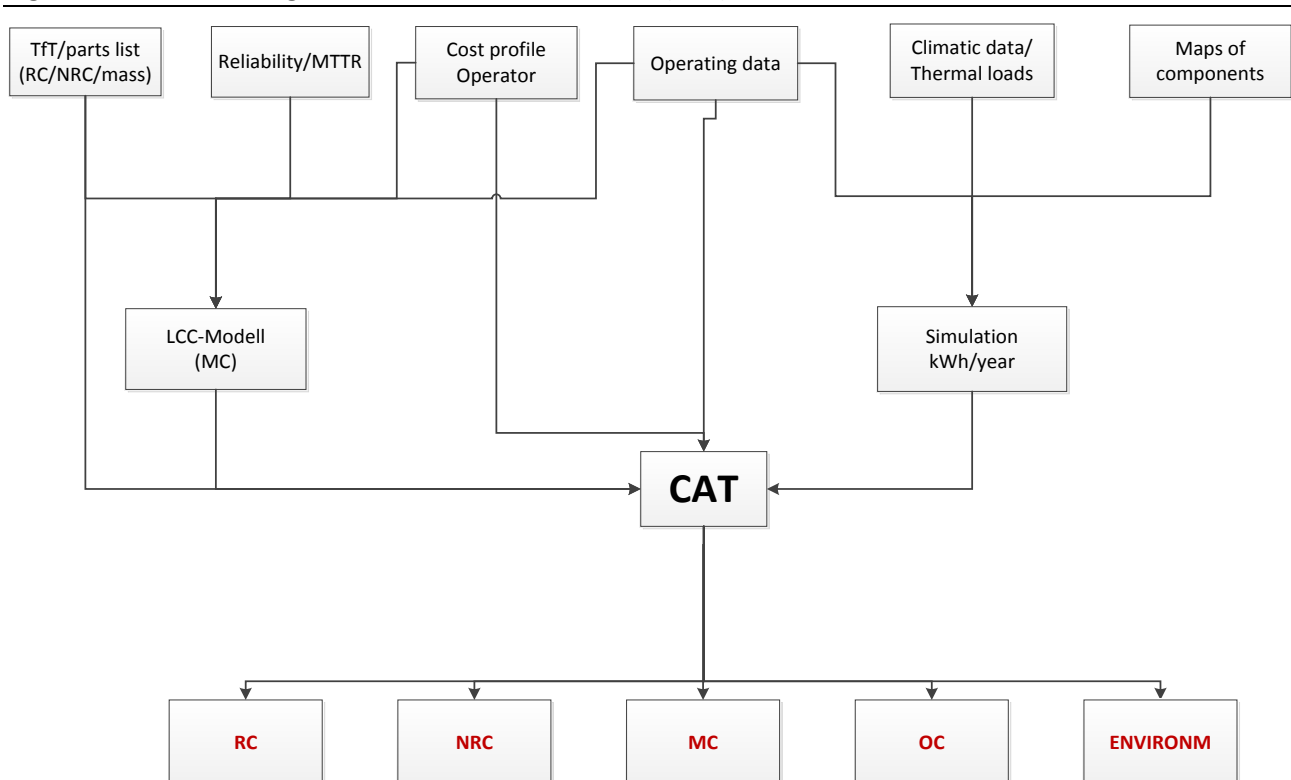
A comprehensive cost analysis was performed for comparison of the economic efficiency of the different heating, ventilation and air-conditioning systems (HVAC systems). A tool originally developed for aviation was used for this purpose. The Cost Assessment Tool (CAT) can be used to compare the costs that carriers incur for different equipment variants on aircraft. The outcome of analysis is the cost over the life cycle of the aircraft ("Total Cost of Ownership") per flight hour that are incurred with the applicable equipment.

When using the CAT for railways, the costs are stated in Euros per year per HVAC system (that is per carriage) against the life cycle of the railway vehicle. It is possible to compare existing and future systems.

Various tools are linked to generate the results. The structure of the cost calculation is shown in Figure 116. The input data are taken from cost planning (item for item cost planning) or from the bill of materials, which are used to determine the production costs and the unit weights. Based on the bill of materials, the Maintenance Cost is determined in the Life Cycle Cost (LCC) tool with reliability data for the components (MTTR-mean time to repair) and information from the operator about the method of operation and maintenance.

The system simulation relies on the performance data of the components and calculates a forecast of the energy consumption using the operating profile of the vehicle and the climate data.

Figure 116: Design of the Cost Assessment Tool (CAT)



Design of the Cost Assessment Tool (CAT Tool); MTTR = mean time to repair; Tft - Teil für Teil Kostenplanung = part per part cost planning; LCC= Life cycle cost; further abbreviations in the text. Source: own illustration, Liebherr

The result is a distribution of different cost types based on the annual costs per HVAC system for each version of a system considered.

- ▶ RC - Recurring Cost
- ▶ NRC- Non-Recurring Cost (development costs, engineering, prototype production, tests)
- ▶ MC - Maintenance Cost
- ▶ OC - Operating Cost
- ▶ ENVIRONM/Environmental Cost (CO₂ tax, retrofitting for environmentally friendly refrigerant)
- ▶ CAT Index/Sum of all costs per year

In principle, the Tool can also be used to perform a dynamic analysis. Dynamic developments can be investigated by specifying indexes for imputed interest or inflation indexes, in general or separately for energy and environmental costs. In this project, this was treated as neutral, i.e. imputed interest, development of the equity of the operating company, inflation, and energy price and environmental cost progression were treated as = 0.

2.4.2.2 Specific comparison of the HVAC systems

It is essential for comparison that identical operating conditions are simulated for the HVAC systems. For this reason, all the systems were based on a reference vehicle, carriage TW7 of ICE 3 trainset 301 from the field data analysis.

In the first step (comparison A), both of the systems, which have been in operation for many years, were compared or projected onto the reference vehicle (compared systems according to section 2.3.3.4):

- ▶ ICE-T vapour cycle system with R134a refrigerant with variable-speed compressor and the option for reheating (corresponds to system 2)
- ▶ ICE 3 2nd series - Air-cycle HVAC system with reverse loop air-cycle system (corresponds to system 1)

The second step (comparison B) shows a future scenario. Obvious potential for improvement and the next generation air-cycle system technology were compared here:

- ▶ ICE-T system concept, energy-optimised (corresponds to system 3)
- ▶ ICE 3 system concept, maintenance-optimised (corresponds to system 2; however, potential improvements identified during analysis of the maintenance data were taken into account in the Maintenance Cost model)
- ▶ Next generation air-cycle system, open direct loop (corresponds to system 6, section 2.3.3.4)

Figure 117: Overview for system comparison using the Cost Assessment Tool (CAT)

CAT Comparison					
Version	Comparison A		Comparison B		
Refrigerant	R134a	Air	Air	R134a	Air
HVAC equipment-Version	ICE-T	ICE3.2 (Reverse loop)	Reverse loop state of the art	ICE-T without counter heating	Next Generation ACS: Open direct loop
Regulation	speed controlled screw compressor, 2 condenser fans switched on demand, optionally counter heating	speed controlled air cycle machine	speed controlled air cycle machine	speed controlled screw compressor, 2 condenser fans switched on demand, hotgas bypass	speed controlled air cycle machine
Selected train for reference	ICE3, trainset 301 - TW7, 74 seats				

Overview for system comparison using the Cost Assessment Tool (CAT). Source: own illustration, Liebherr

2.4.2.3 Input variables for the analysis of economic efficiency

NRC – Non-Recurring Cost

The development costs were compensated for to ensure a fair comparison of conventional and future technologies, as the development costs for a new air conditioning technology are not transferred to just one production series or one type of carriage. It was assumed that the NRC in the long term would approach €1,000,000 per HVAC system and vehicle type for all systems. The current CAT model is based on a series of 500 carriages, across which the stated NRC is distributed.

RC - Recurring Cost

The recommended prices for the Recurring Cost (RC) for the reference vehicle, as expected for the current market, are as follows:

- ▶ RC for vapour cycle system: €40,000 (without refrigerant bypass)
- ▶ RC for vapour cycle system: €41,000 (with refrigerant bypass)
- ▶ RC for ACS reverse loop, analogous to ICE 3, 2nd series: €65,000
- ▶ RC for ACS direct loop, "Next generation ACS": €55,000

The manufacturing costs of air-cycle systems are a little higher than for vapour cycle systems, but the potential for economies of scale has not been taken into account. As demand for air-cycle technology increases and the quantities of corresponding components increases, one would expect a reduction in unit costs.

OC - Operating Cost

The principles for determining the energy consumption are presented in section 2.4.1.2. Table 13 shows the combined result for cooling operation and heating operation as the mean from the 3 climate zones of Braunlage, Kassel, Mannheim (data from the test reference year (TRY)) for the 74 seats of the reference vehicle. The energy consumption is at the pantograph, i.e. including losses from the on-board power supply and traction motor.

Table 13: Annual energy consumption for the Cost Assessment Tool (CAT) related to the reference vehicle, based on the field data

Operating conditions	Energy consumption in comfort mode			
	Field data		Models/simulation	
	ACS_UntDP ICE 3 Measurement MWh/year	VCS_f/U_GH ICE-T Measurement MWh/year	ACS_ÜbDP Simulation MWh/year	VCS_f/U_BP Bypass: Assumption MWh/year
Primary energy consumption	84.1	92.1	79.0	81.8
Secondary energy consumption	4.9	8.5	5.7	8.3
Total	89.1	100.6	84.7	90.2

ACS_UntDP: ACS with reverse loop - ICE 3, 2nd series concept

VCS_f/U_GH: VCS with frequency-controlled compressor and option for reheating = ICE-T concept

ACS_ÜbDP: ACS with direct loop = "Next generation ACS" concept

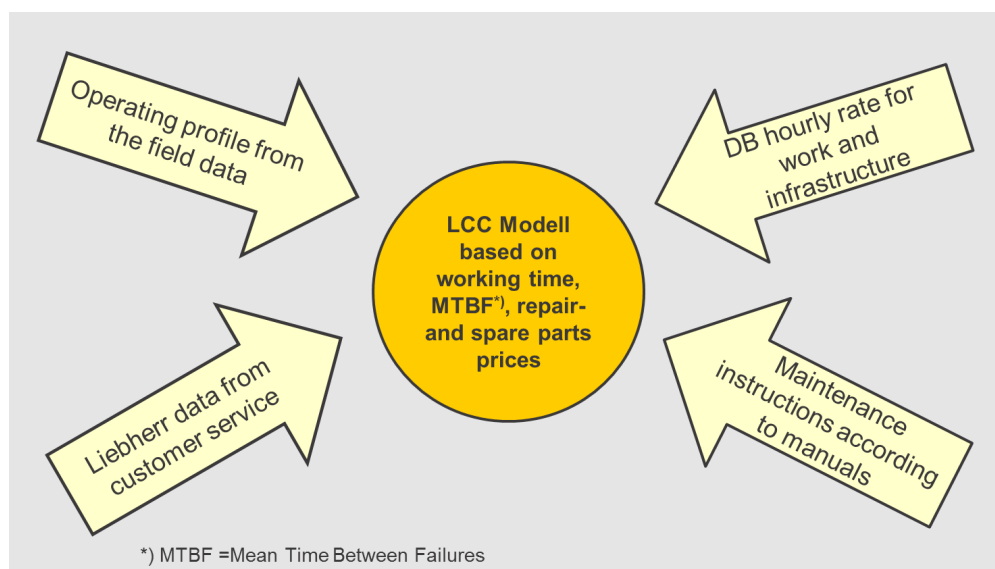
VCS_f/U_BP: VCS with variable-speed compressor and refrigerant bypass = ICE-T concept with bypass

The Operating Cost for primary energy consumption (operation of the HVAC system) and secondary energy consumption (travel resistance from exchanging air with the environment) was calculated based on an electricity tariff of 11.59 Euro cents/kWh.

MC – Maintenance Cost

A model showing the corrective and preventive maintenance cost for the reference vehicle based on field data, information from the operating company and the data basis from the Liebherr customer service is used to determine the Maintenance Cost.

Figure 118: Source data for the Life Cycle Costs (LCC) model



Life Cycle Costs (LCC) model source data; MTBF (Mean Time Between Failures) - for repairable units. Source: own illustration, Liebherr

Field data acquisition

- Operating hours for cooling and heating for the reference vehicle

Operating company information

- Hourly rate of €90/h for work and infrastructure

Liebherr Customer Service

- Quantity and price of repairs, quantity and price of delivery of spare parts

Maintenance instructions

- Preventive maintenance according to the system manual

For the air-cycle system with direct loop, referred to as the “next generation ACS” in comparison B, there are, of course, not yet data available from customer service or the maintenance manual, so that data from the other systems were taken for comparable components or model values based on manufacturer information were applied.

Table 14: Comparison A - Maintenance Cost for the ICE-T and ICE 3 2nd series air-conditioning systems on the reference vehicle according to calculation in the Cost Assessment Tool (CAT)

Liebherr LCC model		
Cost for	ICE-T	ICE 3, 2nd series
Cooling/ventilation	€3,790	€4,030
Heating system	€400	€450
CAT comparison of costs for cooling/heating/ventilation	€4,190	€4,480

ICE-T: ICE-T concept with reheating

ICE 3, 2nd series: ICE 3, 2nd series concept

Table 15: Comparison B - Maintenance Cost for three optimised air-conditioning systems on the reference vehicle according to calculation in the Cost Assessment Tool (CAT)

Liebherr LCC model			
Cost for	ICE 3 Opt	ICE-T bp	ACS NG
Cooling/ventilation	€3,200	€3,820	€3,250
Heating system	€450	€370	€450
CAT comparison of costs for cooling/heating/ventilation	€3,650	€4,190	€3,700

ICE 3 Opt: Concept for ICE 3, 2nd series, maintenance-optimised

ICE-T bp: same as the ICE-T concept, but additionally with refrigerant bypass for capacity control

ACS NG: Next generation air-cycle system, open direct loop

The vapour cycle system has differences between the version with electric reheating and the version with hot-gas bypass. They are the result of the different corrective maintenance required for the heating system and refrigeration circuit, but they balance out. For this reason, the model shows the same total amounts for the Maintenance Cost for both versions (Table 15).

ENVIRONM – Environmental Cost of the vapour cycle system

In comparison A (review), the Environmental Cost for the ICE-T was calculated based on the refrigerant leaks. It consists of the Emission Cost in Euro/CO₂-equivalent from refrigerant leaks and the costs for filling refrigerant.

- ▶ Total filling quantity of refrigerant: 9 kg R134a
- ▶ Global warming potential (GWP) of R134a: 1430
- ▶ Leaks: 5% per annum
- ▶ Refrigerant price: €36/kg R134a
- ▶ Emission Cost assessment of refrigerant leaks: €4.55/t CO₂ equivalent*)

Comparison B (future scenario) assumed the system will change to a refrigerant drop-in after 5 years of operation. The low global warming potential (GWP) of replacement refrigerants is based on their low service life, i.e. they are relatively quickly degraded in the atmosphere. For this reason, limited durability is assumed for the selected replacement refrigerant R513A so that the refrigerant fill must be replaced every 2 years due to the high number of operating hours in railway operations.

- ▶ Total filling quantity of refrigerant: 9 kg R134a
- ▶ After 5 years, switch to refrigerant R513A (mixture of R134a and R1234yf)
- ▶ Drop-in refrigerant, i.e. simple refrigerant replacement without retrofitting costs for the HVAC system
- ▶ Global warming potential (GWP) of R513A: 547
- ▶ Leaks: 5% per annum
- ▶ Complete replacement of refrigerant every 2 years
- ▶ Refrigerant price: €50/kg R513A
- ▶ Emission Cost assessment of refrigerant leaks: €4.55/t CO₂ equivalent*)

*) European Union Emissions Trading System (European Energy Exchange AG, 2016)

Environmental Cost of air cycle system

Since the Emission Cost from electricity generation is already included in the electricity price, the value for the Environmental Cost of the air cycle systems is set at €0.

2.4.2.4 Result of the analysis of economic efficiency

Comparison A – Review

As described in section 2.4.2.2, 2 tried and tested systems are compared here:

- ▶ ICE-T - vapour cycle system with variable-speed compressor and the option for reheating
- ▶ ICE 3, 2nd series - Air-cycle HVAC system with reverse loop

Table 16 and Figure 119 shows the costs per year and HVAC system, broken down into the relevant single items. It is clear that the NRC and Environmental Cost play a secondary role and are practically negligible. The largest share of the costs comes from energy consumption. Although the air cycle system has benefits, they are offset again by the higher Recurring Cost (RC). The Maintenance Cost is about the same for the two systems. The CAT Index, i.e. the sum of the costs, is within the same order of magnitude for both systems, whereby the air cycle system has a small cost advantage of approx. €200/year.

Table 16: Comparison A: Total Cost of Ownership – Index determined using the Cost Assessment Tool (CAT)

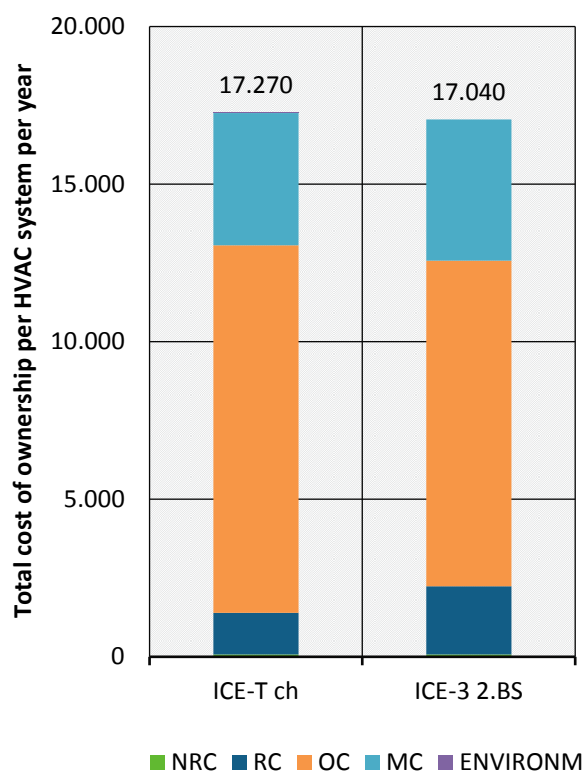
**Comparison A:
Cost analysis in the Cost Assessment Tool (CAT)**

Cost type	ICE-T	ICE 3, 2nd series
CAT Index (total costs/ year/HVAC system)	€17,270	€17,040
ENVIRONM – Environmental Cost	€20	€0
MC – Maintenance Cost	€4,190	€4,480
OC – Operating Cost	€11,660	€10,330
RC – Recurring Cost	€1,330	€2,170
NRC – Non-Recurring Cost	€70	€70

ICE-T: ICE-T concept - R134a vapour cycle system with reheating

ICE 3, 2nd series: ICE 3, 2nd series concept, air-cycle system

Figure 119: Comparison A: Total Cost of Ownership – Index determined using the Cost Assessment Tool (CAT)



ICE-T: ICE-T concept, vapour cycle system with reheating; ICE 3 2nd series: ICE 3, 2nd series concept - air-cycle system
 NRC - Non Recurring Cost; RC - Recurring Cost; OC - Operating Cost; MC - Maintenance Cost;
 ENVIRONM - Environmental Cost. Source: own illustration, Liebherr

Comparison B – Future scenario

In the future scenario (comparison B), optimised systems were compared with each other, as would be designed for the reference vehicle today based on 2.4.2.2.

- ▶ ICE 3 Opt – Air-cycle system: Air-cycle HVAC system with reverse loop, maintenance-optimised (see section 2.4.2.3)
- ▶ ICE-T bp - Vapour cycle system R134a with variable-speed compressor with hot gas bypass, without electric reheating
- ▶ ACS NG – Air-cycle system: Air-cycle HVAC system with direct loop (next generation ACS)

Table 17 and Figure 120 shows the breakdown of annual costs. In contrast to comparison A, the Environmental Cost for the future scenario is of greater importance. The vapour cycle system is now energy-optimised, i.e. their energy consumption corresponds to that of the air cycle system with the reverse loop process. However, this improvement is partially offset by the Environmental Cost. The largest share of the costs, however, is still from energy consumption.

For the next generate air cycle system, one would expect improvements compared to today's air cycle systems in terms of procurement costs and energy consumption, which would result in a cost benefit of approx. €1,000/year compared to state-of-the-art cold vapour systems.

Table 17: Comparison B: Total Cost of Ownership – Index determined using the Cost Assessment Tool (CAT)

Comparison B: Cost analysis in the Cost Assessment Tool (CAT)

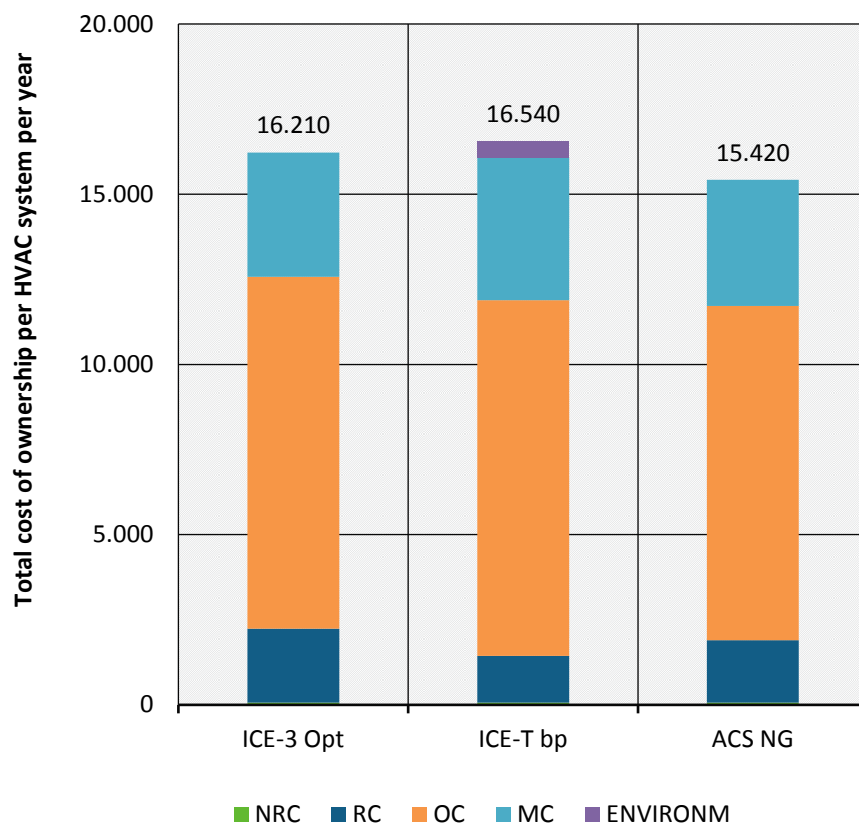
Cost type	ICE 3 Opt	ICE-T bp	ACS NG
CAT Index (total costs/ year/HVAC system)	€16,210	€16,540	€15,420
ENVIRONM – Environmental Cost	€0	€470	€0
MC – Maintenance Cost	€3,650	€4,190	€3,700
OC – Operating Cost	€10,330	€10,450	€9,820
RC – Recurring Cost	€2,170	€1,370	€1,830
NRC – Non-Recurring Cost	€70	€70	€70

ICE 3 Opt: Concept for ICE 3, 2nd series, maintenance-optimised

ICE-T bp: same as the ICE-T concept, but additionally with refrigerant bypass for capacity control

ACS NG: Next generation air-cycle system, open direct loop

Figure 120: Comparison B: Total Cost of Ownership – Index determined using the Cost Assessment Tool (CAT)



ICE 3 Opt: Concept for ICE 3, 2nd series, maintenance-optimised; ICE-T bp: same as the ICE-T concept, but additionally with refrigerant bypass for capacity control; ACS NG: Next generation air-cycle system, open direct loop; NRC - Non Recurring Cost; RC - Recurring Cost; OC - Operating Cost; MC - Maintenance Cost; ENVIRONM - Environmental Cost. Source: own illustration, Liebherr

2.4.3 Discussion of results & conclusions

2.4.3.1 Results for power and energy consumption

The presented results are for the comfort mode of heating, ventilation, air-conditioning systems (HVAC systems) over 6,570 operating hours per year, where comfort mode covers passenger service. The underlying operating conditions (weighting matrices), in particular the distribution of outside ambient temperature, affect the result. Assuming that a train is operated with equal frequency in the climate zones (cool (Braunlage), moderate (Kassel) and warm (Mannheim)), the air-cycle system with reverse loop (ICE 3) resulted in average savings of 28% for primary annual energy consumption in cooling operation, compared to a vapour cycle system with variable-speed compressor and reheating option for the low part-load range (ICE-T).

Similarly, the advanced air-cycle system with direct loop (simulation) produces savings of 16% compared to a vapour cycle system with variable-speed compressor and refrigerant bypass (bypass assumed by calculation).

For the annual energy consumption for cooling operation, the air-cycle technology therefore has a clear advantage.

In heating operation, there are no relevant technical differences between the air-cycle system and the vapour cycle system. Depending on the ratio of the annual energy consumption for heating operation and cooling operation, the savings in cooling operation have a different impact on the total annual energy consumption.

Taking an analytical approach, this study also examined the secondary power and energy consumption as a result of air intake by the HVAC system. This secondary power consumption must be provided by the traction motor. Depending on the HVAC system and operating conditions, the secondary energy consumption is 5% to 15% of the total annual energy consumption (primary and secondary, heating and cooling) or 9% to 22% of the total annual energy consumption (primary and secondary) for cooling. Consequently, the secondary energy consumption is non-negligible.

The difference between the HVAC systems is in cooling operation, where the air-cycle systems require a significantly lower air volume for cooling in each case compared to the vapour cycle system. In cooling operation, this means that air-cycle systems see savings for secondary energy consumption of more than 50%, when comparing the systems implemented in railway vehicles, and savings of 23% to 38% for the air-cycle systems in simulation. The lower secondary energy consumption is another advantage of the air-cycle technology.

In absolute numbers, the three investigated climate zones of Braunlage, Kassel and Mannheim on average have total energy savings for the air-cycle system with reverse loop (primary and secondary energy consumption for heating and cooling) of 11.50 MWh/year compared to the vapour cycle system with speed control and reheating in the low part-load range, for a carriage based on TW7 of ICE 3 (74 passengers) and 6,750 hours in comfort mode. The calculated savings in this case, when comparing the air-cycle system with direct loop with the vapour cycle system with speed control and assumed bypass, are approx. 5.41 MWh/year.

The significance of these energy savings can be illustrated with the following example: The energy saved by the air-cycle technology per year and per carriage (5.41 MWh or 11.50 MWh) could be used to drive an electric vehicle⁵ around the equator 1.1 or 2.3 times. Translated into a more practical example, it could provide the electricity required per annum by 3 or 6.5 electric passenger cars⁶ or the electricity required per annum for 1.6 or 3.3 households⁷ in Germany. These comparisons show that the energy saved by the air-cycle technology per carriage and year are significant in scale:

2.4.3.2 Conclusion on economic efficiency

Air-cycle railway air-conditioning systems are already a successfully tested, environmentally friendly and economical alternative to conventional vapour cycle systems with fluorinated refrigerants. For the HVAC systems compared here, which have been in standard service for many years, it is evident that the proven environmentally friendly air-cycle technology is at least equivalent in terms of economic efficiency. If the potential for optimisation identified in this study and new developments are implemented, then the air-cycle systems have an economic advantage.

⁵ E.g., the VW e-Golf: Power consumption: 12.7 kWh/100 km, combined, 100 kW motor (Volkswagen, 2017)

⁶ For the average mileage of a passenger car in Germany: 14,015 km/year (Kraftfahrt-Bundesamt, 2017) (Federal Motor Transport Authority, 2017)

⁷ Number of households in Germany in 2012: 39,707,000

(Umwelt Bundesamt, Bevölkerungsentwicklung und Struktur privater Haushalte, 2017)

(Federal Environmental Agency, Population development and structure of private households, 2017)

Electricity consumption of households in Germany in 2012: 137 TWh/year (Umwelt Bundesamt, Stromverbrauch, 2017) (Federal Environmental Agency, Electricity consumption, 2017)

The higher investment costs for the air-cycle air-conditioning technology are offset by lower operating costs.

Generally, compared to the energy and maintenance costs, the investment costs play a subordinate role and amount to about 10% for conventional VCS and about 14% for air-cycle systems annually.

In the course of the project, additional potential for improvement was identified for maintenance of the existing system ICE 3, 2nd series, implementation of which should deliver significant cost savings.

The potential of air-cycle technology far from exhausted. There is a very positive outlook for the air-cycle air conditioning of railway vehicles with further development of the architecture.

2.5 Technical discussion and publication (WP 5)

On 25 January 2018, the public technical presentation and discussion of the results of the project took place as part of the technical discussion organised by LVF with the support of the UBA and DB at the press and visitor centre of the Federal Press Office in Berlin. Figure 121 shows the programme for the technical discussion.

The goals of this technical discussion were to describe the measurements, the analysis of the measured values, the results for power and energy consumption and for the Life Cycle Costs and the additional insights gained in the project and to discuss the scientific, technical and economic aspects in detail with the specialists with an interest in the field.

The presentations at the technical discussion were published on the UBA website⁸.

Figure 121: Programme for the technical discussion of the air-conditioning project, held in Berlin on 25 January 2018

09:30	<i>Eintreffen und Begrüßungskaffee</i>
10:00	Begrüßung Jochen Flasbarth - Staatssekretär im Umweltministerium / BMUB Dr. Thomas Holzmann - Vizepräsident des Umweltbundesamtes / UBA Projektpartner - Liebherr - Dirk Junghans / Geschäftsführung Liebherr - DB Systemtechnik GmbH - Nils Dube / Leiter Business Line Engineering
10:50	Inhalt und Durchführung des Forschungsprojektes Maik Wollweber / Liebherr
11:20	<i>Kaffeepause</i>
11:35	Projektanteil der DB Systemtechnik Dr. Peter Claus / DB Systemtechnik GmbH
12:05	Analyse und Systemvergleich anhand der Leistungsaufnahme Dr. Christian Luger / Liebherr
12:50	<i>Mittagspause</i>
13:35	Systemvergleich anhand der Wirtschaftlichkeit Roland Friedrich / Liebherr
14:15	Ausblick Air-Cycle-Technologie Reinhard Aigner / Liebherr
14:30	Diskussion der Ergebnisse
ca. 16:00	<i>Ende der Veranstaltung</i>

Programme for the technical discussion of the air-conditioning project, held in Berlin on 25 January 2018, Source: UBA

⁸ Link to UBA website: <https://www.umweltbundesamt.de/service/termine/fachgesprach-klimatisierung-von-zuegen>, 12/07/2018

2.6 Need for and relevance of the project

This project is the first time that measurement on a train and an air-conditioning system and subsequent detailed evaluation of the data has been carried out in such detail. The project also provides an analysis of the Life Cycle Cost of train air-conditioning systems for the first time. The results of the project include critical findings and base data for evaluating air-conditioning technologies on trains to identify the need for changing over to environmentally friendly train air conditioning, as the global phasedown of fluorinated greenhouse gases progresses.

2.7 Applicability of the results

2.7.1 Economic prospects of success

For LfV and DB, the great potential of this project is that it presents the economic efficiency of an air-cycle system (ACS) compared to a conventional vapour cycle system (VCS). This provides manufacturers of air-conditioning systems that use natural refrigerants with significantly more weight when arguing in favour of such systems and for future calls for tenders.

In addition to discussing energy efficiency, this project also explains and demonstrates economic efficiency, providing good arguments for an expansion of the use of air-cycle systems on railway vehicles.

This project also serves to increase knowledge of the factors of energy consumption and economic efficiency as well as acceptance of systems that use natural refrigerants in general and acceptance of air-cycle systems in particular by train manufacturers and operating companies.

2.7.2 Prospects for scientific success

The findings of the overall project obtained through measurements will support the improvement and further development of air-conditioning systems, and air-cycle technology in particular, in further research and development projects and, as a result, identify additional potential for reducing energy consumption and the Total Cost of Ownership (TCO).

2.7.3 Prospects for scientific and commercial follow-up projects

At present, no follow-up research and development (R&D) project is planned which would look at the acquisition of field data. However, the insights gained will be used in all R&D projects by the contractor, LfV, to continue working on the efficiency of railway air conditioning and also to create commercial incentives for the use of natural refrigerants by train manufacturers and operating companies.

In the long term, these and similar projects will promote the changeover from environmentally unfriendly refrigerants to environmentally neutral refrigerants and systems.

2.8 Advances by other bodies

Additional projects on train air conditioning have been started in the meantime (see the note in section 2.3.3.3 about system 3).

2.9 Publications

The public technical presentations on 25 January 2018 were published on the UBA website.

Technical discussion of Air cycle airconditioning for railways: Wollweber M.: Inhalt und Durchführung des Forschungsprojektes; Claus, P., Kretschmann, K.-P.: Felddatenanalyse ICE 3 Tz 301 - Projektanteil der DB Systemtechnik; Luger C.: Vergleich des elektrischen Energiebedarfs von Bahn-Klimaanlagen mit den Kältemitteln Luft und R134a; Friedrich R., Krawanja A.: Wirtschaftlichkeitsanalyse von Bahn-Klimaanlagen mit den Kältemitteln R729 (Luft) und R134a; Aigner R.: Ausblick Air Cycle Technologie. Umweltbundesamt. Berlin 2018. URL:

<https://www.umweltbundesamt.de/service/termine/fachgesprach-klimatisierung-von-zuegen>

The results of the entire project were published in 2018 in the railway journal ZEVrail in two articles:

- Luger C., Krawanja A., Aigner R., Claus P., Vergleich des Jahresenergiebedarfs von Bahn-HLK-Systemen mit den Kältemitteln Luft und R134a, ZEVrail 142 (2018) 08, 308-314.
- Krawanja A., Luger C., Aigner R., Claus P., Vergleich der Gesamtbetriebskosten von Bahn-HLK-Systemen mit den Kältemitteln Luft und R134a, ZEVrail 142 (2018) 09, 378-384.

3 Bibliography

- Aigner, R. (2007). Synthetic and Natural Refrigerants for Rail HVAC units and their impact on the Annual Energy consumption. RTA International Workshop.
- Bell, Wronski, Jorrit, Quoilin, Sylvain, Lemort & Vincent. (2014). Pure and Pseudo-pure Fluid Thermophysical Property Evaluation and the Open-Source Thermophysical Property Library CoolProp. Industrial Engineering Chemistry Research, 53(6), p. 2498-2508.
- Claus, P. (2016). Liebherr-Transportation Systems und Deutsche Bahn AG führen Felddatenanalyse an luftgestützter Klimaanlage durch [Liebherr-Transportation Systems and Deutsche Bahn AG conduct field data analysis on air-cycle systems]. ZEVrail, no. 140, p. 396-397, 2016.
- Deutsche Bahn AG. (2008). Daten zur Passagierbesetzung aus dem Reisenden-Erfassungs-System [Data for passenger occupancy from the Passenger Acquisition System]. Unpublished.
- Deutsche Bahn AG. (08. 05 2017). Fahrzeuglexikon für den Fernverkehr 2016 [Vehicle lexicon for long-distance trains]. Retrieved on 01/09/2017 from http://download-data.deutschebahn.com/static/datasets/fahrzeuglexikon/Fahrzeuglexikon_2017.pdf.
- Deutscher Wetterdienst. (2014). Testreferenzjahre von Deutschland für mittlere, extreme und zukünftige Witterungsverhältnisse [Test reference years of Germany for average, extreme and future weather conditions].
- Deutscher Wetterdienst. (2017). Climate Data Center. Retrieved from <https://www.dwd.de/DE/leistungen/cdcftp/cdcftp.html>.
- DIN 4710:2003-01. (2003). Statistics on German meteorological data for calculating the energy requirements for heating and air conditioning equipment.
- DIN EN 13129:2016-12. (2016). Railway applications - Air conditioning for main line rolling stock - Comfort parameters and type tests.
- European Energy Exchange AG. (2016). Market data environmental markets. Accessed on 22/07/2016 at <https://www.eex.com/en/market-data/emission-allowances/spot-market>.
- EU (2014). Regulation (EU) No 517/2014 of the European Parliament and of the Council of 16 April 2014 on fluorinated greenhouse gases and repealing Regulation (EC) No 842/2006. Official Journal of the European Union. Vol. L 150/195, 20/05/2014.
- Luger C., Krawanja, A., Aigner R., Claus, P. (2018): Vergleich des Jahresenergiebedarfs von Bahn-HLK-Systemen mit den Kältemitteln Luft und R134a [Comparison of yearly energy demand of rail HVAC systems with refrigerants Air and R134a]. ZEVrail, no. 142 (8) p.308-314, 2018.
- Krawanja, A., Luger C., Aigner R., Claus, P. (2018): Vergleich der Gesamtbetriebskosten von Bahn-HLK-Systemen mit den Kältemitteln Luft und R134a [Comparison of Total Cost of Ownership of rail HVAC systems with refrigerants Air and R134a]. ZEVrail, no. 142 (9) p.378-384, 2018.
- Luger, C. (2017). Virtual development and optimization of HVAC systems in rail vehicles. Dissertation: Technical University of Graz.
- Luger, C., Kallinovskiy, J., & Rieberer, R. (2016). Identification of representative operating conditions of HVAC systems in passenger rail vehicles based on sampling virtual train trips. Advanced Engineering Informatics, p. 157-167.
- Meister, M. (10 2012). Vergleichende betriebliche Messungen zur Bestimmung des Energieverbrauchs von Klimaanlage mit Luft und R134a als Kältemittel [Comparative operational measurements for determining the energy consumption of air-conditioning systems with air and R134a as refrigerant]. ZEVrail no. 136 (10), p. 402-409, 2012.
- Morgenstern, J., & Ebinger, I. (December 2008). Anforderungen an zukünftige Klimaanlage für Schienenfahrzeuge [Requirements for future air-conditioning systems for railway vehicles]. El-Eisenbahningenieur, 12, p. 24-31, 2008.
- Schmitt, & Berlitz. (2014). Energie-Verbrauchszyklus zur Bestimmung der Energie-Effizienz von Schienenfahrzeug-Klimaanlagen [Energy consumption cycle for determining the energy efficiency of railway vehicle air-conditioning systems]. ZEVrail, no.138, p. 190-194, 2014.
- Schmitt M., Berlitz T., David Ch., Danzer P.(2015). Anwendung des DB-Energie-Verbrauchszyklus DC2013 für Klimaanlage in Schienenfahrzeugen [Applying the DB Duty cycle DC2013 for air conditioning units of railway rolling stock]. ZEVrail, no. 139 (6-7), p.2-8 , 2015.